



UNIVERSITY OF NIŠ  
FACULTY OF OCCUPATIONAL SAFETY  
Department of Preventive Engineering  
Noise and Vibration Laboratory



"POLYTECHNICA" UNIVERSITY OF TIMISORA  
FACULTY OF MECHANICAL ENGINEERING  
Department of Mechanics and Vibration  
Noise and Vibration Laboratory

PROCEEDINGS OF PAPERS

26<sup>th</sup> INTERNATIONAL  
CONFERENCE



NOISE & VIBRATION

6 - 7, December 2018.  
Niš, Serbia

**26<sup>th</sup> INTERNATIONAL CONFERENCE**

# **NOISE AND VIBRATION**



**PROCEEDING OF PAPERS**

**Niš, December 6 - 7, 2018.**

**Publisher:** *University of Niš, Faculty of Occupational Safety, 2018*

**For the publisher:** *Prof. Momir Prašćević, Ph. D.  
dean*

**Editors of proceeding of papers:**

*Prof. Dragan Cvetković, Ph. D.*

*Prof. Vasile Marinca, Ph. D.*

*Prof. Nicolae Herisanu, Ph. D.*

*Prof. Momir Prašćević, Ph. D.*

**Graphic design and prepress:**

*Darko Mihajlov, Ph. D.*

*Rodoljub Avramović*

**Printout:** "Unigraf x-copy" Niš

**No. of copies:** 100

**ISBN: 978-86-6093-088-2**

**CIP - Каталогизacija u publikaciji - Narodna biblioteka Srbije, Beograd**

534.83(082)

62-752(082)

614.872(082)

628.517(082)

INTERNATIONAL Conference Noise and Vibration (26th ; 2018 ; Niš)

Proceeding of Papers / 26th International Conference Noise and Vibration, Niš, December 6 - 7, 2018.;

[organizers University of Niš, Faculty of Occupational Safety of Niš, Department of Preventive Engineering [and] "Politehnica" University of Timisoara, Faculty of Mechanical Engineering,

Department of Mechanical Engineering ; editors Dragan Cvetković et al.]. - Niš : University Faculty of Occupational Safety,

2018 (Niš : Unigraf x-copy). - 183 str. : ilustr. ; 30 cm

Tekst štampan dvostubačno. - Tiraž 100. - Bibliografija uz svaki rad.

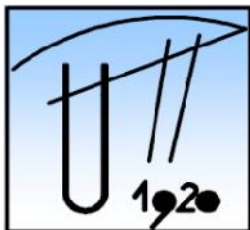
ISBN 978-86-6093-088-2

1. Fakultet zaštite na radu (Niš)

a) Бука - Зборници b) Вибрације - Зборници COBISS.SR-ID 270804748

## ORGANIZER

---



**University of Niš**

**Faculty of Occupational Safety of Niš**

Department of Preventive Engineering

Noise and Vibration Laboratory

[www.znrfak.ni.ac.rs](http://www.znrfak.ni.ac.rs)

**"Politechnica" University of Timisoara**

**Faculty of Mechanical Engineering**

Department of Mechanical Engineering

Noise and Vibration Laboratory

[www. http://www.mec.upt.ro](http://www.mec.upt.ro)

## AUSPICE

---



**Ministry of Education, Science and Technological Development Republic Serbia**

[www.mpn.gov.rs](http://www.mpn.gov.rs)

## GENERAL SPONSOR

---

**Brüel & Kjær** 

[www.bksv.com](http://www.bksv.com)

## CONFERENCE REVIEW

---

---

1 <sup>st</sup> Yugoslav Conference	Belgrade	1978
2 <sup>nd</sup> Yugoslav Conference	Belgrade	1979
3 <sup>rd</sup> Yugoslav Conference	Belgrade	1980
4 <sup>th</sup> Yugoslav Conference	Belgrade	1981
5 <sup>th</sup> Yugoslav Conference	Belgrade	1982
6 <sup>th</sup> Yugoslav Conference	Belgrade	1983
7 <sup>th</sup> Yugoslav Conference	Belgrade	1984
8 <sup>th</sup> Yugoslav Conference	Belgrade	1985
9 <sup>th</sup> Yugoslav Conference	Belgrade	1986
10 <sup>th</sup> Yugoslav Conference	Belgrade	1987
11 <sup>th</sup> Yugoslav Conference & 1 <sup>st</sup> International Conference	Belgrade	1988
12 <sup>th</sup> Yugoslav Conference	Belgrade	1989
13 <sup>th</sup> Yugoslav Conference	Niš	1991
14 <sup>th</sup> Yugoslav Conference & 2 <sup>nd</sup> International Conference	Niš	1993
15 <sup>th</sup> Yugoslav Conference & 3 <sup>rd</sup> International Conference	Niš	1995
16 <sup>th</sup> Yugoslav Conference with international participation	Niš	1998
17 <sup>th</sup> Yugoslav Conference with international participation	Niš	2000
18 <sup>th</sup> Yugoslav Conference with international participation	Niš	2002
19 <sup>th</sup> Conference with international participation	Niš	2004
20 <sup>th</sup> Conference with international participation	Tara	2006
21 <sup>st</sup> Conference with international participation	Tara	2008
22 <sup>nd</sup> Conference with international participation	Niš	2010
23 <sup>rd</sup> Conference and 4 <sup>th</sup> International Conference	Niš	2012
24 <sup>th</sup> International Conference	Niš	2014
25 <sup>th</sup> International Conference	Tara	2016
26 <sup>th</sup> International Conference	Niš	2018

## PROGRAM COMMITTEE

---

- Prof. Dragan Cvetković, Ph. D.,**  
University of Niš, Faculty of Occupational Safety – chairman
- Prof. Vasile Marinca, Ph. D.,**  
"Politehnica" University of Timișoara, Romania – co-chairman
- Prof. Petar Pravica, Ph. D.,**  
University of Belgrade, Faculty of Electrical Engineering
- Prof. Giangiacomo Minak, Ph. D.,**  
University of Bologna, Italy
- Prof. Marek Grzybowski, Ph. D.,**  
Gdynia Maritime University, Poland
- Prof. Holger Stark, Ph. D.,**  
Heinrich Heine University Düsseldorf, Germany
- Prof. Miloš Manić, Ph. D.,**  
University of Idaho, USA
- Prof. Nicolae Herisanu, Ph. D.**  
"Politehnica" University of Timișoara, Romania
- Prof. Vasile Bacria, Ph. D.,**  
"Politehnica" University of Timișoara, Romania
- Prof. Liviu Bereteu, Ph. D.,**  
"Politehnica" University of Timișoara, Romania
- Prof. Gheorghe Draganescu, Ph. D.,**  
"Politehnica" University of Timișoara, Romania
- Prof. Tihomir Trifunov, Ph. D.,**  
National Military University „Vassil Levski“ of Veliko Turnovo, Bulgaria
- Prof. Koleta Zafirova, Ph. D.,**  
Faculty of Technology and Metallurgy, Skopje, Macedonia
- Prof. Nikola Holeček, Ph. D.,**  
Environmental Protection College, Velenje, Slovenia
- Prof. Valentina Golubović-Bugarski, Ph. D.,**  
Faculty of Mechanical Engineering, Banja Luka, Rep. of Srpska
- Prof. Pero Raos, Ph. D.,**  
Faculty of Mechanical Engineering, Slavonski brod, Croatia
- Ratko Uzunović, Ph. D.,**  
VIBEX system
- Zoran Stojanović, Ph. D.,**  
Vinča Institute for nuclear sciences, University of Belgrade
- Prof. Ljiljana Živković, Ph. D.,**  
University of Niš, Faculty of Occupational Safety
- Prof. Nenad Živković, Ph. D.,**  
University of Niš, Faculty of Occupational Safety
- Prof. Predrag Kozić, Ph. D.,**  
University of Niš, Faculty of Mechanical Engineering
- Prof. Nikola Lilić, Ph. D.,**  
University of Belgrade, Faculty of Mining and Geology

**Prof. Slobodan Gajin, Ph. D.,**  
University of Novi Sad, Faculty of Civil Engineering in Subotica

**Prof. Zoran Perić, Ph. D.,**  
University of Niš, Faculty of Electronic Engineering

**Prof. Zoran Petrović, Ph. D.,**  
University of Kragujevac, Faculty of Civil and mechanical Engineering in Kraljevo

**Prof. Zlatan Šoškić, Ph. D.,**  
University of Kragujevac, Faculty of Civil and mechanical Engineering in Kraljevo

**Prof. Dejan Ćirić, Ph. D.,**  
University of Niš, Faculty of Electronic Engineering

**Prof. Aleksandar Cvjetić, Ph. D.,**  
University of Belgrade, Faculty of Mining and Geology

## **ORGANISATION COMMITTEE**

---

**Prof. Momir Prašćević, Ph. D.,**  
University of Niš, Faculty of Occupational Safety – chairman

**Prof. Nicolae Herisanu, Ph. D.,**  
"Politehnica" University of Timișoara, Romania – co-chairman

**Prof. Vasile Marinca, Ph. D.,**  
"Politehnica" University of Timișoara, Romania

**Prof. Dragica Milenković, Ph. D.,**  
University of Niš, Faculty of Mechanical Engineering

**Prof. Jasmina Radosavljević, Ph. D.,**  
University of Niš, Faculty of Occupational

**Prof. Miomir Raos, Ph. D.,**  
University of Niš, Faculty of Occupational Safety

**Prof. Branko Radičević, Ph. D.,**  
University of Kragujevac, Faculty of Civil and mechanical Engineering in Kraljevo

**Prof. Nebojša Bogojević, Ph. D.**  
University of Kragujevac, Faculty of Civil and mechanical Engineering in Kraljevo

**Prof. Darko Mihajlov, Ph. D.,**  
University of Niš, Faculty of Occupational Safety

**Emir Ganić, Ph. D.,**  
University of Belgrade, Faculty of Transport and Traffic Engineering

**Prof. Mladena Lukić, Ph. D.,**  
University of Niš, Faculty of Occupational Safety

**Marko Ličanin, MSc,**  
University of Niš, Faculty of Occupational Safety

## CONTENT

---

### INVITED PAPERS

- Livija Cvetičanin** 9  
*Overview on vibration energy harvesting systems*
- Miomir Mijić, Dragana Šumarac Pavlović, Miloš Bjelić** 15  
*Some actual problems in making an acoustic comfort*
- Ivana Kovačić, Neil Ferguson, Hans Bodén** 21  
*ERASMUS+ project: Strengthening educational capacities by building competences and cooperation in the field of noise and vibration engineering (SENVIBE)*

### NOISE

- Jelena Tomić, Nebojša Bogojević, Branko Radičević, Zlatan Šoškić** 25  
*Application of genetic algorithm in developing of traffic noise prediction model*
- Branko Radičević, Milan Kolarević, Nicolae Herisanu, Mišo Bjelić, Tanja Miodragović** 29  
*Sound absorption of recycled plastic material*
- Milan Kolarević, Branko Radičević, Vladan Grković, Ivana Ristanović, Marina Ivanović** 35  
*Acoustic properties of recycled plastic*
- Aleksandra Petrović, Mladen Rasinac, Vladan Grković, Marina Ivanović** 41  
*An experimental plan for noise analysis and chatter detection in milling depending on the cutting parameters*
- Aleksandra Igić, Slavko Zdravković, Dragana Turnić, Sandra Šaković, Vesna Zdravković** 45  
*The research of acoustics from aspect of sound source*
- Nikola Holeček, Tomaž Bregar** 49  
*Psychoacoustics in household appliances*
- Milan Veljković, Snežana Živković** 55  
*Noise sensitivity among surface miners and underground miners*
- Emil Živadinović, Marija Jevtić, Sanja Bijelović, Nataša Dragić, Siniša Milošević, Živojin Lalović** 59  
*Modeling basic noise indicators of environmental noise for the period 1985 - 2010*
- Aleksandar Gajicki** 65  
*Differences in strategic noise mapping by NMPB '96 and CNOSSOS-EU methods on Velika Plana-Markovac section*
- Emir Ganić, Vinh Ho-Huu, Obrad Babić, Sander Hartjes** 69  
*Air traffic assignment to reduce population noise exposure and fuel consumption using multi-criteria optimisation*
- Jovan Miočinović, Biljana Beljić Durković** 77  
*Industrial impulsive noise and hearing: evaluation according to the regulations and applicable standards and possible additional risk on hearing comparing to the effect of steady noise*
- Momir Prašćević, Darko Mihajlov, Marko Ličanin** 85  
*Noise monitoring on the territory of the city of Niš - Overview of the methodologies and results*
- Violeta Stojanović, Zoran Milivojević** 93  
*Analysis of acoustic parameters in Serbian orthodox churches*

<b>Darko Mihajlov, Momir Praščević, Marko Ličanin</b> <i>Defining the environmental noise indicators measurement time interval using multi-criteria optimization</i>	99
<b>Ana Đorđević, Dejan Ćirić</b> <i>Problem of excessive noise generated by industrial machinery</i>	107
<b>Marko Milivojčević, Filip Pantelić, Dejan Ćirić</b> <i>Comparison of frequency characteristics of sound generated by internal combustion engines depending on fuel</i>	115
<b>Jovica Jovanović, Jovana Jovanović</b> <i>Health effects of industrial noise</i>	121
<b>Mladenka Vujošević</b> <i>Noise level control in primary schools in Podgorica</i>	125
<b>Boris Mihaylov</b> <i>Strategic Noise Mapping combined with dedicated long and short term noise monitoring. Experience, output.</i>	127
<b>Marko Ličanin, Momir Praščević, Darko Mihajlov</b> <i>Realization of the low-cost noise measurement monitoring station using MEMS microphone technology and micro PC</i>	133
 <b><u>VIBRATION</u></b>	
<b>Karoly Menyhardt, Ramona Nagy, Remus Stefan Maruta</b> <i>Control signal generation for random vibration tests</i>	137
<b>Miomir Jovanović, Goran Radoičić, Predrag Milić, Taško Maneski</b> <i>Application of frequency simulation for detecting the risk of extreme events on transport machines</i>	141
<b>Slavko Zdravković, Dragan Zlatkov, Andrija Zorić, Sandra Šaković</b> <i>The dissipation and the dissipation function of seismic energy</i>	147
<b>Miljan Cvetković, Boban Cvetanović, Mário Fedatto Neto</b> <i>The evaluation of the whole-body vibration exposure of vibratory roller operators</i>	151
<b>Igor Jovanović, Ljubiša Perić, Uglješa Jovanović, Dragan Mančić</b> <i>Stressing issue of a piezoceramic sectional cylinder with a circular polarization</i>	155
<b>Nikola Vučić, Zoran Perić, Bojan Denić</b> <i>Design of switched QL quantizer of Laplacian source with GR codes for medium quality of reconstructed signal</i>	161
<b>Dragan Jovanović, Milena Mančić, Miomir Raos, Slobodan Jovanović, Milan Banić, Marko Mančić</b> <i>Vibrodiagnostic methods for detection of structural and functional failure of machines</i>	167
<b>Jovan Miočinović, Biljana Beljić Durković</b> <i>Evaluation of WBV by ISO 2631-1 for workers of broadcasting and communications company in transport to and from mountain repeater station</i>	173
<b>Nicolae Herisanu, Vasile Marinca</b> <i>Analytical investigation to Duffing harmonic oscillator</i>	177
<b>Vasile Marinca, Nicolae Herisanu</b> <i>Free vibrations of tapered beams</i>	181

University of Nis  
Faculty of Occupational Safety

„Politehnica“ University of Timisoara  
Faculty of Mechanical Engineering



26<sup>th</sup> International Conference

**NOISE AND VIBRATION**

Niš, 6 - 7. 12. 2018.

# 1<sup>st</sup> SESSION

# INVITED

# PAPERS





## OVERVIEW ON VIBRATION ENERGY HARVESTING SYSTEMS

Livija Cveticanin<sup>1,2</sup>

<sup>1</sup> University of Novi Sad, Faculty of Technical Sciences, Serbia, cveticanin@uns.ac.rs

<sup>2</sup> Obuda University, Doctoral School of Safety and Security Sciences, Budapest, Hungary

**Abstract** - In this paper an overview on vibration energy harvesters (EH) which are the electric energy generators for small energy consumers in the system is presented. The principle of energy transformation in the system is described. Devices which transform the ambient mechanical energy especially the vibration energy in electricity are considered. Special attention is given to EH with piezoelements. Advantages and disadvantages of this type of EH are discussed. Various applications of EH devices are shown. In conclusion optimization of the system in the sense of increasing of power supply is suggested.

### 1. INTRODUCTION

Recently, there are a lot of devices that need quite small energy for their powering. These devices are micro-electro-mechanical systems (MEMS), like sensors and actuators, but also measuring and control systems, small electronic components and remote sensors for different disciplines of engineering field, such as mechanical, aerospace, electrical and civil [1] and so on. The evolution of low-power-consuming electronics and small-scale electronic mobile devices developed the need to give wireless solutions to these problems and led to the investigation in energy harvesting. Usually the energy sources for these devices are batteries. Unfortunately, in spite of their efficiency and low price, batteries have many disadvantages like limited working life and represent an environmental pollutant. In the concept of ecological frame the chemical waste produced by batteries has to be reduced. It is suggested that the new energy sources use ambient waste energy. It has to be converted into useful electrical energy. It would be a renewable energy source. It is found that the waste ambient energy is a good starting point for further investigation. The most convenient energy sources are based on solar power [2], thermal gradients [3], fluid flow or energy produced by normal range of human activity [4]. Roundy et al. [5] stated that the power available from ambient conditions is:  $380 \mu\text{W}/\text{cm}^3$  from air flow,  $17 \mu\text{W}/\text{cm}^3$  from pressure variation,  $330 \mu\text{W}/\text{cm}^3$  from human power and  $380 \mu\text{W}/\text{cm}^3$  from vibrations. It is concluded that the vibration energy plays a major role due to the fact that is almost universal present: from ground shaking to human movements, from ambient sound to thermal noise. This energy is suitable to be transformed into the electric energy and energy harvesters are produced.

The first electric energy harvesters are applied for powering of clocks. Namely, in the second half of the 20<sup>th</sup> century a new mechanism for clocks with quartz crystal oscillator is developed. The mechanism is done by engineers in Neschatel

in Swiss in 1967 [6]. The clocks were more accurate than the conventional mechanical ones and since that time it becomes the leading one on the market. Electric energy is obtained by transforming the mechanic energy of hand motion, and these clocks have more sophisticated functions [7].

The waste mechanical energy of vibration has to be converted into electricity. Devices, which convert energy and also storage it, are called energy harvesters (EH) [8]. As the sources of waste vibration have quite low energy, the main question is how to make this transformation in the most effective way to obtain the energy enough for powering devices. Various procedures for energy transformation are already developed. Dependently on mechanism of energy transformation the EH may be different. Thus, thermal EH converse thermal energy into mechanical work. Temperature of the body is varying due to energy adding or losing and it causes molecule motion and energy transformation. Photo-voltage EH directly convert light into electricity on atomic level. Some of materials have the property of the photo-electric effect i.e., they absorb photons and break free electrons which produce the electric current.

The aim of this paper is to give the overview on principles of energy production with EH, to describe various types of EH and to give a short description of application of EH. Special types of EH which transform the kinetic energy of motion into electric one [9] are also presented. They produce low voltage electricity with special frequencies. These energy harvesting devices are widely used, but it is still being explored about lost energy on the human body and machines, its storage and using of concentrated energy. Namely, the energy harvesting market has the tendency of increasing mostly in medicine, automotive, transportation, industry and also in building.

### 2. TECHNIQUES IN ELECTRICAL ENERGY HARVESTING

Presented three main techniques of harvesting energy from ambient vibrations have been shown to be capable of generating output power levels in the range of  $\mu\text{W}$  to  $\text{mW}$  [10]. Techniques of vibration energy harvesting is based on three concepts: piezoelectric, electromagnetic and electrostatic.

Electromagnetic generators employ the electromagnetic induction which is the result of relative motion between a conductor and a magnet with variable magnetic flux gradient [11]. The electromagnetic generators offer good powering for small spring/mass configurations. The produced electricity is

with low voltage and high output current level. The disadvantage of the system is associated with problems in assembly and alignment of sub-millimeter scale electromagnetic system [1].

To generate energy, electrostatic generators utilize the relative movement between electrically isolated charged capacitor plates [10]. The work done against the electrostatic force between the plates provides the harvested energy. The energy density of the generator can be increased by decreasing the capacitors spacing. However, the energy density is decreased by reducing the capacitor surface area. Electrostatic generators can utilize electrets to provide the initial charge and these are capable to store charge for many years. The output voltage produced by the device is relatively high and results in a limited current supply capability and capacitances can lead sometimes to reduce generator efficiency.

However, the piezoelectric generators are the most widely applied ones. Due to their simple design and small size, they have the advantage in comparison to the previous ones. Namely, there are no requirements for complex geometry and numerous additional components. Piezoelectric generators convert directly structural vibrations into a voltage output by using a piezoelectric material. Piezoelectric materials generate a charge when mechanically stressed. Materials are usually artificial and of composite type. Mechanical properties of the material will limit the overall performance and the lifetime.

Piezoelectric generators are capable to produce relatively high output voltages but only at low electrical currents. The generators are useful in micro engineering and are widely applied in structural health monitoring devices or sensors of these devices.

The piezoelectric effect was discovered by brothers Pierre Curie and Jacques Curie in 1880. They demonstrated the effect of piezoelectricity with tourmaline, quartz, topaz, cane sugar and Rochelle salt. If the certain crystal material is pressed electricity is generated. The inverse effect was proved mathematically by Gabriel Lippmann in 1881. It is called ‘inverse piezoelectric effect’ [8]. The first applications were made during World War I with piezoelectric ultrasonic transducers. Since that time, various types of piezoelectric materials as artificial composites are produced. They are built in various devices for producing electric current in inaccessible places where the power from outside is not possible or the battery supply is not a good option.

### 3. PRINCIPLE OF PIEZOELECTRIC EH

Vibration-based energy harvesting has received growing attention over the last decade. Recently, piezoelectric EH with piezoelectric materials, for converting energy from one form to another, are developed. The most often applied piezomaterials in EH are crystals and ceramics [12]. The most famous crystal applied for piezoelectric effect is quartz i.e., silicium-dioxid ( $\text{SiO}_2$ ) and the most often applied ceramic is lead-zirconate-titanate ( $\text{Pb}[\text{Zr}_x\text{Ti}_{1-x}]\text{O}_3$  ( $0 \leq x \leq 1$ )), or shortly PZT. This ceramic material is convenient due to its low prize and to its dipole property are high temperatures.

Most off the piezoelectric EH are cantilever beams with one or two piezomaterial layers which form mono-morph or bimorph structures [13]. The piezoelement is mounted on the

vibrating structure. In Fig.1 the cantilevered bimorph piezoelectric EH is plotted.

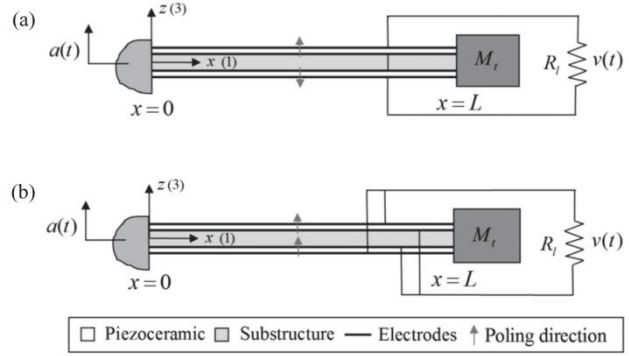


**Fig. 1** Cantilevered bimorph piezoelectric energy harvester configurations under base excitation: (a) series and (b) parallel connection [13].

The vibrating structure is excited with a force on the left end. On the right end of the beam a tip mass  $M_t$  is mounted [13]. The cantilever beam – mass system may be of various types [14]. In Fig.2 the wide, narrow and trapezoidal beams with variable masses are plotted.

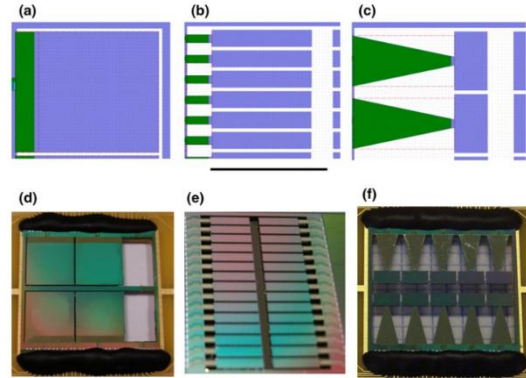


**Fig. 2** Schemes of cantilever beam (green) - mass (purple) systems : a, d) wide beam, b, e) narrow beam, c, f) trapezoidal beam [14].

Every type of beam – mass system has some advantages and disadvantages. The wide beam gives the high density of current, while the narrow beam has high bandwidth, while the trapezoidal beam is the optimal in the both components.

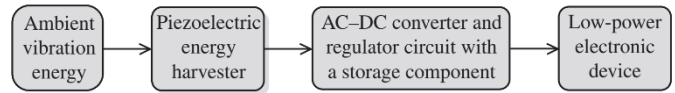


**Fig. 3** Schematic representation of the concept of a piezoelectric energy harvesting system [13].

The connection between the beam and piezoelectric elements is serial (Fig.1a) or parallel (Fig.1b). The strain induced in the layer results in an alternating voltage output (AC) across their electrodes. AC is stabilized and transported into a capacitor which is the part of the AC-DC convertor (Fig.3). The obtained energy is enough for battery charging, for example [8].

#### 4. APPLICATION OF PIEZOELECTRIC EH

As it is already mentioned, vibration represents the side effect of every motion and can be treated by applying of EH. The application of the obtained electric energy is very wide. So, it can be applied for powering of the screen for monitoring of system state, for the so called Health and Usage Monitoring System, in various machines, transportation devices, airplanes, etc. [15] but also civil structures [16]. Wang et al 2012 in MRS suggest the application of EH in: pressure imaging system, pressure sensor, photon sensor/imaging, force sensor, biomedical sensors, touch sensor, smart gloves, actuator, nanorobots, implantable devices, LED, solar cell, active flexible electronics, nanogenerator, touch pad electronics, human-Si CMCS interfacing, 4D electronic signature etc. Generally, EH are applied in human health monitoring, structural health monitoring, in industry, automotive, military (Fig.4).

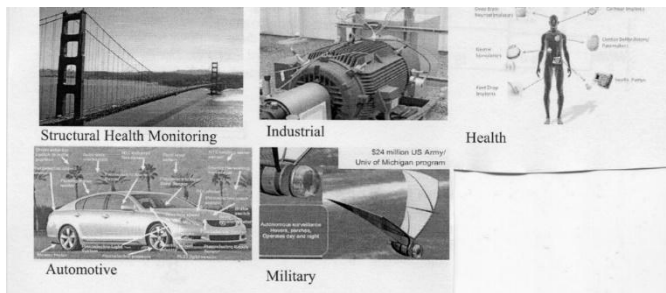


Fig. 4 Application of piezoelectric EH [9].

Number of sensors in the system may be significant. Thus, in automotive following small energy consumers are evident: pressure sensor for fuel injecting, GPS and inertial navigation system, accelerometer at airbags, microphone for noise elimination, sensors for corrosion, pressure sensor for tire, pressure sensor and controller in break, accelerometer for control of amortization, pressure sensor for air flow, pressure sensor for air condition, silicon sensors for fuel injecting, sensor for exhaust gases [17].

##### 4.1 Humans activity and EH

For electrical power generation over longer durations, energy harvest from everyday human activities is desirable. It is a challenge to produce substantial electricity from walking. Biomechanics developed EH which generates electric current during walking. EH are settled on the knees and selectively activate the production of electricity at the end of bending of the leg. Many devices can utilize the obtained energy, for example, battery lamp, radio, charger for mobile phone, etc. Mechanical energy originates from motion of human body parts during walking (from knees, heel, skeletal joint, hip bone, shoulder, elbow) [18]. Piezoelectric generator gives the energy stimulated by muscles. The generator is not incorporated into the human body but is an exterior leg denture (Fig.5). Active motor nerve challenges a contraction force in the muscle which loads the piezoelectric material.

At the moment energy harvesting research has focused on generating electricity from the compression of the shoe sole during walking (Fig.6).

It is interesting to be mentioned that the microtechnology is utilized in medicine: in physiology, cardiology but also in other multidisciplinary sciences.



Fig. 5 Human powered generation [18].

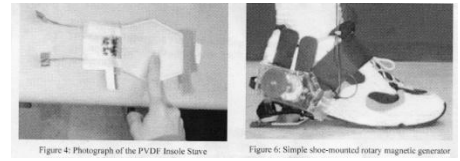


Fig. 6 a)Piezoelectric element, b)EH generation in the shoe [18].

One of the most important devices which prolonged the life of patients is the implanted pacemaker which is settled into the heart for 20 years. The device is of cylindrical shape with dimensions 5,8x23 mm and is implanted into the top of the right hear chamber across femoral venue and right pre-chamber (Fig. 7a) [19].

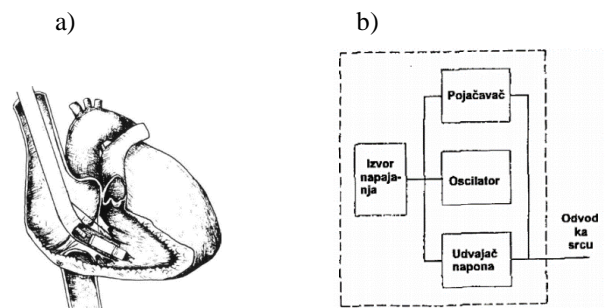
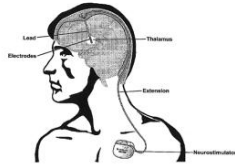


Fig. 7 a)Implanted pacemaker/catheter in the right chamber, b)Schematic diagram of components in implanted pacemaker [19].

To understand the purpose of the pacemaker it is necessary to analyze the operation of the 'natural pacemaker' using the states of physiology of medicine [20]. Some of the heart cords have the ability of self excitation, automatically and periodically to make impulses and contractions. These are the cords of the sinus knots which control the frequencies of the whole heart. Due to exchange i.e., membrane permeability of calcium and natrium ions there is the variation of the voltage and the signal is activated. In addition, the permeability of ions can be blocked and due to alternative processes the rhythmic impulses occur. This activation is repeating continually during the whole life. The activation is independent on brain intervention and because of that the heart is autonomous organ. Electric signal which is formed in sinal atrial (SA) knot and is transmitted through the atrial ventricular (AV) knot and Hissov's bundle up to the Purkins cords on the top of chamber for their contraction. For artificial generating of these occurrence, simulation of natural processes are made by pacemaker (Fig. 7b) [21].

For the case of pathologic obesity the gastric pacemakers are implanted into the stomach wall of the patient. By stimulating with hormones which encourage the extraction of the digestive enzymes, the weight of the patient decreases. Healing of obesity potential illnesses as diabetes are prevented [22]. These pacemakers are activated with HE systems.

Pulse in the veins can be used for generation of electric energy and supply of medicine nanodevices and sensors for monitoring of the vital organs of human body like the heart and the blood pressure [18].



**Fig. 8** Scheme of neuro-simulator [21].

Microtechnology is utilized for stimulation of parts of brain. Patients with impaired mobility and other types of neurologic illnesses are healed with impulse generator which is incorporated in torso (Fig. 8).

#### 4.2 Vehicle interaction with road and track in EH

Moreover, another major issue prevalent in harvesting energy is from railroad tracks were usually the irregular pulse-like nature of railroad track vibrations and low amplitude of displacement of the railroad track are applied. Setting the EH devices in tracks the electric energy is generated which is used for powering of the auxiliary devices of the rail transport. Devices of the railway infrastructure need 10-100 W. Let us mention some of them: device for signalization, various switches, system state screens etc. [23].

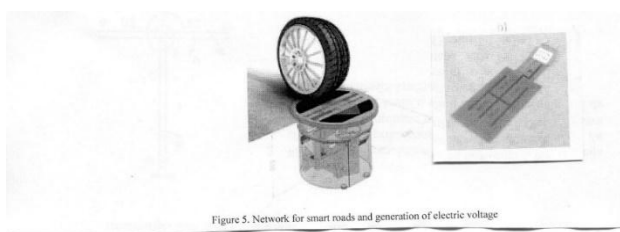


Figure 5. Network for smart roads and generation of electric voltage

**Fig. 9** a) Wheel – EH interaction, b) Piezoelectric element [12].

It is used in construction where piezoelectric materials append for making smart roads [12]. Wheels of car and other vehicle are driven over a road covered with a thin piezoelectric layer and generate electricity. This kind of energy is free, so it becomes an excellent solution for the deficiency of electricity in some countries. Thus, due to vibration and the human or vehicle interaction with roads the wasted energy from roadways is kept captive and harvested [12]. This energy it is concentrated, and saved for future use.

#### 4.3 Micro-electro-mechanical system (MEMS)

As it is already mentioned the piezoelectric EH are devices which work by using the ambient energy. The waste vibration energy is converted into electric energy and it gives the effective use of environmental energy. EH is a useful energy source in devices where a small amount of powering energy is necessary. EH substitutes batteries which are intensive environment pollutants. As EH is a suitable source for powering small energy consumers it is applied for powering micro sensors and low voltage electric circles. Nowadays, new micro-electro-mechanical systems (MEMS) are developed. These are small devices which register changes in environment, analyze them and act. MEMS contain mechanic elements, sensors, actuators, electric and electronic devices

[24]. The trend of energy scaling in the last ten years gives as the result that the energy consumption is decreased on 10-100  $\mu$ W for the digital signal processors of electric circuit with low and up to middle bandwidth. As the properties of EH are improved, they become mobile energy sources instead of chemical batteries. Recently, the technology requires the voltage of 3V or higher, which is obtained using the piezoelectric EH with d33 piezoelectric regime.

#### 4.4 Application of EH in civil engineering

In [13] the application of EH on the large structures is considered. It is shown that the energy harvesting is possible to be utilized on heavy bridges, too. The electric energy is generated due to moving of a load on the bridge causing excitation of slender bridges and surface strain fluctuation of large structures. Two types of EH are applied: a bimorph located on an arbitrary position on the slender bridge and the piezoceramic patch covering a region of a bridge.

In [14] the explore ways of harvesting energy from a building are presented. To be more specific, the conversion of mechanical energy into electrical energy using piezoelectric materials is studied. Applications of piezoelectric materials in actuators are also explored, with particular interest in the question: what is the maximum moment that an actuator, whose energy comes from piezoelectricity, can develop when attached to a beam.

Duan et al. [16] investigated the structural health monitoring using devices powered with piezoelectric HE. It is shown that the piezoelectric material is obvious to be applied for repairation of certain damages as a kind of smart material.

### 5. FURTHER INVESTIGATION

We suggest the development of EH in two directions:

1. Optimize the EH. EH are power generators for small devices. Unfortunately, the produced energy is very low and very often the frequency region is not convenient. The proper choice of harvester parameters is necessary for obtaining of the optimal rate between the broadband energy harvesting combined with vibration reduction. As a piezoelectric material cannot generate much energy, and often requires amplification, the goal is to optimize the circuit linked to the piezoelectric material to obtain as much power as possible [14]. In addition, there is a problem of optimizing vibration reduction of the primary structure and the quantum of harvested power production. When the vibration of the structure is reduced the power, that can be scavenged from the structure, decreases.
2. Production of portable EH. Already there are some portable medical devices [25], but their improvement is necessary.

### ACKNOWLEDGEMENT

The investigation was supported by the Faculty of Technical Sciences in Novi Sad (Proj. No. 054/2019).

## REFERENCES

- [1] S. Priya and D. Inman, *Energy Harvesting Technologies*, New York: Springer, 2009.
- [2] [www.science.nasa.gov/science-news/science-at-nasa/2002/solarcells](http://www.science.nasa.gov/science-news/science-at-nasa/2002/solarcells)
- [3] [www.energetskiportal.rs/obnovljivi-izvori-energije/](http://www.energetskiportal.rs/obnovljivi-izvori-energije/)
- [4] R. Riemer and A. Shapiro, "Biomechanical energy harvesting from human motion: theory, state of the art, design guidelines, and future directions", *Journal of Neuroengineering and Rehabilitation*, vol. 8, no. 1, 2011.
- [5] [www.piezomaterials.com](http://www.piezomaterials.com)
- [6] C. Piguet, "The first quartz electronic watch", *Integrated Circuit Design. Power and Timig Modeling, Optimization and Simulation*, vol. 2451, no. 1, p.p. 1-15, 2002.
- [7] A. Glasmeier, "Technological discontinuities and flexible production networks: The case of Switzerland and the world watch industry", *Research Policy*, vol. 20, no. 5, p.p. 469-485, 1991.
- [8] A. Erturk and D.J. Inman, *Piezoelectric Energy Harvesting*, Chichester: John Wiley & Sons, 2011.
- [9] [www.kinergizer.com](http://www.kinergizer.com)
- [10] S. Beeby, M. Tudor and N White, "Energy harvesting vibration sources for microsystems applications", *Measurement Science and Technology*, vol. 17, pp. 175-195, 2006.
- [11] N. Kumar and S. Kolangiammal, "Fully self-powered electromagnetic energy harvesting system", *International Journal of Science and Research*, vol. 2, no. 5, p.p. 305-308, 2013.
- [12] A. Abbasi, "Application of piezoelectric materials in smart roads and MEMS, PMPG power generation with transverse mode thin film PZT", *International Journal of Electrical and Computer Engineering*, vol. 3, no. 6, p.p. 857-862, 2013.
- [13] A. Erturk, "Piezoelectric energy harvesting for civil infrastructure system applications: Moving loads and surface strain fluctuations", *Journal of Intelligent Material System and Structures*, vol. 22, no. 17, p.p. 1959-1973, 2011.
- [14] A. Ledoux, *Theory of piezoelectric materials and their applications in civil engineering*, MSc thesis, Boston: MIT, 2011.
- [15] M. Stamos, C. Nicoleau, R. Torah, J. Tudor, N. Harris, A. Niewiadomski and S. Beeby, "Screen printed piezoelectric generator for helicopter health and usage monitoring system", *Proceedings of PowerMEMS 2008+ microEMS2008*, 2008.
- [16] W.H. Duan, Q. Wang and S.T. Quek, "Applications of piezoelectric materials in structural health monitoring and repair: Selected research examples", *Materials*, vol. 3, p.p. 5169-5194, 2010.
- [17] T. Djakov, I. Popovic and Lj. Rajakovic, "Mikro-elektromehanički sistemi (MEMS)-Tehnologija za 21.vek", *Hemijska industrija*, vol. 68, no. 5, p.p. 629-641, 2014.
- [18] J. Donelan, Q. Li, V. Naing, J. Hoffer, D. Weber and A. Kuo, "Biomechanical energy harvesting: generating electricity during walking with minimal user effort", *Science*, vol. 319, no. 5864, p.p. 807-810, 2008.
- [19] P.E. Vardas, C. Politopoulos, E. Manios, F. Parthenakis and C. Tsagarakis, "A miniature pacemaker introduced intravenously and implanted endocardially. Preliminary findings from an experimental study", *European Journal of Cardial Pacing Electrophysiology*, vol. 1, no. 1, p.p. 27-30, 1991.
- [20] A. Guyton and J. Hall, *Medicinska fiziologija*, Beograd: Savremena administracija, 2003.
- [21] M. Andrasi, *Generisanje električnih signala u ljudskom organizmu. Električni signali srca*, Diplomski rad, Novi Sad: Univerzitet u Novom Sadu, 2005.
- [22] F. Favretti, M. De Luca, G. Segato, L. Busetto, A. Ceoloni, A. Magon and G. Enzi, "Treatment of morbid obesity with the Transcend Implantable Gastric Stimulator (IGS): A prospective survey", *Obesity Surgery*, vol. 14, no. 5, p.p. 666-670, 2004.
- [23] T. Lin, J. Wang and L. Zuo, "Energy harvesting from rail track for transportation safety and monitoring", *University Transportation Research Center*, 2014.
- [24] N. Jackson, R. O'Keeffe, F. Waldron, M. O'Neill and A. Mathewson, "Evaluation of low-acceleration MEMS piezoelectric energy harvesting device", *Microsystem Technologies*, vol. 20, no. 4-5, p.p. 671-680, 2013.
- [25] J. Paulo and P.D. Gaspar, "Review and future trend of energy harvesting methods for portable medical devices", *Proceedings of the World Congress on Engineering*, vol. 2, 2010.



# CENTER OF TECHNICAL DIAGNOSTICS & NOISE AND VIBRATION LABORATORY



UNIVERSITY OF NIŠ  
FACULTY OF OCCUPATIONAL SAFETY  
Čarnojevića 10a, 18000 Niš  
Tel.: 018 529-747; Fax: 018 529-748

## Environmental noise & Occupational noise - measurement and analysis

- ◆ Rating noise level;
- ◆ Frequency analysis;
- ◆ Statistical analysis;

## Human vibration

- ◆ Hand-arm vibration;
- ◆ Whole body vibration;



## Sound power of noise sources

- ◆ Sound pressure method;
- ◆ Sound intensity method;



## Predictive/preventive maintenance of machine

- ◆ Vibration condition monitoring;
- ◆ Vibrodiagnostics;
- ◆ Balancing of rotating machine;

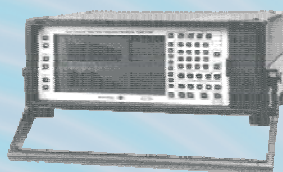


## Design of noise and vibration control systems

- ◆ Design of noise insulation and absorption system;
- ◆ Design of vibration insulation and absorption system;
- ◆ Design of room acoustics;

## Room acoustics

- ◆ Time reverberation;
- ◆ Airborne sound reduction index;
- ◆ Impact sound reduction index;



## Urban noise

- ◆ Noise monitoring;
- ◆ Noise zoning;
- ◆ Strategic noise maps;



## Education

- ◆ Workshops;
- ◆ Courses;
- ◆ Long-term learning;





## SOME ACTUAL PROBLEMS IN MAKING AN ACOUSTIC COMFORT

Miomir Mijić, Dragana Šumarac Pavlović, Miloš Bjelić

University of Belgrade, Faculty of Electrical Engineering, Serbia, emijic@etf.rs

**Abstract** – *Acoustic comfort is a specific dimension in overall building quality that has become very important in residential buildings today. Efforts to achieve such a quality in new designed dwellings in Serbia very often suffer the negative influences of some specific factors. Those are: (1) lack of adequate architects' knowledge, (2) objective difficulties in achieving the required level of acoustic comfort and (3) some inadequacy in the actual legislation that do not follow modern living. In this paper three issues are discussed: lack of information concerned with contemporary sound insulation theory among all participant in building design and construction, the complexity of the sound transmission through some partitions widely used today and changes in the acoustic environment in dwellings induced by the overall development of building technology. The paper consider the effects of those factors on the acoustic comfort in dwellings.*

### 1. INTRODUCTION

Acoustic comfort is one of the tasks challenging the building erection today. It is well known that such comfort is primarily achieving by adequate sound insulation. The issue how to fulfil the required sound insulation in buildings has long been an expert topic in the architectural acoustics [1,2,3]. Solving that task is achieved in three phases: through the approved criteria, that is, by prescribing minimum requirements, through the calculations of the relevant parameters values and through the rules of good builder practice in the realization of what has been designed. The first documents in this field in Serbia dated from the mid of twentieth century [4,5], which led to publishing of the still actual standard JUS U.J6.201 in 1982 [6] (today only renamed to SRPS U.J6.201 [7]). This explicitly indicated to all participant in the process of buildings design and construction that there is an acoustical comfort as a topic, and that some minimal acoustic isolation criteria must be met. However, that was the time when the apartments were donated to people, and the dwelling houses erection was a social action that had to provide housing and a “better future” for all. And generally such gifts were not critically analyzed. That was also the time when engineers were distinguished themselves by proving new methods of quick and cheap constructions using of prefabricated elements and innovative constructive solutions. All that permanently changed the characteristics of the physical environment in which somehow the sound have to be stopped.

Long time has passed since then, but the standard U.J6.201 with unchanged content is still the only document that

prescribes the sound isolation criteria in Serbia [6]. However, in housing and building constructions significant changes are going on today. They are generally manifested in several dimensions: in the evolution of the dwellings user demands and their general ideas about living, in changes of architectural concepts, in changes of building technology, in dissemination of very extensive installations of all types through the residential buildings, as well as in the improvements in regulation concerned with acoustic comfort which happened in European countries during last decade. All this has combined in a complex way influencing the sound insulation in buildings.

All these changes have not influenced yet more serious impact on the design and construction routine in Serbia. That is why the time is now to redefine the practice of acoustic comfort achievement in residential buildings, but also to intensely search for innovative practical solutions that will follow the changes. In this paper, some recognized problems in design and construction of the residential buildings that directly induced difficulties in reaching the acoustic comfort in them are presented and discussed.

### 2. CALCULATION OF SOUND INSULATION IN CURRENT BUILDING DESIGN

The first algorithms for the calculation of the partition's sound isolation index in building have been proposed in the literature more than sixty years ago [3]. Issue of the analysis is one partition with all its layers and physical characteristic of applied materials, defining the graph of the sound insulating index  $R$  as a function of frequency. With some small variations in formulas, introduced by some our older generation acousticians the calculation procedure have found their place in popular textbooks of building acoustics published in Serbia. With the very appearance of computers, some of these formulas was incorporated in software and thus long ago come in the practice of building design bureaus. Thus, in about last thirty years programs for calculation based on theory known in that time have been widely used. Figure 1 presents an illustration taken from such a software. That approach conceals an important shortcoming giving the results that are without all important influences appearing in the reality of building construction.

An important shift in sound insulation design rules was made in the year 2000. by appearance of the standards series denoted as EN12354, part 1, 2 and 3. These documents are also accepted in Serbia ten years ago [8,9,10]. The essence of

this major change is fact that the calculation implies an analysis of the structure of partitions in the building and takes into account all the sound paths between two adjacent rooms, and not only the partition that directly separates them. Fig. 2 symbolically presents main categories of the sound energy path between two adjacent rooms that determine value of the sound reduction index of the construction between them [8]. Beside direct sound path Dd there are also flanking sound paths Df, Ff and Fd. To make more observable a simplified 3D presentation of sound energy paths is presented in Fig. 3 [11,12]. In such approach to calculation all partitions are represented by the value of their sound reduction index measured in the laboratory, but also taking into account the influence of the connection type between them (rigid, elastic, T or X).

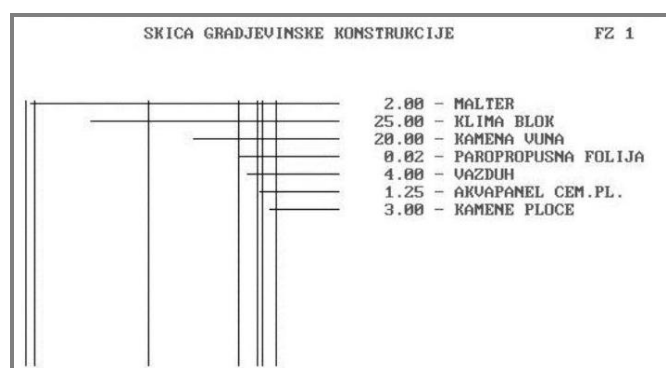


Fig. 1 The illustration of an old calculation method applied in a present-day residential building design

An interesting fact is that that change in calculation methodology, although defined in actual standards, has not yet been reflected in the building design practice in Serbia. Unfortunately, an old approach is still widely applied, although the results obtained by such calculation in a greater or lesser extent do not correspond to reality. The reason for this is, apparently, the lack of information and knowledge among building designers. There is also lack of any feedback from the output of building erection process, which is a finished building and certification of its quality, to the process entry which is the building designers and their design methods.

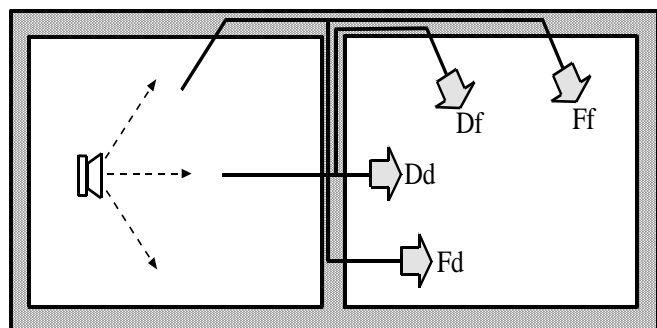


Fig. 2 Symbolical presentation of main sound energy paths between two adjacent rooms [8]

Therefore, the first problem in achieving acoustic comfort in buildings is a certain inertia and designers' ignorance concerned with existing standards and modern calculation algorithms for sound insulation prediction which give more

precise results. Until now some obligation to apply new standards in building design process has not explicitly confirmed, thus the problem is partly in the absence of such a rulebook that would precisely express that obligation. In the mean time archaic methods are still in use.

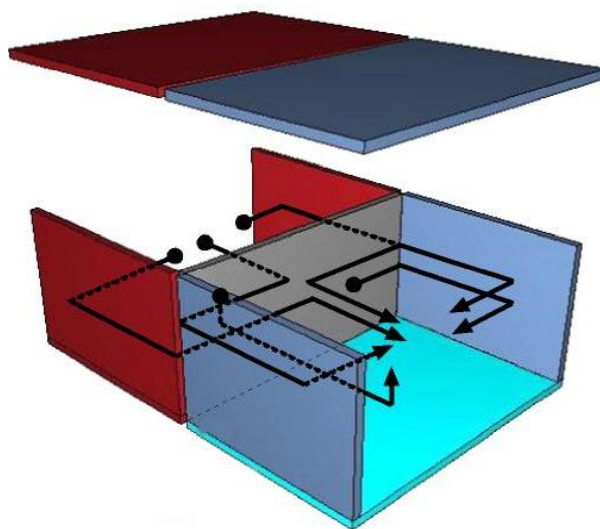


Fig.3 A simplified 3D presentation of sound energy paths between two adjacent rooms [11,12]

### 3. ACOUSTICAL PROBLEMS INDUCED BY ENERGY EFFICIENCY REQUIREMENTS IN BUILDINGS

A huge change in the design and construction of buildings occurred with introducing the concept of energy efficiency. The main consequence was some changes in standard approaches to building construction. One of such consequence is obligation of making the thermal insulation between adjacent dwellings. Thus the wall between the dwellings, along with standard acoustic requirements, has to satisfy the requirements of thermal insulation, too. That mandatory introduced an appropriate thermal insulation layer positioned somewhere into the structure of partitions separating the adjacent dwellings. In contemporary building constructions in Serbia the extensively applied solution is a double massive wall with some thermal insulation material between them. That mostly led to about 30 cm thick walls, a centimetre more or less.

The application of double massive partitions revealed problems after sound insulation measurements in some realized buildings. It has been found that sound insulation does not meet expected value, i.e. does not meet existing norm or satisfy just lower permissible value, although the calculations in building design stage had shown larger value. That was a confusing result, because the double wall with the space between two layers gave smaller value of sound insulation index than the wall with materials of two layers connected into one unique wall. Thus, this topic has come in the focus of interest among investors and builders of residential buildings (unfortunately, with less interest among building designers). That initiated, among other things, various laboratory measurements of the double walls insulating properties with different materializations, both massive materials and insulation between.

The idea of sound insulation properties improvement for a double massive wall at the first moment led to different variations of materials applied in space between two massive layers. Two such results are shown in Figures 4 and 5 taken from the literature [13]. Figure 5 present the measurement result of a double wall made of massive brick 12 + 12 cm with about 5 cm space between them. Both side of the partitions are plastered. Measurements were performed with three different mineral wool quality (density) placed in the gap (R1, R2 and R3). The results reveal that the variation of the filling between the layers did not bring about any change in value of the sound insulation index. The quality of the wool has been changed in wide limits, but the results have been positioned in the range of only 1 dB, which is inside the interval of measurement uncertainty.

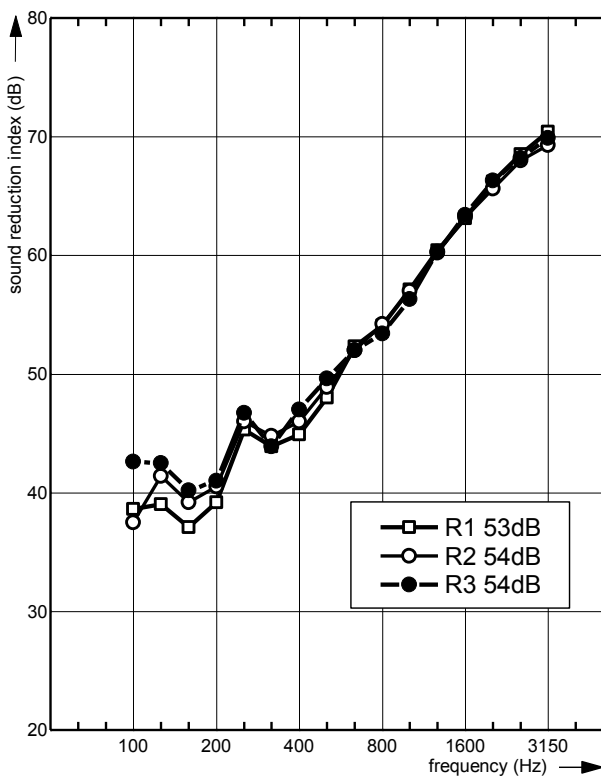


**Fig. 5** Sound reduction index of massive brick double walls 12+12 cm with different characteristic of mineral wool in gap between layers [13]

One more idea for improvement of the double massive wall sound insulation properties was the insertion of one plasterboard into the middle of the gap and with mineral wool in rest of the space. Such possibility was analysed on the example of a double wall made of massive blocks with material density of about  $1900 \text{ kg/m}^3$ . The sound insulation measurement was done in two cases: with only a mineral wool in the gap between layers (R8) and with a plasterboard inserted in the partition (R10). One can see that the measured change of rated sound insulation index for these two structures is rather small, only 1 dB, i.e. again within the interval of measurement uncertainty for that type of measurement.

These results, as well as results of some other measurements performed in meantime can be found in the literature [13]. All those results reveal an important fact that any valuable

improvement of the double massive wall insulating properties cannot be achieved by modification in the air gap, even with “magic” insulation materials one can find at the market. There are obviously some hidden physical processes that make the sound path through the air gap between layers less relevant for overall wall’s insulation properties. It was clear that the problem of sound insulation between rooms with double massive walls separating them have to be analysed in more detail.

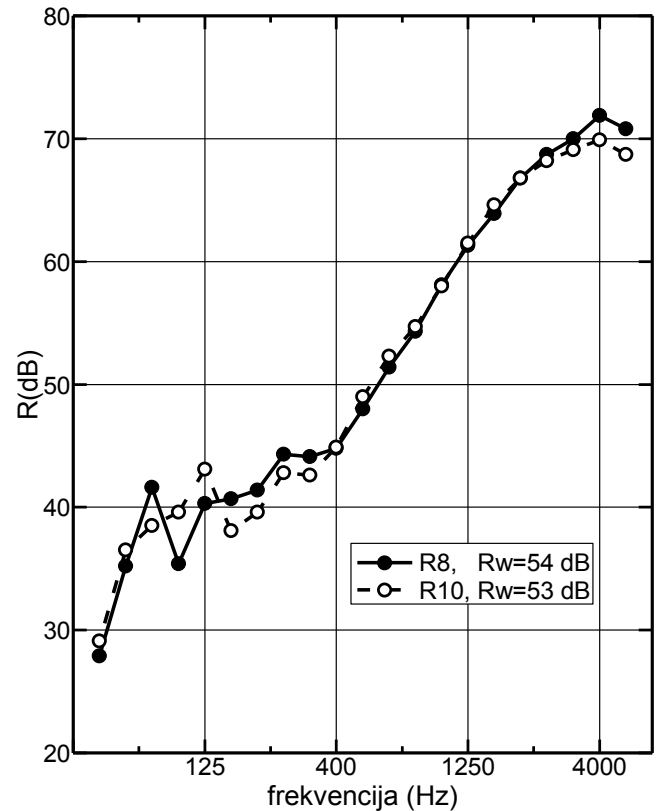


**Fig. 6** Sound reduction index of massive double walls made of bricks 12+12 cm with and without gypsum plate in gap between layers [13]

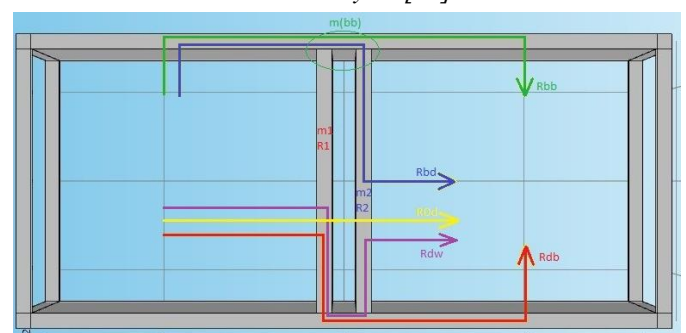


**Fig. 7** Sound energy paths between two adjacent rooms in case of double massive wall between them

Figure 7 presents schematically the construction of two adjacent rooms with a double massive wall between them. The picture shows all the paths of sound energy between the rooms separated by double layers construction. At each path one can identify corresponding sound insulation index. There is a direct path (marked in Fig.7 with yellow line) as in all conventional partitions. On that path the first wall layer receives the sound energy from the source room and forwards it through the air gap to the second layer and further into the

receiver room. It is clear that such direct sound transmission through a double layers has a greater attenuation due to the discontinuity of the materials, i.e. the sound reduction index at that path  $R_{dd}$  is greater than for the single layer monolith wall of the same surface mass.

However, the rigid connections between two layers of the double wall and the adjoining partitions establish parallel paths of sound energy, thus resulting in reduction in the overall sound insulation index of complete partition. In the configuration of double walls the energy received by the first layer is transferred to the second layer via a common joints all around the partition's perimeter. The impact of this paths (marked in Fig. 7 with violet colour) is quantified by the sound reduction index  $R_{dw}$ . That inevitably reduces the sound reduction index achieved by separating the wall into two layers. Direct transmission through such a partition, instead of a single path that exists in the monolith wall, now extends with several parallel paths formed through wall joints to all four boundary surfaces (two side walls, floor and ceiling). This effect is present in laboratory measurements, too. In addition, double walls commonly have some additional physical connections due to static reasons.

In process of sound energy transmission between adjacent rooms separated with double wall there are also other "normal" flanking paths of sound energy as well (blue and red lines in Fig. 7). The paths are going through one of the wall lining and side walls. In Fig. 7 sound reduction index at those paths are labelled as  $R_{db}$  and  $R_{bd}$ . Those paths of sound energy occur also in monolith wall as well, but the difference is in the fact that here they are formed through the wall having a smaller surface mass and whose sound insulating properties are therefore lower. As a consequence, the sound energy attenuation in the wall joints has been changed. That is modification compared to the monolith massive wall of the equivalent surface mass positioned at the same location. It is phenomenon that makes a difference in results between *in situ* measurement in real building and laboratory measurement.

There is no data in literature about double walls' insulating properties that involve structural transmission through lateral partitions, or their parts, as indicated in Figure 8. The most common data on double walls implies complete dilation between their layers, which is rarely applied in local building design practice. Unlike massive double walls, double lightweight walls made of plasterboards have been analysed in numerous papers because in the western world countries such system is widely used type of walls, so-called "dry construction". There are also numerous publications of materials and dry construction systems manufactories, which include, among others, their insulating properties.

An illustration of the described impacts on the double massive wall insulating properties is shown in Figure 8. The diagram presents values of measured sound reduction index for walls made of brick with total massive material thickness 24 cm, but with different internal configuration. The sound reduction index of the homogeny massive wall made of brick with 24 cm thickness and a double wall with structure 12 + 12 cm, which means with the same surface mass, are shown [13]. The diagram reveal the reduction of values in the case of a double wall compared to single wall with same mass. The diagram also shows two measured results of the

same double walls made of brick, but in real conditions between two rooms in one building. The effects of changing conditions around the wall perimeter are manifests at higher frequencies. Similar results with an even greater influence of flanking paths were obtained for double massive walls made from other materials such as various types of blocks.

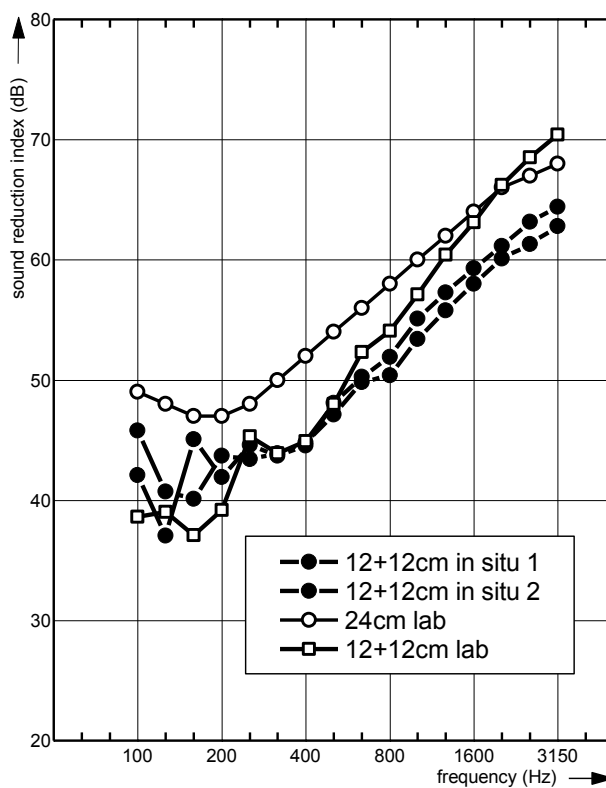


Fig. 8 Sound reduction index of brick walls with same total thickness of massive material, i.e. with the same surface mass, but with different structure and at different locations

#### 4. THE PROBLEM OF MINIMUM REQUIREMENTS OF SOUND INSULATION - THE CASE OF "DEEP" SILENT

Acoustic comfort in buildings as a designer's topic includes two directions of action: noise protection and privacy protection [7]. It is known that the comfort is realised by an adequate level of sound insulation of the partitions, walls and ceilings. Based of such fact, the minimal required values of sound reduction index for partitions in buildings are written in the legislation. The currently valid norm in Serbia determines that the acceptable level of acoustic comfort in dwellings requires 52 dB as a minimal value of sound reduction index between adjacent dwellings. However, various practical problems appeared in everyday practice have shown that such a minimal requirement is not sufficient to ensure an acceptable state of acoustic comfort in all circumstances. Unfortunately, when one discover such problem in a building, its solving is very complex, at least not in an elegant way. And sometimes it's impossible. It is therefore necessary to understand the reasons for such phenomena and to take measures to prevent appearance of such problems in the future.

In the literature it was established a parameter for expressing the privacy quality in buildings. It is called the "Speech Privacy Class" - SPC [15,16], and represents a measure of the

level of privacy between the two adjacent rooms. Its value, by definition, is the sum of the sound insulation between the rooms D and the level of ambient noise in the receiving room:

$$SPC = D + L_b \text{ (dB)}$$

where D is sound insulation between adjacent rooms defined as mean value of sound insulation measured in 1/3 octave bands in frequency range relevant for speech, from 160 Hz to 5 kHz, and  $L_b$  is noise level defined as mean value of levels measured in 1/3 octave bands in the same frequency range. It has been experimentally shown that with sufficient accuracy the SPC can be obtained from the usual data measured in buildings [17]:

$$SPC = R_w + L_{Aeq} \text{ (dB)}$$

where  $R_w$  is measured value of rated sound reduction index measured according to standards and  $L_{Aeq}$  is value of equivalent noise level measured according to relevant standard.

Such an approach to the quantification of acoustic comfort shows the important fact that the feeling the comfort, more precisely the privacy of the speech in the room, does not depend only on the sound insulation quality, but also on the masking effect of the ambient noise present in a room. Those two factors together summarize the condition of acoustic comfort in rooms, and not only the quality of the partitions separating them. It has been shown in the literature that conditions that can be classified as "standard privacy protection" require SPC value about 80 dB, and for a high level of privacy, a value of as much as 90 dB is required [15].

When analyzing the criteria from the existing norm in Serbia [6], one can see that the maximum allowed ambient noise level, better to say expected silence in the bedrooms, is set at 30 dBA. With the required sound insulation index of the partitions between adjacent dwellings set at 52 dB, one can roughly estimate that the standard prescribes an SPC of about 80 dB. Therefore, the existing norm in Serbia implicitly stated request the speech privacy in dwelling that can be labeled as "standard", but not as "high".

In the past period of time various innovations have occurred in the concept of housing construction, due to which the conditions influencing the value of SPC have also changed. More recent experiences with various residential buildings in Belgrade have shown that in luxury apartments ambient noise during night has a level far below 30 dBA assumed in local legislation. That is contributed by a number of factors, such as high-quality façade windows (often with triple glazing if the facade of the building is intensively exposed to the sun), the quieter housework constantly working appliances such as refrigerators and the like, almost all demanded by the energy efficiency and energy saving concept. Some measurements performed in Belgrade have shown that today in the number of apartments' bedrooms the noise level at night is not about 30 dBA, but nearly about 20 dBA. Curiosity is an apartment in the residential area of Belgrade where was found the room noise level of only 17 dBA, measured at 10 o'clock in the evening. With the sound insulation of the order of magnitude about 50 dB, as required by local legislation, the SPC value is only about 70 dB. This is characterized in the literature as "minimal speech privacy", and stated that with such SPC value "...speech sounds will frequently be audible".

Therefore, lowering the level of ambient noise in dwellings, which is an ideal for many people, has to some extent unexpectedly caused the opposite effect, that is, the possibility of hearing the noise from neighbors. Even worst, to hear their conversation. Surprisingly, such a problem is induced by some improvements in other aspects of building construction, for example in the energy efficiency requirements, as well as the progress in home appliance technology. The social consequence of such appearance is that in some circumstances tension appears between the builder, who has proof that the quality of the building is satisfactory, and the tenants who say that the acoustic comfort is below their expectation. From all that one can conclude that in buildings where higher expectations of comfort was set due to corresponding price of apartments, the existing legislation for sound insulation does not provide adequate dwellings' acoustical quality. That further triggers the need to revise the principles of building construction from the point of view of acoustics.

## 5. CONCLUSION

All aspects of acoustic comfort presented in this paper have a goal to point out several important aspects in the design and construction of buildings.

1. It is necessary to make revision of minimal requirements in sound insulation that residential buildings should satisfy today. The main topic have to be minimal requirements for the sound insulation index of the partitions between the two adjacent dwellings, which is now defined at 52 dB.
2. It is necessary to review the current building design and construction practice not only in the selection of partition structures, but also in the search for completely new construction possibilities, such as:
  - introduction of dilatations in building construction as more as possible;
  - introduction of elastic connections between the partitions wherever possible;
  - exploring the possibility of applying double massive walls, but with the simultaneous development of their optimal configurations and practical details for their realisation in building;
  - application of drywalls and additional plasterboards linings at massive walls, wherever that does not make vulnerable functionality of the rooms.
3. It is necessary to organize big action for education of the building designers and the builders, i.e. architects and civil engineers, about all acoustical aspects of building construction and about actual standards in acoustic comfort domain.
4. It is necessary to innovate the legislation concerned with the acoustic comfort in buildings.

## REFERENCES

- [1] P.Brüel, „Sound insulation and room acoustics“, Chapman and Hall, London, 1951.
- [2] L.Beranek, Noise reduction, McGraw-Hill Bookm Company, New York, 1960.

- [3] H.Kurtović, „Osnovi tehničke akustike“, Naučna knjiga, Beograd, 1982.
- [4] „Pravilnik o minimalnim tehničkim uslovima za izgradnju stanova“, Službeni list SFRJ broj 45/67, 1967.
- [5] „Pravilnik o tehničkim merama i uslovima za zvučnu zaštitu zgrada“, Službeni list SFRJ broj 35/70, 1970.
- [6] SRPS U.J6.201 „Akustika u zgradarstvu – Tehnički uslovi za projektovanje i građenje zgrada“
- [7] JUS ISO 6242-3 „Visokogradnja. Izražavanje zahteva korisnika, Deo 3: Akustički zahtevi“, 1997.
- [8] SRPS EN 12354-1:2008 Akustika u građevinarstvu - Ocena zvučne zaštite zgrada na osnovu akustičkih performansi građevinskih elemenata - Deo 1: Zvučna izolacija između prostorija
- [9] SRPS EN 12354-2:2008 Akustika u građevinarstvu - Ocena zvučne zaštite zgrada na osnovu akustičkih performansi građevinskih elemenata - Deo 2: Izolacija od zvuka udara između prostorija
- [10] SRPS EN 12354-3:2008 Akustika u građevinarstvu - Ocena zvučne zaštite zgrada na osnovu akustičkih performansi građevinskih elemenata - Deo 3: Zvučna izolacija od spoljašnjeg zvuka
- [11] [www.ursa.rs/softver-akustika](http://www.ursa.rs/softver-akustika)
- [12] URSA AKUSTIKA, softver za proračun zvučne izolacije, Elektrotehnički fakultet, Beograd
- [13] <https://www.datakustik.com/en/products/bastian>
- [14] Dragana Šumarac Pavlović, Miloš Dinić, Vlada Bezbradica, Miloš Bjelić, „Analiza izolacionih moći dvostrukih pregrada - laboratorijska merenja“, ETRAN 2017, Zbornik radova, AK1.3.1-6, ISBN 978-86-7466-618-0
- [15] ASTM E2638 – 10, „Standard Test Method for Objective Measurement of the Speech Privacy Provided by a Closed Room“, 2017.
- [16] J.Bradley, B.Gover, „Speech Privacy Class for Rating the Speech Privacy of Meeting Rooms“, Canadian Acoustics, Vol. 36 No. 3 (2008) 22-23
- [17] M.Bjelić, T.Miljković, D.Šumarac Pavlović, M.Mijić, paper in preparation for publishing
- [18] Miloš Dinić, Dragana Šumarac Pavlović, Miloš Bjelić, Ivana Ristanović, „Dileme u proceni izolacionih osobina dvostrukih masivnih pregrada pomoću procedura iz standarda SRPS 12354-1“, ETRAN 2017, Zbornik radova, AK1.4.1-4, ISBN 978-86-7466-618-0



## ERASMUS+ PROJECT: STRENGTHENING EDUCATIONAL CAPACITIES BY BUILDING COMPETENCES AND COOPERATION IN THE FIELD OF NOISE AND VIBRATION ENGINEERING (SENVIBE)

Ivana Kovacic<sup>1</sup>, Neil Ferguson<sup>2</sup>, Hans Bodén<sup>3</sup>

<sup>1</sup> Project Coordinator, University of Novi Sad, Faculty of Technical Sciences, Serbia, [senvibe@uns.ac.rs](mailto:senvibe@uns.ac.rs)

<sup>2</sup> University of Southampton, Institute of Sound and Vibration Research ISVR, United Kingdom

<sup>3</sup> Kungliga Tekniska Högskolan KTH, Stockholm, Marcus Wallenberg Laboratory for Sound and Vibration Research, Sweden

**Abstract** - *SENVIBE* is the acronym of the project 'Strengthening educational capacities by building competences and cooperation in the field of Noise and Vibration Engineering', which has been approved for financing under the call Erasmus+ Capacity Building in Higher Education EAC/A05/2017, and will be coordinated by University of Novi Sad during the period 15 Nov 2018 – 14 Nov 2021. This paper provides the description of the motivation for the project, its wider and specific objectives, expected multifold impact and the project consortium formed to achieve them.

### 1. INTRODUCTION

The motivation behind the Erasmus+ SENVIBE project entitled 'Strengthening educational capacities by building competences and cooperation in the field of Noise and Vibration Engineering' [1] is the recognized and urgent need to improve national educational capacities and build cooperation and competences in dealing with engineering, environmental and occupational noise and vibration (No&Vib) issues in Serbia.

Sound is a common part of our everyday life. We take it for granted but there is a lot more to it from the scientific and educational side which largely influences our lives, occupations, living and working environment, health, etc. It can be enjoyable when listening to music or singing of birds, but at the same time, it can be disturbing, annoying and threatening. When it is unpleasant or unwanted, we typically call it noise. Vibration, which is so naturally linked to the sound as sound is often generated by a vibrating object, can have beneficial or detrimental effects. Some essential activities of a human body, such as breathing, speaking, hearing or heart beating, involve some kind of vibration. In engineering systems, vibration has been found to improve the efficiency of certain machining, welding, dentist's drills, etc. However, faulty design or poor manufacturing can cause imbalance and vibration, which result in rapid wear of machine parts, failure and excessive noise. The transmission of vibration to human bodies can result in discomfort and adverse health effects. Health hazards of Environmental and Occupational Noise and Vibration (No&Vib) have been clearly recognized and are subject to regulations and standards aimed at preventing damage to health and

minimizing annoyance. Environmental No&Vib are related to traffic, industry, construction or other outdoor activities, while Occupational No&Vib are associated with workplace hazards. Initially, No&Vib have been linked to engineering systems, but today we are fully aware of the Environmental and Occupational No&Vib which requires proper attention from the very beginning - during the process of education of future experts in the area. Serbian National Strategy for Occupational Health and Safety explicitly states the need for continuous theoretical and practical lifelong learning in these fields. This is a direct implication that these issues have not been properly addressed previously in the Serbian education system and that creating tailor-made curricula and expertise can bring the much needed innovation in this field of higher education. Chapter 27 on Environmental Protection in Serbia's EU accession negotiations [2] clearly identifies this problem as multispectral and emphasizes that 'no progress has been made in the field of noise. What is needed is strategic planning, strengthening capacities and more investments...'. This is exactly what the SENVIBE project addresses relying on the national priorities for Serbia defined by the Erasmus+ Key Action 2 Capacity Building in Higher Education: in Curriculum development, SENVIBE concerns Engineering and engineering trades; SENVIBE also covers the priority of University-enterprise cooperations, including support for students' practical placement.



Fig. 1 SENVIBE logo

Motivated by the state-of-the-art facts, needs and priorities identified, the SENVIBE project shall rely on the synergy between the partners who possess the know-how and experience in the area - the two renowned Higher Education Institutions (HEIs) from the EU: University of Southampton, Institute of Sound and Vibration Research ISVR and Kungliga Tekniska Högskolan KTH, Marcus Wallenberg Laboratory for Sound and Vibration Research, who will transfer the knowledge to boost the practices of four HEIs

from Serbia dealing with No&Vib: University of Novi Sad, University of Nis, University of Kragujevac and EDUCONS University from Sremska Kamenica. The two international partners already have a good cooperation portfolio and have good understanding of the topic and joint results. Further support is secured from non-academic partners: the local authority - Provincial Secretariat for Urban Planning and Environmental Protection of Autonomous Province of Vojvodina, stakeholders from industry (Vojvodinian Association of Employers) and the Institute for Occupational Safety and Health. Their complementarity will bring added value to the pool of No&Vib issues for students to experience during their practical placement or to analyse in their individual projects (theses), which is fundamentally different from the existing situation in which they mainly work on theoretical problems. On the other hand, these non-academic partners will have some of their No&Vib issues identified and resolved, sharing their experience and gaining new ones, establishing mutual cooperation for the first time. A promising associate partner is the Chamber of Commerce and Industry of Serbia, situated in Belgrade, with a well-developed network over the whole country, which will be beneficial for establishing intensive links and cooperation with industry and public enterprises. A refreshing associate partner is the Young Acousticians Network - a non-profit entity gathering young (mainly) European acousticians who deal with sound and vibration topics and who will undoubtedly support project dissemination and sustainability. The structure of the SENVIBE Consortium is shown in Fig. 2.

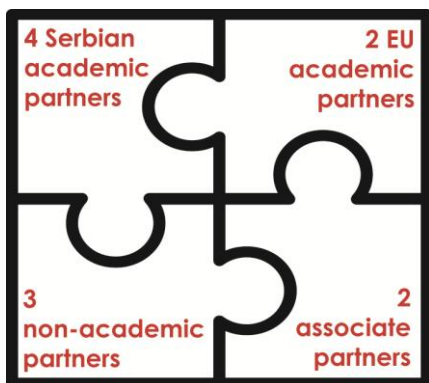


Fig. 2 SENVIBE Consortium

## 2. DESCRIPTION OF THE PROJECT

### 2.1 Aims and objectives

The wider aim of the SENVIBE project is to improve and build national educational capacities, cooperation and competences in dealing with environmental and occupational No&Vib engineering issues in accordance with ongoing EU integration strategies and the needs identified in Serbia.

There are four Specific Project Objectives (SPOs), Fig. 3:

SPO1. To modernise existing courses in the field of No&Vib as well as to develop and implement new courses tailor-made for students of undergraduate programmes of different engineering departments. Among the existing courses are those for the students of Environmental Engineering, Occupational Safety Engineering, Mechanical Engineering and Electrical

Engineering; the new course will be developed for the students of Civil Engineering and Traffic Engineering at the Serbian HEIs involved;

SPO2. To create and implement two types of Life-Long Learning (LLL) courses for practitioners in the fields of No&Vib Engineering, Environmental Protection and Occupational Safety;

SPO3. To develop and implement a new MSc programme in Vibro-Acoustic Engineering (VAE) at the University of Novi Sad;

SPO4. To establish a No&Vib Hub - a central unit launching and facilitating strategic cooperation among the key stakeholders engaged in No&Vib management: academia, local industry and local and national authorities.

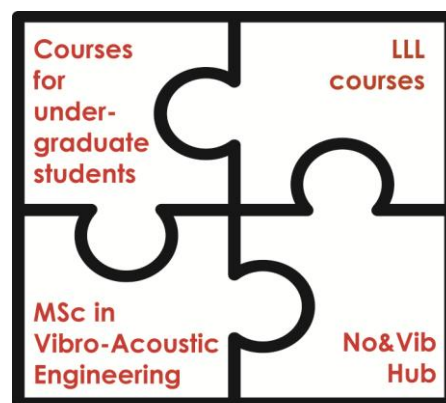


Fig. 3 SENVIBE Specific Objectives

Besides these aims, all the educational activities are also accompanied with the additional aim to introduce new teaching methodologies, including the use of e-tools and b-learning approaches, aiming either at facilitating more intensive interaction between teachers and students/trainees or enabling them to fit the activities planned into their everyday activities with a possibility for distance learning or repetitive insights into learning material, including experiments. The equipment will be either modernised when it exists, or new hardware will be installed if the HEI does not have it. It should be emphasised that the distribution of No&Vib equipment in Serbia is rather non-homogenous, so is the related budget required in this project. The purpose is to give all students/trainees the opportunity to do certain measurements and analyses by themselves in order to get a better feeling of different phenomena or control possibilities. The current teachers and university staff, including technicians, will be trained on the new courses, methodologies and equipment.

### 2.2 Expected impact

The target group for the project are students, professionals, academia, institutions, businesses, industries, non-profit entities, national and local authorities interested or involved into No&Vib issues, their control, monitoring and management. The courses for students of undergraduate programmes of different engineering departments will be primarily focused on students of Environmental, Occupational Safety, Mechanical, Electrical, Civil

Engineering and Traffic Engineering. The HEIs from Serbia engaged in this project include these departments - either all of them (University of Novi Sad) or some of them (all others), which is a good starting point for promotion and initiation of modernisation, upgrade or the implementation of new courses on No&Vib. These students will certainly provide the starting, straightforwardly accessible pool and will be easily motivated to continue their studies onto a higher level at the new VAE MSc programme

Furthermore, the LLL courses will be promoted at the institutions and among all non-academic partners and through their own their well-developed networks/unions at the national level and will also be directly related to the No&Vib Hub. Thus, the interested candidates will be promptly informed about the LLL courses provided. Within them, there might also be candidates who would like to apply for the new VAE MSc programme as well. These are professionals who would recognise an opportunity to gain higher/enhanced level of education and improve their competence and position in the market and in society.

The establishment of the No&Vib Hub will have multifold impact both during the duration of the SENVIBE project and afterwards. This Hub is of paramount importance for strategic networking and collaboration between the key stakeholders in the No&Vib fields. The key stakeholders are directly involved as partners in this projects, but others will be reached extending this network directly by each partner. Note that three consortium members represent the Association, the Chamber and the Network, and, thus, already include multiple target groups and databases, which can be reached easily via internal communication mechanisms covering both the whole country and the international communities as they have the well-developed channels at this level as well.

The Hub's mission includes developing effective mechanisms of cooperation through Student Internship Programme, Industrial scholarship/fellowship program, realisation of joint projects (including providing practical subjects for MSc theses), co-financed activities, monitoring of reform policies, development and implementation of professional training, seminars and workshops for companies and the unemployed, promotions, prompt and wide dissemination activities and exchange of info/knowledge on the related legislation, monitoring results, new issues, etc.

### **2.3 Activities and methodology**

The SENVIBE project consists of nine Work Packages (WPs), all of which comprise a specific set of deliverables, indicators and their measures.

The preparation activities in WP1 include the survey and comparative analysis of relevant courses in the EU and in Serbia - matching and benchmarking. Learning outcomes, contents, teaching methodologies and resources available and needed are of interest for three separate analyses: courses for undergraduate students of different engineering departments (developed and implemented in WP3), LLL courses (developed and implemented in WP4) and VAE MSc programmes (one of them will be developed, accredited and implemented in WP5). In addition, WP1 comprises matching the EU trends with the needs in Serbia with respect to the No&Vib Hub (established in WP6), compiling the list of

stakeholders, analysing mutual and individual contributions to the project goals and establishing a modus operandi. An important deliverable, which is also a major milestone, is the report resulting in the needs analysis and gaps compiled through comparative research.

The planned preparation activities in WP2 are concerned with resources, facilities and equipment. They first include setting requirements and designing the ICT platform and its tools. The platform will be crucial for WP3-WP5 for learning purposes and it will enable the application of e-learning and b-learning methodologies. Thus, its functionality is also a milestone. Besides this, the Hub's activities, services and programmes from WP6 will also be linked to the ICT platform via a certain moodle. WP2 also contains procurement, installation and activation of the equipment, which will be used for experiments and lab exercises. Training of Serbian teachers and technicians on the new courses, methodologies and equipment is also included.

WP3 is concerned with the development and implementation of six No&Vib courses for students of undergraduate programmes of six different engineering departments. Four of them already exist (for students of Environmental Engineering, Occupational Safety Engineering, Mechanical and Electrical Engineering), but they need to be modernised and enhanced in accordance with the findings of WP1 and using the resources, facilities and equipment from WP2. Two new courses for students of undergraduate programmes of Civil and Traffic Engineering will be developed, as they do not exist.

WP4 concerns the development and implementation of LLL courses. An earlier analysis has shown that they are needed for practitioners from SMEs and large enterprises (e.g. Mechanical, Civil, Environmental, Traffic engineers/technicians who are faced with No&Vib issues, but have not received formal/adequate education about it), and for local authorities, whose legal obligations include continuous noise monitoring (but progress in this respect has been rather poor). Two types of LLL courses are planned in accordance with the conclusions from WP1 and will be accompanied with the relevant learning material. A SENVIBE Glossary (hardcopy and e-version) will be published - a specific vocational register aimed at trainees at other stakeholders in the field.

The activities planned for WP5 are related to the development of the new MSc curriculum in Vibro-Acoustic Engineering in correlation with WP1 and WP2. This curriculum will include compulsory courses and elective courses. The development of e-learning and b-learning materials is planned. This is then followed by the accreditation process, enrolment of the MSc students and the implementation of the MSc VAE studies. Student Internship, which is also a compulsory part of master programmes in Serbia, will be organised and realised through the No&Vib Hub (WP6) with the help of stakeholders from industry and authorities. It is also expected that these stakeholders engaged in the No&Vib Hub provide a list of recommended MSc theses so that students work on the relevant, practical and contemporary subjects or issues.

WP6 comprises the activities related to the establishment of the No&Vib Hub. Based on the findings of WP1, a

framework for cooperation between the stakeholders will be defined. The specification of activities aimed at students and at the wider society will be made. The space foreseen for the No&Vib Hub, division of roles and responsibilities will be defined, and the No&Vib Hub will be established. Note that its activities are related both to the students, as mentioned above, but it will also provide a good pool for recruiting trainees for the LLL course and for the dissemination related to the project, courses, the MSc programme and No&Vib issues.

WP7 regards Quality Control, Assurance and Monitoring. It comprises the development of quality control mechanisms and conducting internal and external reviews of the project processes and outcomes. In addition, students', trainees' and stakeholders' evaluation of the realised activities will be performed and analysed.

WP8 is concerned with the dissemination and exploitation activities that will raise general awareness and use of the project results. It includes the preparation of the Project Dissemination Strategy with the Key Performance Indicators for the assessment of the achievement with respect to those originally projected. The SENVIBE website will be developed and continuously maintained. Promotional material (hardcopies and e-versions) will be prepared and different media, enrolment and promo campaigns carried out. The Exploitation Plan will be prepared and activities related to institutional sustainability conducted.

WP9 concerns project management, which includes establishing project internal management structures (Steering Committee, Project Management Team), organizing project coordination meetings (Kick-off meeting, other meetings, urgent consultations), developing management and reporting procedures and the internal communication plan as well as daily project management.

### 3. CONCLUSIONS AND FUTURE PROSPECTS

The SENVIBE project will address the need for strengthening educational capacities by building competences and cooperation in Serbia in the No&Vib fields. These capacities will be strengthened in several ways. First, through the modernisation of the existing courses or development of new ones in No&Vib for students of different engineering departments. Then also through innovative LLL courses and a new MSc programme in Vibro-Acoustics, which exists in the EU, but does not exist in Serbia. All the courses will be enriched with virtual and real experiments. In addition, e-methodologies and b-learning methodologies will be implemented. For these purposes, a special ICT platform will be created. A new No&Vib Hub will be established. The Hub's activities, services and programmes will also be linked to the ICT platform via a certain moodle with plugins for extending the features of its functionality. The cooperation in the Hub will continue to grow and attract more stakeholders and decision makers within the No&Vib fields, aspiring to initiate a better cooperation between HEIs and other sectors for the sake of improving the current situation criticised in Chapter 27 [2] as well as for wider societal benefits.

**ACKNOWLEDGEMENT:** This SENVIBE (598241-EPP-1-2018-1-RS-EPPKA2-CBHE-JP) project has been funded with the support from the European Commission. This publication (communication) reflects the views only of the authors, and the Commission cannot be held responsible for any use which may be made of the information contained therein.

### REFERENCES

- [1] [www.senvibe.uns.ac.rs](http://www.senvibe.uns.ac.rs)
- [2] <http://www.eu-pregovori.rs/eng/negotiating-chapters/chapter-27-environment/>

University of Nis  
Faculty of Occupational Safety

„Politehnica“ University of Timisoara  
Faculty of Mechanical Engineering



26<sup>th</sup> International Conference

**NOISE AND VIBRATION**

Niš, 6 - 7. 12. 2018.

# 2<sup>nd</sup> SESSION

# NOISE





## APPLICATION OF GENETIC ALGORITHM IN DEVELOPING OF TRAFFIC NOISE PREDICTION MODEL

Jelena Tomić<sup>1</sup>, Nebojša Bogojević<sup>1</sup>, Branko Radičević<sup>1</sup>, Zlatan Šoškić<sup>1</sup>

<sup>1</sup>Faculty of Mechanical and Civil Engineering in Kraljevo, University of Kragujevac, Serbia

**Abstract** - *In order to control noise levels it is necessary to have a suitable calculation method for traffic noise prediction. Since 1950s many mathematical models for estimation of traffic noise pollution have been developed, and most of available models found in literature are based on regression analysis. This paper presents the application of genetic algorithm in development of simple mathematical model for prediction of equivalent A-weighted level of road traffic noise in urban areas of the city of Kraljevo. Predictions of developed mathematical model are compared to experimental data collected by traffic noise measuring, as well as to predictions of commonly used traffic noise models, and obtained results of statistical analysis of differences between measured and calculated noise levels are shown in this paper.*

### 1. INTRODUCTION

Although technological and industrial development contributes to the progress of civilization, the development of industrial and transport capacities causes not only air, soil and water pollution, but also increase in levels of communal noise. The results of strategic noise mapping in the European Union (EU) clearly indicate that road traffic represents dominant source of noise pollution in urban environments. According to noise maps of the EU agglomerations and major roads, close to 68 million EU citizens are exposed to daytime road traffic noise levels above the excess exposure threshold, fixed by the EU at 55 dB(A) [1]. In the past decades many studies [2-4] have shown that long term noise exposure causes stress, sleep disturbance, cardiovascular problems, and therefore significantly affects human psycho-physical health and productivity of the population.

In order to manage and reduce the impact of noise pollution on human health and environment, it is necessary to have a suitable calculation method for prediction of road traffic noise levels. The calculation method represents an important tool for the process of noise mapping and noise action planning, and therefore can be of fundamental importance in the process of urban planning and designing, as well as for the traffic noise reduction through the process of traffic management. Although software packages for noise prediction are numerous, their price is high and their usage is highly complex. This is the reason why numerous mathematical models for traffic noise prediction have been developed by establishing a functional relationship between experimentally measured noise levels and selected road traffic

parameters. Since early 1950s many researchers have offered a large number of mathematical models for traffic noise prediction and most of the available models are developed using linear regression analysis. Also, several publications use soft computing methods such as artificial neural networks (ANN) [5-7] or genetic algorithms [8-9] for developing or predicting traffic noise levels. The critical review of some of the most used models are given in [10], and one of the conclusions given in paper is that each model is strongly influenced by certain characteristics of the traffic flow and environment, such as pavement type, driving skills, road and vehicles maintenance, etc.

This paper presents a novel mathematical model for prediction of traffic noise levels in the territory of the city of Kraljevo. The model is developed based on experimental results of noise level measuring carried out in the city of Kraljevo and therefore reflects the specificities of the traffic flow in the areas near the city major roads. A functional relationship between A-weighted noise level and the traffic flow parameters is obtained using genetic algorithm. For the purpose of the model validation, traffic noise prediction levels obtained by developed model are compared to measurement results, as well as to predictions of several commonly used traffic noise models.

### 2. MODEL BACKGROUND

The most of the available mathematical models for estimation of road traffic noise levels enable prediction of the equivalent A-weighted continuous noise level,  $Leq$  [dBA], which is recommended as a suitable descriptor for the use in motor vehicle noise assessment by many national and international regulatory agencies [11]. Almost all mathematical models available in literature are developed based on experimental results of noise level monitoring by performing the regression analysis in approximation of functional relationship between the equivalent noise level and traffic flow and road parameters.

Some of the most used mathematical models for road traffic noise prediction are those proposed by Burgess [12], Griffith [13] and Fagotti [14]. Based on experimental data collected in the territory of Sidney, Australia, Burgess determined functional relationship between the equivalent noise level  $Leq$  and road traffic parameters:

$$Leq = 55.5 + 10.2 \log(Q) + 0.3p - 19.3 \log(d)$$

In the given equation  $Q$  represents the total number of vehicles per hour,  $p$  percentage of heavy vehicles, while the distance between the observation point and center of the traffic lane is denoted with  $d$ .

According to Griffiths and Langdon, equivalent noise level and percentile levels ( $L_{10}$ ,  $L_{50}$  and  $L_{90}$ ) at distance  $d$  from the center of the traffic lane can be calculated according to the following equations:

$$\begin{aligned} Leq &= L_{50} + 0.018 \cdot (L_{10} - L_{90})^2, \\ L_{10} &= 61 + 8.4 \log(Q) + 0.15p - 11.5 \log(d), \\ L_{50} &= 44.8 + 10.8 \log(Q) + 0.12p - 9.6 \log(d), \\ L_{90} &= 39.1 + 10.5 \log(Q) + 0.06p - 9.3 \log(d). \end{aligned}$$

Fagotti et al. proposed simple mathematical model for estimation of the equivalent noise level based on the number of light motor vehicles  $N_c$ , motorcycles  $N_m$ , heavy vehicles  $N_{hv}$  and buses  $N_b$  per hour:

$$Leq = 33.5 + 10 \log(N_c + N_m + 8N_{hv} + 88N_b).$$

Since the mathematical models for traffic noise prediction have been developed from experimental results of noise level measuring by performing the statistical analysis, each model is strongly influenced by the composition and characteristics of road traffic flow, as well as certain characteristics of the measurement locations. This is the reason why the application of the available models is often limited to the environment where the noise levels monitoring was conducted. Therefore, a simple mathematical model is developed for the purpose of road traffic noise prediction in the urban area of the city of Kraljevo. As the equivalent noise level represents a logarithmic function of the total number of motor vehicles, it was modeled by the following equation

$$Leq = L_0 + 10 \cdot \log(N_{lv} + a_{hv} \cdot N_{hv}) - 10 \log(d / d_0)$$

where  $L_0$  is the average A-weighted noise level of a light motor vehicle at distance  $d_0$  from the centre of road lane, while the coefficient  $a_{hv}$  represents the equivalent number of light motor vehicles that generate approximately the same noise level as one heavy vehicle. Referent distance  $d_0$  was adopted to be 7.5 m, while the distance between the measurement point and the road center lane is denoted by  $d$ . The third member in the sum accounts for sound spreading.

In order to develop a novel model for prediction of noise levels in the areas near the major roads of the city of Kraljevo, after measuring of A-weighted equivalent noise levels and collecting of traffic flow data in the urban areas of Kraljevo, traffic noise model parameters  $L_0$  and  $a_{hv}$  were estimated by the experimental data fitting using genetic algorithm.

### 3. MEASUREMENTS

For the purpose of noise level monitoring and development of traffic noise prediction model, measurements of A-weighted equivalent noise levels were performed with Brüel&Kjær 2250 sound level meter on 28 measurement locations near the major roads of the city of Kraljevo. All measurements were carried out in dry weather conditions, without snow coverage,

and with wind speeds lower than 5 m/s. Measurement positions were distant from the intersections and traffic-control lights, so it was assumed that all vehicles moved at a steady speed of 50 km/h, which is the speed limit for the territory of Kraljevo. The measuring points were far away from the airports, railway traffic, construction sites and industrial plants, so the road traffic can be considered as the only source of noise. A total of 690 measurements during the 15-minute time periods were carried out at 28 measurement locations. During each of the measurements, the numbers of light motor vehicles  $N_{lv}$  and heavy motor vehicles  $N_{hv}$  were collected.

### 4. GENETIC ALGORITHM

Genetic algorithm (GA) represents a powerful metaheuristic and evolutionary algorithm which is inspired by the process of biological evolution [15, 16]. Since it is capable of finding a global optimum in a space with multiple local extrema, genetic algorithm is often used in the optimization problems solving.

Genetic algorithm begins by creating a random population of the individuals. Each individual represents a candidate solution of the optimization problem. The quality of each member of the population is estimated using the fitness function. In every iteration of the algorithm, by simulating the processes of natural selection, mutation and crossover (reproduction), new generation of individuals is formed. By applying mechanism of selection, higher quality individuals survive and create new offspring. During the process of crossover new individuals are created by recombination of genetic materials between the pairs of survived individuals. The process of mutation causes a random change in the gene values. Since it introduces a new genetic material into the population, mutation represents the basic mechanism for prevention of premature convergence of the genetic algorithm. The searching process repeats until the maximum number of iterations is reached or error tolerance is met. The highest quality individual of the last generation represents an approximate solution of the given problem.

The simple functional dependence between traffic noise level and traffic flow parameters was optimized using genetic algorithm with rank based selection. According to this method of selection, after sorting the individuals based on their fitness values, the probability of an individual selection is determined according to on its rank (i.e. the position in the sorted array). If  $S$  represents the size of the population, the probability of selecting a individual with a rank  $i$  can be calculated with the following equation:

$$P_i = \frac{i}{\sum_{j=1}^S j}.$$

After selecting two different parental individuals, one child is formed by applying BLX- $\alpha$  crossover [17] of the parental genes. After offspring creation, a non-uniform gene mutation [18] (with a low mutation probability  $p_m=0.05$ ) is applied. The values of GA parameters used in the optimization process are given in the Table 1. The traffic noise model parameters ( $L_0$  and  $a_{hv}$ ) were estimated using 494 experimental data sets collected at 20 measurement locations, and the result of the algorithm is a set of parameters that

minimize the mean square difference between the measured and calculated noise levels. The results of the optimization are given in Table 2.

**Table 1** GA parameters

Number of individuals	40
Selection method	rank based selection
Crossover method	BLX- $\alpha$ ( $\alpha=0.5$ )
Method of mutation	non-uniform mutation
Mutation probability	0.05
Number of iterations	500

**Table 2** Optimized parameters

$L_0$	$a_{hv}$
42.6	13

#### 4. RESULTS

Traffic noise prediction results of developed mathematical model are compared with experimental results of noise level monitoring and prediction results obtained applying Burgess, Griffith and Fagotti mathematical models for estimation of traffic noise levels. Statistical analysis of differences between measured and calculated noise levels was carried out for all 690 measurement data sets. The mean values of the absolute

differences between measured and calculated noise levels ( $\Delta L$ ), standard deviations of the differences ( $\sigma$ ) and correlation coefficient ( $r$ ) were calculated and shown in the Table 3. The obtained results of statistical analyses are separately presented for 494 measurement data sets used in the optimization process (index “optim”) and 196 testing data sets collected at 8 remaining measurement locations which were not used in the process of optimization (index “test”). Furthermore, for each of the applied models, the total number of predictions  $m$  with error larger than 3 dB and the largest value of prediction errors ( $\Delta L_{\max}$ ) are given in the Table 4. Figure 1 shows a comparative chart of measured and calculated noise levels. The results are shown for randomly selected 50 of 196 measurements used for model testing.

The results of the statistical analysis clearly show that the application of novel mathematical model for prediction of road traffic noise levels presented in this paper leads to more accurate estimation of noise pollution in the urban areas of the city of Kraljevo. It is important to notice that the number of predictions with an error larger than 3 dB is significantly reduced. The reason for superior performance of presented model is that it is developed on the basis of experimental results of noise monitoring in the city of Kraljevo, and, therefore, it is tuned to the characteristics of the road traffic in this city.

**Table 3** Comparison of different models for traffic noise prediction

Model	$\Delta L$	$\Delta L_{\text{optim}}$	$\Delta L_{\text{test}}$	$\sigma$	$\sigma_{\text{optim}}$	$\sigma_{\text{test}}$	$r$	$r_{\text{optim}}$	$r_{\text{test}}$
Novel model	1.32	1.26	1.47	0.88	0.86	0.93	0.89	0.9	0.87
Burgess	1.66	1.56	1.90	1.31	1.22	1.50	0.86	0.87	0.84
Griffith	4.38	4.39	4.35	1.67	1.67	1.68	0.87	0.88	0.86
Fagotti	3.75	3.74	3.76	1.62	1.61	1.67	0.88	0.89	0.86

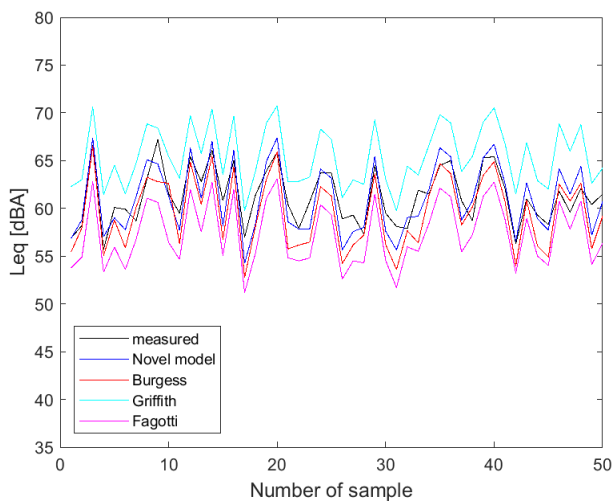


**Fig. 1** Comparative chart of noise levels

**Table 4** Prediction error statistic

Model	$m$	$m_{\text{optim}}$	$m_{\text{test}}$	$\Delta L_{\max}$	$\Delta L_{\max}^{\text{optim}}$	$\Delta L_{\max}^{\text{test}}$
Novel model	36	19	17	4.01	3.65	4.01
Burgess	12 6	77	49	6.19	5.37	6.19
Griffith	52 8	377	151	7.75	7.75	7.61
Fagotti	43 1	310	121	7.23	7.20	7.23

#### 5. CONCLUSIONS

Noise levels predicted by extensively used mathematical models for traffic noise prediction deviate significantly from the experimental results of noise level monitoring in the territory of the city of Kraljevo, which indicates the need for development of a new model for equivalent noise level prediction. In order to develop more precise model, a total of 690 noise level measurements were performed during the 15-minute time periods at 28 measurement locations near the city

major roads. Functional relationship between equivalent A-weighted noise level and traffic flow parameters was established using genetic algorithm.

The validation of developed mathematical model was performed by statistical analysis of the deviations between predicted and measured noise levels, as well as the correlation analysis of these levels. Results of statistical and correlation analysis show good agreement between measured and calculated values. A comparative analysis of the results obtained by proposed models and some of frequently used models for road traffic noise prediction has shown that the application of proposed models enables not only more precise prediction of traffic noise levels, but also significantly lower number of predictions with error larger than 3 dB.

## ACKNOWLEDGEMENT

The authors wish to express their gratitude to Serbian Ministry of Education and Science for support through project TR37020.

## REFERENCES

- [1] De Vos, P.; Licitra, G. "Noise maps in the European Union: An overview". In Licitra, G. (Ed.), *Noise mapping in EU: Models and Procedures*, pp. 285–310, USA: CRC Press, 2013.
- [2] Ohrstrom, E.; Rylander, R. "Sleep disturbance by road traffic noise - A laboratory study on number of noise events". *Journal of Sound and Vibration*, vol. 143, no. 1, pp. 93–101, 1990.
- [3] Fyhri, A.; Klboe, R. "Road traffic noise, sensitivity, annoyance and self-reported health - A structural equation model exercise". *Environment International*, vol. 35, no. 1, pp. 91-97, 2009.
- [4] Pirreera, S.; Valck, E. D.; Cluydts, R. "Nocturnal road traffic noise: A review on its assessment and consequences on sleep and health". *Environment International*, vol. 36, no. 5, pp. 492–498, 2010.
- [5] Cammarata, G.; Cavalieri, S.; Fichera, A. "A neural network architecture for noise prediction". *Neural Networks*, vol. 8, no. 6, pp. 963-973, 1995.
- [6] Genaro, N.; Torija, A.; Ramos-Ridao, A.; Requena, I.; Ruiz, DP.; Zamorano, M. "A neural network based model for urban noise prediction". *The Journal of the Acoustical Society of America*, vol. 128, pp. 1738-1746, 2010.
- [7] Givargis, S.; Karimi, H. "A basic neural traffic noise prediction model for Tehran's roads". *Journal of Environmental Management*, vol. 91, pp. 2529-2534, 2010.
- [8] Gundogdu, O.; Gokdag, M.; Yuksel, F. "A traffic noise prediction method based on vehicle composition using genetic algorithms". *Applied Acoustics*, vol. 66, no. 7, pp. 799-809, 2005.
- [9] Rahmani, S.; Mousavi, S.; Kamali, M. J. "Modeling of road-traffic noise with the use of genetic algorithm". *Applied Soft Computing*, vol. 11, no. 1, pp. 1008-1013, 2011.
- [10] Quartieri J.; Mastorakis N. E.; Iannone G.; Guarnaccia C.; D'Ambrosio S.; Troisi A.; Lenza T.L.L. "A Review of Traffic Noise Predictive Models", *Proc. of the 5th WSEAS Int. Conf. on "Applied and Theoretical Mechanics" (MECHANICS'09)*, Puerto De La Cruz, Canary Islands, Spain, December 14-16, 2009. ISBN: 978-960-474-140-3 / ISSN: 1790-2769, pp. 72-80.
- [11] C. G. Balachandran. "Urban Traffic Noise in Environmental Impact Assessments". In: *Proceedings of 14<sup>th</sup> International Congress on Acoustic*, paper E1-4, Beijing, China, 1992.
- [12] Burgess, M. A. "Noise prediction for Urban Traffic Conditions - Related to Measurement in Sydney Metropolitan Area". *Applied Acoustics*, vol. 10, pp. 1-7, 1977.
- [13] Griffiths, I. D.; Langdon, F. J. "Subjective Response to road traffic noise". *Journal of Sound and Vibration*, vol. 8, pp. 16-32, 1968.
- [14] Fagotti, C.; Poggi, A. "Traffic Noise Abatement Strategies. The Analysis of Real Case Not Really Effective", in *Proc. of 18th International Congress for Noise Abatement*, pp. 223-233, Bologna, Italy, 1995.
- [15] David Beasley, David R Bull, and Ralph Robert Martin. *An overview of genetic algorithms: Part 1, fundamentals*. *University computing*, 15(2):56-69, 1993
- [16] David Beasley, David R Bull, and Ralph Robert Martin. *An overview of genetic algorithms: Part 2, research topics*. *University computing*, 15(4):170-181, 1993.
- [17] M Čangalović. *Opšte heuristike za rešavanje problema kombinatorne optimizacije*. *Kombinatorna optimizacija: Matematička teorija i algoritmi*, pages 320-350, 1996
- [18] AE Eiben. *Genetic algorithms + data structures = evolution programs: Z. Michalewicz*. Springer, Berlin, 1996, (appeared in 1992), 387 pp.(hardcover), 68 figures, 36 tables, 1997.



## SOUND ABSORPTION OF RECYCLED PLASTIC MATERIAL

Branko Radičević<sup>1\*</sup>, Milan Kolarević<sup>1</sup>, Nicolae Herisanu<sup>2</sup>, Mišo Bjelić<sup>1</sup>, Tanja Miodragović<sup>1</sup>

<sup>1</sup>University of Kragujevac, Faculty of Mechanical and Civil Engineering, Kraljevo, Serbia, radicevic.b@mfkv.rs

<sup>2</sup>„Politehnica“ University of Timisoara, Faculty of Mechanical Engineering, Timisoara, Romania

**Abstract** - In this paper an empirical model to predict the acoustic properties of materials, recycled plastics and polyurethane resins as a binder is developed. The parameters of model were determined on the basis of samples of thicknesses from 10 mm to 50 mm. Measurement of the sound absorption coefficient was performed in an impedance tube – Transfer function method (SRPS EN ISO 10534-2:2008). In order to form an empirical model, on the same samples was carried out measuring the resistance of the air flow according to the method SRPS ISO 9053:1994.

**Keywords:** recycled plastic, absorption coefficient, passive noise protection

### 1. INTRODUCTION

Research by various authors has shown that materials from the recycled plastic can be made with the desired acoustic properties.

Energy consumption in the construction sector can reach up to 40% of the total energy demand of an industrial country. Sustainable materials can play an important role, as less energy is usually needed for their production than is required for conventional materials. In the past few years, many new noise control materials have been studied and developed as alternatives to traditional (glass or stone wool); these materials are natural (cotton, cellulose, hemp, wool, clay, etc.) or made of recycled materials (rubber, plastics, carpets, cork etc.). [1]

In recent years, many new noise control materials have been studied and developed as alternatives to traditional (glass and stone wool); these are natural materials (cotton, cellulose, hemp, wool, clay, etc.) or recycled (rubber, plastic, carpet, cork, etc.) [2]

In the paper [3], the possibilities of attenuation of noise by means of absorption materials are shown, among which are plastic materials, which can be used for the production of sound barriers.

Murugan in his work [4] presents the ways of using recycled plastic waste for sound absorption.

Wood-plastic composites are a new group of materials that can be used because of their acoustical properties in the range of 25 Hz to 2000 Hz. A wide range of polymers such as polypropylene, polyethylene, polyvinyl chloride and so on are used in the production of wooden plastic composites. [5].

To address noise pollution, materials such as rock wool, glass wool and asbestos in the past used as sound absorbers for

decades. These materials are harmful to both producers and consumers and could endanger human health [6,7].

The effect of density on the dissipation of sound energy will require further study of the microstructure. Compared to conventional noise reduction materials, wood-plastic composites have excellent absorption characteristics at medium and low frequencies, and in addition require less space for installation. The results showed that the wood-plastic composites have a wide potential applications, particularly in view of their ability to further recycling. [8]

The sound absorption of various fibrous materials, including a series of plastic, was experimentally tested. The results show the relationship between sound absorption and air resistance. Higher airflow resistance always gives better sound absorption, but for air resistance greater than 1000, sound absorption has less value, because in that case there are difficulties in moving sound waves through the material. [9]

Polyester fibrous materials made from recycled plastic bottles (PET) have also been studied. [10]

In recent years, researchers such as [11-13] have been working on composites with a combination of plastic and rubber granular material. Embedding granular materials such as rubber crumb, increases the density of filling and the resistance of composite materials. [14]

Composite materials are increasingly used for sound insulation. Particularly are important composites that can be characterized as "green" that include different recycled materials such as, recycled rubber, recycled plastics, and waste materials from industrial processes. Zainulabidin [15] and others have studied the acoustic properties of two kinds of materials: rubber sponges and fibers of glass wool.

Soleimani [16] and others examined the acoustics mixture of wood fibers and recycled plastics. Samples are dried and cast in molds for a certain amount of time. The research show that the addition of nano-clays to the composite, the water absorption decreased and that the plastic has a negligible water absorption.

The acoustic properties of rubber were the subject of many studies [17-21] in order to examine the possibility of using rubber barriers and panels for noise reduction.

In works by Radičević, Ristanović, Kolarević [22-25], experimental research on the acoustic and non-acoustic properties of recycled rubber and recycled plastics material have been demonstrated, on the basis of which an empirical

model for the prediction of the acoustic properties of these materials have been formed.

The assumption is that the empirical models that exist for the recycled rubber can also be useful for recycled plastics, bearing in mind that it is also a granular material that is bound with a polyurethane resin.

## 2. MATERIAL

The basic raw materials used for the preparation of the samples is obtained by grinding a recycled plastic. Grain size in the granulate ranges from 1mm to 3mm. The average density of the samples for testing was 759.5 kg / m<sup>3</sup>. The percentage of the binding agent (polyurethane resin) was 10%.

Test samples were made from recycled plastics granules from insulation from automotive cables (granule dimensions 3 to 5mm) and polyurethane resin binding agent. Samples were 10mm, 20mm, 30mm, 40mm and 50mm thick and were cast in molds of 100mm diameter without pressing to ensure porosity of the samples (Figure 1.). Recycled plastics belongs to a group of PVC materials .



**Fig. 1** The appearance of the test sample



**Fig. 2** Structure of the sample from recycled plastic

When sound is spread in interconnected pores of a porous material, it loses its sound energy. This energy loss is due to the complex heterogeneous microstructure and the viscous

effects of the boundary layer, so that the sound energy is dissipated through friction with the pore walls. As with viscous effects, there are losses due to thermal conductivity from the air to the porous material, which are expressed in low frequencies [22].

Due to the accelerated global depletion of raw materials, especially oil, it is expected that waste plastic in the future will have the character of a valuable resource.

## 3. METHODS

The measurement of absorption was done in the impedance tube by using the transfer function method between two microphones, defined in the EN ISO 10534-2 [26]. This method is based on the decomposition of the standing wave which is formed in the tube by recording signals from two microphones and calculating their transfer function. The reflection coefficient is calculated from the transfer function, and then the absorption coefficient is calculated under conditions of normal incidence.

$$\alpha = 1 - |R|^2 \quad (1)$$

where  $R$  is the reflection coefficient calculated according to the expression:

$$R = \frac{H - e^{-jks}}{e^{jks} - H} e^{j2k(l+s)} \quad (2)$$

where:  $H$  – the corrected transfer function,  $s$  – the distance between the microphones,  $l$  – the distance between the closer microphone and the sample,  $k$  – the wave number.

In order to form an empirical model for determining the acoustic impedance and material coefficient, measurement of the resistance to air flow was also performed.

Air resistance is one of the main non-acoustic parameters that shows the behavior of porous materials used in sound absorption systems. The standard SRPS ISO 9053 specifies two methods for measuring airflow resistance: a steady state airflow method and an alternating airflow method. The paper presents the results of measurements using the method of constant air flow.

The vacuum pump ZAMBELLI, type ZB1, is used as the device for creation of airflow. The pump is of a membrane type and can realize the maximum free flow of 30 l/min. The underpressure produced by the pump is higher than 0.773 bar (580 mmHg). The pump has two airflow metres, which operates on the principle of the ball rotametre. Smaller airflows in the range of 0.2÷6 l/min are measured by means of the smaller rotametre, and higher flows in the range of 5÷30 l/min are measured by means of the bigger rotametre. The maximum flow measurement error is ± 2%. The pump allows the fine control of flow and the stability of flow in the part of the measuring cell which is behind the sample. By its characteristics, the pump provides a sufficiently small air velocity so that the measured airflow resistance could not depend on air velocity. The pump enables airflow velocity of  $0,4 \cdot 10^{-3}$  m/s in the measuring cell, which completely corresponds to the recommendations by the standard SRPS ISO 9053 ( $0,5 \cdot 10^{-3}$  m/s).

In the measuring cell, the atmospheric pressure is on one side of the sample, and the underpressure produced by the vacuum pump is on the other side of the sample. In order to provide the conditions for maintaining underpressure, the measuring cell must be well sealed on one side. The differential pressure gauge TESTO 512 is used for measuring the difference in pressures on both sides of the sample. This gauge has a measuring range of 0 to 200 Pa with the resolution of 0.1 Pa. The equipment used allows measurement of differential pressure up to the accuracy  $\pm 5\%$  of the specified value.



**Fig. 3** The appearance of a measuring system for determining the air flow resistance

The measuring cell has the form of a circular cylinder, and it is made of plexiglass so that placing of the sample could be visually monitored. The inner diameter of the measuring cell is 100 mm, which satisfies the requirement of the standard SRPS ISO 9053 that the inner diameter must be longer than 95 mm. [27]

#### 4 PROPOSAL FOR A NEW EMPIRICAL MODEL FOR DETERMINING THE ACOUSTIC PROPERTIES OF COMPOSITES OF GRANULAR MATERIALS

Theoretical models require five input parameters, which can not often be easily and reliably determined. This is the basic lack of the so-called phenomenological or micro models for determining the acoustic properties of porous materials. Therefore, in this paper, an experimental macro model for predicting acoustic properties of recycled rubber and plastic materials has been developed. The basic advantage of such models is that they have one input parameter - longitudinal resistance to air flow.

The propagation of sound in an isotropic homogeneous material can be represented by the characteristic impedance ( $Z_c$ ) and the sound propagation constant in the absorption material.

$$Z_c = R + jX \quad (3)$$

$$\gamma = \alpha + j\beta \quad (4)$$

Starting from the well-known Delany & Bazley relations:

$$R = \rho_0 c_0 \left[ 1 + C_1 \left( \frac{\rho_0 f}{r} \right)^{-C_2} \right] \quad (5)$$

$$X = -\rho_0 c_0 \left[ C_3 \left( \frac{\rho_0 f}{r} \right)^{-C_4} \right] \quad (6)$$

$$\alpha = \left( \frac{2\pi f}{c_0} \right) \left[ C_5 \left( \frac{\rho_0 f}{r} \right)^{-C_6} \right] \quad (7)$$

$$\beta = \left( \frac{2\pi f}{c_0} \right) \left[ 1 + C_7 \left( \frac{\rho_0 f}{r} \right)^{-C_8} \right] \quad (8)$$

where  $R$  and  $X$  are real and imaginary parts of characteristic acoustic impedances  $Z_c$ , and  $\alpha$  i  $\beta$  real and imaginary parts of propagation constant ( $\gamma$ ) of the sound in absorption material,  $\rho_0$  - air density,  $f$  - frequency and  $r$  - longitudinal resistance to air flow.

Starting from equations (9) to (13) and the recommendations of European norm EN 12354-6: 2003, the diffuse coefficient of sound absorption of porous materials can be calculated. For a diffuse acoustic field, the absorption coefficient  $\alpha_s$  can be determined as:

$$\alpha_s = \int_0^{\pi/2} \alpha_\varphi \sin 2\varphi d\varphi \quad (9)$$

$$\alpha_\varphi = 1 - |r_\varphi|^2 \quad (10)$$

$$r_\varphi = \frac{Z' \cos \varphi - 1}{Z' \cos \varphi + 1} \quad (11)$$

$$Z'_c = \frac{Z_c}{\rho_0 c_0} \quad (12)$$

$$Z' = Z'_c \coth \gamma d \quad (13)$$

where:

- $\varphi$  - angle of incidence, in radians,
- $\alpha_\varphi$  - the absorption coefficient for a plane sound wave, bound to the angle  $\varphi$ ,
- $r_\varphi$  - reflection coefficient for plane sound wave, bound to the angle  $\varphi$ ,
- $Z'$  - normalized surface impedance layer
- $Z'_c$  - normalized characteristic impedance of absorbent material,
- $d$  - layer thickness m.

An empirical macroscopic model for the determination of the acoustic properties of recycled plastic materials can not be found in the available scientific literature. A new model for the prediction of the acoustic properties of composites of recycled rubber and plastics was developed using the method of the smallest squares. By calculating the coefficients  $C_1, \dots, C_8$ , the deviation of the absorption coefficient is minimal in relation to the values obtained by measuring in the impedance tube.

**Table 1** Basic parameters of the new empirical model

Material	Recycled plastic
Longitudinal resistance to air flow, $r$ [Pas/m <sup>2</sup> ]	5045
Characteristic impedance, $Z_c$	$Z_c = \rho_0 c_0 \left[ (1 + 0.570 \cdot C^{1.221}) - i(1.74E-07 \cdot C^{1.649}) \right]$ (14)
Coefficient of expansion, $\gamma$	$\gamma = \frac{2\pi f}{c_0} \left[ (0.174 \cdot C^{0.843}) + i(1 + 0.680 \cdot C^{0.0594}) \right]$ (15)
Coefficient of absorption EN 12354-6:2003	$\alpha_s = \int_0^{\pi/2} \alpha_\varphi \sin 2\varphi d\varphi$ (16)
Medium absolute error, $\Delta\bar{\alpha}$	0.0384
Medium relative error, $\bar{\varepsilon}$ [%]	28.0

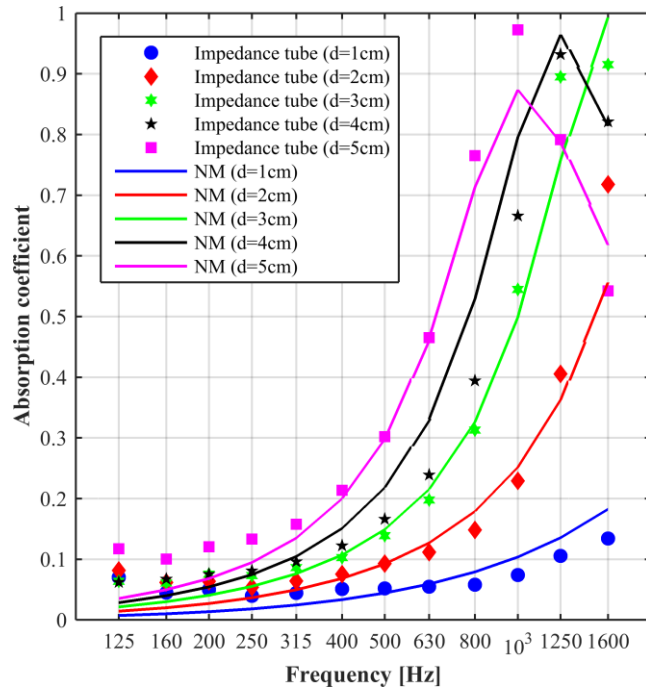


**Fig. 4** The absorption coefficient of the recycled plastic material according to the prediction of the new model in relation to the measured values in the impedance tube

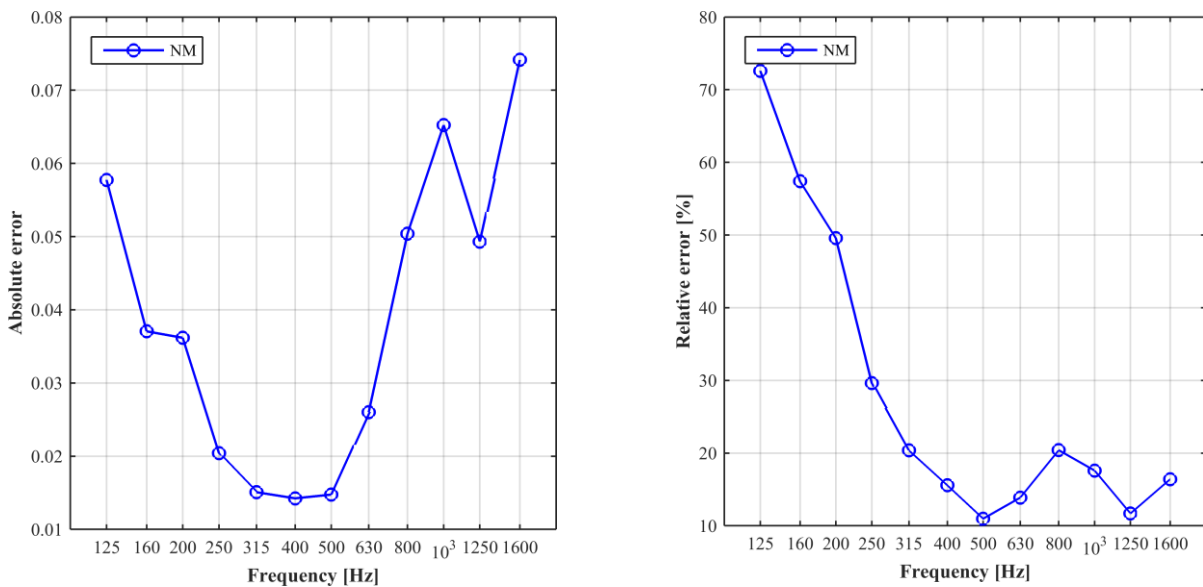


**Fig. 5** Absolute and relative error of model

The deviation of the absorption coefficient obtained using the new proposed model in relation to the impedance tube measurement is 3.84%, [28] which is very good compared to the most frequently used limit value of 10% from the available scientific literature.

## 5 CONCLUSION

The paper presents the methodology for the formation of the empirical macroscopic model for predicting the acoustic properties of composites from recycled plastic. As the input parameter in the model, the measured longitudinal resistance to air flow was used for five different sample thicknesses.

The new model has confirmed the good absorption properties of composites of recycled plastics. The average absolute error of the new model is 3.84% in relation to the measured values of the sound absorption coefficient in the impedance tube. On this basis, the new model can be considered as adequate for assessing acoustic properties of recycled plastics, where polyurethane resin is used as a binding agent.

With the increase in the number of materials to which a new model can be applied, it can also be expected to improve it in terms of prediction of acoustic properties of porous materials. Considering that the grain structure material has been analyzed, it is realistic to expect that this model can be applied to predict acoustic properties and other porous materials with a grain structure.

## ACKNOWLEDGEMENTS

The authors express their gratitude to the Ministry of Education, Science and Technological Development of the Republic of Serbia for the support to this research through the project TR37020.

The authors owe special gratitude to the Laboratory for Acoustics of the Faculty of Electrical Engineering in Belgrade, where measurements of the sound absorption coefficient in the impedance tube were performed.

## REFERENCES

- [1] F. Asdrubali, "Green and sustainable materials for noise control in Buildings", in *Proc. 19th International Congress on Acoustics - ICA2007MADRID*, Madrid, 2-7 September 2007.
- [2] F. Asdrubali, "Survey on the acoustical properties of new sustainable materials for noise control", In *Proc. of Euronoise (Vol. 30). Tampere: European Acoustics Association*, May 2006.
- [3] L.A. Al-rahman, I.R. Raja, and R.A. Rahman, "Attenuation of noise by using absorption materials and barriers: a review", *International Journal of Engineering and Technology*, vol. 2(7), pp. 1207-1217, 2012.
- [4] D. Murugan, S. Varughese, and T. Swaminathan, "Recycled polyolefin-based plastic wastes for soundabsorption", *Polymer-Plastics Technology and Engineering*, vol. 45(7), pp. 885-888, 2006.
- [5] Z. Daeipour, V. Safdari, and A. Nurbakhsh, "Evaluation of the Acoustic Properties of Wood-Plastic-Chalk Composites", *Engineering, Technology & Applied Science Research*, vol. 7(2), pp. 1540-1545, 2017.
- [6] J. Lee and G.W. Swenson, "Compact sound absorbers for low frequencies", *Noise Control Engineering Journal*, vol. 38(1), pp. 109-117, 1992.
- [7] S.V. Joshi, L.T. Drzal, A.K. Mohanty, and S. Arora, "Are natural fibercomposites environmentally superior to glass fiber reinforcedcomposites", *Composites Part A: Applied Science Manufacture*, vol. 35(1), pp. 371-376, 2004.
- [8] L.T. Chang and F.C. Chang, "Sound absorption properties of wood plastic composites made of recycled materials", in *Proc. 7th World Convention on Waste Recycling and Reuse*, pp. 35, Tokyo, 16-17 May 2018. DOI: 10.4172/2475-7675-C1-003.
- [9] H.S. Seddeq, "Factors influencing acoustic performance of sound absorptive materials". *Australian Journal of Basic and Applied Sciences*, vol. 3(4), pp. 4610-4617, 2009.
- [10] R. Dragonetti, C. Ianniello, and R. Romano: "The evaluation of intrinsic non-acoustic parameters polyester fibrous materials by an optimization procedure", in *Proc. of Euronoise 2006, Structured Session Sustainable Materials for Noise Control*, Tampere, Finland, 30 May – 1 June 2006.
- [11] R. Maderuelo-Sanz, J. M. Barrigon Morillas, M. Martin-Castizo, V. Gomez Escobar, and G. Rey Gozalo, "Acoustical performance of porous absorber made from recycled rubberand polyurethane resin", *Latin American Journal of Solids and Structures*, vol. 10(3), pp. 585–600, 2013.
- [12] R. Maderuelo-Sanz, A.V. Nadal-Gisbert, J.E. Crespo-Amoros, and F. Parres-Garcia, "A novel sound absorber with recycledfibers coming from end of life tires (ELTs)", *Applied Acoustics*, vol. 73(4), pp. 402–408, 2012.
- [13] J. Pfretzschner, "Rubber Crumb as Granular Absorptive AcousticMaterial", *Instituto de Acustica*, Madrid, Spain, 2002.
- [14] H. Mamtaz, M.H. Fouladi, M. Al-Atabi, and S. Narayana Namasivayam, "Acoustic absorption of natural fiber composites". *Journal of Engineering*, pp.1-11, 2016. DOI: 10.1155/2016/5836107.
- [15] M. H. Zainulabidin, M. H. Abdul Rani, N. Nezere, and A. L. Mohd Tobi, "Optimum Sound Absorption by Materials Fraction Combination," *Int. J. Mech. Mechatronics Eng.*, vol. 14(02), pp. 118 –121, 2014.
- [16] H. Soleimani, B. Kord, M. M. Pourpasha, and S. Pourabbasi, "The Relationship Between Plastic Virginity and Engineering Properties of Wood Plastic Composites," *World Appl. Sci. J.*, vol. 19(3), pp. 395–398, 2012.

- [17]J. Pfretzschner, "Rubber crumb as granular absorptive acoustic material," *Forum Acusticum*, Sevilla, Spain, pp. 1–6, 2002.
- [18]H. Zhu, and D. D. Carlson, "A Spray Based Crumb Rubber Technology in Highway Noise Reduction Application," *Journal of solid waste technology and management*, vol. 27(1), pp. 27-32, 2001.
- [19]M. Sobral, A.J.B. Samagaio, J.M.F. Ferreira, and J.A. Labrincha, "Mechanical and acoustical characteristics of bound rubber granulate," *J. Mater. Process. Technol.*, vol. 142(2), pp. 427–433, 2003.
- [20]J. Pfretzschner, and R.M. Rodriguez, "Acoustic properties of rubber crumbs," *Polym. Test.*, vol. 18(2), pp. 81–92, 1999.
- [21]G. Iannace, L. Maffei, and M. Masullo, "Proprietà acustiche di materiali granulari ottenuti dalla triturazione di pneumatici fuori uso," *In Proceedings of the 33rd National Congress of the Italian Association of Acoustics (AIA)*, pp. 635-638, Ischia, Italy, January 2006.
- [22]B. Radičević, and I. Ristanović, "Koeficijent apsorpcije materijala od recikliranog gumenog otpada," 58. *ETRAN*, pp. AK3.6.1–6, Vrnjačka Banja, Srbija, 2014.
- [23]B. Radičević, and I. Ristanović, "Koeficijent apsorpcije materijala od reciklirane gume," 58. *ETRAN*, pp. AK3.6.1–6, Vrnjačka Banja, Srbija, 2014.
- [24]B. Radičević, M. Kolarević, and I. Ristanović, "Predviđanje akustičkih osobina kompozita od reciklirane gume i plastike", 60. *ETRAN*, pp. AK3.6., Zlatibor, Srbija, 2016.
- [25]M. Kolarević, B. Radičević, V. Grković, and Z. Petrović, "A Realization of the System for Measuring Airflow Resistance," *FACTA Univ. Work. Living Environ. Prot.*, vol. 12(1), pp. 83–94, 2015.
- [26]*Determination of sound absorption coefficient and impedance in impedance tubes - Part 2: Transfer - function method*, EN ISO 10534-2:2001.
- [27]*Acoustics - Materials for acoustical applications - Determination of airflow resistance*, ISO 9053:1991.
- [28]B. Radičević, "Razvoj modela odlučivanja za izbor optimalne smeše zvučno apsorpcionih materijala," Doktorska disertacija, Fakultet za mašinstvo i građevinarstvo u Kraljevu, Univerzitet u Kragujevcu, Srbija, 2016. Link: <http://www.mfkv.kg.ac.rs/documents/disertacije/2016/Disertacija-BrankoRadicevic.pdf>. [Pristup: 08-Jul-2016].



## ACOUSTIC PROPERTIES OF RECYCLED PLASTIC

Milan Kolarević<sup>1\*</sup>, Branko Radičević<sup>1</sup>, Vladan Grković<sup>1</sup>, Ivana Ristanović<sup>2</sup>, Marina Ivanović<sup>1</sup>

<sup>1</sup> University of Kragujevac, Faculty of Mechanical and Civil Engineering, Kraljevo, Serbia, kolarevic.m@mfv.rs

<sup>2</sup> Visoka škola tehničkih strukovnih studija, Čačak, Srbija

**Abstract** - This paper presents the results of testing acoustic properties of samples formed of recycled plastics granules and a binding agent made of polyurethane resins. The testing was performed in an impedance tube with the diameter of 100 mm by using the transfer function method between two microphones defined by the standard SRPS EN ISO 10534-2. The samples with the thickness between 10mm and 50mm were tested. The results show that recycled plastics has excellent absorption properties and that the increase in thickness of the material leads to the increase in the values of the sound absorption coefficient at lower frequencies..

**Keywords** – recycled plastics, absorption coefficient, passive noise protection

### 1. INTRODUCTION

The acoustic properties of polyurethane foams, fibrous and granular materials were examined within the project TR 37020 “Development of Methodologies and Means for Noise Protection in Urban Environments” financed by the Ministry of Education, Science and Technological Development of Republic of Serbia [1]. Special attention was given to recycled materials such as recycled rubber and recycled plastics and their possible application for noise protection.

Acoustic properties of rubber and the possibility of using rubber for passive noise protection have been the subject of a lot of research [2-6]. It has been shown that the preliminary results of the absorption coefficient of these tyre samples, under normal incidence conditions, are rather high.

In addition to rubber, a large part of industrial waste is also taken up by plastic waste. This paper presents the initial results of the research organised for the purpose of finding possibilities for mastering new products on the basis of recycled plastics granules obtained by removing the worn electric cables.

#### 1.1. Research plan

The research plan involves testing of acoustic properties of recycled rubber granules in the frequency range 125Hz-1600Hz as well as the dependence of the sound absorption coefficient on the material thickness. The factors tested and the intervals of their change are presented in Table 1.

#### 1.2. Material and preparation of samples

The testing samples were made of recycled plastics granules (granule dimensions from 3 to 5mm) and a binding agent made of polyurethane resins. The samples were 10 mm,

20 mm, 30 mm, 40 mm and 50 mm thick and they were cast in moulds whose diameter was 100mm without pressing in order to provide the porosity of samples (Figure 1).

**Table 1** Factors for response surface study

Factor	Name	Mark	Units	Low Level (-1)	High Level (+1)
A	frequency	<i>f</i>	Hz	125	1600
B	thickness	<i>d</i>	m	0.01	0.05

Enlarged view of the structure of the granulate from recycled plastic is shown in Figure 2.

The physical properties of recycled plastic materials have not been tested and will be subject to future research.

### 1.3 Method and equipment

The absorption coefficient was measured in an impedance tube at the Laboratory for Acoustics at the Faculty of Electrical Engineering in Belgrade. Transfer function method between two microphones, described in the SRPS EN ISO 10534-2 standard was used [7].

This method is based on the decomposition of the standing wave which is formed in the tube by recording signals from two microphones and calculating their transfer function. The reflection coefficient is calculated from the transfer function, and then the absorption coefficient is calculated. This method results in obtaining the values of the absorption coefficient at normal incidence, in the frequency range defined by the physical dimensions of the tube and the distance between the microphones. By using this method, it is possible to obtain fast measurements for normal incidence, using small samples.

$$\alpha = 1 - |R|^2 \quad (1)$$

where R is the reflection coefficient calculated according to the expression:

$$R = \frac{H - e^{-jks}}{e^{jks} - H} e^{j2k(l+s)} \quad (2)$$

where:

- *H* - the corrected transfer function,
- *s* - the distance between microphones ,
- *l* - the distance between the closer microphone and the sample, and
- *k* - the wave number.



**Fig. 1** Samples made of recycled plastics



**Fig. 2** Enlarged view of the structure of the granulate from recycled plastic

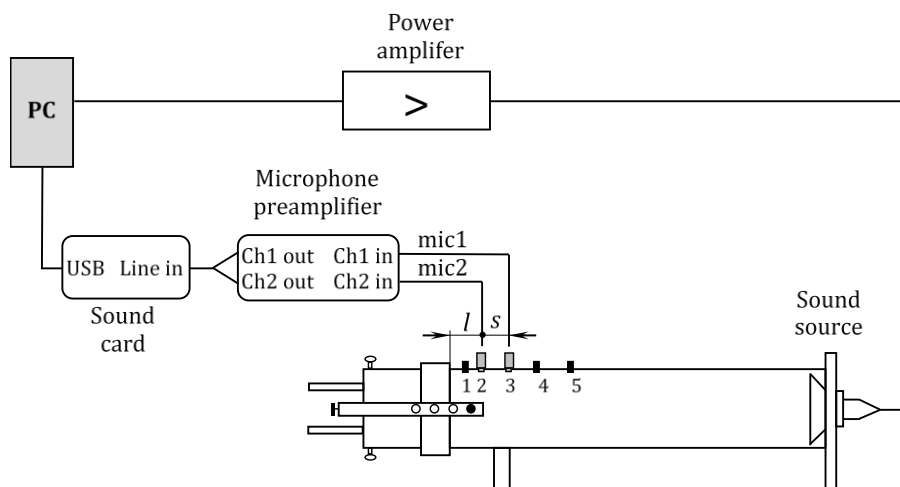


**Fig. 3** System for measuring absorption according to the standard SRPS EN ISO 10534-2 [7]

The method of the impedance of that tube has numerous advantages, which are described in the literature [7], the most important of them being:

- the measuring device is of small dimensions, so that is very practical for use ,
- the samples themselves have small dimensions, which facilitates their preparation for measurement,
- small costs of the experiment.

The disadvantages of this method:

- only normal incidence of waves are measured, although it is possible to apply correction to obtain a value of the absorption coefficient with random incidence,

- different diameters of tubes and samples are necessary in order to cover a wider frequency range.

## 2. RESULTS AND DISCUSSION

### 2.1. Experimental results

Experimental values of the absorption coefficient per 1/3 octave bands for different material thicknesses obtained by measuring in the impedance tube are shown in Table 2.

From Table 2. and Figure 4. the following can be noted:

- At low frequencies up to 400Hz, recycled plastic does not have pronounced absorption properties.

- The absorption coefficient ranges in the interval from 0,05 for the thickness of 10mm to 0,21 for the material thickness of 50mm.
- The absorption coefficient increases with the increase in the material thickness.
- For the material thicknesses from 10mm to 30mm the maximum value of the absorption coefficient is at the frequency of 1600Hz as follows: for  $d=10\text{mm}$  it is  $\alpha=0,13$ , for  $d=20\text{mm}$  it is  $\alpha=0,72$  and for  $d=30\text{mm}$  it is  $\alpha=0,91$ .
- For the plastics thickness of  $d=40\text{mm}$ , the maximum value of the absorption coefficient is  $\alpha=0,93$  for the frequency  $f=1250\text{Hz}$  while this value decreases at higher and lower frequencies.
- For the plastics thickness of  $d=50\text{mm}$  the maximum value of the absorption coefficient is  $\alpha=0,97$  for the frequency  $f=1000\text{Hz}$  while this value decreases at higher and lower frequencies.

It can be concluded that the absorption coefficient of recycled plastic increases with the increase in the material thickness, but at the same time its maximum moves toward relatively lower frequencies up to 1000Hz. In comparison with recycled

rubber [8], recycled plastic has slightly more advantageous absorption properties.

**Table 2** Values of the absorption coefficient for recycled plastic

$f$ (Hz)	$d$ (cm)				
	1	2	3	4	5
125	0.07045	0.08159	0.06360	0.06229	0.11737
160	0.04500	0.06167	0.06059	0.06724	0.10029
200	0.04998	0.06342	0.07518	0.07554	0.12036
250	0.03962	0.05359	0.07307	0.08124	0.13322
315	0.04424	0.06393	0.08620	0.09630	0.15780
400	0.05110	0.07538	0.10281	0.12230	0.21353
500	0.05196	0.09267	0.13902	0.16619	0.30182
630	0.05469	0.11156	0.19746	0.23917	0.46519
800	0.05815	0.14845	0.31262	0.39413	0.76533
1000	0.07396	0.22894	0.54481	0.66599	0.97240
1250	0.10531	0.40526	0.89514	0.93225	0.79133
1600	0.13402	0.71772	0.91522	0.82113	0.54213

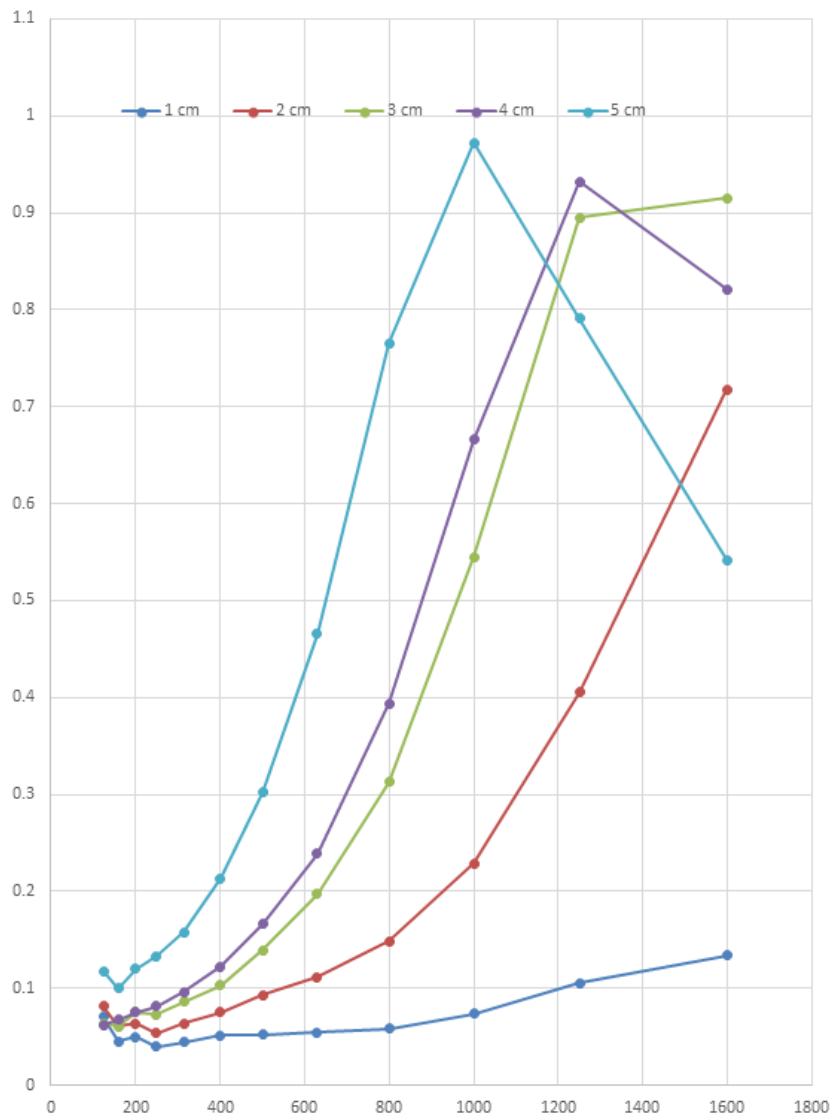


**Fig. 4** Values of the absorption coefficient for recycled plastic

## 2.2. Procession and analysis of the experimental results

The data procession was performed in the software package Design Expert v.9.0.6.2. [9-11]. Out of the available mathematical models, the models proposed have the form of third and fourth degree polynomials (Table 3).

**Table 3** Summary statistics of possible mathematical models

Source	Std. Dev.	R-Squared	Adjusted R-Squared	Predicted R-Squared	PRESS	
Linear	0.39	0.8466	0.8412	0.8212	10.02	
2FI	0.37	0.8652	0.8580	0.8076	10.78	
Quadratic	0.34	0.8900	0.8798	0.8277	9.65	
Cubic	0.11	0.9890	0.9870	0.9821	1.00	Suggested
Quartic	0.10	0.9917	0.9891	0.9725	1.54	Suggested
Fifth	0.095	0.9935	0.9905	0.9616	2.15	Aliased

The cubic model was adopted. In order to improve the results of the analysis, it was necessary to perform the transformation of the response function by means of the natural logarithm (Natural Log,  $k=0$ ,  $\lambda=0$ ). After reduction of nonsignificant members from the proposed model, the analysis of variance (ANOVA) for the transformed cubic model was performed.

**Table 4** ANOVA report for recycled plastic

ANOVA for Response Surface Cubic model						
Source	Sum of Squares	df	Mean Square	F Value	p-value Prob > F	
Model	55.39	9	6.15	497.56	< 0.0001	significant
A-f	9.02	1	9.02	729.60	< 0.0001	
B-d	1.85	1	1.85	149.85	< 0.0001	
AB	0.35	1	0.35	28.64	< 0.0001	
A <sup>2</sup>	1.00	1	1.00	80.59	< 0.0001	
B <sup>2</sup>	2.05	1	2.05	165.43	< 0.0001	
A <sup>2</sup> B	2.18	1	2.18	175.93	< 0.0001	
AB <sup>2</sup>	2.34	1	2.34	189.49	< 0.0001	
A <sup>3</sup>	0.58	1	0.58	47.20	< 0.0001	
B <sup>3</sup>	0.44	1	0.44	35.44	< 0.0001	
Residual	0.62	50	0.012			
Cor Total	56.01	59				

The high F value of the model ( $F=497,56$ ) and the low value of probability ( $p<0,0001$ ) indicate that the model is significant. The coefficient of determination (R-Squared) and other statistic (Table 5.) have good values, which justifies the selection of the adopted mathematical model.

The final equation of the mathematical model which adequately describes the dependence of the sound absorption coefficient of recycled plastic on the frequency and the material thickness is:

$$Ln(\alpha) = -2.77031 - 5.63955E-003 \cdot f + 54.58375 \cdot d + 0.29244 \cdot f \cdot d + 5.00031E-006 \cdot f^2 - 3554.33097 \cdot d^2 - 7.15031E-005 \cdot f^2 \cdot d - 2.61071 \cdot f \cdot d^2 - 1.37120E-009 \cdot f^3 + 50369.01689 \cdot d^3 \quad (1)$$

**Table 5** Calculation values of the statistics for the evaluation of the mathematical model

Std. Dev.	0.11
Mean	-1.92
C.V. %	5.80
PRESS	1.00
R-Squared	0.9890
Adj R-Squared	0.9870
Pred R-Squared	0.9821
Adeq Precision	68.485

The value of regression coefficients of the mathematical model, the standard error, 95% confidence intervals and the Variance inflation factor (VIF) of regression coefficients are presented in Table 6.

**Table 6** Values of coefficients of the mathematical model and confidence intervals

Factor	Coefficient Estimate	df	Standard Error	95% CI		VIF
				Low	High	
Intercept	-1.05	1	0.032	-1.12	-0.99	
A-f	1.95	1	0.072	1.81	2.10	9.55
B-d	0.83	1	0.067	0.69	0.96	11.02
AB	0.18	1	0.034	0.11	0.25	1.43
A <sup>2</sup>	-0.38	1	0.042	-0.46	-0.29	1.10
B <sup>2</sup>	-0.51	1	0.040	-0.59	-0.43	1.33
A <sup>2</sup> B	-0.78	1	0.059	-0.90	-0.66	3.17
AB <sup>2</sup>	-0.77	1	0.056	-0.88	-0.66	2.76
A <sup>3</sup>	-0.55	1	0.080	-0.71	-0.39	8.30
B <sup>3</sup>	0.40	1	0.068	0.27	0.54	9.03

The diagnostics of statistical characteristics of the model (diagram of normal distribution of residuals, BoxCox diagram, etc.) show that residuals are normally distributed and that the model has satisfactory statistical characteristics.

The graphical presentation of the mathematical model described by Eq. (1) is shown in Figures 5. and 6.

Design-Expert® Software  
 Factor Coding: Actual  
 Original Scale  
 Alfa (PLASTIC)  
 0.9724  
 0.039622  
 X1 = A: f  
 X2 = B: d

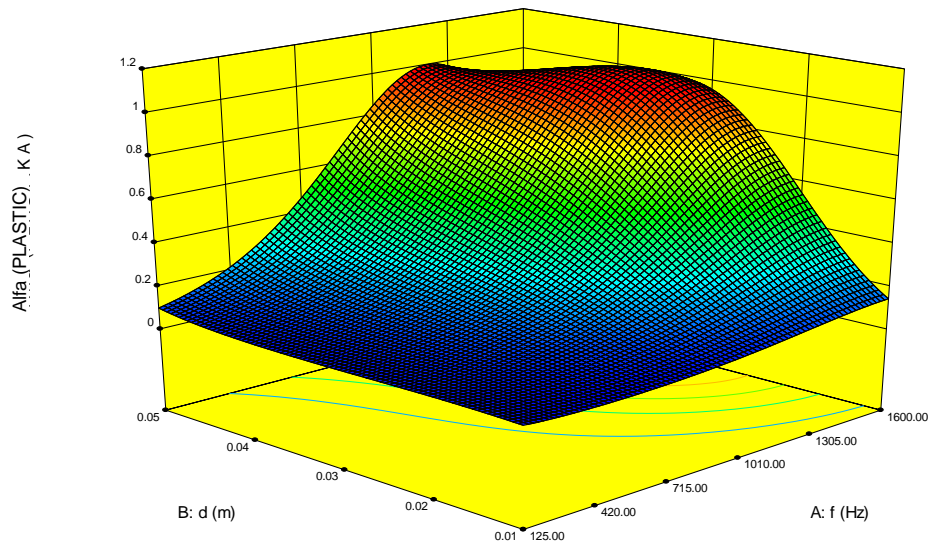


**Fig. 5** 3D graphical presentation of the dependence of the absorption coefficient on the material thickness in the examined frequency range

Design-Expert® Software  
 Factor Coding: Actual  
 Original Scale  
 Alfa (PLASTIC)  
 X1 = A: f  
 X2 = B: d

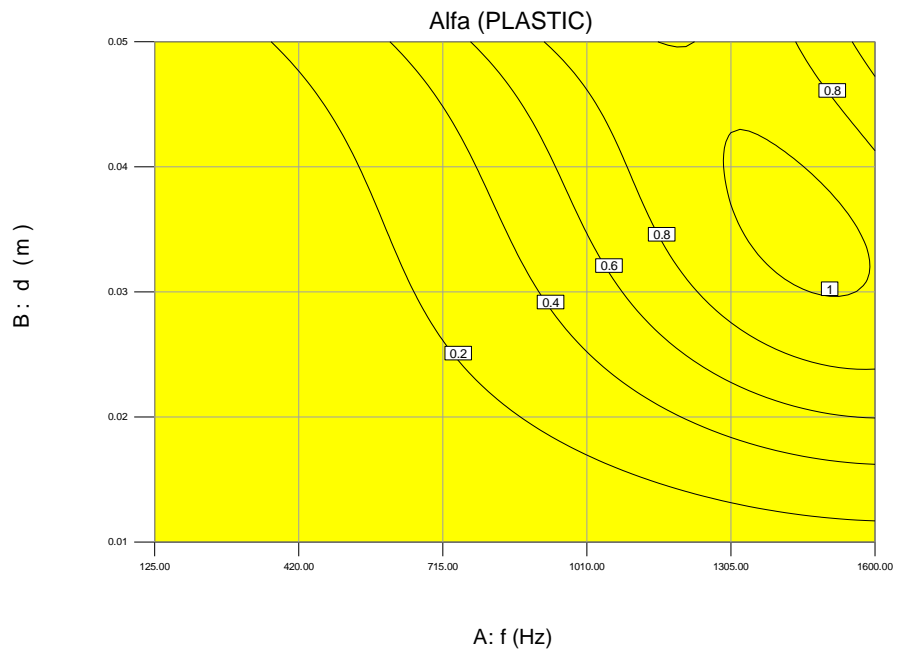


**Fig. 6** Contour 2D presentation of the mathematical model for recycled plastic

### 3. CONCLUSION

Experimental results show that the absorption coefficient of recycled plastic increases with the increase in frequency up to the value of 1250Hz and after that it decreases. The best values of absorption coefficient are obtained in the interval of 800Hz do 1600Hz.

At higher frequencies above 1250Hz the thickness of the material has a significant effect on increasing the absorption coefficient to a thickness of 30mm and after that has a negative effect which causes a slight decrease of the absorption coefficient.

It can be concluded that these materials manifest a high level of sound absorption in the medium frequency range, which is not characteristically in most absorption materials, and as

such can have a wide range of applications in the field of noise protection.

### ACKNOWLEDGEMENTS

The authors express their gratitude to the Ministry of Education, Science and Technological Development of the Republic of Serbia for the support to this research through the project TR37020.

The authors owe special gratitude to the Laboratory for Acoustics of the Faculty of Electrical Engineering in Belgrade, where part of the measurements presented in this paper was performed.

## REFERENCES

- [1] M. Kolarević, Z. Šoškić, Z. Petrović, and B. Radičević, "Noise Protection in Urban Environment-Description of a Project", *Mechanics, Transport Communications*, vol. 3, pp. IV-69/IV-78, 2011.
- [2] J. Arenas, and M. Crocker, "Recent Trends in Porous Sound-Absorbing Materials", [www.SandV.com](http://www.SandV.com)
- [3] G. Pispola, and K.V. Horoshenkov, "Consolidated granular media for sound insulation: Performance evolution through different methods", *International Congress on Sound and Vibration*, Lisbon (Portugal) 2005.
- [4] C. Aciu, "Possibilities of the Recycling Rubber Waste in the Composition of Martars", *ProEnvironment*, vol. 6, pp. 479-483, 2013.
- [5] M.J. Swift, P. Bris, and K.V. Horoshenkov, "Acoustic absorption in re-cycled rubber granulates", *Applied Acoustics*, vol. 57, pp. 203-212, 1999.
- [6] J. Pfretzschner, "Rubber crumb as granular absorptive acoustic material", in *Proc. of the Forum Acusticum Sevilla 2002*, pp. 43.50.Rq, 43.55.Ev, Sevilla (Spain), 16-20 Sep 2002.
- [7] SRPS EN ISO 354:2008, *Akustika - Merenje zvučne apsorpcije u reverberacionoj komori*.
- [8] M. Kolarević, B. Radičević, N. Herisanu, M. Rajović, and V. Grković, "Acoustic Properties of Recycled Rubber at Normal Incidence", in *Proc. IX International Conference "Heavy Machinery- HM 2017"*, F.15-F.22, Zlatibor, 28 June – 1 July 2017, ISBN 978-86-82631-89-7.
- [9] Design Expert v.8 User's Guide, Stat-Ease, [http://www.statease.com/dx8\\_man.html](http://www.statease.com/dx8_man.html)
- [10] Stat-Ease. Handbook for Experimenters version 09.01.03, Stat-Ease, Inc. 2014, [www.statease.com/pubs/handbk\\_for\\_exp\\_sv.pdf](http://www.statease.com/pubs/handbk_for_exp_sv.pdf)
- [11] D. Montgomery, "*Design and Analysis of Experiments*", 5th edition, John Wiley&Sons, INC, New York, 2001.

## AN EXPERIMENTAL PLAN FOR NOISE ANALYSIS AND CHATTER DETECTION IN MILLING DEPENDING ON THE CUTTING PARAMETERS

Aleksandra Petrović<sup>1</sup>, Mladen Rasinac<sup>1</sup>, Vladan Grković<sup>1</sup>, Marina Ivanović<sup>1</sup>

<sup>1</sup> University of Kragujevac, Faculty of Mechanical and Civil engineering, Serbia, petrovic.a@mfv.kg.ac.rs

**Abstract** – Improving the performance of cutting operations has led to an increase in noise levels, especially when milling. Main source of noise in milling are self-excited vibrations, i.e. chatter vibrations. In the literature is usual to compare noise level according to the spindle speed, feed per tooth, axial depth of cut and radial depth of cut. Purpose of that comparisons is to gain insight in effect of cutting parameters on occurrence of noise and vibrations. Here are presented plan of experiments and variants of the sample forms for identification of noise generated by chatter vibrations, in dependence of mentioned cutting parameters. That experiments we can use to get conclusions about cutting parameters that causes instability of process through vibrations and reduce productivity. Based on results obtained it is possible to select cutting parameters which enable us to improve productivity and part quality by avoiding unstable regions.

### 1. INTRODUCTION

The main goal for manufacturers of machine parts is to produce with as little cost as possible. Manufacturing technologies have advanced significantly, as well as machine tools. Accuracy, flexibility and productivity are constantly increasing in order to satisfy the demands of the market. Current trends, thanks to the advancement of computers and sensors, are focused on on-line monitoring, measurement and control of the process. [1], [3]

Vibrations of machine tools have a big impact in decreasing productivity. Excessive vibrations cause a wear and breakage of tools, poor surface quality, damage of the spindle bearings, waste of energy, excessive noise,... [1]

In metal cutting, there are three types of mechanical vibrations, which are due to deficiency of mechanical stiffness of system: machine tool, tool holder, cutting tool and workpiece.

These vibrations are:

- Free vibrations,
- Forced vibrations, and
- Self-excited vibrations. [1]

Self-excited vibrations use energy of interaction between cutting tool and workpiece to start and grow during the cutting process. These type of vibrations causes instability and that is the most undesirable type of vibrations. [1]

Chatter in milling can be detected by machine operator who analyzes the sound emitted, or by computer application who monitors the milling process sound and analyze the amplitudes and frequencies to identify chatter. [2] In that way, analysing the frequency and amplitude of the sound emitted give us a possibility to conclude which characteristics has a sound obtained, generated by chatter vibrations.

In [2] are presented experimental methodology for identification of stability lobes diagram – SLD (Fig. 1), who shows the boundary between chatter-free operations and unstable process, which is obtained as dependence between axial depth of cut and spindle speed. Based on SLDs it is possible to choose a suitable combination of these parameters and prevent the occurrence of chatter vibrations and high noise level. [2] On diagram can be seen that for the certain depths of cut, at any spindle speed cutting process remains stable. Maximum value of depth of cut at which cutting process is always stable is critical depth of cut. That methodology is particularly convenient for smaller companies which does not have enough resources to implement more complicated methods. For more precise SLDs, i.e. for some another combinations of machine, tool holder, tool and workpiece material it is necessary to carry out a large number of experiments. [5], [6]

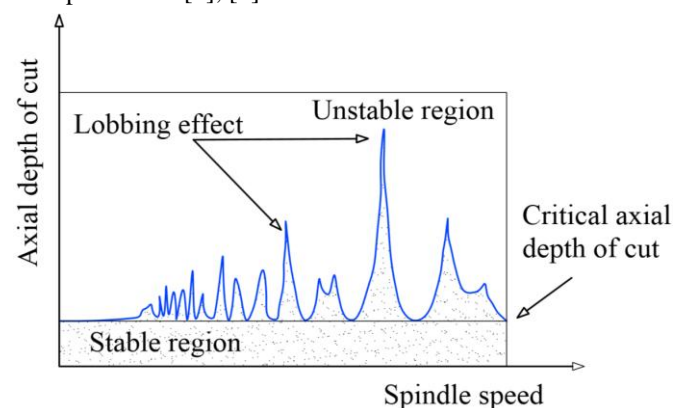


Fig. 1 Stability lobes diagram

### 2. NOISE EMISSION IN MILLING

In face milling, noise can be classified into idling noise and cutting noise. Idling noise consists of aerodynamic noise, noise because of cutter vibration caused by flow of air around the cutter teeth and noise due to rotation of spindle. [4]

In operation of milling, impacts of the cutting edge causes vibrations because of interaction between elements of the system.

During the milling, vibrations are spreading through the air and create noise that contains information about the milling process. [2]

Noise is directly dependent of vibrations. By analyzing sound emitted i.e. its frequency and amplitude, we can see when self-excited vibrations occur and that experimental results can be used to plot the dependence between cutting parameters and level of noise, based on methodology developed in [2].

### 3. PLAN OF EXPERIMENTAL ANALYSIS

In this section are presented some experiments that can be used to measure sound pressure level (SPL, [dBA]) in dependence of cutting parameters. Equipment that is necessary for those measurements consists of machine (vertical milling machine), milling cutter of proper diameter at each experiment, samples - workpieces with defined shape and dimensions and microphone for measuring SPL. In [4] are proposed that the distance between the centre of the cutter and microphone should be at least 10 times of cutter radius, because the measured values of SPL varies as a function of that distance. In our case distance should be 250 [mm] in first set of experiments, 100 [mm] in second experiment and 110 [mm] in third experiment.

#### 3.1 First set of experiments

First set of experiments consists of measuring SPL when changing cutting parameters (axial depth of cut, feed per revolution, spindle speed and radial depth of cut). In addition to measuring noise, the operator will register when chatter vibrations occur (at which value of the parameter that we change).

In this experiments it is suitable for samples to have quadratic form (Fig. 2).

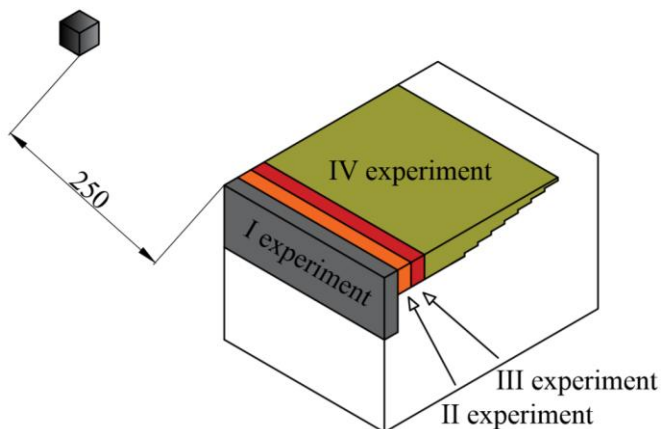


**Fig. 2** Schematic representation of sample form and surfaces obtained by 8 passes in first set of experiments

In Tables 1-4 can be seen proposed values of cutting parameters we are changing, while the others are constant. The material of workpiece should be carbon steel, and a diameter of the cutter is 50 [mm].

**Table 1** Proposed values of axial depth of cut in first experiment

FIRST EXPERIMENT								
No.	1	2	3	4	5	6	7	8
Axial depth of cut [mm]	0.5	1.0	1.8	2.5	3.0	3.5	3.8	4.0
SPL [dBA]								

**Table 2** Proposed values of feed per revolution in second experiment

SECOND EXPERIMENT								
No.	1	2	3	4	5	6	7	8
Feed per revolution [mm/rev]	0.1	0.2	0.3	0.4	0.5	0.6	0.7	0.8
SPL [dBA]								

**Table 3** Proposed values of spindle speed in third experiment

THIRD EXPERIMENT								
No.	1	2	3	4	5	6	7	8
Spindle speed [rpm]	60	80	100	120	140	160	180	200
SPL [dBA]								

**Table 4** Proposed values of radial depth of cut in fourth experiment

FOURTH EXPERIMENT								
No.	1	2	3	4	5	6	7	8
Radial depth of cut [mm]	15	20	25	30	35	40	45	50
SPL [dBA]								

In Fig. 3a are shown 8 passes in which difference is in axial depth of cut while other parameters are the same at every pass.

Second experiment (Fig. 3b) represents method for measuring of SPL where at every pass is different feed per revolution.

In third experiment (Fig. 3c) we change spindle speeds.

While in fourth (Fig. 3d) we change radial depth of cut.

In Table 5 are shown cutting parameters which are constant at each pass.

**Table 5** Proposed values of constant cutting parameters in set of experiments

CUTTING PARAMETERS				
EXPERIMENT	Axial depth of cut [mm]	Feed per revolution [mm/rev]	Spindle speed [rpm]	Radial depth of cut [mm]
1	-	1	100	5
2	1	-	200	5
3	1	0.6	-	5
4	1	0.8	150	-

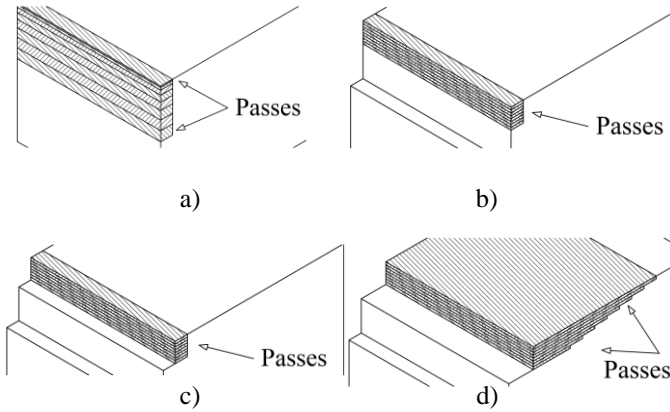


**Fig. 3** Schematic representation of sample forms and 8 passes in set of experiments for measuring SPL

Purpose of this experiments presented above, is to get conclusions about dependence between noise generated and cutting parameters, and detection of chatter vibrations. Based on this results, we can see which parameters mostly affect the noise level and vibration increase.

### 3.2 Second experiment

Second type of experiment (Fig. 4) is based on experiments conducted in [2]. In that research, methodology for identifying stability lobes diagram is based on empirical tests where the workpiece has a inclined surface with gradual increase of the axial depth of cut in the feed direction. Axial depth of cut represents ordinate axis (y) of the SLD and spindle speed represents abscissa axis (x) which is increased between passes. The cutting process is stopped when the chatter is detected. In that way SLD is physically machined on the workpiece. [2] Measuring noise with a microphone of chatter vibrations, we can take conclusions about level of noise in dependence of spindle speed and axial depth of cut.

In Table 6 are shown cutting parameters in this experiment. There can be seen that axial depth of cut varying from 0 – 3 [mm], and spindle from 80 – 480 [rpm] with a step up of 20. Where the diameter of the cutter is 20 [mm], and material of the workpiece is carbon steel.

**Table 6** Cutting parameters

CUTTING PARAMETERS				
EXPERIMENT	Axial depth of cut [mm]	Spindle speed [rpm]	Feed per revolution [mm/rev]	Radial depth of cut [mm]
	0 - 3	80 - 480	0.8	20

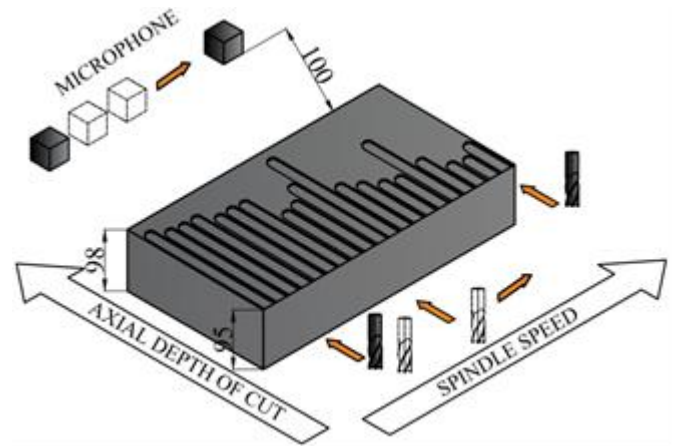


**Fig. 4** Schematic representation of experiment for measuring SPL of chatter vibrations

### 3.3 Third experiment

In third experiment, proposed here, aim is to obtain the level of noise in dependence of radial depth of cut ( $a_e$ ) which is increasing linearly from 0 to 20 [mm] that is the diameter of the cutter, (Fig. 5). As it is used the SLD where we can see dependence between spindle speed and axial depth of cut, also SLD can be obtained by plotting the values of radial depth of cut. Material of the sample form is carbon steel.

In Table 7 are given cutting parameters in this experiment.

**Table 7** Cutting parameters

CUTTING PARAMETERS				
EXPERIMENT	Radial depth of cut [mm]	Axial depth of cut [mm]	Feed per revolution [mm/rev]	Spindle speed [rpm]
	0 - 20	1	0.8	100

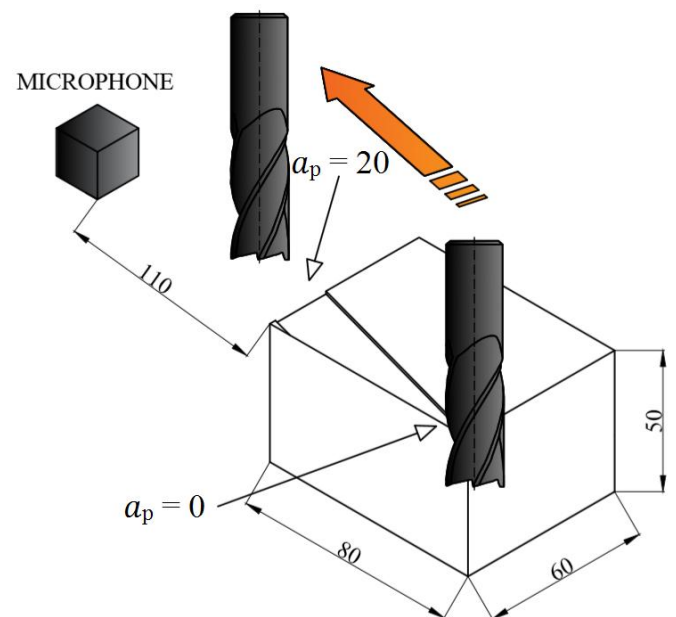


**Fig. 5** Schematic representation of experiment for measuring SPL at varying radial depth of cut

#### 4. CONCLUSIONS

In today industry, vibrations is the main problem, especially in process of high speed milling. Researchers have dealt with problem of vibrations as the main cause of noise, especially chatter vibrations. Measurements of noise levels can be used to capture frequencies and amplitudes at which chatter vibrations occur. It allows us to make the process of cutting stable (without chatter), by customizing the cutting parameters. In this paper are proposed three different types of experiments to measure noise level, i.e. SPL generated and detection of chatter vibrations. In first we measure SPL in dependence of cutting parameters and detect when vibrations occur, second measures noise induced by chatter vibrations and analyzes its frequency and amplitude. In third experiment idea is to see how noise changes with radial depth of cut that increases linearly. Generally, the aim of this three types of experiments is to determine the dependence between different cutting parameters of milling and noise and vibrations, with the aim of determining stable regions of cutting process. Results that would be obtained can be used for further investigations of that dependence. Based on obtained results we can conclude which parameters is most critical and adjust them to avoid high level of noise during process of milling in practical application. This plan of experiments is only initial step in our further research in this field. Next step would be some other experiments that should be conducted with different types of material, cutter, parameters of the process (cutting parameters), using of accelerometers for determining vibrations, etc.

#### REFERENCES

- [1] G. Quintana and J. Ciurana, "Chatter in machining process: A review", *International Journal of Machine Tools and Manufacture*, vol. 51, pp. 363-376, 2011.
- [2] G. Quintana, J. Ciurana and D. Teixidor, "A new experimental methodology for identification of stability lobes diagram in milling operations", *International Journal of Machine Tools and Manufacture*, vol. 48, pp. 1637-1645, 2008.
- [3] J. Rech, F. Dumont, A. Le Bot and P. J. Arrazola, "Reduction of noise during milling operations", *CIRP Journal of Manufacturing Science and Technology*, vol. 18, pp. 39-44, 2017.
- [4] K. Sampath, S.G. Kapoor and R.E. DeVor: "Modeling and Analysis of Aerodynamic Noise in Milling Cutters", *Journal of Manufacturing Science and Engineering*, vol. 129, pp. 5-11, 2007.
- [5] Y. Altintas: "Manufacturing automation - metal cutting mechanics, machine tool vibrations and CNC design", 2<sup>nd</sup> edition, *Cambridge University Press*, 2012, New York, USA
- [6] A. Petrović: "Optimization of the path of milling cutter at high-speed contour milling", Ph. D. thesis, *University of Kragujevac, Faculty of mechanical and civil engineering*, Kraljevo, 2016

## THE RESEARCH OF ACOUSTICS FROM ASPECT OF SOUND SOURCE

Aleksandra Igić<sup>1</sup>, Slavko Zdravković<sup>1</sup>, Dragana Turnić<sup>1</sup>, Sandra Šaković<sup>1</sup>, Vesna Zdravković

<sup>1</sup> University of Nis, Faculty of Civil Engineering and Architecture, Serbia, igic.aleksandra91@gmail.com

**Abstract** - Acoustics as a science of sound is especially important from the aspect of isolation and the absorption of space for work and housing. Frequency of 20Hz to 20kHz is significant for the people's sense of hearing. The frequency of hearing is individual and decreases for years. The basic characteristics of each tone are: height, color and intensity. The calculations of their own frequencies of oscillations of different sources, such as the intensity and levels of sound are given. The terms echo and echo are explained, and the acoustics of the rooms are described by the equation and the solution of the wave equation. The absorbers of the sound of materials and constructions are of particular importance, as well as the time of reverberation. Noise protection is actually a reduction in sound passage through the partition walls of the building, ie the use of suitable acoustic materials, that is, insulating absorbent materials.

### 1. BASIC CHARACTERISTICS OF SOUND

Acoustics is a science of sound. By sound in a narrow sense, it means mechanical waves that can be registered with a hearing sense, that is, the frequency is in the range of 20 Hz to 20 kHz. Sound in physical sense is synonymous with mechanical waves in general, with waves whose frequency below 20 Hz is called infrasound, and those whose frequency is above 20 kHz is ultraviolet. The volume of hearing frequencies is, however, an individual characteristic, and the above values should be understood as adopted statistical values. Also, the frequency bandwidth decreases over the years for each individual.

If the sound wave is a free sine wave, then such sound is called a free tone. However, sound waves are most often complex waves. If, by explaining these waves, one can get the final, i.e. countless infinite number of free waves then that sound is called a complex tone. If the sound wave is not periodic, ie it can not be explained on free waves, such a type of sound is called noise. Therefore, we can divide the sound to tone and noise, with tones being free or complex.

If we plot the wave amplitude obtained by the decomposition of a complex wave in the function of frequency, we obtain an amplitude spectrum. The spectrum of the tone is linear, ie it contains lines at the frequencies  $\nu_0$ ,  $\nu_1=2\nu_0$ ,  $\nu_2=3\nu_0$ , etc.

All complex tones except basic ones are called higher harmonics.

The basic characteristics of each tone are: height, color and intensity (intensity). The height of the tone is determined by the value of the basic tone frequency. The color of the tone is

determined by the relative relationships of the amplitude of the basic or higher harmonics.

By color, we distinguish tones produced by the voices of different people or by using different musical instruments. The volume of the tone is the intensity of a complex wave and is equal to the sum of:

$$I = I_0 + I_1 + I_2 + I_3 + \dots \quad (1)$$

where  $I_0$  is the intensity of the base tone,  $I_1$  the intensity of the first accordion, the  $I_2$  intensity of the second accordion, etc.

The noise has a continuous spectrum, unlike tones. For this reason, amplitude spectrum ordinates in the noise are taken from the amplitude density  $g_I = dI/d\nu$ . There are different types of noise, depending on the shape of the spectrum. The spectra of tones and noise are shown in Fig. 1.

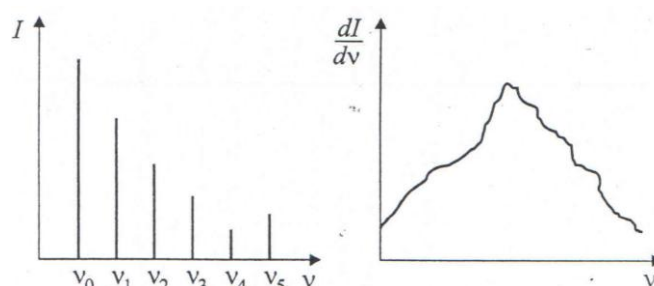


Fig. 1. Spectrum of sound and noise

One of the important characteristics of the sound is its velocity. It depends on the environment through which the sound moves.

### 2. SOUND SOURCES

Any mechanical oscillator that can oscillate properly by creating tones is called a sound source. Strained wires, rods, air pillars, membranes and plates are the most commonly used sound sources.

#### 2.1 Tightened wires

Calculation (2) shows the fluctuations of the wire tightened by force  $F$  between the two fixed supports. If the direction of the wire is driven by the oscillation of one of its points, a transverse wave will be created. In order for the created wave to be standing, the length of the wire must be equal to the total number of wavelengths half, and hence can determine the own frequency of the oscillation of the wire of various noise.

$$l = n \frac{\lambda}{2}, \quad v_n = \frac{n}{2l} c = \frac{n}{2l} \sqrt{\frac{F}{\mu}} \quad (2)$$

## 2.2 Rods

With rods it is possible to educate both transversal and longitudinal oscillations. The own oscillations of the rods depend on the hook of the stick. In any case, the knots of the standing waves are formed at the points of fastening and the trunks at the places of the free ends of the rod. If the rod is fixed at one end, then:

$$l = (2n+1) \frac{\lambda}{4}, \quad v_n = (2n+1) \frac{c}{4l} \quad (3)$$

and if, for example, there are two fixing points, then it applies (2). The velocity of sound propagation  $c$  depends on whether it is transversal or longitudinal waves and is given by the expressions (4) and (5). The speed of the expansion of transverse waves in a solid body is given by the expression:

$$c = \sqrt{\frac{F}{\mu}}, \quad (4)$$

where  $F$  is the tensile force, and  $\mu$  is the mass per unit length (longitudinal mass).

Speed of longitudinal waves in the solid body:

$$c = \sqrt{\frac{E_y}{\rho}}, \quad (5)$$

where  $E_y$  - Jun's modulus of elasticity, and  $\rho$  - density of the environment.

## 2.3 Air columns

The oscillation of the air columns depends on whether they are open at one or both ends.

For air columns open at one end it is valid (3) and for those open at both ends (2).

## 3. CHARACTERISTICS OF SPEECH AND MUSIC

The two most important types of sound signals that transmit the desired information received by the hearing organ are speech and music. In addition to speech and music, the ear

receives a large number of different sounds. Most of them fall into unwanted sounds that we consider subjectively as noise.

### 3.1 Characteristics of speech

A man speaks with organs of speech, which includes: the lungs, the dorsal, the larynx with the vocal cords (vocal cords), the spittle with the reservoir, the oral cavity (palate, tongue, teeth) and the nasal cavity, also called the vocal tract. The work of the speech organ can be compared with the work of gadgets: the bellows produce a constant flow of air that plays the modulus, turning it into a pulsating flow of a certain frequency. In the body of the lungs, they respond to the bellows, and the vocalists played.

The vocalists narrow the vocal tract, leaving the opening in the form of a narrow cracks, whose opening and closing periodically interrupts the air current and forms the sound signal that is further processed in various slaves and chambers which, by their position, form a resin, palate, tongue, teeth

and lips. In this way, with the given basic frequency of the sound, different spectra can be created, on the basis of which the individual voices differ from one another.

Voices are phonetically divided into vowels and consonants. All vowels are sound, and consonants can be audible and voiceless.

### 3.2 Characteristics of music

Time changes are the basic elements of music. Changing the tone height creates a melody and changing the sound volume creates dynamics. Successive emphasis is rhythm.

If two or more tones are produced simultaneously, they create a composition. A compound of two tonnes that is comfortable for hearing is called consonance, and what is unpleasant dissonance. In order to create a consonance, it is necessary that the tones are approximately equal to the intensity, and that their basic frequencies are in the ratio of small integers, i.e. the harmonic is even better if two tonnes compose in a number of accordions. The most agreeable consonance is a two-tone acceleration with a frequency of 1: 2, and is called an octave [4].

## 4. INTENSITY AND LEVEL OF SOUND

The sound intensity is actually the intensity, the most commonly complex, sound waves. Sound propagation causes a volume deformation of the medium through which the sound is transmitted, leading to the appearance of excessive  $p_m$  at each point in the center:

$$I = \frac{\rho v_0^2}{2} c = \frac{p_m^2}{2\rho c} = \frac{1}{2} \rho \omega^2 A^2 c. \quad (6)$$

As there is a lower and upper boundary frequency for the extent to which the ear of pressure changes feels like sound, there are also limits for the intensity of sound. The minimum value of the volume that a human ear can hear is called the sound intensity on the threshold of audibility, or a shorter threshold of audibility. It depends on the state of the hearing organ (it is different for different people and it also changes with the same man for years), but also from the frequency of the sound signal. The noise level for flat waves in the free space, standardized for 1000 Hz, was determined by experimental, statistical testing of young and healthy people, and it is:

$$I_0 = 10^{-12} \frac{W}{m^2} = 1 \frac{pW}{m^2}. \quad (7)$$

The upper limit of the intensity of the sound that a shell's ear can hear is determined by the onset of pain due to the existence of high pressure on the bumps, so it is called the pain limit. It also depends on the state of the hearing organ and the frequency of the acoustic signal, and for 1000Hz the threshold of audibility is slightly more than 1012 times.

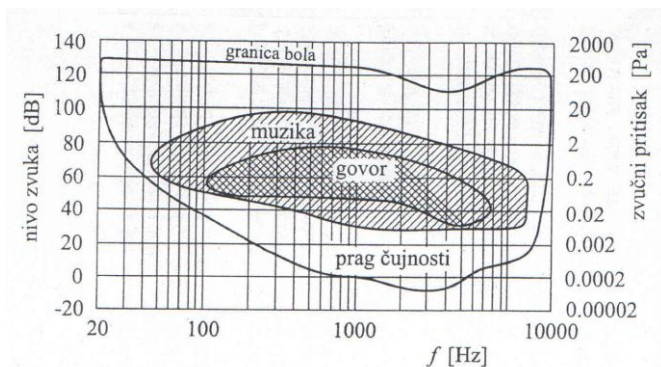


**Fig. 2** Audible area and area of speech and music

A large range of sound intensity in the field of audibility is unusual. Also, the human ear, as the hearing sense organ, has a logarithmic sensitivity. It is therefore appropriate to introduce a new size, the sound level:

$$L = 10 \log \frac{I}{I_0} [=] dB, \quad (8)$$

which is a measure of the relative intensity of sound that is observed in relation to the threshold of audibility. Now the entire audio range is set at an interval of -10 to 130 dB. Typically (averaged) audible area of speech and music, as well as the entire sound area shown in the sun, Fig. This picture shows that the mean dynamics of music is greater than the dynamics of speech.

## 5. THE SUBJECTIVE STRENGTH OF SOUND

Although the scale in decibels is well suited to the subjective sense of volume change, due to the frequency dependence of the threshold of sensitivity and pain limits, the sound level can not be the right measure for a subjective sense of strength. For example, if we observe two sounds of the same level  $L = 20$  dB, the frequency of 100 and 1000 Hz, we see that the first one is not heard while the other is falling into the field of sensibility. That's why a new physical size is introduced, called the subjective volume, and its unit called *the phon*. By definition, two sounds that have the same number of phons for the human ear appear to be of equal strength, regardless of the value of their sound levels, which may be different.

## 6. ACOUSTIC SPACE

During the reflecting of the noise from the obstacle, a storm and echo are appeared. Assuming that the pronunciation of the style lasts about 0.1 s and the sound velocity is about 340 m/s, then, if the distance of the obstacle is less than about 17 m, the reflected sound returns to the sound source during the duration of the style. This phenomenon is called a streak. If, however, the reflecting surface is at a distance of greater than about 17 m, an echo appears, ie the reflected sound returns to the source after the finished pronunciation of the style.

In closed rooms there is the creation of standing waves, ie for each room there are its resonant frequencies. Let's look at a parallelepiped room with ideally rigid walls of dimension  $l_x$ ,  $l_y$ ,  $l_z$ . We will assume that the sound wave in the room can be described by the equation:

$$\psi(x, y, z, t) = A \sin(k_x x + \phi_x) \sin(k_y y + \phi_y) \cdot \sin(k_z z + \phi_z) \sin \omega t \quad (9)$$

for which it can be shown to represent a solution of the wave equation, where it follows that it must be:

$$\left(\frac{2\pi}{\lambda}\right)^2 = k^2 = k_x^2 + k_y^2 + k_z^2. \quad (10)$$

Acoustic materials used for acoustic room processing can be divided into:

- Porous materials for high frequency absorption;
- Mechanical resonators designed for medium frequency absorption;
- Acoustic resonators designed for low frequency absorption.

Porous materials are various porous structures, which are made on the basis of polyurethane, pre-fabricated mineral or stone wool, textile fibers, their combination or similar materials of similar genesis.

The acoustic resonator is essentially any construction constructed of a sufficiently massive material consisting of a closed air-filled chamber with a relatively small opening. In the acoustical sense, the volume plays a significant role, but not its shape.

## 7. CONCLUSION

Acoustics is a science of sound and for our sense of hearing the frequency is in the interval from 20 Hz to 20 kHz, but the individual character and the frequency of the audio volume are decreasing over the years. Sound waves are the tones and they are characterized by: height, color and intensity - intensity. The picture shows a spectrum of tones and the woods have a continuous spectrum.

The most commonly used sound sources are listed: tensioned wires, rods, air columns, membranes and plates and formulas for calculating their own frequency - oscillation frequency, except for membranes and plates due to their diversity. The characteristics of speech and music are analyzed in particular. The maximum sound power levels that a human ear can hear is called the sound intensity at the threshold of audibility. The threshold is determined by the onset of pain due to the high pressure on the bumps, so it is called the pain limit, and the unit for the subjective volume of the sound is called the phon.

Because of the reflection of the sound from the obstacles, the storm and the echo are appeared.

The propagation of the sound wave in the room is described by the equation, and the solution of the wave equation is presented. The terms of sound absorption and the time of reverberation are explained. Basically, there are three groups of absorbers of sound of the matrix and constructions, which are: porous materials - high frequencies, acoustic materials - medium frequencies and mechanical resonators - low frequencies. Due to the passage of sound through the partition walls, we have three methods of noise protection: the suppression of noise at the source, the removal from noise sources and acoustic isolation of rooms. This problem concerns the so-called architectural-construction acoustics, as well as acoustic (sound) isolation using insulating and absorbent materials.

### Acknowledgement

This research is conducted at The Faculty of Civil Engineering and Architecture of University of Niš in the framework of the project in the field of technological development in the period 2011-2019, and titled „Experimental and theoretical investigation of frames and plates with semi-rigid connections from the view of the second order theory and stability analysis“ (TR 36016), financed by the Ministry of Education, Science and Tehnological development of the Republic of Serbia.

### REFERENCES

- [1] H. Kurtović, *Osnovi tehničke akustike*, Naučna knjiga, Beograd, 1982.
- [2] D. Cvetković, M. Praščević, *Buka i vibracije*, fakultet zaštite na radu, Univerzite u Nišu, 2005.
- [3] S. Zdravković, D. Turnić, S. Ljubenić, "Buka i vibracije u životnoj i radnoj sredini", *XXII Konferencija sa međunarodnim učešćem, Buka i Vibracije*, Fakultet zaštite na radu Univerziteta u Nišu, pp. 191-195, Oktobar, 2010.
- [4] J. Karamarković, *Fizika*, Građevinsko-arhitektonski fakultet Univerziteta u Nišu, Niš, 2005.
- [5] H. Kurtović, M. Mijić, *Zbirka rešenih zadataka iz tehničke akustike*, Naučna knjiga, Beograd, 1987.
- [6] T. Jelačić, *Zvuk. Sluh. Arhitektonska akustika*, Školska knjiga, Zagreb, 1978.
- [7] D. Cvetković, D. Petković, "Simuliranje akustičnog opterećenja u cilju prognoziranja rizika od oštećenja sluha bukom", *XXX Jugoslovenska konferencija ETAN-a*. Herceg Novi, 1986.



## PSYCHOACOUSTICS IN HOUSEHOLD APPLIANCES

Nikola Holeček<sup>1</sup>, Tomaž Bregar<sup>1</sup>

<sup>1</sup>Gorenje d.d., Parizanska 12, SI-3503 Velenje, Slovenija, nikola.holecek@gorenje.com

**Abstract** - Household appliances are often located in the living area; therefore the appliances should be as silent as possible when operating. For this purpose, noise level is already given on energy labels of all household appliances. Quiet and efficient appliances are attractive for customers on the market today. Automotive and aviation industry recently started using in the development process the so-called psychoacoustic parameters, besides the overall sound power level. The main purpose of psychoacoustics and its parameters is an objective and qualitative understanding of perceiving and experiencing sound/noise. Since the human interpretation of sound is subjective. If we take for example two similar products with the same sound power level, it may be that, due to the frequency content of noise one of them, the human ear would perceive it more silent or less annoying than another. Psychoacoustic parameters give us qualitative information on the interpretation of noise, and thus enable the objective characterization of noise.

In this paper, established psychoacoustic parameters such as loudness, tonality, roughness and fluctuation strength will be presented. In addition to these basic parameters, there are various general factors that can determine the sound quality. One of the qualitative factors is the psychoacoustic annoyance factor with which we can determine the overall level of annoyance of noise. The use of psychoacoustic parameters in the development of household appliances enables us to evaluate the noise of the appliance at the very stage of development of the new product, while also providing information about the customer perception of noise.

### 1. INTRODUCTION

Historically sound power level (SPW) has been the main design variable associated with sound quality. However, products can sound annoying or even unappealing although they are relatively quiet [1]. Therefore, evaluating product sound quality only by SPW can lead to misleading results. For that reason, the color of sound also needs to be considered.

A special field of acoustics is the so-called psychoacoustics, which main goal is the objective quantification of human perception of sound [2]. First psychoacoustic model for estimating loudness was developed by Zwicker [3]. Loudness aside, there are four additional psychoacoustic parameters which are also well established: roughness, sharpness, fluctuation strength and tonality. Psychoacoustic parameters can be combined to assess the overall annoyance [4, 5] or pleasantness [6] of sound.

The objective of this paper is to present a comparison between SPW and psychoacoustic evaluation of a centrifugal fan. The main source of noise in this type of fan is aerodynamical. Noise associated with the fan has both tonal and broadband characteristics. However, tonal noise is dominant in this exact fan design. Tonal noise is associated with blade passing frequency (BPF) [7, 8]. Reduction of BPF noise can be achieved with several solutions [9, 10]. In this paper cut-off clearance and lip curvature was modified with different lip design. Noise from different design shapes was recorded inside a semi-anechoic chamber. SPW and psychoacoustic parameters were evaluated and compared. The last design shape, which had the lowest A-weighted SPW also exhibited the best psychoacoustic pleasantness. Therefore, psychoacoustic parameters can be used as an additional design variable to gain more information about the overall sound quality.

The paper is organized as follows. The next section summarizes the psychoacoustic parameters together with two combined parameters (psychoacoustic pleasantness and annoyance). The third section presents experimental setup and in the fourth section results of SPW and psychoacoustic evaluation are presented. In the last section a summary and contributions are presented.

### 2. PSYCHOACOUSTIC PARAMETERS

Human interpretation of sound characteristics is highly complex and subjective. Evaluation of sound quality with psychoacoustic experiments can be time consuming, therefore different models have been proposed which enable us to objectively predict sound quality of a product. Basic psychoacoustic quantities are loudness, fluctuation strength, roughness, sharpness and tonality.

#### 2.1 Loudness

Loudness is directly connected with human interpretation of sound amplitude level. Model for calculating loudness has been proposed by Zwicker [3] in 1960 and was improved in [11,14]. Loudness is defined as integral of specific loudness  $N'$  over Bark frequency scale:

$$N = \int_0^{24 \text{ Bark}} N' dz \text{ [sone].}$$

Specific loudness is defined with the following expression:

$$N' = 0.08 \left( \frac{E_{TQ}}{E_0} \right)^{0.23} \left( \left( 0.5 + 0.5 \frac{E}{E_{TQ}} \right)^{0.23} - 1 \right), \quad (2)$$

where  $E_0$  is the excitation that corresponds to the reference intensity ( $I_0 = 10^{-12} \text{ W/m}^2$ ),  $E_{TQ}$  is the excitation level at the threshold of quiet and  $E$  is the considered excitation level. Zwicker's loudness model has been standardized in international standard ISO 532B [12] and in national standard DIN 45 631 [13].

### 2.3 Roughness

Roughness is a hearing sensation related to temporal variations of a sound and reaches a maximum for modulation frequencies around 70 Hz. Roughness can be explained by the temporal-masking pattern of sounds [6].

Roughness can be calculated with the following equation:

$$R = 0.3 \frac{f_{\text{mod}}}{\text{kHz}} \int_0^{24 \text{ Bark}} \frac{\Delta L_E(z) dz}{\text{dB/Bark}} \text{ [asper]}, \quad (3)$$

where  $f_{\text{mod}}$  is the modulation frequency and  $\Delta L_E(z)$  is related to temporal masking depth and can be defined as:

$$\Delta L_E(z) = 20 \log \left( \frac{N_{\text{max}}}{N_{\text{min}}} \right) \text{ [dB]}, \quad (4)$$

where  $N_{\text{max}}$  and  $N_{\text{min}}$  are the maximum and minimum loudness levels in the current critical band.

### 2.2 Fluctuation strength

Fluctuation strength is similar to roughness as is also related to temporal variations of a sound. However, fluctuation strength reaches maximum at modulation frequencies of around 4 Hz. Model of fluctuating strength was developed by Fastl [14]:

$$F = \frac{0.008 \int_0^{24 \text{ Bark}} (\Delta L(z)/\text{dB Bark}) dz}{(f_{\text{mod}}/4 \text{ Hz}) + (4 \text{ Hz}/f_{\text{mod}})} \text{ [vacil]}, \quad (5)$$

where  $\Delta L(z)$  is masking depth and is defined as:

$$\Delta L(z) = 20 \log \left( \frac{N'_{\text{max}}}{N'_{\text{min}}} \right) \text{ [dB]}, \quad (6)$$

where  $N'_{\text{max}}$  and  $N'_{\text{min}}$  are the maximum and minimum specific loudness levels in the current critical band.

### 2.4 Sharpness

Sharpness is related to sharp, high-frequency sound and can be regarded as a measure of tone colour [15]. It is defined as comparison of the amount of high frequency energy to the total energy and can be calculated with the following equation:

$$S = 0.11 \frac{\int_0^{24 \text{ Bark}} N' g(z) z dz}{\int_0^{24 \text{ Bark}} N' dz} \text{ [acum]}, \quad (7)$$

where  $g(z)$  is the weighting function, which is equal to 1 under 3 kHz and increases to value of 4 from 3 kHz to 20 kHz.

### 2.5 Tonality

Human ear is very sensible to pure harmonic sounds. Parameters which is related to the pitch strength of sound is tonality. Tonality can be calculated by different models, the most common is Aures model [4] and is defined by the following equations Eq. (8-11).

$$T = c \left( \sum_{i=1}^n [q'_1(\Delta z_i) q'_2(f_i) q'_r(\Delta L_i)] \right)^{\frac{0.29}{2}}. \quad (8)$$

$$\cdot \left( 1 - \frac{N_{\text{Gr}}}{N} \right)^{0.79} \text{ [tu]}, \quad (9)$$

$$q'_1(\Delta z) = \frac{0.13}{\Delta z + 0.13}$$

$$q'_2(f) = \left( \sqrt{1 + 0.2 \left( \frac{f}{700} + \frac{700}{f} \right)^2} \right)^{-0.29} \quad (10)$$

$$q'_3(\Delta L) = \left( 1 - e^{-\frac{\Delta L}{15}} \right)^{0.29} \quad (11)$$

## 2.6 Combined psychoacoustic parameters

Combining of aforementioned psychoacoustic parameters has proven useful for prediction of overall sound quality. In this paper two different composed parameters are used that is psychoacoustic annoyance and psychoacoustic pleasantness.

### 2.6.1 Psychoacoustic pleasantness

Aures [5] proposed psychoacoustic pleasantness parameter  $P$  which can be calculated with the following relation:

$$P = e^{-0.55R} e^{-0.113S} (1.24 - e^{-2.2T}) e^{-(0.023N)^2}, \quad (12)$$

where  $R$ ,  $S$ ,  $T$  and  $N$  are roughness, sharpness, tonality and loudness.

### 2.6.1 Psychoacoustic annoyance

Fastl and Zwicker [6] proposed the psychoacoustic annoyance parameter  $PA$  which is calculated from loudness, fluctuation strength, roughness and sharpness:

$$PA = N_5 (1 + \sqrt{w_s^2 + w_{FR}^2}), \quad (13)$$

where  $N_5$  is percentile loudness,  $w_s$  constant describing effect of sharpness Eq. (15) and  $w_{FR}$  constant describing effect of roughness and fluctuation strength Eq. (16). Proposed model was able to estimate annoyance of different noises, however since it neglected tonality it underestimated annoyance of sound with strong tonal components [16]. Improved psychoacoustic annoyance was proposed by Guoging [16] which includes effect of tonality:

$$IPA = N_5 (1 + \sqrt{w_s^2 + w_{FR}^2 + w_T^2}), \quad (14)$$

where  $w_T$  is a constant describing effect of tonality Eq. (17).

$$w_s = \begin{cases} (S - 1.75) 0.25 \lg(N_5 + 10) & S > 1.75 \\ 0 & S < 1.75 \end{cases} \quad (15)$$

$$w_{FR} = \frac{2.18}{N_5^{0.4}} (0.4F + 0.6R) \quad (16)$$

$$w_T = \frac{6.41}{N_5^{0.4}} T \quad (17)$$

## 3. EXPERIMENTAL SETUP

Experiment was carried out to evaluate sound quality of a centrifugal fan which is built-in range hood. Measurements were performed in semi-anechoic chamber (with volume of  $220 \text{ m}^3$ ) as depicted in Fig. 1. Semi-anechoic chamber is in conformity with ISO 3744 [17]. Radial fan was connected with standardized muffler designed in conformity with [18].

For calculating psychoacoustic parameters binaural recording of sound is needed. In this experiment measurement of sound pressure level was obtained from B&K UX-331-

UN microphone array with B&K type 4957 microphones. Measured sound was filtered using head related transfer functions (HRTF) to replicate measurements which should otherwise be made with head and torso simulator (HAT). Functions were obtained from opensource CIPIC HRTF Database [19]. HRTF at zero elevation and for different azimuth angles are shown on Fig. 2.

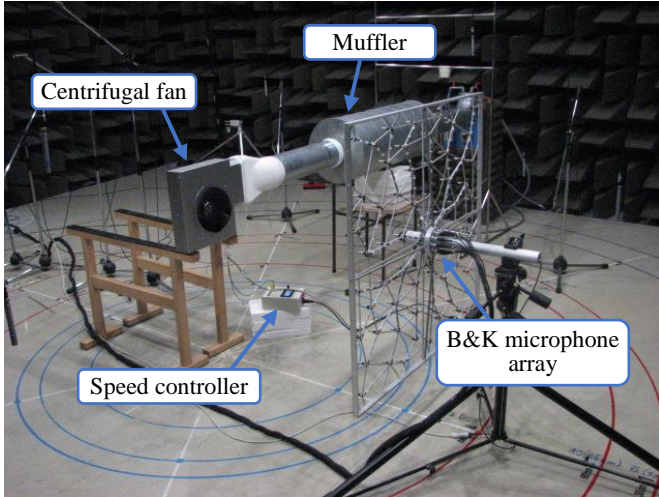


**Figure 1:** Experimental setup in semi-anechoic chamber.

Simultaneously sound power level (SPW) was measured and calculated according to ISO 3744 [17] (20x B&K type 4189 A21 microphones were used). For more information about the system used to measure SPW reader is referred to [20].

Airflow was not measured throughout the presented experiment. Measurements of airflow and overall efficiency were made additionally and are not presented in this paper.

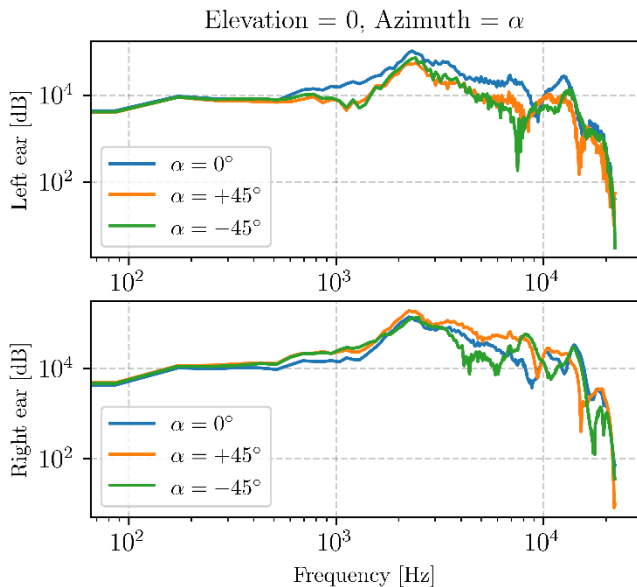


**Figure 2:** Head related transfer functions (HRTF) at different azimuth angles from CIPIC database [19].

### 3.1 Lip geometry

The main source of noise with this type of centrifugal fan is the so called blade passing frequency noise (BPF) [9, 7, 21]. In this paper effect of different designs of lip shape on sound

quality is evaluated at different motor speed settings. Impeller and chasis of the fan stayed the same throughout the whole experiment. Different designs of lip shapes are depicted on Fig. 3.

It is expected that shape 0 design will have the best airflow performance and highest overall SPW. Shape 3 is expected to have the worst airflow efficiency while having the lowest SPW.

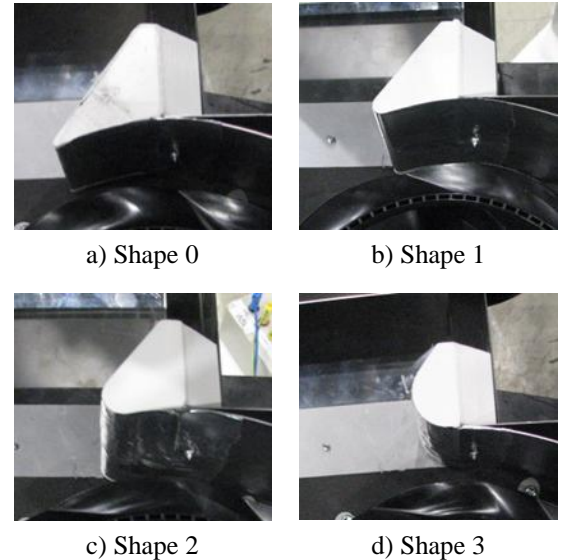


**Figure 3:** Different designs of lip shape at centrifugal fan outlet.

## 4. RESULTS AND DISCUSSION

Sound measurements were made after fan operated for approximately 2 minutes to achieve steady state conditions.

Firstly, sound power levels were compared for different designs of lip shape. Secondly, all psychoacoustic parameters were calculated and compared for different designs of lip shape at five different motor speed settings (12%, 20%, 40%, 60% and 100%). Additionally, psychoacoustic pleasantness and psychoacoustic annoyance were calculated and evaluated.

### 4.1 SPW evaluation

A-weighted sound power level for different design shapes at 100% motor speed setting is shown in Fig. 4. A distinct peak in SPW at 400 Hz can be seen, which is a direct consequence of BPF. At higher frequencies (above 4 kHz) shape 3 has the highest SPW levels.

Fig. 5 represents comparison between each design shape at different speed setting. At low speed settings (12% and 20%) it can be seen that design of lip shape has little to none effect on overall SPW level. However, at higher speed settings (40%, 60% and 100%) a clear improvement in SPW for each subsequent design can be identified.

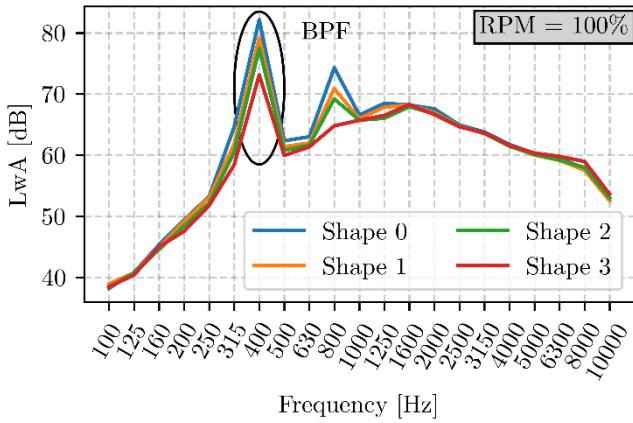


**Figure 4:** Sound power level for different design shapes at 100% motor speed setting.

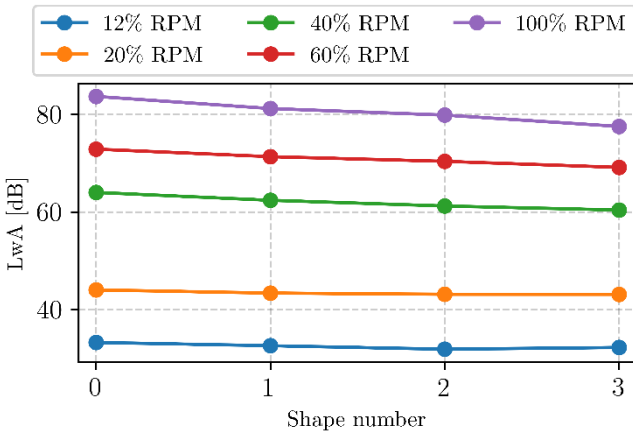


**Figure 5:** Sound power level for each design shape at different motor speed settings.

#### 4.2 Psychoacoustic evaluation

Loudness at 100% motor speed setting is shown in Fig. 6. If loudness is compared with SPW in Fig. 4 it can be concluded that the two parameters are in fact correlated. A peak at 4 Bark (350-400 Hz) is consistent with BPF. At higher frequency range shape 3 design has the highest SPW and loudness levels.

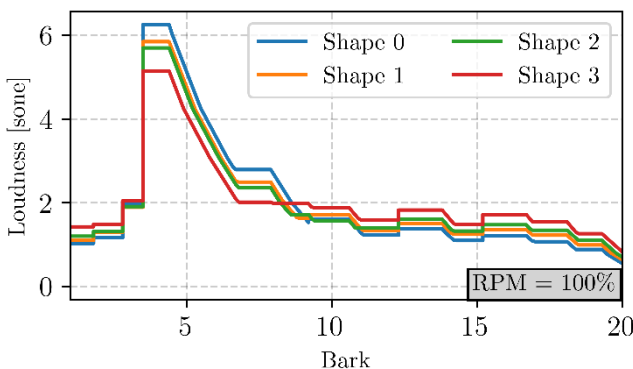


**Figure 6:** Loudness for different design shapes at 100% motor speed setting.

In Fig. 7 loudness for each design shape at different motor speed settings is shown. It can be seen that lip shape has smaller effect on overall loudness level compared with effect on SPW (Fig. 5).

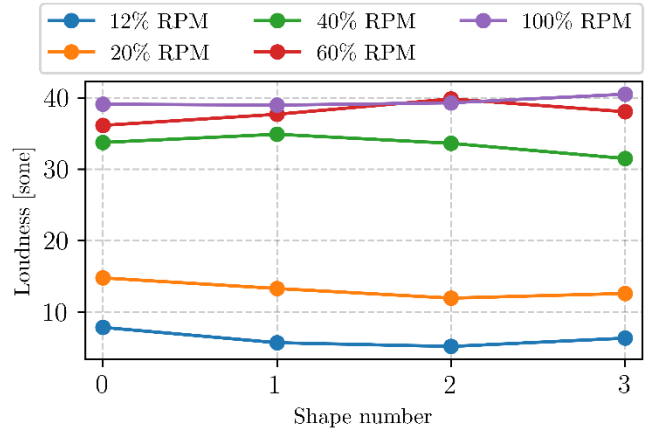


**Figure 7:** Loudness for each design shape at different motor speed settings.

Roughness at 100% motor speed setting is shown in Fig. 8. It can be observed that design of lip shape has negligible effect on roughness.

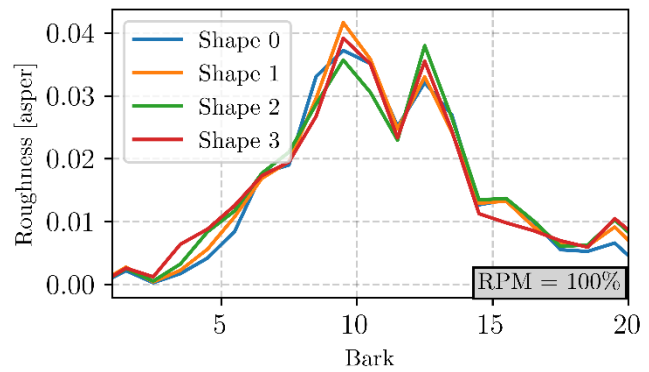


**Figure 8:** Roughness for different design shapes at 100% motor speed setting.

In Fig. 9 fluctuation strength at 100% motor speed settings is shown. At BPF (4 Bark) shape 3 design has the highest fluctuation strength levels. However, overall levels of fluctuation strength are not significant.

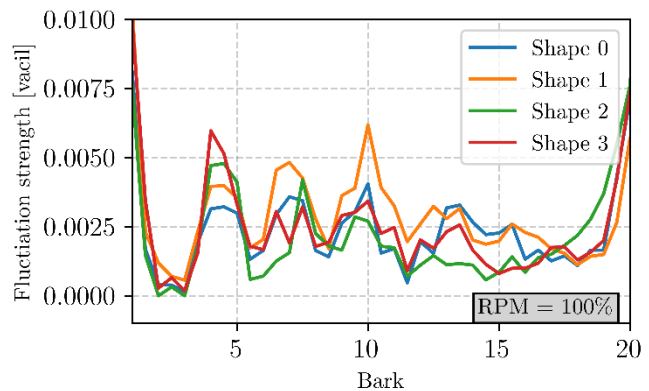


**Figure 9:** Fluctuation strength for different design shapes at 100% motor speed setting.

Sharpness at 100% motor speed setting is shown in Fig. 10. It is evident that at BPF shape 3 design outperforms shape 0 design. However, at higher frequency range shape 3 design has the highest sharpness levels.

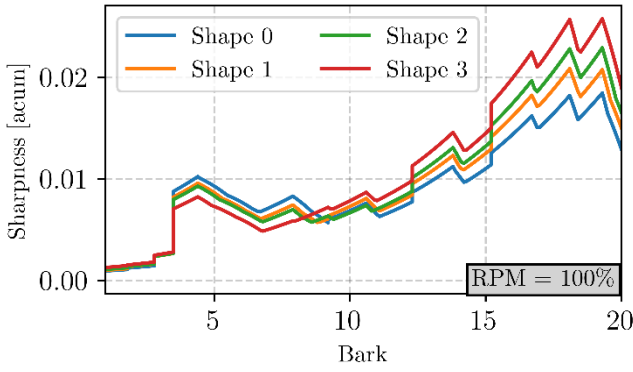


**Figure 10:** Sharpness for different design shapes at 100% motor speed setting.

In Fig. 11 sharpness for each design shape at different motor speed settings is shown. A similar relation can be seen as with overall SPW level (Fig. 5). At lower speed settings design of lip shape has negligible effect on overall sharpness level. On the other hand, at higher speed settings shape 0 design clearly outperforms shape 3 design.

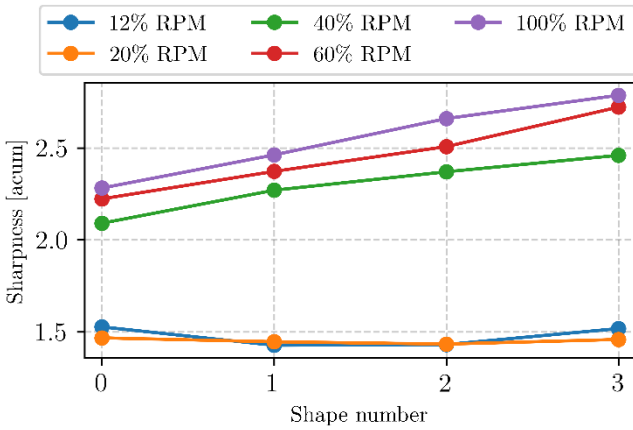


**Figure 11:** Sharpness for each design shape at different motor speed settings.

In Fig. 10 overall tonality level is shown for each design shape at different motor speed settings. At lower speed settings design of lip shape has also negligible effect on overall tonality level. At higher speed settings a clear improvement with shape 3 design can be seen.

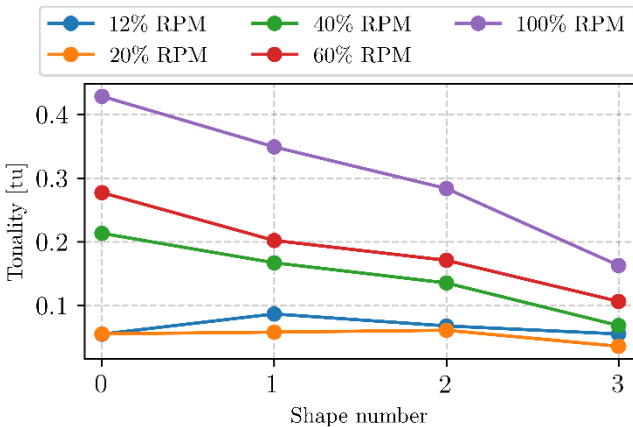


**Figure 12:** Tonality for each design shape at different motor speed settings.

### 4.3 Psychoacoustic annoyance and pleasantness

Psychoacoustic pleasantness has been evaluated according to Eq. (12). In Fig. 13 results are shown for each design shape at different motor speed settings. A distinct similarity can be observed between psychoacoustics pleasantness and SPW shown in Fig. 5. Best overall pleasantness can be recognized from shape 3 design, with exception at the lowest speed setting, where shape 2 has a slightly more pleasant sound.

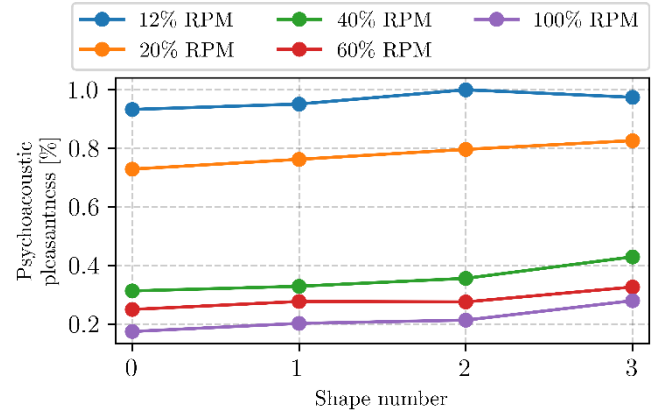


**Figure 13:** Psychoacoustic pleasantness for each design shape at different motor speed settings.

Psychoacoustic annoyance can be evaluated with or without the effect of tonality. In Fig. 14. psychoacoustic annoyance without effect of tonality Eq. (13) is shown. At low speed settings it can be seen that lip design has small to negligible effect on overall annoyance. At higher speed settings it can be seen that shape 3 design shows the highest annoyance levels. This is directly related to sharpness (Fig. 12) and tonality (Fig. 13), Since the basic psychoacoustic annoyance model neglects tonality, shape 3 design will exhibit increased annoyance because of increased sharpness at higher speed settings.

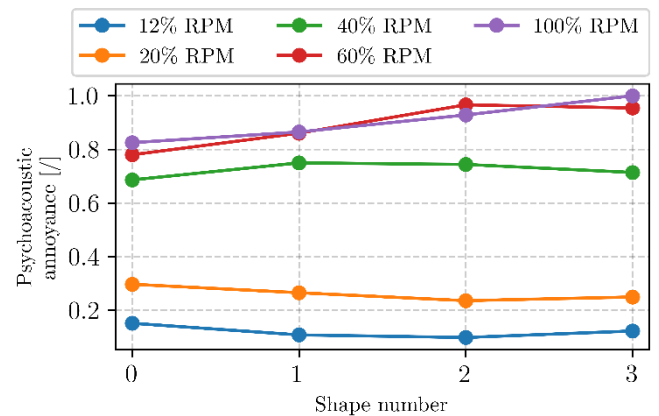


**Figure 14:** Psychoacoustic annoyance for each design shape at different motor speed settings.

Improved psychoacoustic annoyance Eq. (14), which includes the effect of tonality is shown in Fig. 15. It can be seen that at almost all motor speed levels now lip design has almost negligible effect on psychoacoustic annoyance.

The analysis of all psychoacoustics parameters has confirmed that shape 3 design exhibits the most overall pleasant noise and the lowest SPW. However, it can be expected that shape 3 design will have the lowest airflow efficiency which was not evaluated in this paper and should be considered.

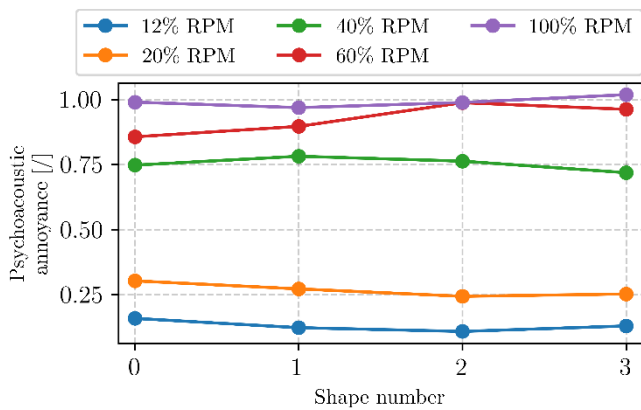


**Figure 15:** Improved psychoacoustic annoyance for each design shape at different motor speed settings.

## 5. CONCLUSIONS

This paper presents a research on effect of different lip design in centrifugal fan on its psychoacoustics performance. Mathematical models of psychoacoustic parameters enable us to objectively quantify the subjective human interpretation of sound. The study revealed that psychoacoustics parameters can be used as an additional design variable when considering sound quality of a product. The last shape design, which had the lowest A-weighted SPW also exhibits the best psychoacoustic pleasantness.

In future work the overall quality of product sound should be evaluated with psychoacoustic experiments. In this experiment person judges the sound quality with semantic differentials (calm-exciting, loud-soft, etc.). Results obtained from experiments should be used to validate current findings.

## REFERENCES

- [1] J. J. Chatterley, J. D. Blotter, S. D. Sommerfeldt, T. W. Leishman, "Sound Quality Assessment of Sewing Machines", *Noise Control Engineering Journal*, vol. 54, pp. 212-220, 2006.
- [2] W. A. Yost, "Psychoacoustics: A Brief Historical Overview", *Acoustical Society of America*, vol. 11, pp. 46-53, 2015.
- [3] E. Zwicker, H. Fastl, "A portable loudness meter based on ISO 532 B", *Proc. 11<sup>th</sup> Int Congr Acoustics*, vol. 8, pp. 135-137, 1983.
- [4] W. Aures, "Sensor euphony as a function of psychoacoustic sensations", *Acustica*, vol. 58, pp. 282-290, 1985.
- [5] W. Aures, "Berechnungsverfahren für den Wohlklang beliebiger Schallsignale, ein Beitrag zur gehörbezogenen Schallanalyse", *PhD thesis*, Munich University, 1994.
- [6] H. Fastl, E. Zwicker, "Psychoacoustics – facts and models", *Heidelberg: Springer-Verlag*, Berlin, 2007.
- [7] M. Boltežar, M. Mesarić, A. Kuhelj, "The influence of uneven blade spacing on the SPL and noise spectra radiated from radial fans", *Journal of Sound and Vibration*, vol. 4, pp. 697-711, 1998.
- [8] W.H. Jeon, et. al., "Analysis of the aeroacoustic characteristics of the centrifugal fan in vacuum cleaner", *Journal of Sound and Vibration*, pp. 1025-1035, 2003.
- [9] W. Neise, "Noise reduction in centrifugal fans: a literature survey", *Journal of Sound and Vibration*, vol. 45, pp. 375-403, 1976.
- [10] W. Neise, "Review of noise reduction methods for centrifugal fans", *J Eng. Ind.*, vol. 151, pp. 151-161, 1982.
- [11] E. Zwicker, K. Deuter, W. Peisl, "Loudness meters based on ISO 532 B, with large dynamic range", *Proc Internoise 85*, vol. 2, pp. 1119-1122, 1985.
- [12] ISO 532B, "Method for calculating loudness level", 1975.
- [13] DIN 45631, "Berechnung des Lautstärkepegels und der Lautheit aus dem Geräuschspektrum", 1991.
- [14] H. Fastl, "Beschreibung dynamischer Hörempfindungen anhand von Mithörschwellen-Mustern", *Hochschul-Verlag*, 1982.
- [15] G. Von Bismarck, "Sharpness as an attribute of the timbre of steady sounds", *Acustica*, vol. 30, pp. 159-172, 1974.
- [16] D. Guoqing, "An improved psychoacoustic annoyance model based on tonal noises", *Internoise*, pp. 21-24, 2016.
- [17] ISO 3744, "Acoustics -- Determination of sound power levels and sound energy levels of noise sources using sound pressure -- Engineering methods for an essentially free field over a reflecting plane", 2012.
- [18] IEC 60704-2-13, "Household and similar electrical appliances - Test code for the determination of airborne acoustical noise - Part 2-13: Particular requirements for range hoods", 2016.
- [19] S. Lee, S. Heo, C. Cheong, "The CIPIC HRTF Database", *IEEE Workshop on Applications of Signal Processing to Audio and Electroacoustics*, pp. 21-24, 2001.
- [20] N. Holeček, "Modeliranje aerodinamičnih lastnosti kondenzatorjev sušilnih strojev nove generacije", *Ph.D. thesis*, Faculty of mechanical engineering, University in Ljubljana, 2006.
- [21] V.R. Algazi, R. O. Duda, D. M. Thompson, C. Avendano, "Prediction and reduction of internal blade-passing frequency noise of the centrifugal fan in a refrigerator", *International Journal of Refrigeration*, vol. 30, pp. 1129-1141, 2010.



## NOISE SENSITIVITY AMONG SURFACE MINERS AND UNDERGROUND MINERS

*Milan Veljković, Snežana Živković*

University of Nis, Faculty of Occupational Safety, Serbia, milan.veljkovic@znrfak.ni.ac.rs

**Abstract** - Mining is a branch of economy with a large number of occupational hazards. Miners are exposed to a number of risk factors at work. For physical factors, they are exposed to extremely high noise. The survey was conducted on a sample of 108 employees at the mine "Lece", which differed in terms of age, years of service and workplace. Questionnaire used in this study were: Weinstein's Noise Sensitivity Scale that measured subjective noise sensitivity, consisting of 21 statements with proposed degrees of agreement. Noise annoyance was measured with a self-rating ten-graded scale. A short general questionnaire referred to age, years of service and workplace. The results showed that a positive relation between noise sensitivity and reported noise annoyance was highly significant in both workplaces. No significant differences in average noise sensitivity scores with respect to age and years of service were found between the underground and surface mining workplace. There is negative correlation between years of service and self-report noise annoyance in underground mining workplace.

### 1. INTRODUCTION

Mining is one of the oldest economic activities. In itself, it is dangerous and destructive, both for environment and for man. Every day of work in the mine is different from the previous one and poses a danger to itself, since moving through the long distance cave room leads to strange and dangerous things, which certainly complicates the functioning of the security system and the protection of miners lives. In spite of undertaking comprehensive measures to fulfill the safe work, in certain situations, there may be increased risks due to the reduced functionality of the person himself. No working position is completely safe and secure, in addition to all the protection measures taken. Therefore, all employees must be informed daily about existing hazards and ways of preserving their own health and safety. To have personal protection, a person must be aware of the risk, because awareness of the risk is strengthened by the defense forces of our organism. The key considerations regarding safety at work in the mine relate to safe mining technology, the problem of dust, noise, vibration and chemicals. Miners are exposed to a number of risk factors at work. For physical factors, they are exposed to extremely high noise. Occupational noise in mines originates from mining equipment and processes such as blasting, drilling, excavating and crushing [1]. noise levels range from 85db to 106 db, and a study shows that this noisy environment within 10m is potentially detrimental to health

[1]. The main aim of the research was to establish if there is a correlation between the noise sensitivity and the noise annoyance of miners that work in the underground and surface mining.

### 2. NOISE SENSITIVITY AND ANNOYANCE

The noise is defined as any unwanted sound in the environment where people live and work, which causes discomfort or may adversely affect the health. Auditory environmental pollution, generally referred to as noise, is one of the most common physical stressors. The negative effects of noise are widespread. Noise is an unwanted or unpleasant sound phenomenon that affects the mental and physical status of human beings, plasters and reduces labor productivity and the rest of people and creates anxiety and mood when it is of a certain intensity. Noise is pervasive in everyday life and can cause both auditory and non-auditory health effects. People are usually not passive recipients of sound irritation and can develop coping strategies to reduce noise impact. If people do not like the noise, they can take steps to avoid it by moving away from a noisy environment, or if you are unable to move, by developing coping strategies. There is a common denominator, however: unwanted sound. Harmful effects of noise depend on its characteristics, as well as time exposure, weather volatility and direction of the noise, and finally the individual susceptibility of the person exposed to that noise. One of the main characteristics that affect the assessment of noise as unwanted is their volume or experienced intensity. The volume consists of sound intensity, tonal sound distribution and duration. The sound is necessary but not sufficient to produce the noise. The psychological component of sound and its physical components play a key role in noise perception.

The results of several studies suggest that the physiological effects and the health complaints are more closely associated with the subjective reactions to noise than with the physical characteristics of the noise. [1], [2]. Psychological factors have a greater effect on noise as a stressor( 50%) than actual physical characteristics and noise exposure( 9- 29%) [3]. Sound level is only a minor factor in response to noise. Although social studies often report a positive correlation between noise intensity and the average level of sensed annoyance, intensity alone rarely explains more than one-quarter of the variance in individual annoyance. Stansfeld[2] concluded that "noise sensitive people attend more readily to

noise, perceive more threat from noise and may react to noise more than less sensitive people, perceiving noise as an environmental threat and lack of environmental control and are less adaptable to noise than people who are less sensitive". For the assessment of the harmful effects of noise and the through undertaking certain measures of protection in specific circumstances, it is necessary to determine certain parameters of noise measurement. Measurements of noise can be subjective and objective. Objective measurements mean the determination and monitoring of the physical parameters relevant to the state of the environment in which the noise occurs. Objective measurements are made using a variety of instruments and appliances. The second group consists of subjective measurement methods aimed at assessment of disturbing and harmful noise effects. The conditions under which measures noise parameters must be uniform and sufficiently well-known to each other and the results were comparable.

Noise causes the organism to have many vegetative, visceral and psychological reactions. They are not equal in all animals and in all people and can range from mild transient symptoms to violent reactions and severe permanent damage, all of which depend on the intensity and characteristics of noise in most cases. If the noise exposure is chronic and exceeds certain levels, the negative health consequences can be observed. Although people tend to get used to the noise exposure, those able to fully adapt are rare. Harmful effects of noise depend on its characteristics, as well as time exposure, weather volatility and direction of the noise, and finally the individual susceptibility of the person exposed to that noise. One of the main characteristics that affect the assessment of noise as unwanted is their volume or experienced intensity. The volume consists of sound intensity, tonal sound distribution and duration. The degree of adaptation to noise differs from person to person [4].

The vibrations are seen as an addition to loud noise. In most studies of noise they are found to be an important factor in determining the inconvenience, especially because they are usually perceived through the other senses. Fields [5] found that, after controlling the level of noise, the disturbance caused by noise increases with the fear of the dangers of noise sources, sensitivity to noise, the belief that the noise cannot be controlled, awareness of others (unremarkable) impacts and the belief that the source of the noise is not important. The perception of the noise source control can reduce the risk of noise and the belief that it can be harmful.

Weinstein [4] concluded that a critical or uncritical attitude to the assessment of environmental stressors explained a significant part of the experience of anxiety caused by noise. The tendency to be critical is associated with greater susceptibility to noise and greater sensitivity to other stressors from the environment. The people who are critical toward the stressors better discriminate the degree of the presence of stressors and have more negative attitudes toward them compared to the people who do not have a critical attitude.

### 2.1.1. Noise sensitivity

There are an extensive variety of ways to determine noise sensitivity. According to Stansfeld [6] it is a measure of attitudes to noise in general. It constitutes a personality trait

covering attitudes towards an extensive variety of environmental noises [6]. Noise sensitivity is more probable related to disposition to respond to noise in general than to the physical properties of noise [7]. Noise sensitivity is a predictor of annoyance [6]. Job (1999) refers to physiological and psychological internal states of any individual, which increase the degree of reactivity to noise in general. Noise sensitive people pay more readily attention to noise, perceive more threat from noise and may respond more to noise than less sensitive people [6]. Noise sensitivity and annoyance are considered to be related but not identical concepts [7]. Noise sensitivity can be determined as a personality trait covering attitudes towards noise in general and as a predictor of annoyance. The main refinement is that while annoyance is related to noise level, sensitivity is definitely not. According to [8] annoyance has in the same way been resolved as a multifaceted psychological concept, covering immediate behavioral noise effects aspects, like disturbance and interfering with intended activities, and evaluative aspects like "aggravation", "nuisance", "disturbance", "unpleasantness", and "repulsiveness". In spite of the fact that annoyance is related to acoustic factors, they don't assume play an overwhelming role in the concept of annoyance. The key distinction is that while annoyance is related to noise level, sensitivity is not.

## 3. METHODS AND INSTRUMENTS

The survey was conducted on a sample of 108 employees at the mine "Lece", which differed in terms of age, total work experience, working hours in the mine, level of education and workplace (miners that works in underground mining and miners that works on surface). Questionnaire used in this study were: SNS was assessed with the Weinstein's Noise Sensitivity Scale [9], consisting of 21 statements with proposed degrees of agreement. Noise annoyance was measured with a self-rating ten-graded scale. Grade 1 represented "not annoyed", while grade 10 represented extreme annoyance. A short general questionnaire referred to age, total work experience, working hours in the mine, level of education and workplace.

### 3.1. Data analysis

For determination of scores on SNS descriptive statistics has been used (Table 1). To determine the correlation between the variables, Pearson's correlation coefficient correlation techniques were used. For determination of the difference between groups, the ANOVA technique was used.

**Table 1.** Scores on Noise sensitivity scale.

	N	M	Min	Max
Noise sensitivity	108	43	94	69.92

## 4. RESULTS

Normal distribution of the scores on the Noise Sensitivity Scale was both in the underground mining and in surface mining.

Conversely, the distribution of scores on the Noise Annoyance Scale was asymmetrical, with the grouping

towards higher scores in the underground mining, and towards lower scores in surface mining workplace.

Positive relation between Noise Sensitivity Scale and reported noise annoyance was highly significant in both areas (Pearson  $r = 0.475$  and  $0.224$ ,  $P < 0.00016$  (Table 2 and Table 3).

#### Underground workplace - medium correlation

**Table 2.** Correlation between noise sensitivity scale and noise annoyance and in underground mining workplace.

		Noise annoyance	Noise Sensitivity Scale
Noise annoyance	Pearson Correlation	1	,475
	Sig. (2-tailed)		,000
	N	108	108
Noise Sensitivity Scale	Pearson Correlation	,475	1
	Sig. (2-tailed)	,000	
	N	108	108

#### Surface workplace - low correlation

**Table 3.** Correlation between noise annoyance and noise sensitivity scale in surface mining workplace.

		Noise annoyance	Noise Sensitivity Scale
Noise annoyance	Pearson Correlation	1	,224
	Sig. (2-tailed)		,000
	N	108	108
Noise Sensitivity Scale	Pearson Correlation	,224	1
	Sig. (2-tailed)	,000	
	N	108	108

No significant differences in average noise sensitivity scores with respect to age and years of service were found between the underground and surface mining workplace (Table 3).

**Table 3.** ANOVA Between groups Age, Years of service and Workplace

		F	Sig
Age	Between groups	3,208	,021
Years of service	Between groups	2,150	,042
Workplace	Between groups	3,341	,041

There is negative correlation between years of service and self-report noise annoyance in underground mining workplace (Pearson  $r=-0.416$ ,  $p<0.05$ ) (Table 4).

**Table 4.** Correlation between noise annoyance and years of service.

		Noise annoyance	Years of service
Noise annoyance	Pearson Correlation	1	-,416
	Sig. (2-tailed)		,027
	N	108	108
Noise Sensitivity Scale	Pearson Correlation	-,416	1
	Sig. (2-tailed)	,027	
	N	108	108

## 5. CONCLUSION AND DISCUSSION

According to Stansfeld [6] noise sensitivity is a measure of attitudes to noise in general. It constitutes a personality trait covering attitudes towards a wide range of environmental noise. The way that subjects were all students, obviously, demonstrates that they have possessed the capacity to adapt and adjust to commotion levels of noise in both locations. This study showed that subjective noise sensitivity was a personality variable independent of noise exposure. Age has been widely investigated as determinants of noise annoyance, but frequently conflicting results are reported. Some studies have found that noise sensitivity increases with age [7], [10]. According to Moreira Belojevic [11] noise sensitivity does not depend upon age. In this study no significant differences in average noise sensitivity scores with respect to age and gender were found between the noisy area and not-noisy environment. Regardless, these factors are applicable as intermediaries for different variables that adjust the individual's perception of and reactions to environmental stimuli. Other factors, which may have limited any chances of significance, are the limited sample size. More noise sensitive subject reported more noise annoyance what is logic. In general annoyance is defined as a feeling of displeasure that is tied to a cause that is believed to affect negatively an individual or a group of individuals. The non-auditory effects of noise are generally viewed as stress-related. Annoyance is one of the first reactions to environmental noise [12]. Annoyance reactions to noise have often been associated with reported interference of noise in everyday activities [6]. Annoyance is also the most common outward symptom of stress in individuals exposed to noise. Annoyance is correlated with noise sensitivity [13], [10], [6], [14]. Noise sensitivity increases annoyance independently from, and above, level of noise exposure. Noise sensitive individuals are likely to be more annoyed by noise than non-noise sensitive individuals at all noise levels [15]. Highly noise sensitive subjects have demonstrated significantly higher noise annoyance in high noise areas [14],[6]. In a future study, it would be desirable to explore other problems related to noise such as personal experience of noise as a stress factor in relation to physical characteristics and noise exposure itself. Future research should examine how much time is needed for adaptation to the noise, increase sample size, ask people whether do they live in urban or rural area and assign personality test, for motivation and sleeping quality questionnaire.

## REFERENCES

- [1] Donoghue AM, Frisch N, Olney D. Bauxite mining and alumina refining: process description and occupational health risks. *J Occup Environ Med.* 2014;56(5 Suppl):S12-7.
- [2] Passchier-Vermeer, W., & Passchier, W. F. (2000). Noise exposure and public health. *Environmental Health Perspectives Supplements*, 108, 123–131.
- [3] Stansfeld, S., Haines, M., & Brown, B. (2000, 43–82). Noise and health in the urban environment. *Reviews on Environmental Health*, 15.
- [4] Bell, P. A., Greene, T. C., Fisher, J. D., & Baum, A. (2001). Environmental psychology.
- [5] Weinstein, N.D. (1980). Individual differences in critical tendencies and noise annoyance. *J. Sound Vib.*, 68, 241–248.
- [6] Fields JM. (1984). The effect of numbers of noise events on people's reactions to noise. An analysis of existing survey data. *J Acoust Soc Am*; 75: 447–67
- [7] Stansfeld, S. V. (1992). Noise, noise sensitivity and psychiatric disorder: epidemiological and psychophysiological studies. *Psychological Medicine Monograph Supplement*, 22, 1–44.
- [8] Nivison, M. E., & Endresen, I. M. (1993). An analysis of relationship among environmental noise, annoyance and sensitivity to noise, and the consequences for health and sleep. *Journal of Behavioral Medicine*, 16, 257–276.
- [9] Guski, R., Felscher-Suhr, U., & Schuemer, R. (1999). The concept of noise annoyance: how international experts see it. *J of Sound Vibration*, 223, 513–527.
- [10] Weinstein, N. D. (1978). Individual differences in reaction to noise: a longitudinal study in a college dormitory. *Journal of Applied Psychology*, 63, 458-466.
- [11] Matsamura Y, Rylander R. Noise sensitivity and road traffic annoyance in a population sample. *J Sound Vib* 151, 415–419, 1991
- [12] Belojevic G, Slepcevic V, Jakovljevic B. Mental performance in noise: the role of introversion. *J Environ Psychol* 21 (2), 209–213(5), 2001.
- [13] Ouis D. Annoyance caused by exposure to road traffic noise: an update. *Noise Health* 4(15), 69–79, 2002.
- [14] Lopez Barrio I, Carles JL . Subjective response to traffic noise. The importance given to noise environment in choosing a place of residence. In *Noise as a Public Health Problem* (M. Vallet editor) 2, France, Arcueil, 1993, 205–208.
- [15] With regard to neurophysiological sensitivity, subjective noise sensitivity and personality variables. *Psychol Med*, 118, 605–613, 1988a.
- [16] Van Kamp I, Job RF, Hatfield J, Haines M, Stellato RK, Stansfeld SA. The role of noise sensitivity in the noise-response relation: a comparison of three international airport studies. *J Acoust Soc Am* 116(6), 3471–3479, 2004.



## MODELING BASIC NOISE INDICATORS OF ENVIRONMENTAL NOISE FOR THE PERIOD 1985 - 2010

*Emil Živadinović<sup>1</sup>, Marija Jevtić<sup>1,2</sup>, Sanja Bijelović<sup>1,2</sup>, Nataša Dragić<sup>1,2</sup>, Siniša Milošević<sup>1</sup>, Živojin Lalović<sup>1</sup>*

<sup>1</sup> Public Health Institute of Vojvodina, Novi Sad, Serbia, [emil.zivadinovic@izjzv.org.rs](mailto:emil.zivadinovic@izjzv.org.rs)

<sup>2</sup> University of Novi Sad, Faculty of Medicine, Novi Sad, Serbia

**Abstract** - Noise is recognized as a physical hazard in the environment, it causes adverse effects to human health and it is also potentially harmful form of energy in the environment. Although the hazards and the risks to human health from noise are generally much higher in the occupational, however, the exposure of the entire population to the different frequencies environmental noise for a long time, leads to population health impairments, which is in the field of the research of medical ecology. The noise measurement results in the City of Novi Sad (NS) since 1985, show that the environmental noise, dominated from road traffic, is a long-lasting physical hazard. Since 2011, the experts from the Public Health Institute of Vojvodina (IZJZV) conduct 24-hour outdoor environmental noise measurements and directly determine the values of basic noise indicators ( $L_{day}$ ,  $L_{evening}$ ,  $L_{night}$ ,  $L_{den}$ ). In order to examine the environmental noise as a physical hazard and in order to determine the percentage of the population annoyed by noise for a long time, based on the 387 analyzed 24-hour noise measurements in the period 2011-2016, using linear regression, in this paper we established the predictive equations for determining the basic noise indicators. The equations are used in the purpose of modeling the basic noise indicators for the period 1985-1990. For that time period, IZJZV possess the equivalent noise levels ( $L_{Aeq}$ ) from a series of 15-minute measurements. Using this approach of modeling, we achieve the quality insight into the environmental noise levels and the population annoyance by the noise in the NS for a period of three decades.

### 1. INTRODUCTION AND THE AIM OF THE WORK

#### 1.1 Introduction

The environmental noise is, due to European Noise Directive (END), unwanted / harmful outdoor sound created by human activities, including noise emitted by means of transport, road traffic, rail traffic, air traffic, and from sites of industrial activity [1]. Except it is subjectively disagreeable, noise is recognized as a physical hazard from environment, it causes adverse effects to human health and it is also potentially harmful form of energy in the environment. Although the hazards and the risks to human health are generally much higher in the occupational [2], however, the exposure of the

entire population to the different frequencies environmental noise for a long time, leads to population health impairments, which is in the field of the medical ecology research. The noise effect on humans depends on many factors - noise level, duration, frequency, variability over the time, time when a man is exposed (day, evening, night), individual sensitivity, health condition and mental health. The basic classification of noise effects on humans is: the effect on the hearing system - the auditory effect of noise and the effect on other organs and organic systems - the extraauditive noise effect.

According to contemporary scientific insights of the World Health Organization (WHO), the European Environment Agency (EEA) and the Environmental Protection Agency (EPA), environmental noise is recognized as a factor that leads to anxiety, hearing impairments, sleep disturbance, cognitive disorders in children and cardiovascular diseases. The environmental noise is, also, a stressogenic factor that affects human mental health as well [3].

Noise makes difficult to people perform complex tasks, change their social behavior and cause annoyance. The noise is a psychosocial stressor and activates the sympathetic and endocrine system [4]. During the response to stress, the hormonal system of hypothalamic-pituitary-adrenal axis is activated. That results in increased secretion of catecholamines, such as adrenaline, and corticosteroids, such as cortisol. This hormonal imbalance, speeds up heart rate and increases the blood pressure, also affects many other metabolic processes in the body. Therefore, noise is recognized as a risk factor for myocardial infarction, because it is a stressor, activating the hormone system, also, noise potentiates the most significant risk factors for this myocardial infarction, such is an arterial hypertension [5].

Exposed to noise, people are annoyed and disturbed. Introverts had more pronounced subjective effects of annoyance, poor concentration and fatigue during mental performance in noise compared to quiet conditions [6]. Residents living in the neighborhood of the airports and noisy streets are frequently complained of headache, and have a feeling of tension and tiredness. High levels of aircraft noise were associated with increased risks of stroke, coronary heart disease, and cardiovascular disease for both hospital admissions and mortality in areas near large airports [7].

The studies showed that respondents from noisy area significantly more often reported difficulty in falling asleep, being woken up, poor sleep quality, tiredness after sleep, and use of sleep medication than residents from quiet areas. The sleep disturbance is the major health effect of urban environmental noise. Also, it is known that noise may restrict the use of parts of the house, prevent windows or doors from being opened, and cause distraction when reading, writing, or having a conversation [8, 9].

WHO estimates, in total, the number of deaths linked to the unhealthy environments amounts to 12.6 million per year (based on 2012 data). WHO also estimates that 23% of global deaths are due to environmental factors [10]. Results indicate that at least one million healthy life years are lost every year from traffic related noise in the western part of Europe (DALYs - disability-adjusted life-years) [11]. For the City of Belgrade, it is estimated that total DALY due to road traffic noise equals 107 years / million inhabitants [12].

Based on one published research, daytime traffic noise affects heart diseases in 3% of all heart disease cases, night time background noise causes sleep disturbance in 2% of all Europeans, total noise causes annoyance of 15% of all Europeans, traffic noise causes 3% of all tinnitus cases, daytime and night-time noise leads to slower learning by children in 0,01%, and, also, loud music causes in hearing loss from "leisure noise" in 1,8% of 7 to 19 year olds in Europe [13].

In one Serbian cross sectional interview study, it is showed that highly noise disturbed adult male residents were under increased risk of arterial hypertension and myocardial infarction, compared to subjects slightly annoyed, or not annoyed by noise [14]. During 2006, the average daytime noise of 69 dB in the City of Novi Sad was a contributing factor to the burden of ischemic heart diseases in 14% of cases [15]. Another study has identified the presence of public transport at daytime and at night as a significant and independent predictor of high noise annoyance [16].

Recent studies on long term noise exposure, especially night noise  $\geq 55$  dB, have reported relationship with pathogenesis of male infertility. Large epidemiological studies on community noise have reported its relationship with breast cancer, stroke, type 2 diabetes, and obesity [17]. Further research is needed to examine coping strategies and possible health consequences of adaptation to noise [18].

### 1.2 The aim of this work

The aim of this paper is to show the model of using historical data on environmental noise measurements. These data can be used for modeling basic noise indicators. Using this approach of modeling, we achieve the quality insight into the environmental noise levels, and also into the population annoyance by noise for a period of three decades. These approach shows that the environmental noise, dominated from road traffic, is a long-lasting physical hazard in the urban city of Novi Sad.

## 2. MATERIALS AND METHODS

### 2.1 Environmental noise measurements in Novi Sad for the time period 1985- 2010

The city of Novi Sad is the largest city in the AP Vojvodina. The City is administrative, cultural, scientific, medical, university and political center center, while 300.000 of people is exposed to the environmental noise levels shown in this paper.

Public Health Institute of Vojvodina (IZJZV) possess an environmental noise data since 1985, to the present day. For the time period 1985 - 2010, data are available in the form of average daily / monthly / annual equivalent noise levels ( $L_{eq}$ )

The oldest available reports in the archives of the IZJZV about measuring environmental noise in Novi Sad date from April 1985. Since 1985, environmental noise measurements were carried out each month in three day intervals (06:30, 14:00, 17:00) on two measuring sites in the course of a single day. Night-time measurements were conducted in two intervals (0:30, 03:30) on all measuring sites where day-time measurements were done. With minor changes, this methodology was maintained until 2011. Ever since then, 24-hour measurements have been conducted. At all times, noise measurements were accompanied by counting number of vehicles on the streets, and, also, measuring of microclimatic parameters.

In regard to equipment used for measuring noise levels, records show that in the period 1985 – 1989 the Noise level meter Type 2205 by Brüel and Kjær was used, from 1990 to 2002, the Brüel&Kjær 4427 was used, from 2002 to 2009 the Brüel & Kjær 2260 Investigator was used with the 4231 type calibrator, condenser microphone type 4189 and the Software Noise Explorer Type 7815 Version 4.15.

Since April 2009, the IZJZV has been using a system which consists of: The Brüel&Kjær Noise meter type 2250, Brüel&Kjær type 3535-A (a protective case that acts as physical protection equipment), Brüel&Kjær Outdoor Microphone type 4952, BZ 5503 Utility Software and the Noise Explorer Type 7815 Software.

From 1985 to 2017, environmental noise in the City of Novi Sad was measured at more than forty measuring sites. Measuring sites have been changed in time, because of the request of city administration or because of technical problems (equipment safety, availability of electricity, works under construction...)

## 2.2 Methodology of modeling basic noise indicators for the time period 1985- 2010

In order to examine the environmental noise as a long-lasting physical hazard, also in order to identify the percentage of population annoyed by noise, we established the predictive equations for modeling basic noise indicators ( $L_{day}$ ,  $L_{night}$ ,  $L_{evening}$ ,  $L_{den}$ ). We analyzed 387 24-hour noise measurements from the latest period (2011-2016), and established the predictive equations applying the linear regression. The equations are used in the purpose of modeling the basic noise indicators for the period 1985-1990. For that time period, IZJZV possess the equivalent noise levels ( $L_{Aeq}$ ) from a series of 15-minute measurements. Using this approach of modeling, we achieve the quality insight into the environmental noise levels and the population annoyance by the noise in the city for a period of three decades.

The established predictive equations are:

$$L_{day} = L_{Aeq} \cdot 1,003 + 1,110$$

$$L_{evening} = L_{Aeq} \cdot 0,949 + 2,820$$

$$L_{night} = L_{Aeq} \cdot 0,993 - 3,718$$

Coefficients of determination for the given equations is:  $R^2=0,96$  for  $L_{day}$  equations ;  $R^2=0,63$  for  $L_{evening}$  and  $R^2=0,67$  for  $L_{night}$ .

Note:  $L_{den}$  is calculated from the modeled basic noise indicators using the standard equation:

$$L_{den} = 10 \lg \left[ \frac{1}{24h} (t_{day} \cdot 10^{0,1L_{day,12}} + t_{evening} \cdot 10^{0,1(L_{evening,4+5dB})} + t_{night} \cdot 10^{0,1(L_{night,8+10dB})}) \right] dB$$

## 3. RESULTS

This paper shows measured annual equivalent noise levels ( $L_{eq}$ ), and then the modeled values of the basic noise indicators for one representative measuring site used in 1985 - 2010, "Novo Naselje" in Novi Sad.

The position of the measuring point within the "Novo Naselje" has been moved during decades (the reasons are City administration demands, and also technical issues, electricity, works under construction). For that reason, only shown data in this paper are for the year when the measuring point was located near "the Stoteks store" at Jovan Dučić Boulevard, or closer to the corner of Boulevard Jovan Dučić and Bate Brkić Street (Table 1).



**Fig. 1** Historical photo, measuring site "Novi Naselje" in 2009, Novi Sad / View to the corner of Jovan Ducic Boulevard and Bate Brkic Street

**Table 1** Measured annual equivalent noise levels ( $L_{eq}$ ) and modeled values of the basic noise indicators for one representative measuring site used in 1985 - 2010, "Novo Naselje" in Novi Sad

Year	Measured values / dB	Modeled values of the basic noise indicators / dB			
	* Annual equivalent noise levels ( $L_{eq}$ )	$L_{day}$	$L_{evening}$	$L_{night}$	$L_{den}$
1985	69,0	70,3	68,3	64,8	72,8
1986	69,0	70,3	68,3	64,8	72,8
1987	68,0	69,3	67,4	63,8	71,8
1988	68,2	69,5	67,5	64,0	72,0
1989	69,1	70,4	68,4	64,9	72,9
1990	-	-	-	-	-
1991	-	-	-	-	-
1992	-	-	-	-	-
1993	-	-	-	-	-
1994	-	-	-	-	-
1995	69,0	70,3	68,3	64,8	72,8
1996	60,0	61,3	59,8	55,9	63,9
1997	62,0	63,3	61,7	57,8	65,9
1998	66,0	67,3	65,5	61,8	69,8
1999	63,0	64,3	62,6	58,8	66,9
2000	64,0	65,3	63,6	59,8	67,9
2001	65,0	66,3	64,5	60,8	68,8
2002	63,0	64,3	62,6	58,8	66,9
2003	61,0	62,3	60,7	56,9	64,9
2004	63,0	64,3	62,6	58,8	66,9
2005	62,3	63,6	61,9	58,1	66,2
2006	-	-	-	-	-
2007	-	-	-	-	-
2008	64,9	66,2	64,4	60,7	68,7
2009	65,5	66,8	65,0	61,3	69,3
2010	64,6	65,9	64,1	60,4	68,4

\* Sources of data: IZJZV reports for the period 1985 - 2010

Note: the environment noise in the City of Novi Sad, the subject of this paper, is the road traffic noise. There are no data about railway noise or air traffic noise in Novi Sad - Novi Sad has no airport, also, rail traffic is not monitored, the railroad does not pass through parts of the city covered by environmental noise monitoring network.

The Serbian national norm from 2010 [19] prescribes the equation for calculating the percentage of highly annoyed population (% HA) by road traffic noise.

$$\% \text{ HA} = 9.868 \cdot 10^{-4} \cdot (L_{\text{den}} - 42)^3 - 1.436 \cdot 10^{-2} \cdot (L_{\text{den}} - 42)^2 + 0.5118 \cdot (L_{\text{den}} - 42)$$

Based on modeled data from previous decades, it is assessment that highly annoyed population percentage (%HA) by road traffic noise in "Novo Naselje", Novi Sad, for time period 1985 - 2010, is in the range 16 - 31% (table 2).

**Table 2** The assessment of highly annoyed population percentage (% HA) by road traffic noise in "Novo Naselje", Novi Sad, 1985 - 2010

Year	Modeled values / dB / $L_{\text{den}}$	Highly annoyed population percentage (%HA)
1985	72,8	31
1986	72,8	31
1987	71,8	29
1988	72,0	29
1989	72,9	31
1990	-	-
1991	-	-
1992	-	-
1993	-	-
1994	-	-
1995	72,8	31
1996	63,9	15
1997	65,9	18
1998	69,8	24
1999	66,9	19
2000	67,9	21
2001	68,8	22
2002	66,9	19
2003	64,9	16
2004	66,9	19
2005	66,2	18
2006	-	-
2007	-	-
2008	68,7	22
2009	69,3	23
2010	68,4	22

#### 4. DISCUSSION

The possibility of using these predictive equations for modeling basic noise indicators ( $L_{\text{day}}$ ,  $L_{\text{evening}}$ ,  $L_{\text{night}}$ ,  $L_{\text{den}}$ ) should be examined on the example of some other noise data from some other communities.

Once again, it should be noted, the predictive equations were established applying the linear regression, using analyzed 387

24-hour noise measurements from the latest period (2011-2016), and variability of  $L_{\text{day}}$  can be explained by this equation in 96% of cases, and variability  $L_{\text{evening}}$  and  $L_{\text{night}}$  in two thirds of cases (relative to the  $L_{\text{eq}}$  in the 24-hour period). However, the one model that can predict every possible scenario with 100% security - does not exist. Therefore, this model can be improved. Different predictive equations can be established, e.g. for the measured noise levels ( $L_{\text{eq}}$ ) in the ranges of 50-55dB, 55-60 dB, 60-65 dB, 65-70 dB and > 70 dB. Of course, all of this can be done if there exists a need for better processing of historical data.

This paper presents that highly annoyed population percentage (%HA) by road traffic noise in "Novo Naselje", Novi Sad, for time period 1985 - 2010, is in the range 16 - 31%.

In relation to measured average five-year  $L_{\text{den}}$  in city zones, according to urban use of the space in the City of Novi Sad, during the 2012-2016, %HA was 11% in "residential areas", 21% in "city center and city traffic", 18% in "recreation areas and hospital areas" and 25% in "business and residential areas". Therefore, in representative zones of the City of Novi Sad, %HA was in the range 11 - 25% [20].

The higher values of noise levels during the 1980s and 1990s, compared to the values from the last decade at the same measuring points in the City of Novi Sad, can also be interpreted from the aspect of used different measurement equipment and different methodologies.

Also, historical data show that minimum and maximum values of the noise level are approaching to each other. This indicates that the noise in the city is more and more "equally distributed" and presented everywhere. This was demonstrated by professional papers from IZJZV [21,22].

#### 5. CONCLUSION

The predictive equations for modeling basic noise indicators ( $L_{\text{day}}$ ,  $L_{\text{evening}}$ ,  $L_{\text{night}}$ ,  $L_{\text{den}}$ ) can be useful model for other cities and institutions which possess historical environment noise data.

In this way, historical data can be analyzed in a modern way, and can also be used for other purposes, for example, making noise maps.

The data presented in this paper examine the environmental noise as a long-lasting physical hazard.

#### Aknowegdments

This paper was supported by the Ministry of Education and Science of the Republic of Serbia through the Project "Biosensing Technologies and Global System for Continues Research and Integrated Management" No. 43002

## REFERENCES

---

- [1] Directive 2002/49/EC. The European Parliament and The Council. Official Journal of the European Communities, 2002
- [2] Maja Miškulin. Fizikalni čimbenici okoliša. U: Dinko Puntarić, Maja Miškulin, Jasna Bošir i suradnici. Zdravstvena ekologija. Medicinska naklada, Zagreb 2012
- [3] WHO. Environmental noise guidelines for the European Region. Copyright© (2015) by EAA-NAG-ABAV, ISSN 2226-5147. Available on <http://www.na-paw.org/WHO-noise-guidelines-Euronoise-2015.pdf>
- [4] Anne-Sophie Evrard, Liacine Bouaoun, Patricia Champelovier, Jacques Lambert, Bernard Laumon. Does exposure to aircraft noise increase the mortality from cardiovascular disease in the population living in the vicinity of airports? Results of an ecological study in France. *Noise health*. 2015 Sep-Oct; 17(78) 328-336. doi: 10.4103/1463-1741-165058
- [5] Maschke C, Rupp T, Hecht K. The influence of stressors on biochemical reactions--a review of present scientific findings with noise. *Int J Hyg Environ Health*. 2000 Mar;203(1):45-53.
- [6] Belojević G, Slepčević V, Jakovljević B. Mental performance in noise: The role of introversion. *Journal of Environmental Psychology* 21(2):209-213, June 2001. DOI: 10.1006/jevp.2000.0188
- [7] Hansell AL, Blangiardo M, Fortunato L, Floud S, de Hoogh K, Fecht D, et al. Aircraft noise and cardiovascular disease near Heathrow airport in London: small area study. *BMJ*. 2013; 347:f5432.[DOI: 10.1136/bmj.f5432] [PMID: 24103537]
- [8] Stansfeld S, Haines M, Brown B.( 2000) Noise and health in the urban environment. *Rev. Environ. Health*. 15(1-2):43-82.
- [9] Stošić Lj, Belojević G, Milutinović S. Effects of Traffic Noise on Sleep in an Urban Population. September 2009, *Archives of Industrial Hygiene and Toxicology* 60(3):335-42. DOI: 10.2478/10004-1254-60-2009-1962
- [10] Prüss-Ustün, A., Wolf, J., Corvalán, C., Bos, R., and Neira, M. Preventing Disease through Healthy Environments: A Global Assessment of the Environmental Burden of Disease From Environmental Risks. World Health Organization, 2016
- [11] Burden of Disease From Environmental Noise – Quantification of Healthy Life Years Lost in Europe. World Health Organization. Regional Office for Europe, Copenhagen; 2011
- [12] Paunović K, Belojević G. Burden of myocardial infarction attributable to road-traffic noise: A pilot study in Belgrade. November 2014, *Noise and Health* 16(73):374-9. DOI: 10.4103/1463-1741.144415
- [13] Kamp I. Noise annoyance - Concept, Measurement, Dose Response Curves, G2G 2011, Beograd
- [14] Belojević G, Sarić-Tanasković M. Prevalence of Arterial Hypertension and Myocardial Infarction in Relation to Subjective Ratings of Traffic Noise Exposure. *Noise Health*. 2002;4(16):33-37.
- [15] Bijelović S. Činioci životne sredine kao pokazatelji uticaja na zdravlje ljudi. Doktorska disertacija. Medicinski fakultet Univerziteta u Novom Sadu, 2011.
- [16] Paunović K, Belojević G, Jakovljević B. Noise annoyance is related to the presence of urban public transport. *Sci total environ*. 2014 may 15;481:479-87. Doi: 10.1016/j.scitotenv.2014.02.092. Epub 2014 mar 12.
- [17] Belojević g, Paunović k. Recent Advances In Research On Non-Auditory Effects Of Community Noise. *Srp Arh Celok Lek*. 2016 JAN-FEB;144(1-2):94-8.
- [18] Stansfeld SA, Matheson MP. Noise pollution: non-auditory effects on health. *Br Med Bull*. 2003;68:243-57.
- [19] Uredba o indikatorima buke, graničnim vrednostima, metodama za ocenjivanje indikatora buke, uznemiravanja i štetnih efekata buke u životnoj sredini, Sl. glasnik br. 75/2010
- [20] Živadinović E. Uznemirenost stanovništva bukom iz životne sredine. Završni rad iz uže specijalizacije iz Medicinske ekologije. Medicinski fakultet Univerziteta u Novom Sadu, 2018
- [21] Bijelović S, Živadinović E. Assessment of noise annoyance in the city of Novi Sad. Proceedings from 42nd International Congress and Exposition on Noise Control Engineering (INTER-NOISE 2013), September 15-18, 2013, Innsbruck, Austria. (Fool papers in electronic form) 0481
- [22] Živadinović E, Bijelović S, Dragić N, Popović M, Milosevic S, Lalovic Z. Environmental Noise Monitoring And Measurement in The City of Novi Sad in 2012. *Internoise 2013*, September 15-18, 2013, Innsbruck, Austria (441, Paper 0478) / 42nd International Congress and Exposition on Noise Control Engineering 2013 (INTER-NOISE 2013): Noise Control for Quality of Life (2929), ISBN: 978-1-63266-267-5

# Environmental Noise Monitoring

Noise monitoring is being adopted throughout the world as a means to reduce noise impact from the everyday activities that go on around us. Monitoring produce trend information for planning and compliance purposes as well as process data to highlight noise disturbances for investigation – working with you to reduce noise!



## Sound and Vibration - Brüel & Kjær!

Brüel & Kjær is a global company providing local sales, service, and support in more than 55 countries.

### Contact your local sales representative:

RMS d.o.o.  
Partizanske avijacije 12/3,  
11070 Novi Beograd, Srbija,  
Tel.: +381(0)11 2280 951  
Fax: +381(0)11 2280 751  
<http://www.rms.rs>

Brüel & Kjær Sound & Vibration Measurement A/S / Export Sales  
Skodsborgvej 307, DK-2850 Nærum, Denmark  
Tel.: +45 7741 2000 – Fax: +45 7741 2015  
E-mail: [export@bksv.com](mailto:export@bksv.com) – Website: <http://www.bksv.com>



## DIFFERENCES BETWEEN STRATEGIC NOISE MAPPING BY NMPB '96 AND CNOSSOS-EU METHODS FOR VELIKA PLANA-MARKOVAC SECTION

Aleksandar Gajicki

Institute of Transportation CIP, Nemanjina 6, 11000 Beograd, Serbia, gajickia@sicip.co.rs  
PhD Student, University of Nis, Faculty of Occupational Safety, Serbia, aleksandar@gajicki.com

**Abstract** - Use of the new European calculation method CNOSSOS-EU will be mandatory from 01.01.2019 on. PE "Roads of Serbia" have done strategic noise maps for 834 km of roads using the NMPB '96 method. Transition to the new calculation method opens the question of whether the results obtained by NMPB '96 and CNOSSOS-EU methods are comparable, and to what extent. In this paper preliminary comparative annoyance analysis between result of obtained by NMPB '96 and CNOSSOS-EU are performed.

### 1. INTRODUCTION

According to the Environmental Noise Directive EC 2002/49/EC (END) every Member State has an obligation to prepare and publish strategic noise maps every 5 years. In Europe, the first round of strategic mapping was carried out in 2007, the second round was carried out in 2012 and the third round was carried out in 2017. The first three rounds for road traffic were performed using recommended NMPB '96, or an appropriate national method.

The new harmonized European calculation method, CNOSSOS-EU was published in 2015 and it is specified in Directive 2015/996/EC. Its use will be mandatory from 01.01.2019.

The Republic of Serbia has a prescribed obligation that the first round of strategic noise map shall be done no later than June 30, 2015 and must include agglomerations with more than 250,000 inhabitants, major roads with average annual traffic flow of more than 6,000,000 vehicles, main railway lines with the average annual traffic flow of more than 60,000 trains and major airports.

The second round of strategic noise maps shall be done no later than December 31, 2020 and must include agglomerations with more than 100,000 inhabitants, major roads with average annual traffic flow of more than 3,000,000 vehicles, main railway lines with the average annual flow traffic of more than 30,000 trains and airports that were not included in the first round of mapping.

PE "Roads of Serbia" within its competences and in accordance with the Law on Noise Protection in the Environment ("Official Gazette RS", 36/09 and 88/10) has produced strategic noise maps for IA, IB and IIA category state roads in the length of 834 km. All calculations were done using „the old“ calculation method NMPB '96.

In the next round of road strategic noise mapping in Serbia, calculations must be performed using „the new“ calculation

method CNOSSOS-EU. Therefore information about the degree of comparability between data obtained by „the old“ and „the new“ calculation method is very important.

As an illustrative example, the results of the strategic noise mapping for section Velika Plana – Markovac are shown, using the NMPB '96 and CNOSSOS-EU methods.

### 2. STRATEGIC NOISE MAPS

A strategic noise map is a map that represents the data on noise levels in a particular area and it is used to estimate the total noise exposure of certain areas from the different noise sources or to predict the total noise in a given area [1].

The process of strategic noise mapping consists of seven phases. Each stage of the process is defined by the preceding stages such that requirements and specifications are captured ahead of the datasets. The strategic noise mapping process can be defined through [2]:

- Phase 1 - Define areas to be mapped
- Phase 2 - Define noise calculation methods
- Phase 3 - Develop dataset specification
- Phase 4 - Produce dataset
- Phase 5 - Develop noise model dataset
- Phase 6 - Noise level calculation
- Phase 7 - Post processing and analysis in accordance with the requirements of legal regulations of the Republic of Serbia.

The software package which is used to calculate noise indicators must be in accordance with the requirements of Nordtest Method "Framework for the Verification of Environmental Noise Calculation Software", ACOU 107 (Nordtest, Finland, 2001) and DIN 45687 "Acoustics - Software products for the calculation of the sound propagation outdoors - Quality requirements and test conditions", Beuth Verlag GmbH (Germany, 2006).

Post processing and analysis of the strategic noise mapping results were performed by using already prepared templates for displaying numerical data to the public.

### 3. CALCULATION METHODS

To point out the basic differences between NMPB-96 and CNOSSOS-EU calculation methods, a brief comparative analysis is done.

NMPB '96 is a French road noise calculation model which was reviewed and corrected by XP S 31-133. For input data with respect to emissions, this model refers to Guide du Bruit 1980.

Guide du Bruit 1980 recognizes two types of motor vehicles, (light and heavy), traffic flow is divided into four categories (continuous fluid, continuous pulsed, pulsed accelerated and decelerated) and there are three types of profiles (gradients above 2% in downward direction, gradients above 2% in upward direction and gradients until 2%).

In order to take into account meteorological influences in calculating a long-term sound level, NMPB '96 calculates sound levels for two conventional propagation conditions: favorable conditions and homogeneous conditions. It also takes into account several attenuations, like the atmospheric absorption, the ground and diffraction attenuations and the geometrical divergence. Calculation is performed in octave bands from 125 Hz to 4 kHz [3].

The CNOSSOS-EU model has four categories of vehicles and it is based also on breaking down representative source lines into point sources. The sound propagation model is based on the NMPB-Roads-2008. The calculations are made in octave bands from 125 Hz to 4 kHz [3].

### 3. RESULTS COMPARISON

For the purpose of analyses strategic noise maps data for Velika Plana - Markovac is used. The section is part of the IA category state road A1 and Pan-European corridor E-75 which connects Europe with the Middle East.

The section length is 12.0 km, and the calculation boundaries were set at 1000 m on the left and right from the axis of the highway. The total area covered for analysis was 23.5 km<sup>2</sup>.

The acoustical model which represents the real situation of the observed area, consists of DTM (3D terrain model), 6981 houses and two noise sources (left and right highway line).

All calculations are performed by „Predictor-LimA Software Suite - Type 7810“ software package, produced by Brüel & Kjær. For both of the above calculations, exactly the same acoustical model is used, with identical calculation settings within software package.

Collected traffic data needed for NMPB '96 calculation methods are transformed for use in CNOSSOS-EU methods using recommendations from Guide for Mapping Existing National Road Methods to the CNOSSOS-EU Road Source Method [4].

In the case of our example the following should be noted during the conversation [5]:

- The single HGV class in NMPB '96 has a total laden weight of at least 3500 kg, the same as the HGV classes in CNOSSOS-EU. By default it has been split 50/50 amongst the 2 HGV classes in CNOSSOS-EU.

- The road surface type corrections are taken from Commission recommendation 2003/613/EC.
- Other emission attributes, such as speed and gradient will match directly to CNOSSOS-EU, although it is accepted that they may not have the same numerical effect on the calculation.

The number of noise-affected people and the degree of their affection is determined using the LarmKennZiffer - LKZ Method (Noise-Evaluation-Index-Method). The total number of inhabitants included in the exposure analysis was 11026.

The analysis of inhabitants exposed ranges of noise indicators L<sub>den</sub> (day-evening-night period) and L<sub>night</sub> (night period), using NMPB '96 and CNOSSOS-EU methods are shown in Tables 1 and 2.

**Table 1** Population exposure analysis related to L<sub>den</sub>

Noise indicator L <sub>den</sub> [dB(A)]	Number of inhabitants	
	NMPB	CNOSSOS-EU
< 55	9849	10431
55 - 59	740	414
60 - 64	313	137
65 - 69	100	43
70 - 74	24	1
> 75	0	0

**Table 2** Population exposure analysis related to L<sub>night</sub>

Noise indicator L <sub>night</sub> [dB(A)]	Number of inhabitants	
	NMPB	CNOSSOS-EU
< 45	9457	9974
45 - 49	931	675
50 - 54	436	272
55 - 59	453	91
60 - 64	47	14
65 - 69	2	0
> 70	0	0

Difference of inhabitants' exposed ranges of noise indicators L<sub>den</sub> (day-evening-night period) and L<sub>night</sub> (night period) between result obtained by NMPB and CNOSSOS-EU calculation methods, are shown in Tables 3 and 4.

**Table 3** Population exposure analysis related to L<sub>den</sub>

Noise indicator L <sub>den</sub> [dB(A)]	Number of inhabitants
	NMPB - CNOSSOS-EU
< 55	-582
55 - 59	326
60 - 64	176
65 - 69	57
70 - 74	23
> 75	0

**Table 4** Population exposure analysis related to  $L_{night}$ 

Noise indicator $L_{night}$ [dB(A)]	Number of inhabitants
	NMPB - CNOSSOS-EU
< 45	-517
45 - 49	256
50 - 54	164
55 - 59	362
60 - 64	33
65 - 69	2
> 70	0

## CONCLUSION

Strategic noise mapping is a complex and demanding process which has to be done in several phases. Strategic noise maps are accurate and precise as much as the data upon which they are made are accurate and precise [6].

Preliminary comparative annoyance analysis between results obtained by NMPB '96 and CNOSSOS-EU show that differences are big, and that the results are not comparable.

Recommendation setting for data migration data from NMPB '96 to CNOSSOS-EU in our example does not produce satisfactory results. It is necessary to further elaborate the process of adapting existing data in order to provide more detailed information. Where it is possible, the

verification of data by dedicated measurements is strictly recommended.

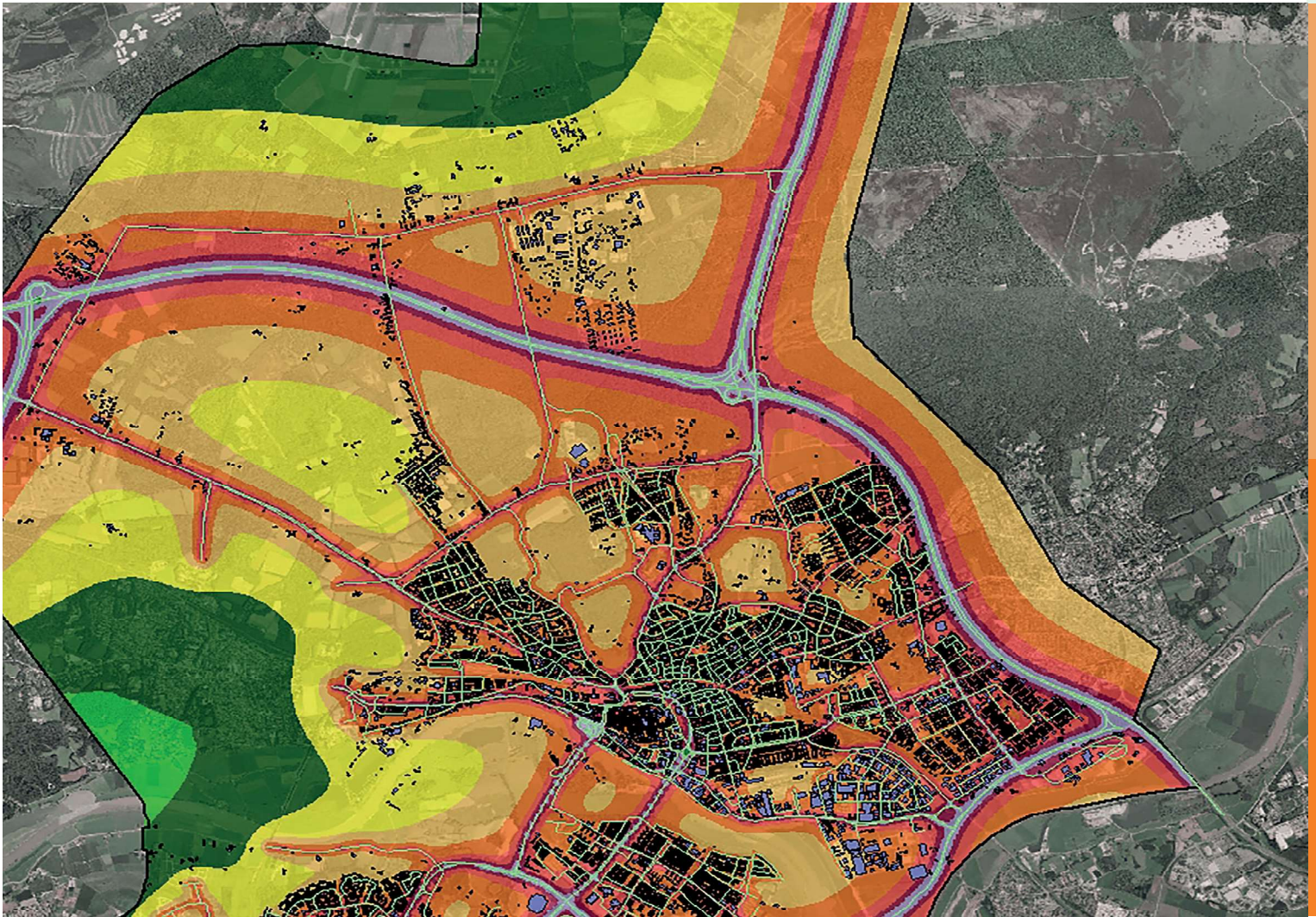
## REFERENCES

- [1] Law on environmental noise protection, "Official Gazette RS", No. 36, 2009 and No. 88, 2010 (In Serbian).
- [2] Environmental Protection Agency, Guidance Note for Strategic Noise Mapping For the Environmental Noise Regulations 2006 - Version 2, Wexford: EPA, 2011.
- [3] J. N. E. C. Ribeiro, Assessment of the CNOSSOS-EU model for road traffic noise prediction, Tecnico Lisboa, 2016.
- [4] Guide for Mapping Existing National Road Methods to the CNOSSOS-EU Road Source Method, [https://circabc.europa.eu/sd/a/00a6a620-b570-4f57-9dbb-76f66a48b325/CNOSSOS-EU%20Road%20Equivalence%20Table\\_Final\\_v2.pdf](https://circabc.europa.eu/sd/a/00a6a620-b570-4f57-9dbb-76f66a48b325/CNOSSOS-EU%20Road%20Equivalence%20Table_Final_v2.pdf) (accessed November 1, 2018)
- [5] S. Shilton et al, Conversion of existing road source data to use CNOSSOS-EU, EuroNoise 2015, Masstricht, pp. 469-474
- [6] A. Gajicki, V. Babić, M. Prašćević, D. Mihajlov, Strategic Noise Maps for Major Roads - First Results in Serbia, FACTA UNIVERSITATIS, Series: Working and Living Environmental Protection Vol. 12, No 1, 2015, pp. 17 - 27

SOFTWARE SUITE

# POWERFUL AND INTUITIVE ENVIRONMENTAL NOISE CALCULATION AND MAPPING

## Predictor-LimA™





# AIR TRAFFIC ASSIGNMENT TO REDUCE POPULATION NOISE EXPOSURE AND FUEL CONSUMPTION USING MULTI-CRITERIA OPTIMISATION

Emir Ganić<sup>1</sup>, Vinh Ho-Huu<sup>2</sup>, Obrad Babić<sup>1</sup>, Sander Hartjes<sup>2</sup>

<sup>1</sup>University of Belgrade, Faculty of Transport and Traffic Engineering, Belgrade, Serbia, [e.ganic@sf.bg.ac.rs](mailto:e.ganic@sf.bg.ac.rs)

<sup>2</sup>Delft University of Technology, Faculty of Aerospace Engineering, Delft, The Netherlands

**Abstract** - Air traffic assignment to departure and arrival routes has a major impact on the population noise exposure in the vicinity of the airport. In some cases, by choosing the suitable air traffic assignment it is possible to avoid overflying populated areas and reduce number of people affected by noise. However, such an approach almost always leads to an increase in route length, and therefore an increase in fuel consumption and CO<sub>2</sub> emissions. Although aircraft noise and fuel consumption reduction are conflicting goals, they both represent pivotal aspects of air transport sustainable development. In this paper, the methods of multi-criteria optimisation are applied, which are generally used when it is necessary to make an optimal decision that requires a compromise (trade-off) solution between two or more conflicting goals. The aim of this research is to develop a mathematical model and to propose an algorithm for air traffic assignment to departure and arrival routes that will, through the Pareto optimality concept, find the approximation of a set of nondominated solutions that minimize population noise exposure and fuel consumption. The approach was demonstrated on Belgrade airport to show the benefits of the proposed model on a real data example. Since all Pareto optimal solutions are considered equally good, from all obtained air traffic assignments the three representative solutions were compared to the actual air traffic assignment (Base case). The obtained results indicate that the proposed approach can provide solutions which offer a good trade-off between the concerned metrics.

## 1. INTRODUCTION

Major commercial airports generate benefits to their neighbouring communities, providing more investment and employment, increasing mobility, as well as providing a strong stimulus to the globalization of the industry, business and long distance tourism. However, external costs are associated with these benefits and any increase in aircraft movement causes adverse environmental impacts. It is widely accepted that the most significant environmental impacts related to the operation of airports arise from the noise generated by aircraft and fuel consumption leading to global CO<sub>2</sub> emissions increase.

Considerable efforts have been invested in order to alleviate the noise nuisance and reduce fuel consumption. On the European level, the Environmental Noise Directive 2002/49/EC (END) relating to the assessment and management of environmental noise has been introduced [1]. In the framework of implementing the requirements set in

this Directive, many airports have developed strategic noise maps and noise action plans [2]–[4]. Numerous initiatives to reduce fuel consumption and emissions have been launched in recent years including Atlantic Interoperability Initiative to Reduce Emissions (AIRE), Asia and South Pacific Initiative to Reduce Emissions (ASPIRE), ACI Airport Carbon Accreditation, The European Advanced Biofuels Flightpath.

In addition to these initiatives that require enormous budgets and are more focused on the strategical level, on a practical level it was observed that the variation of aircraft/airport operational procedures could bring short-term improvements and could be less costly in comparison with the other options [5].

The literature shows that efforts to design optimal departure and arrival routes with less noise and fuel burn have been well studied over the past decades, and various strategies have been proposed. Besides the attempts to design environmentally friendly departure/arrival routes, the allocation of aircraft and operational procedures to specific routes could also help to considerably diminish the environmental impacts. For instance, Frair [6] proposed a nonlinear integer programming model to minimize community annoyance at an airport by allocating aircraft to the existing arrival and departure trajectories. Zachary et al. [7] investigated the optimization problem which aims at finding an optimal combination of approach and departure routes, operational procedures and fleet composition to optimize noise and pollutant emissions. Kim et al. [8] built an optimization model to minimize the total emissions on the airport surface and in the terminal area by allotting aircraft to runways and scheduling the arrival and departure operations on these runways concurrently.

Several air traffic assignment strategies have been proposed in order to allocate noise more wisely. Netjasov suggested the model that was based on the categorization of aircraft according to engine type and wake turbulence category and the assignment of specific runways for take-off and landing for each aircraft category [9]. Hebliij et al. developed the Noise Allocation Planning Tool that maintained an equal noise level over a wider area, effectively reducing peak levels [10]. Zaporozhets and Tokarev formulated and solved several problems related to minimisation of aircraft noise impact, including a selection of optimum operations around an airport by distributing the aircraft between the routes [11]. On a tactical level, Nibourg et al. have developed Runway Allocation Advice System (RAAS) which is currently in

operation at Amsterdam Airport Schiphol (AAS) and Basel Euro Airport and which allows controllers to choose the optimal runway (combination) in any given situation with respect to noise preferential runway system in place [12]. Kuiper et al. proposed an optimization approach that aims to minimize the risk of exceeding the limit at any predefined location in the vicinity of the airport by distributing flights over different runways [13].

Each decision regarding the assignment of aircraft to routes should consider the number of people who will be exposed to adverse noise levels. Due to population daily migrations, number of people in some residential areas could significantly differ from census data. Ott was one of the first researchers to spot the drawback when relying to census data since it leads to overlooking the fact that some residents spend a long time far from the area, which is supposed to represent their exposure [14]. Ganić et al. [15] incorporated population daily migrations into air traffic assignment optimisation model with the aim to reduce the number of people exposed to noise but without taking into account fuel consumption. Although the importance of analysis of daily migrations has been recognized in many transportation studies [16]–[21], to the best of the authors’ knowledge, none of the air traffic assignment strategies addressed trade-off between population noise exposure and fuel consumption in combination with temporal and spatial variations in population in an airport’s vicinity.

The idea presented in this paper is to tailor air traffic assignment of aircraft to departure and arrival routes taking into account temporal and spatial variations in population in an airport’s vicinity in order to reduce the number of people exposed to noise as well as fuel consumption. The approach was demonstrated on Belgrade airport to show the benefits of the proposed model on a real data example. The obtained results indicate that the proposed approach can provide solutions which offer a good trade-off between the concerned metrics.

The rest of the paper is organised as follows. Section 2 presents the formulation of the multi-objective optimization problem by defining the mathematical model, explaining the necessary input data as well as the proposed (used) NSGA-II algorithm. Section 3 describes the Belgrade airport case study which is used to assess the capability of the proposed air traffic assignment model. The results are presented in Section 4. Finally, Section 5 provides the conclusion and ideas for further research.

## 2. MULTI-OBJECTIVE OPTIMIZATION PROBLEM FORMULATION

To generate optimal air traffic assignment with respect to population daily migrations, the mathematical model of an optimization problem with two objectives is developed. As a continuation of the research done by Ganić et al. [15], besides population noise exposure, this research takes into account fuel consumption as the second objective.

### 2.1. Input data

Description of proposed air traffic assignment model requires following input data:

- air traffic data,
- departure and arrival routes for each runway,

- noise data for each location produced by each aircraft flying over routes,
- fuel consumption data for each aircraft flying over each route,
- population data,
- human mobility patterns based on daily migrations.

Air traffic data includes information about origin and destination, aircraft type, actual take-off time (ATOT), arrival time, runway in use, operation type (take-off or landing) and can be obtained from Air Traffic Control. Real radar data could be used to represent departure and arrival routes or they could be obtained from Aeronautical Information Publication (AIP).

Noise level for each location produced by each aircraft flying over routes could be either measured or calculated. In the first case, noise levels are measured at noise monitoring stations which represent locations. In the second case, noise levels are calculated using some noise prediction and mapping software, such as Predictor-LimA, SoundPlan, Integrated Noise Model (INM), etc. Even though the first approach gives the opportunity to work with real-time data, the second approach seems more appealing since there are no limitations regarding the number of locations and their position.

Selection of locations for which noise levels will be assessed together with the actual number of people exposed to those noise levels during the observed periods is crucial for the population noise exposure assessment. Low level of detail required for this research allows each settlement to be represented by a single point, i.e. location instead of observing each housing unit in particular.

Fuel consumption was calculated using the EMEP/EEA air pollutant emission inventory guidebook – 2016 [22]. Fuel burn for Landing and Take-Off (LTO) flight phases was assessed using information about origin and destination airports, aircraft type (engine type, number of engines), duration for each LTO phase (taxi, take off, climb out, approach) and rate of fuel burn (kg/s/engine). For Climb/Cruise/Descent (CCD) flight phases fuel consumption was calculated based on CCD stage length and aircraft type.

Population data are collected for each location which implies gathering the number of people living in each settlement based on census data. During some period of the day, especially when employees go to work and pupils and students go to schools and faculties, number of people at some residential areas could significantly differ from census data due to population daily migrations. Having that in mind, assessment of human mobility patterns based on daily migration gives an estimation of how many people will actually be present at some location during a defined period of time. Daily migrations presented in this paper include a special form of spatial mobility of economically active population performing an occupation, of pupils and students. This data can be obtained from the National Statistical Office for each municipality around the airport [23].

### 2.2. Mathematical model

To formulate this model, the following notations are used:

Parameters:

$P$  is the set of periods,  $t \in P$

$O_t$  is the set of operations during period  $t$ ,  $i \in O_t$ ,  $t \in P$

$L$  is the set of locations,  $k \in L$

$S_i$  is the set of feasible operational options of operation  $i$ ,  $i \in O_t$

$T_t$  is the duration of period  $t$ ,  $t \in P$

$p_{kt}$  is the number of population living at a location  $k$  during period  $t$

$k_{kt}$  is the legal noise limit at a location  $k$  during period  $t$

$fuel(x_i)$  is the fuel consumption that operation  $i$  costs when option  $x$  is selected

$nl(x_i)$  is the noise level that operation  $i$  cause when option  $x$  is selected

Design variables:

$x = \{x_i, i \in O_t\}$  is the vector of optimal assignment of all operations to routes.

$x_i$ : is an optimal option of operation  $i$ , which is selected from set of all feasible operational options  $S_i$ , ( $x_i \in S_i$ ).

The set of operational options  $S_i = \{1, 2, \dots, M\}$  is defined based on its operational type (departure/arrival) and navigation point, in which  $1, 2, \dots, M$  is the number of options that can be derived for aircraft operation  $i$ . For each option, noise level ( $nl(x_i)$ ) and fuel consumption ( $fuel(x_i)$ ) are predefined.

Objective functions:

$$\min(T_{fuel}(x), N_{pa}(x)) \quad (1)$$

- *Fuel consumption:*

$$T_{fuel}(x) = \sum_{i \in O_t} fuel(x_i) \quad (2)$$

- *Number of people affected by noise:*

$$N_{pa}(x) = \sum_{k \in L} p_k \cdot S_k(x) \quad (3)$$

$$S_k(x) = 2^{0.1 \cdot (N_k(x) - k_k)}, \forall k \quad (4)$$

$$N_k(x) = 10 \log \left( \frac{1}{t} \cdot \sum_{i \in O_t} 10^{0.1 \cdot nl(x_i)} \right), \forall k \quad (5)$$

It should be noted that besides the introduction of a new objective, i.e., fuel consumption, this model also contains a new promising feature in comparison with the model proposed in [15]. Particularly, in the model [15], for each operation, all feasible options it can be assigned to are considered as binary design variables, which means that only one of these options is equal to 1 if it is selected, and the rest of them will be equal to 0. Consequently, the size of optimization problem will be extremely enlarged when the number of operations increases. This may make the problem more difficult to solve by using evolutionary algorithms or even integer nonlinear programming models. On the contrary, in the paper, each operation is considered as a design variable, and all its feasible assignments will serve as its design space. As a result, the number of design variables of the problem will dramatically decrease, and hence the

problem can be effectively solved by using evolutionary algorithms.

### 2.3. NSGA-II algorithm

As described in Section 2.2, the formulated problem is an integer nonlinear optimization problem with two objective functions, which is hard to be solved by gradient-based optimization methods or linear/nonlinear programming models. Fortunately, in recent years, many evolutionary algorithms have been proposed that are capable of effectively solving such kind of problems. Among them, nondominated sorting genetic algorithm II (NSGA-II) proposed by K. Deb et al. [24] emerged as one of the most powerful methods, which has been widely used in many different engineering applications. In this paper, it is therefore utilized to deal with the optimization problem stated above. Since the details of the algorithm have been given in [24], interested readers are encouraged to refer to this reference.

### 3. BELGRADE AIRPORT CASE STUDY

To demonstrate the reliability and applicability of the proposed approach, a case study is carried out in this section. Belgrade airport Nikola Tesla (ANT), the largest and busiest international airport in Serbia, situated 18 km west of downtown Belgrade, has been chosen as the case study. In 2017, the airport handled more than 5 million passengers and approximately 60 thousand aircraft operations with single runway 3400 m long (direction 12/30).

The first step in this case study was to obtain detailed air traffic data for one day. September 16<sup>th</sup>, 2016 has been chosen since it was a summer day with relatively heavy traffic and some of the data was already available from the previous study [25] which also included measured noise levels at one location near Belgrade airport.

Daily traffic consisted of 220 operations, including 109 departures and 111 arrivals. Distribution of operations between runways was slightly in favour of runway 12 which handled 128 operations (58.2%), while the runway 30 was used for 92 operations (41.8%).

Departure and arrival routes for each runway were obtained from radar data since Standard Instrument Departure (SID) and Standard Arrival Routes (STAR) could not be considered accurate due to aircraft vectoring mostly in place at ANT. Taking into account that aircraft vectoring at ANT is usually done in a similar way, radar data could be regarded as constant since changes in departure/arrival routes derived from radar data from one day to another are minor.

From a bundle of radar tracks presented in Fig. 1a, a 27 different routes were selected to represent actual SID/STAR routes. There are seven departure routes and seven arrival routes from runway 12 (Fig. 1b) and six departure routes and seven arrival routes from runway 30 (Fig. 1c). Departure routes are marked in blue while red colour corresponds to arrival routes.

Noise and fuel data are in function of aircraft type. For the observed day, fleet mix consisted of 25 different aircraft types. However, for the purpose of simplifying the calculations, they were classified into 11 groups based on the similarity of aircraft types. In this way, 85% of the operations were presented by the aircraft types that were actually flown that day, while the remaining 15% were presented by aircraft

types that have approximately the same level of noise exposure and fuel consumption as their representative.

Table 1 shows the number of departure and arrival operations per each period per each aircraft type categorised as per the INM [26] and AzB [27] databases.

Before calculating the noise data, it is pivotal to choose the optimal number and position of locations for which the noise and population data will be obtained. Since ANT is surrounded by populated areas, 23 different municipalities were considered to be affected by aircraft noise: 17 Belgrade municipalities and the municipalities of Stara Pazova, Indjija, Irig, Ruma, Pecinci and Pancevo. In order to be certain that adequate locations would be selected, the conservative approach of calculating noise exposure of each location around the airport was applied in the following way: the most unfavourable case for a certain selected location is when all operations are assigned to departure and arrival routes that are closest to that location and when the noisiest aircraft type is overflying the location (in this study it is "Airbus A330-200"). From 306 locations (settlements) for which the noise exposure was calculated using a conservative approach, only 17 locations were selected since the noise levels at these locations were above legal noise limit values (above 55dB  $L_{den}$  and/or 45dB  $L_{night}$ ). Table 2 shows legal noise limits and population data for each selected location.

As it can be seen from Table 2, population data are presented in four different columns. Data in the first column represents 2011 census data [23]. In order to take into account human mobility patterns and to simulate the three-8h working shifts the day has been divided into three-8h periods: Period 1 from 8 am to 4 pm (90 operations), Period 2 from 4 pm to 12 am (79 operations) and Period 3 from 12 am to 8 am (51 operations). In order to obtain data on daily migrations of economically active persons who perform an occupation, pupils and students for each of the 23 municipalities around the airport it was necessary to make private request for special processing of data collected in the 2011 census to the Statistical Office of the Republic of Serbia since this data was not available publicly. Definition provided in 2011 Census methodology describes daily migrants as persons who work

or go to school/university outside the place of their usual residence, but who return on a daily basis or several times a week [23]. Data on daily migrations was the key to calculate the total daily inflow and outflow of inhabitants for each municipality. Based on that, the approximation of total daily inflows and outflows of the inhabitants for each settlement within the municipality was done in proportion to the number of inhabitants in the settlement.

Having in mind that in this way, human mobility patterns are obtained for the whole day only, and not for the separate periods of the day, some assumptions were needed to be made in order to assess how many people would actually be present at each location during a defined period of time. It was assumed that 50% of employees work first shift, 40% work second shift, and 10% work night shift, while pupils and students go to school in two shifts (Period 1 and 2) equally. In this way, for each period population data were calculated based on the census and daily migration data showing the difference in the number of people at the locations between periods. The total number of residents living near these 17 locations based on census data was 238,741.

Legal noise limit values for day, evening and night, given in Table 2, represent the limit values for EU common noise indicators  $L_{den}$  and  $L_{night}$  in the Republic of Serbia, for residential areas (see [28]). For Period 1 and 2, representing the day and evening, legal noise limit values in dB (A) were set to 55dB, while for Period 3 representing the night noise limit value of 45dB was used.

INM software was used to calculate the sound exposure levels (SEL) for each aircraft type in the fleet mix, flying over each route, for each location separately. This data was used as input for noise objective in optimization model. For each operation, standard INM profile settings were used taking into account the fact that different aircraft types overfly locations at different altitudes and thrust settings. In addition, different profile parameters for each aircraft type were assigned including take-off and landing masses, thrust and flaps settings, climb rate, descent angle,...

**Table 1** Flight statistics and aircraft classifications

Aircraft type	Assigned AzB class	INM airplane code	Departure			Arrival		
			Period	Period	Period	Period	Period	
			1	2	3	1	2	3
Boeing 737-300	S 5.2	737300	4	1	3	5	3	1
Boeing 737-800	S 5.2	737800	2	2	1	3	1	0
Airbus A319	S 5.2	A319-131	10	9	9	11	15	3
Airbus A320	S 5.2	A320-211	11	4	6	12	5	5
Airbus A330-200	S 6.1	A330-301	1	1	0	0	1	1
BE20	P 1.4	CNA441	1	0	1	1	0	0
Cessna 560 XL	S 5.1	CNA560XL	1	1	2	2	1	1
SW4	P 2.1	DHC6	1	2	1	3	1	0
ATR 42	P 2.1	DHC8	1	3	0	1	3	0
ATR 72	P 2.1	DO328	7	8	10	6	14	6
Embraer 190	S 5.2	EMB190	4	2	0	3	2	1
		Total	43	33	33	47	46	18

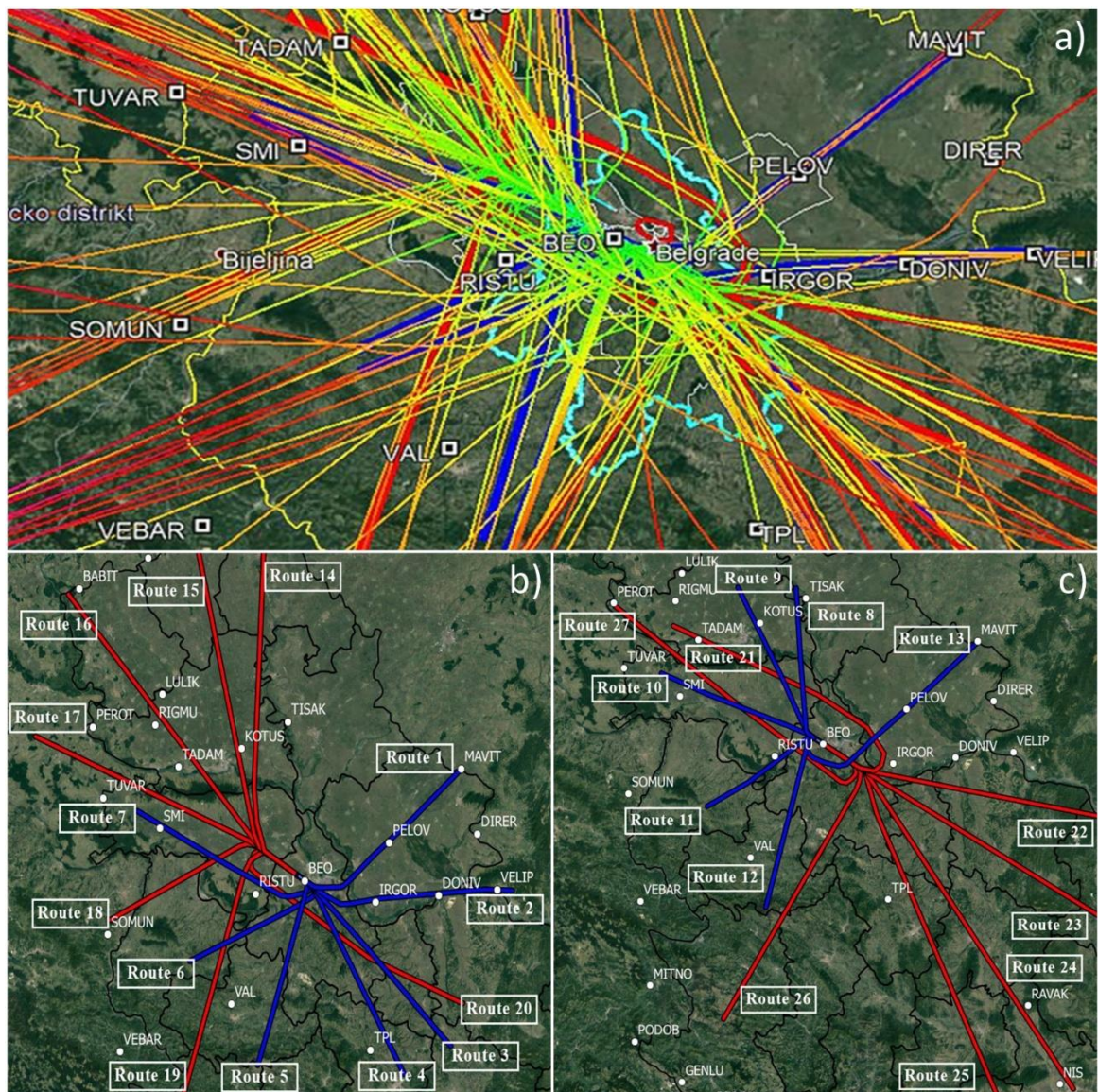


**Fig. 1** Radar data and departure and arrival routes (source: Flightradar24.com, using Google Earth)

**Table 2** Location and population data

No.	Municipality	Settlement	Legal noise limit (dB)		Population			
			Day and Evening	Night	2011 Census	Period 1	Period 2	Period 3
1	Cukarica	Banovo Brdo	55	45	44669	40098	40790	43978
2	Cukarica	Cerak	55	45	43993	39492	40172	43312
3	Cukarica	Zarkovo	55	45	30979	27809	28289	30500
4	Novi Beograd	Bezanijski blokovi	55	45	22455	22725	22610	22570
5	Novi Beograd	Ledine	55	45	6813	6895	6860	6848
6	Novi Beograd	Sava	55	45	18899	19126	19029	18996
7	Rakovica	Kanarevo Brdo	55	45	11389	9975	10194	11170
8	Rakovica	Kosutnjak	55	45	4944	4330	4425	4849
9	Rakovica	Miljakovac	55	45	7622	6676	6822	7476
10	Rakovica	Skojevaska	55	45	4739	4151	4242	4648
11	Surcin	Dobanovci	55	45	8503	8055	8089	8469
12	Vozdovac	Jajinci	55	45	8876	8672	8733	8815
13	Vozdovac	Kumodraz	55	45	6064	5924	5966	6022
14	Vozdovac	Kumodraz 1	55	45	3852	3763	3790	3826
15	Vozdovac	Rakovica	55	45	3292	3216	3239	3269
16	Zemun	Ugrinovci	55	45	10807	10585	10616	10776
17	Stara Pazova	Krnjesevci	55	45	845	809	813	841
Total					238741	222301	224679	236365

#### 4. RESULTS AND DISCUSSION

The results obtained by the proposed approach for three different periods in comparison with those acquired by the base case and the model in [15] are depicted in Fig. 2. At first glance, it can be seen from Fig. 2 that the present approach offers a wide range of solutions (denoted as Pareto front), which try to make a good trade-off between the population noise exposure and fuel consumption. Another observation is that, for all three periods, the proposed model can provide solutions that dominate the base case, while compared with those obtained by [15], they are worse in terms of noise criterion and better regarding fuel burn.

In order to make the comparison more apparent, for each period, three different solutions are selected and highlighted, as shown in Fig. 2. With this selection, solution 1 represents for fuel optimization, solution 3 prefers to noise criterion, whereas solution 2 is one of solutions from the Pareto fronts which is close to the base case. All the metrics derived from these solutions are given in Table 3, where those obtained by the base case and the model in [15] are also provided.

From the table, a common trend for all the periods can be observed. Specifically, compared to base case, solution 1 offers a better performance in fuel burn, solution 2 performs better in noise criterion, while with almost the same amount of fuel consumption, solution 3 achieves a significant

reduction in population noise exposure. For example, in Period 1, solution 1 has a reduction of 0.7% and 0.5% in fuel burn and route length, respectively, and an increase of 3.3% in population noise exposure, compared with the base case. Solution 2 has a very good performance in noise criterion with a considerable decrease of 43.8% in comparison with the base case, which is almost the same with that of the model in [15]. However, it is worse than the base case in term of fuel burn and route length. For solution 3, there is a good trade-off between all the concerned metrics to be found. With the same amount of fuel burn, it gains a great reduction of 42.7% in noise metric, while the one acquired by Ganic et al. [15] has a reduction of 43.8%, but causes a significant increase up to 0.7% in fuel burn.

From the results obtained above, it can be concluded that the proposed approach is reliable and quite effective. It not only provides reliable solutions, but also offers a variety of options for interested users to choose with only one single run. This feature has made the proposed approach dominating other single objective approaches in previous studies. Moreover, with the new form of the optimization problem given in Section 2.2, the problem size is reduced significantly, which allows the proposed model to be capable of solving large scale problems.

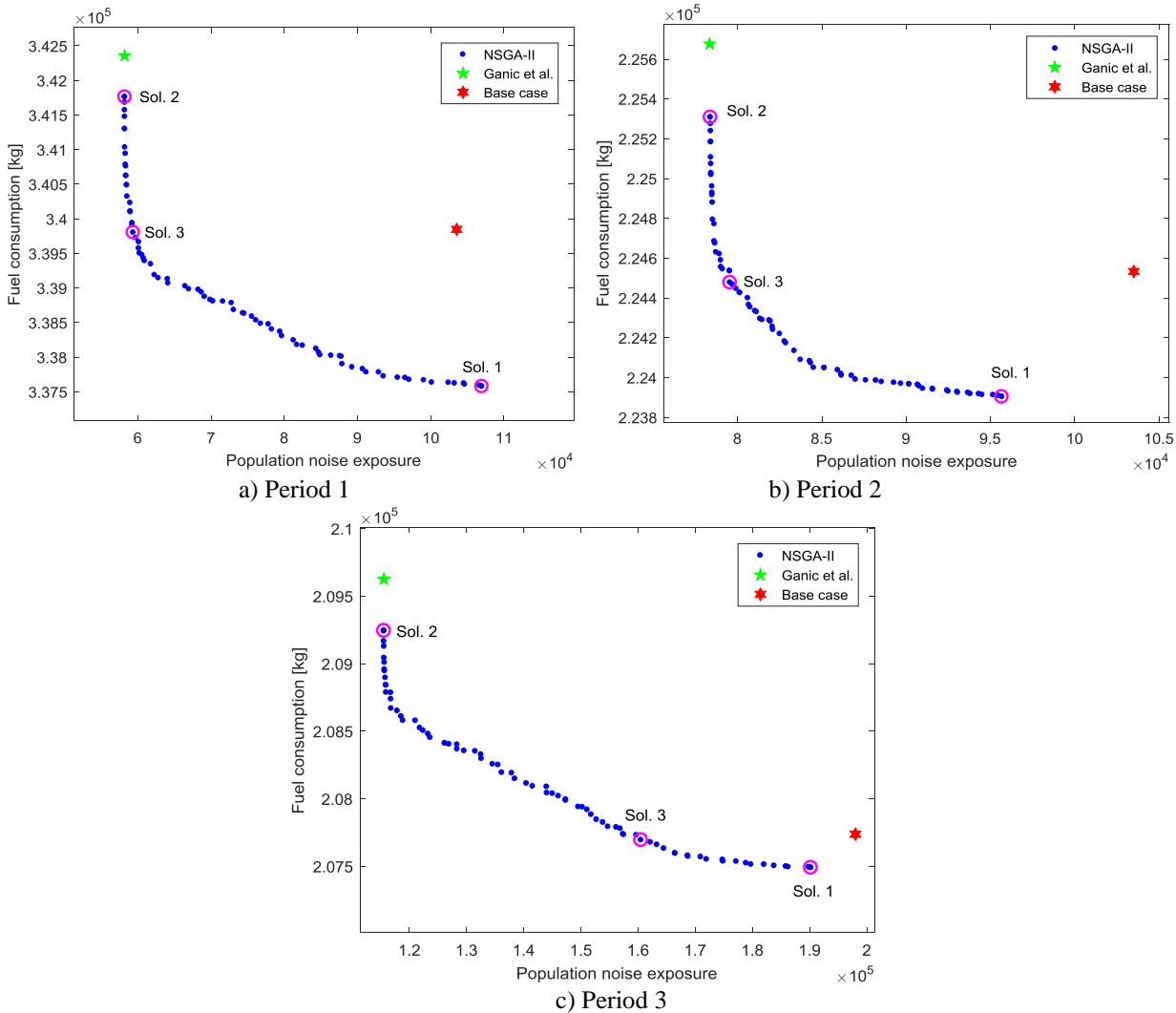


Fig. 2 Pareto front obtained by the NSGA-II algorithm

**Table 3** Comparison of the metrics of the representative solutions and the reference case

Period	Metrics	Base case	Ganić et al. [15]		Solution 1		Solution 2		Solution 3	
			Absolute value	% reduction	Absolute value	% reduction	Absolute value	% reduction	Absolute value	% reduction
1	Population noise exposure	103541	58187	-43.8%	106974	3.3%	58211	-43.8%	59359	-42.7%
	Fuel consumption (kg)	339844	342358	0.7%	337567	-0.7%	341761	0.6%	339798	0.0%
	Route length (NM)	51459	52065	1.2%	51227	-0.5%	51923	0.9%	51647	0.4%
2	Population noise exposure	103506	78332	-24.3%	95643	-7.6%	78356	-24.3%	79518	-23.2%
	Fuel consumption (kg)	224527	225682	0.5%	223897	-0.3%	225315	0.4%	224477	0.0%
	Route length (NM)	38664	38924	0.7%	38515	-0.4%	38833	0.4%	38644	-0.1%
3	Population noise exposure	197999	115514	-41.7%	190204	-3.9%	115539	-41.6%	160493	-18.9%
	Fuel consumption (kg)	207735	209631	0.9%	207488	-0.1%	209248	0.7%	207695	0.0%
	Route length (NM)	33713	34279	1.7%	33639	-0.2%	34191	1.4%	33700	0.0%

## 5. CONCLUSION

In this paper, a new approach for air traffic assignment is developed. The proposed model is based on a new form of the optimization problem, in which two conflicting objective functions, including noise and fuel criteria, are taken into account simultaneously. The formulated problem is then solved by the well-known multi-objective optimization method, named NSGA-II. The reliability and applicability of the proposed approach are demonstrated through a case study at Belgrade Airport in Serbia. Through the evaluation and comparison of the obtained results with those of the base case and the model in [15], it reveals that the proposed method is reliable and quite effective. It does not only provide reliable solutions but also gives a wide range of solutions – featuring a good trade-off between the considered two objectives – which can be a good reference base for users to refer to before making decisions.

Furthermore, thanks to the new ways of formulating the optimization problem, the proposed approach is promising to be extended for solving large problems in busy airports.

## Acknowledgements

This research is supported by the Ministry of Science and Technological Development of the Republic of Serbia and represents a part of the project named “A support to sustainable development of the Republic of Serbia's air transport system” (TR36033).

## REFERENCES

- [1] EC, “Directive 2002/49/EC of the European parliament and the Council of 25 June 2002 relating to the assessment and management of environmental noise,” *Official Journal of the European Communities*, vol. 189, no. 12, pp. 12–25, 2002.
- [2] K. Vogiatzis, “Airport environmental noise mapping and land use management as an environmental protection action policy tool. The case of the Larnaka International Airport (Cyprus),” *The Science of the total environment*, vol. 424, pp. 162–73, May 2012.
- [3] I. Glekas, K. Vogiatzis, and C. Antoniadis, “Strategic noise mapping & action plans for the international airports of Larnaca & Pafos in Cyprus,” in *The 23rd International Congress on Sound and Vibration*, 2016.
- [4] K. Vogiatzis, “Assessment of environmental noise due to aircraft operation at the Athens International Airport according to the 2002/49/EC Directive and the new Greek national legislation,” *Applied Acoustics*, vol. 84, pp. 37–46, Oct. 2014.
- [5] V. Ho-Huu, S. Hartjes, H. G. Visser, and R. Curran, “Integrated design and allocation of optimal aircraft departure routes,” *Transportation Research Part D: Transport and Environment*, vol. 63, pp. 689–705, Aug. 2018.
- [6] L. Frair, “Airport noise modelling and aircraft scheduling so as to minimize community annoyance,” *Applied Mathematical Modelling*, vol. 8, no. 4, pp. 271–281, Aug. 1984.
- [7] D. S. Zachary, J. Gervais, and U. Leopold, “Multi-impact optimization to reduce aviation noise and emissions,” *Transportation Research Part D: Transport and Environment*, vol. 15, no. 2, pp. 82–93, Mar. 2010.
- [8] B. Kim, L. Li, and J.-P. Clarke, “Runway Assignments That Minimize Terminal Airspace and Airport Surface Emissions,” *Journal of Guidance, Control, and Dynamics*, vol. 37, no. 3, pp. 789–798, May 2014.
- [9] F. Netjasov, “A Model of Air Traffic Assignment as a Measure for Mitigating Noise at Airports: The Zurich Airport Case,” *Transportation Planning and Technology*, vol. 31, no. 5, pp. 487–508, Oct. 2008.
- [10] S. J. Heblj, V. Hanenburg, R. A. A. Wijnen, and H. G. Visser, “Development of a Noise Allocation Planning Tool,” in *45th AIAA Aerospace Sciences Meeting and Exhibit*, 2007, pp. 1–7.
- [11] O. I. Zaporozhets and V. I. Tokarev, “Predicted flight procedures for minimum noise impact,” *Applied Acoustics*, vol. 55, no. 2, pp. 129–143, Oct. 1998.
- [12] J. M. Nibourg, H. H. Hesselink, and Y. A. J. R. van de Vijver, “Environment-Aware Runway Allocation Advice System,” Amsterdam, the Netherlands, NLR-

- TP-2008-506, 2012.
- [13] B. R. Kuiper, H. G. Visser, and S. J. Heblj, “Efficient use of an allotted airport annual noise budget through minimax optimization of runway allocations,” *Proceedings of the Institution of Mechanical Engineers, Part G: Journal of Aerospace Engineering*, vol. 227, no. 6, pp. 1021–1035, Jun. 2013.
- [14] W. R. Ott, “Concepts of human exposure to air pollution,” *Environment International*, vol. 7, no. 3, pp. 179–196, 1982.
- [15] E. Ganić, O. Babić, M. Čangalović, and M. Stanojević, “Air traffic assignment to reduce population noise exposure using activity-based approach,” *Transportation Research Part D: Transport and Environment*, vol. 63, pp. 58–71, Aug. 2018.
- [16] M. Hatzopoulou and E. J. Miller, “Linking an activity-based travel demand model with traffic emission and dispersion models: Transport’s contribution to air pollution in Toronto,” *Transportation Research Part D: Transport and Environment*, vol. 15, no. 6, pp. 315–325, Aug. 2010.
- [17] I. Kaddoura, L. Kröger, and K. Nagel, “User-specific and Dynamic Internalization of Road Traffic Noise Exposures,” *Networks and Spatial Economics*, Mar. 2016.
- [18] J. Hao, M. Hatzopoulou, and E. Miller, “Integrating an Activity-Based Travel Demand Model with Dynamic Traffic Assignment and Emission Models Implementation in the Greater Toronto, Canada, Area,” *Transportation Research Record: Journal of the Transportation Research Board*, vol. 2176, pp. 1–13, 2010.
- [19] S. Jiang, J. Ferreira, and M. C. Gonzalez, “Activity-Based Human Mobility Patterns Inferred from Mobile Phone Data: A Case Study of Singapore,” *IEEE Transactions on Big Data*, vol. 3, no. 2, pp. 208–219, Jun. 2017.
- [20] S. Jiang, J. Ferreira, and M. C. González, “Clustering daily patterns of human activities in the city,” *Data Mining and Knowledge Discovery*, vol. 25, no. 3, pp. 478–510, Nov. 2012.
- [21] J. Novák and L. Sýkora, “A City in Motion: Time-Space Activity and Mobility Patterns of Suburban Inhabitants and the Structuration of the Spatial Organization of the Prague Metropolitan Area,” *Geografiska Annaler, Series B: Human Geography*, vol. 89, no. 2, pp. 147–168, Jun. 2007.
- [22] M. Winther, K. Rypdal, L. Sørensen, M. Kalivoda, M. Bukovnik, N. Kilde, R. De Laurentis, R. Falk, D. Romano, R. Deransy, L. Box, L. Carbo, N. T. Meana, and M. Whiteley, *EMEP/EEA air pollutant emission inventory guidebook 2016 – Update July 2017 - 1.A.3.a, 1.A.5.b Aviation*, no. July. European Environment Agency, 2017.
- [23] Statistical Office of the Republic of Serbia, *2011 Census of Population, Households and Dwellings in the Republic of Serbia. Daily Migrants (data by municipalities/cities)*. Belgrade, Serbia: Statistical Office of the Republic of Serbia, 2013.
- [24] K. Deb, A. Pratap, S. Agarwal, and T. Meyarivan, “A fast and elitist multiobjective genetic algorithm: NSGA-II,” *IEEE Transactions on Evolutionary Computation*, vol. 6, no. 2, pp. 182–197, Apr. 2002.
- [25] E. Ganić, M. Radojević, and O. Babić, “Influence of aircraft noise on quiet areas,” in *25th International Conference Noise and Vibration Proceeding of papers*, 2016, pp. 47–53.
- [26] Federal Aviation Administration, “INM v7.0 User’s Guide,” 2007.
- [27] AzB-08, *Anleitung zur Berechnung von Lärmschutzbereichen nach dem Gesetz zum Schutz gegen Fluglärm vom 19. November 2008 in: 1. Verordnung zur Durchführung des Gesetzes zum Schutz gegen Fluglärm (1. FlugLSV) vom 27.12.2008*. 2008.
- [28] Government of Republic of Serbia, *Regulation on noise indicators, limit values, assessment methods for indicators of noise, disturbance and harmful effects of noise in the environment (in Serbian)*, vol. 75/2010. Republic of Serbia, 2010.

# INDUSTRIAL IMPULSIVE NOISE AND HEARING: EVALUATION ACCORDING TO THE REGULATIONS AND APPLICABLE STANDARDS AND POSSIBLE ADDITIONAL RISK ON HEARING COMPARING TO THE EFFECT OF STEADY NOISE

Jovan Miočinović<sup>1</sup>, Biljana Beljić Durković<sup>2</sup>

<sup>1</sup>TEHPRO d.o.o., Serbia, jovan.miocinovic@tehpro.rs

<sup>2</sup>TEHPRO d.o.o., Serbia, biljana.beljiic@tehpro.rs

**Abstract** - When evaluating noise impact on hearing there used to be a difference in rating the steady and impulsive noise. By new Noise regulation, Directive and ISO 9612 standard, the determination of the noise exposure at the workplace for comparison with limit values with respect to risk of hearing damage both are treated equal under condition that peak sound pressure level is limited to corresponding limit values. In practice, at industrial workplaces the impulses rarely exceed those peak limit values (135 or 137 dB(C)). Still, recent studies indicate the additional effect of occupational impulse noise on hearing. Both the Noise regulation and the Directive demand particular attention to any exposure to impulsive noise, yet there is no accepted risk assessment method nor risk criteria for impulsive noise to meet the requirements of the Directive. In this paper the review of past and present evaluation methods are presented, as well as one promising method that includes this additional risk.

## 1. INTRODUCTION

The effect from impulse noise may result in an immediate hearing loss, as for exposure to sudden blasts like explosions in mining industry or military, as well as exposure to shooting of guns and weaponry in military. However, exposures for a long period of time to impulsive noise of high levels (yet lower than instantly damaging ones) that occur in some industries also cause noise induced hearing loss, more severe than exposure to steady state noise of equivalent average sound pressure level. Impulsive noise is present in metal fabrication industry near machinery like angle grinders, metal working machines as punch presses and nailing machines, cutting saws, in hammering and banging on metal objects, in welding and gouging, also in glass industry near bottling machines.

## 2. IMPULSIVE NOISE AND AVERAGE SOUND PRESSURE LEVEL

### 2.1 The definition

Impulsive noise is defined as noise noise consisting of a series of bursts of sound energy, each burst having a duration of less than approximately 1 s [1].

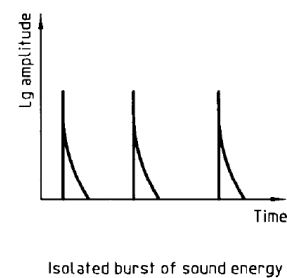


Fig. 1 Pictorial example of impulsive noise. After ISO 12001[1]

Some authors differ impulse noise, which is the product of explosive devices (e.g. gunfire) from impact noise which is generated by banging of hard surfaces (e.g. hammering a nail).

Impulse noise is described by many parameters such as peak level, duration, rise- and fall times, impulse energy, inter-impulse interval, impulse rate and the background continuous noise level.

In the literature the following descriptors may be found [18]. The highest peak in the series of successive peaks, peak level (pressure difference AB in Figure 2), A duration, a duration of of the first overpressure (zero level crossing, time difference AC in Figure 2a) and B duration, the duration from the highest peak level to a point of time when the envelope of pressure fluctuation stays within 20 dB of the peak pressure level, also including the recurrent impulses (time difference AD + EF in Figure 2b). Figure 2a ideally represents impulse noise and Figure 2b impact noise. In real-life situations distinction between impact and impulse noise is blurred due to reflections that add to the initial impulses.

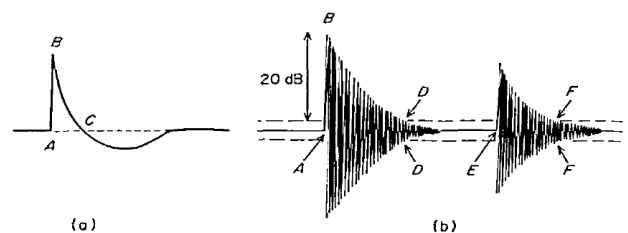


Fig. 2 Idealized oscilloscopic waveforms of impulse noises. After Coles et al. [3]

## 2.2 Measuring impulsive noise

Recent investigation [4] has shown that average sound pressure levels are not an adequate indicator of hearing risk. Instead, the impulsive character of the sound, in addition to its average level, must be considered. Sound level meters with fast response modes have an averaging time of 125 ms, whereas impulse peaks in many sounds occur within 25-50 microseconds. Therefore these meters are unable to measure the true intensity level of such sounds.

Impulsive noise is measured with sound level meter using exponential RMS integration for impulse exponential time constant,  $\tau=35$  ms, that is AI-weighted equivalent continuous sound pressure level,  $L_{pA_{leq}}$  comparing to linear RMS integration for fast time constant,  $\tau=125$  ms that is used for measuring A-weighted equivalent continuous sound pressure level,  $L_{pA_{leq}}$ .

Also, there is a method based on the continuous calculation of crest factor. The crest factor is defined as a difference between peak and RMS level of the noise, and is in relationship to the effective length and to the energy of a single impulse [5]. The definition of impulse noise based to the effective length is:

$$I = L_{Ap} - L_{AS} \geq 15 \text{ dB} \quad (1)$$

where  $L_{Ap}$  is A-weighted peak level,  $L_{AS}$  is A weighted RMS level measured with slow time constant,  $\tau=1000$  ms, and  $I$  is impulsiveness. The numerical value of 15 dB corresponds to an effective duration of 31,5 ms and is close to audibility of impulses.

The other quantity for evaluating impulsive noise is C-weighted peak sound pressure level ([10], [12], [13]).

Another descriptor would be the number of impulses that overpass the given peak pressure during the working day. For limiting the risk of hearing damage common approach is to limit the number of impulses at a given peak pressure over a workday [11].

## 3. NOISE RATING AND EVALUATING ACCORDING TO REGULATIONS

### 3.1 Limit values, criterion levels and exchange rate

#### 3.1.1 Limit values and criterion levels

Evaluation is made by comparing the noise levels to the limit values, or criterion levels. Criterion level is the steady noise level permitted for a full eight-hour shift.

By the national regulation in effect (Regulation on preventive measures for health and safety at work regarding noise exposure [12], in further text: the New Regulation) those are action value:  $L_{EX,8h} = 80$  dB(A) and limit value:  $L_{EX,8h} = 85$  dB(A). In other european countries they are also guided by Directive [13] given values: exposure limit value:  $L_{EX,8h} = 87$  dB(A), upper exposure action value:  $L_{EX,8h} = 85$  dB(A) and lower exposure action value:  $L_{EX,8h} = 80$  dB(A). In other countries, e.g. in Canada and USA criterion levels are 90, 87 or 85 dB(A) depending the state, province or territorial unit.

#### 3.1.2 Exchange rate

In close relation to criterion level is the exchange rate. The exchange rate is the amount by which the permitted sound level may increase if the exposure time is halved. There are two types of exchange rates currently in use: 3 dB(A) and 5

dB(A) exchange rate, or rule. 3 dB rule seems more logical: if the sound level is doubled, then the allowable exposure time should be cut in half. The assumption is that the exposures to equal sound energies during the full shift would produce the same effects. It follows, then, that the allowable time should be halved for every 3 dB(A) increase in sound level. This is precisely the case if the 3 dB(A) exchange rate is used. The 3 dB(A) exchange rate is more stringent. For example (see Table 1), the maximum permitted duration for a 100 dB(A) noise exposure in the 3 dB(A) exchange rate is 15 minutes. With the 5 dB(A) exchange rate, it is one hour. These two exchange rates, with criterion levels of 85 dB(A), give two different sets of exposure guidelines as Table 1 shows. The 3 dB exchange rate is incorporated in present ISO 9612 [10], and consequently by New Regulation and corresponding Directive 2003/10/EC as well as in other european countries. In Canada and USA it is 3 dB or 5 dB depending the state, province or territorial unit. By Old Regulation criterion levels followed 5 dB rule.

**Table 1** Limit values by the Old Regulation regarding the risk of hearing damage and corresponding noise exposure levels by ISO 9612

daily exposure [h]	5 dB rule: The Old Regulation limit value [dB]	3 dB rule: $L_{pA_{eqT_e}}$ [dB] for $L_{EX,8h} = 85$ dB (A) according to ISO 9612
8	85	85,0
4	90	88,0
2	95	91,0
1	100	94,0
0,5	105	97,0
0,25	110	100,0

### 3.2 Calculating daily noise exposure according to ISO 9612

According to ISO 9612 from equivalent sound pressure levels noise exposure is calculated by:

$$L_{EX,8h} = L_{pA_{eqT_e}} + 10 \log \left[ \frac{T_e}{T_0} \right] \text{ dB} \quad (1)$$

where

$L_{EX,8h}$  is daily noise exposure level;

$L_{pA_{eqT_e}}$  is the A-weighted equivalent continuous sound pressure level for the effective duration  $T_e$  of the working day, and  $T_0$  is the reference duration,  $T_0=8$  h.

$L_{pA_{eqT_e}}$  is calculated from measured equivalent sound pressure levels depending on measurement strategy chosen.

### 3.3 Treating and evaluating impulsive noise according to previous regulation and previous ISO 9612

As for treating impulsive noise, corresponding to the previous national regulation (The Regulation on occupational safety measures and norms for noise protection at workplace [8], in further text: the Old Regulation), Council Directive 79/113/EEC [9] and previous ISO 9612 [2] measured equivalent sound pressure levels are adjusted to rating levels for various types of noise, by the Old Regulation for impulsiveness, tonality and intermittency, by Directive [9] and previous ISO 9612 for impulsiveness and tonality.

For impulsive and tonal noise the measured levels are to be adjusted:

$$L_r = L_{pAeq} + K_I + K_T \quad (2)$$

By older regulations (Old Regulation and Directive [9]) and previous ISO 9612 the impulse adjustment for the impulsive noise was determined as the difference between the A-weighted sound pressure level and  $L_{pAeq}$ :

$$K_I = L_{pAeq} - L_{pAeq} \quad (3)$$

By previous ISO 9612, for noise with  $K_I \leq 2$  dB the impulse adjustment may be neglected. If  $K_I$  is not determined by measurement of A-weighted sound pressure level, an impulse adjustment of 3dB or 6 dB may be used depending on the prominence of the impulsiveness in the noise (according to previous ISO 9612) and 5 dB (according to the Old Regulation).

The evaluation is made by comparing the adjusted levels to the limit values.

### 3.4 Treating and evaluating impulsive noise according to current regulation and current ISO 9612

The New Regulation as well as corresponding Directive 2003/10/EC [13] prescribe the noise exposure limits with respect to risk of hearing damage and the evaluation is made by comparing the three noise quantities to the limit values (A-weighted noise exposure level normalized to a nominal 8 h working day, A-weighted noise exposure level normalized to a nominal 8 h working day averaged over the 5 day working week and C-weighted peak sound pressure level).

Corresponding to The New Regulation (and the Directive [13]) impulsiveness of the noise is to be taken into account ([12] Article 10, paragraph 1; [13] Article 4, paragraph 6a). However, in the assessment of noise by present version of ISO 9612 [10], unlike the previous version ([2], Annex C) such adjustments are not mentioned.

By present ISO 9612 it is assumed that the impulsiveness is taken into account by limiting C-weighted peak sound pressure level.

By New regulation action value is  $L_{p,Cpeak} = 135$  dB(C) and limit value is  $L_{p,Cpeak} = 137$  dB(A). In other european countries they are guided by Directive [13] given values: exposure limit value:  $L_{p,Cpeak} = 140$  dB(C), upper exposure action value:  $L_{p,Cpeak} = 137$  dB(C) and lower exposure action value:  $L_{p,Cpeak} = 135$  dB(C). In some other countries, e.g. in Canada and USA noise regulations in several jurisdictions treat impulse noise separately from continuous noise. A common approach is to limit the number of impulses at a given peak pressure over a workday. The exact figures vary slightly, but generally the regulations in which the exchange rate is 5 dB permit 10,000 impulses at a peak pressure level of 120 dB; 1,000 impulses at 130 dB; 100 impulses at 140 dB, and none above 140 dB. By Old Regulation the number of impulses was limited to 100 for sound pressure level of 140 dB and 1000 for sound pressure level of 130 dB.

When 3 dB exchange rate is used, generally there is no separate regulation for impulse noise. It is assumed that the equivalent sound exposure level takes impulse noise into account in the same way as it does that for continuous or intermittent noise.

## 4. IMPULSIVE NOISE DAMAGE RISK CRITERIA

Damage risk criteria are based on data obtained in the temporary threshold shifts (TTS) studies on volunteers, retrospective analysis of the permanent threshold shifts (PTS) in working population and on data obtained in animal studies.

### 4.1 First formulations of damage risk criteria

In 1964 the apparent lack of information on the effect of high-intensity impulse noise on hearing caused research work to concentrate on the formulation of a damage risk criterion (DRC). A programme of research was undertaken by Coles and Rice, in which methods of measuring and specifying the physical characteristics of impulse noise were compared with the temporary threshold shifts (TTS) which such noises produced in volunteer subjects. This research led to the formulation in 1968 by Coles, Garinther, Hodge and Rice [3] of what is thought to be the first authoritative DRC for exposure to gunfire noise.

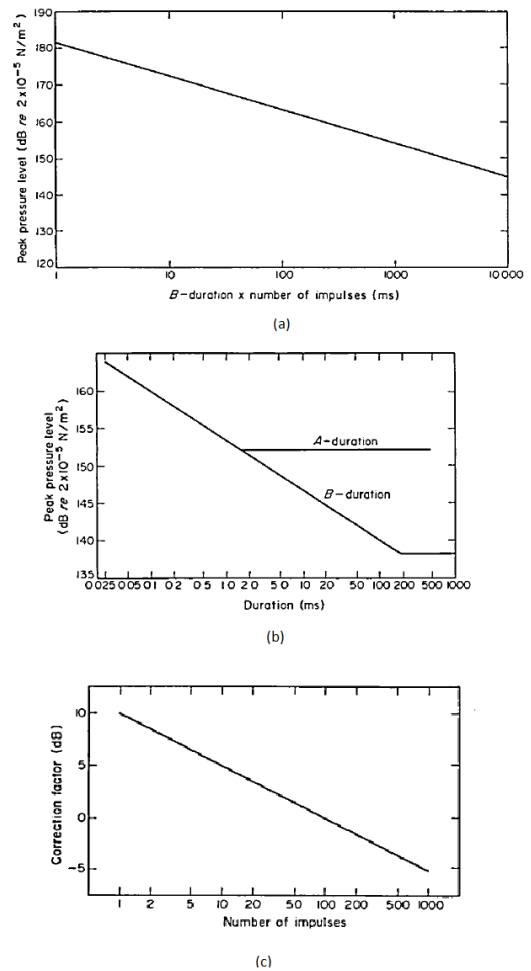


**Fig. 3** Damage risk criterion for impulse noise extended to include the use of relationship between B duration (Figure 3a), after Forrest [14]. Damage risk criterion for impulse noise (Figure 3b), correction factor to DRC for number of impulses (Figure 3c) proposed by CHABA, after CHABA [15]

In TTS studies exposition is exactly known and TTS is measured shortly after the exposition. Sound impulses were produced by sparks, light fire arms, clicker toys, by wood-on-wood or metal-on-metal impacts, and synthetically by loudspeakers, with and without reverberation. When using TTS as a measure of risk of hearing loss, the relation between

TTS and the permanent threshold shifts (PTS) to be expected after repeated exposure to the same noise is not a simple one. Usually, the TTS studies are based upon TTS measured 2 minutes after the exposure. The relation between the TTS and PTS approach improves when TTS is measured later, for example after 200 minutes. However, measurable effects after 200 minutes require higher experimental exposure levels, which meet ethical objections.

The request is that "end of day" TTS should not exceed 10 dB at or below 1000 Hz, 15 dB at 2000 Hz, and 20 dB at or above 3000 Hz in 75 % of the normally-hearing persons exposed. An approximation to the 90th percentile could be made by reducing the criterion peak pressure levels by 5 dB.

The damage risk criterion based on the criterion of Coles at al. [3] proposed by NAS-NRC Committee on Hearing, Bioacoustics and Biomechanics (CHABA) [15] extended to include the use of relationship between B duration (Fig. 2b) and the number of impulses per exposure [14] is represented in Figure 3.

These criteria rely on the assumption that a consistent relationship exists between TTS and PTS. Further specification of the noise (for example, spectral content) wasn't taken into account.

#### 4.2 The equal energy concept

Contemporary with the research on gunfire noise was the work of Burns and Robinson based on retrospective PTS analyses [15]. They were concerned with the evaluation of the effects of continuous noise in industry on the hearing of people habitually exposed during their working lifetime. An important conclusion of this work was that the total A-weighted sound energy received is a representative measure of noise exposure with respect to injury to hearing. In consequence the International Organisation for Standardization (ISO) has utilized these principles in its assessment of occupational noise exposure [16]. Further investigations were directed towards the extension of these continuous noise criteria to the impulse noise situation. Atherley and Martin [17] employed the equal-energy concept when assessing the hazard to hearing from industrial impact noise. They showed that the equal energy principle put forward by Burns and Robinson may be extended to include industrial impact noise and that equivalent A-weighted sound energy is an appropriate measure of hazard to hearing in this case. The equivalence of the criteria may be made under consideration in terms of acceptable hearing damage produced by exposure to an equivalent continuous noise level (ECNL) of 90 dB(A) for a working lifetime of 30 years [18]. The criteria are represented in Figure 4.

It is apparent from Figure 6 that the equivalent energy curve for 90 dB(A) is within about 5 dB of the other criteria. Therefore the equal-energy concept may be said to provide a possible unification and simplification of them. The method of assessment described by Martin and Atherley [17] for industrial impact noise is based on the assumption that the noise has generally broadband frequency characteristics and that the difference between dB(C) and dB(A) measures of the noise is 2,6 dB, and that is assumed also when employing equal energy concept to gunfire noise criterium.

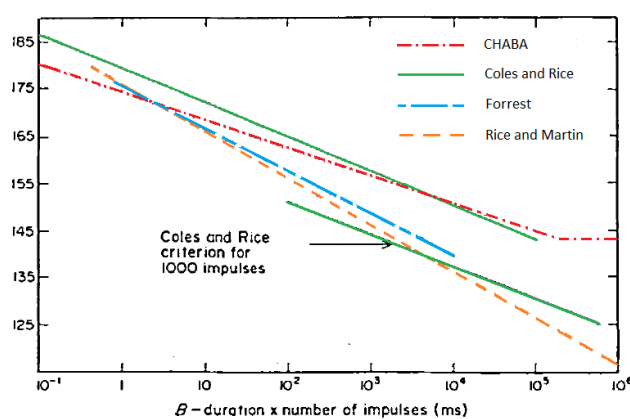


**Fig. 4** Comparison of damage risk criteria for gunfire noise [3, 6] with an equivalent continuous noise level of 90 dB(A) calculated by following the method of Martin and Atherley [18], Coles et al. [3], CHABA [6], Forrest [14], energy concept: ECNL = 90 dB(A), Rice and Martin [18]. All curves corrected for 75 % protected. Maximum number of impulses is 1000 for gunfire criteria [3, 6, 15]. After Rice and Martin [18]

As already said [see 2.1.] impulse noise is described by many parameters and there is no single measure, or assessment method, that enables adequate prediction of auditory hazard from impulse noise. It is very difficult to assess retrospectively the exposure of an individual over periods of years, so it is almost impossible to relate PTS measured in a particular individual, to the individual's impulse exposure history. Yet, the idea to apply equal energy concept to industrial impulsive noise by Atherley and Martin and generalization to gunfire noise by Rice and Martin seem to prevail. Equal energy principal accepted in ISO 1999 based on data collected with broad-band steady non-tonal noise is also sad to be the best available extrapolation to tonal or impulsive noise [19]. The former version of ISO 1999 indicated in a note that the measured exposure level may be increased by 5 dB when the noise contains impulsive or tonal components before applying the dose-effect relations to assess risk of hearing loss. In current version [20] there are no notes on impulsive or tonal noise. The basis for extension of equal energy principal to cover impulsive noise in this standard is the authoritative statement by the body of international experts [21]. According to the statement, there is not yet any clear defensible evidence to separate impulse and non-impulse noise, or their effects; consequently impulse noise and non-impulse noise should not be considered independently over the range up to an unweighted instantaneous peak sound pressure level of approximately 145 dB. It is recommended as a precautionary measure that for impulse noises suspected on the basis of available studies to have hazard potential in excess of the one predicted for continuous noise of equal  $L_{Aeq}$ , hearing conservation programmes should be initiated at a 10 dB lower level both in industrial and military situations.

#### 4.3 Animal studies

The relationship between noise-induced hearing loss and the peak amplitude of an impulse or impact noise is complicated. Systematic research with the chinchilla has shown that at the lower range of exposure to impulse noise ( $L_{p,Cpeak} < 140$  dB(C)) or impact noise ( $L_{p,Cpeak} < 115$  dB (C)),

the chinchilla develops a hearing loss that is proportional to the total energy of the exposure (peak level × number of impulses) [22]. Above these peak sound pressure levels, the auditory system is damaged primarily by the large displacements caused by high peak levels. The dividing line between the “energy” and “peak-level” behavior is referred to as the “critical level.” The critical levels are general approximations for the chinchilla, actual critical level is dependent on the specific waveform of the impulsive noise. Based on across-species comparisons, the critical levels for humans are likely to be approximately 10 dB higher than those observed in chinchillas. However, because of the high risk of hearing loss from high-level impulses and the variability in subsequent noise-induced hearing loss, a more conservative criterion of 140 dB has been adopted.

Impulsive noise also present a heightened risk when occurs with other steady-state background noise (approximately 85 – 95 dB(A)). Experimental studies with laboratory animals have shown that exposure to combinations of relatively benign impact and steady-state noise can lead to multiplicative interactions with hearing loss and cochlear damage, with the effects of the combined exposure being greater than the simple additive effects of impulse or continuous noise.

## **5 STUDIES ON EFFECT OF INDUSTRIAL IMPULSIVE NOISE ON HEARING**

Several studies on effect of industrial impulsive noise on hearing were taken, before and after the braking statement by the body of experts [21] was reported in 1981. Studies show that exposure to impulse noise among workers cause a significant hearing loss [6], [24]. Most of the hearing loss was in the higher frequencies (3–8 kHz). The hearing loss at 4 kHz was approximately 5–10 dB for those under 30 and 35–40 dB for those between 50 and 60 years of age.

Martin et al. (1975) examined hearing in 228 Canadian smelter workers in three different departments and compared it to nonexposed employees from the same factory [23]. The daily noise exposure level was mostly below 90 dB, which was then the Canadian threshold limit value (TLV), and therefore hearing protection was not found to be necessary. The prevalence of a hearing loss, defined as the average >25 dB for the 0,5–2-kHz area, ranged from 14 to 32 % in exposed >50 years, compared to 4 % of the controls. The hearing loss was greatest in areas with impulse noise and lowest in areas with a continuous noise level, LAeq, of 85–90 dB.

Nilsson et al. (1977) examined hearing of 1492 employees at a shipyard with an exposure to noise from LAeq = 88–94 dB and with a lot of impulse noise, typically 2500 impulses per day with peak noise levels from 105 to 135 dB (A) [23]. Despite the fact that almost 90 % used hearing protection, about 60 % had a reduced hearing acuity. After individual age correction to the ISO 1999, there were still about 40 % with reduced hearing acuity, most of them with exposure >5 years. The authors conclude that the noise in shipyards with impulse noise is particularly damaging to hearing.

Mantysalo and Vuori (1984) studied effect of impulsive noise on groups of Finnish metal workers and welders [23]. Three groups of Finnish metal workers and welders, each with 10 subjects, who had been exposed to impulse noise over a

short, medium and long period, respectively, were compared with 12 employees in a cable factory exposed to continuous noise. The longer the duration of impulse noise exposure, the greater the prevalence of hearing loss. It was also concluded that recurrent impulse noise appears to result in permanent hearing loss at frequencies 4 and 6 kHz after a shorter exposure time compared to continuous noise.

Starck and Pekkarinen (1987) evaluated the effect of impulsiveness of noise on hearing in a cross-sectional study on different groups of workers in Finland [5]: forest workers (N = 199) and shipyard workers (N = 179). In a selected group of workers exposure to noise was evaluated both outside and inside the hearing protectors (HPD) to define the lifetime equivalent noise exposure level and impulsiveness by the crest factor method. The exposure data was used to predict the noise-induced hearing loss at 4 kHz by applying ISO 1999 model that takes into the consideration exposure to noise using A-weighted equivalent level, age and gender. Special attention was paid to hearing protection - the types of hearing protectors used and the usage rates was questioned.

Measured and predicted hearing levels were consistent among forest workers. Among shipyard workers measured hearing loss was 10 dB higher than the predicted one. The shipyard workers exposure to noise was impulsive. Expressed by the impulse percentage, outside the HPD the impulse percentage was 4,2 % indicating duration in the noise sample when impulsiveness (I) is above 15 dB.

In another study by Toppila et al. (2000) a further analysis of the effect of impulsiveness was performed on three different groups of workers [5]. The impulse noise group consisted of shipyard workers, and the steady state noise groups of forest workers and paper mill workers. The impulsiveness of noise caused an extra 12 dB permanent threshold shift to shipyard workers who were exposed to high exposure levels. No difference was observed at low exposure levels.

In Russia Suvorov et al. (2001) found hearing loss in a study of the personnel in two workshops, revealing that impulse noise caused a greater hearing loss than one would expect from the estimated A-weighted noise dose [23]. The authors suggested that an extra safety margin of 5 dB should be subtracted from the threshold value for what is considered harmful impulse noise.

Tambs et al. (2006) conducted a Norwegian population study (N = 51 975) [23]. The participants were asked about occupational noise and impulse noise, including shooting. It was a clear but moderate effect on hearing among the relatively few women who were exposed to impulse noise. For women over 64 years, a loss of 4–6 dB was found at 3–8 kHz. For men aged 45–64 years, the corresponding hearing loss was 8 dB. Among men older than 64 years, there was a loss of approximately 7 dB in the range 2–8 kHz. Among men younger than 45 years, the hearing loss was 1–3 dB for the frequency range 3–8 kHz. While continuous noise generally resulted in a U-shaped” audiogram with the greatest loss in 3–4 kHz, impulse noise gave a loss in a much larger frequency range, in the oldest group from 2 to 8 kHz.

## **6 MECHANISMS AND MODELS OF IMPACT OF IMPULSIVE NOISE ON HEARING**

Brüel (1976) explained how impulse noise can cause more damage than the amount of energy calculated would indicate,

compared to continuous noise [7]. The averaging time of the brain is about 35 ms, and therefore these impulses are actually more intensive than they appear to be based on loudness, that is short impulses sound less loud than longer ones of the same intensity. The increased risk to hearing arises because, first of all, these impulses are transmitted with full force to the inner ear (the averaging times of the outer and middle ears being 50 and 35 microseconds respectively). Short impulses with relatively high energy content around 4 kHz are almost always amplified by resonance in the outer and middle ear so that these impulses reach the inner ear with an amplitude 10 - 12 dB higher than other types of noise. Given this amplification, certain loud sounds may damage the nerve ends of the inner ear producing permanent hearing loss, even though a sound level meter with fast time constant would indicate that their level is lower than the danger level.

Clifford and Rogers (2009) gave the new explanation the mechanism how the impulse noise may be more damaging than continuous sound [24]. As sound energy to the cell increases, the mechanism of cochlear damage shifts from biochemical injury to mechanical injury. Outer hair cells appear to be more sensitive than inner hair cells to impulse noise because of their energy requirements, which lead to increased production of reactive oxygen and nitrogen species and self-destruction by apoptosis.

## 7 TOWARD A NEW IMPULSIVE NOISE DAMAGE RISK CRITERIUM

Explanation of Clifford and Rogers has support in statistical model such as kurtosis and animal studies on chinchillas.

Statistical measurements such as kurtosis hold promise for the quantitative prediction of hearing loss. A basic form for noise metrics is designed by combining the equivalent sound pressure level (SPL) and a temporal correction term defined as a function of kurtosis of the noise. Kurtosis is defined as the fourth standardized moment about the mean of the data:

$$\frac{E(x-m)^4}{s^4} \quad (4)$$

where  $s$  is the standard deviation of  $x$ ,  $E(x-m)$  represents the expected value of quantity,  $m$  is the mean of  $x$ . Kurtosis describes the peakedness of a distribution, which is independent of the overall level and was suggested as a metric of impulsiveness by Erdreich [25]. Kurtosis of Gaussian noises is approximately 3. A basic form for noise metrics is designed by combining the equivalent sound pressure level (SPL) and a temporal correction term defined as a function of kurtosis of the noise [26].

Studies on animal exposure by Hamernik et al. [27] have shown that kurtosis effectively discriminates the risk of hearing loss in chinchilla for noise exposures with the same level and different temporal characteristics. Thus, SPL combined with a kurtosis correction term may serve as a good noise metric for assessment of the risk of noise of different temporal characteristics.

Goley et al. [26] showed that the kurtosis correction term significantly improves the correlation of the noise metric with the measured hearing losses in chinchillas. The average SPL of the frequency components of the noise that define the hearing loss with a kurtosis correction term is identified as the best noise metric among tested. One of the investigated metrics, the kurtosis-corrected A-weighted SPL, is applied to

a human exposure study data as a preview of applying the metrics to human guidelines.

## 8 CONCLUSION

Recent studies indicate the additional effect of occupational impulse noise on hearing, yet there is no valid method to combine steady state and impulsive noise. Present methods of assessment of occupational noise exposure and estimation of noise-induced hearing loss like ISO 9612 and ISO 1999 are based on equal energy concept that doesn't differ types of the noise. On the other hand, present regulations demand particular attention to any exposure to impulsive noise. Recently a new promising model of effect of impulsive noise is being considered that explains impact of impulsive noise on tested animals and metrics are being developed to meet the requirements for assessment of the risk of hearing loss in humans for noise exposures with different temporal characteristics.

## REFERENCES

- [1] ISO 12001:1996, SRPS EN ISO 12001:2009 Acoustics -- Noise emitted by machinery and equipment -- Rules for the drafting and presentation of a noise test code
- [2] ISO 9612:1997, SRPS EN ISO 9612:2008 Acoustics — Guidelines for the measurement and assessment of exposure to noise in a working environment
- [3] R. R. A. Coles, G. R. Garinther, D. C. Hodge and C. G. Rice "Hazardous exposure to impulse noise ", *Journal of the Acoustical Society of America* 43, 336—346, 1968.
- [4] [https://www.sfu.ca/sonic-studio/handbook/Damage-Risk\\_Criteria.html](https://www.sfu.ca/sonic-studio/handbook/Damage-Risk_Criteria.html)
- [5] Starck J, Toppila E, Pyykko I. "Impulse noise and risk criteria", *Noise Health* 5:63-73, 2003.
- [6] NAS-NRC Committee on Hearing, Bioacoustics and Biomechanics "Proposed damage-risk criterion for impulse noise (gunfire)", *Report of Working Group 57*, 1968.
- [7] P.V. Brüel, "Do We Measure Damaging Noise Correctly?", *B&K Technical Review*, no. 1, pp. 3-32, 1976.
- [8] Regulation on occupational safety measures and norms for noise protection at workplace. Off. J. SFRJ. 1992, 21, pp. 310-31
- [9] Council Directive 79/113/EEC of 19 December 1978 on the approximation of the laws of the Member States relating to the determination of the noise emission of construction plant and equipment
- [10] ISO 9612:2009, SRPS EN ISO 9612:2016 Acoustics — Determination of occupational noise exposure — Engineering method
- [11] [https://www.ccohs.ca/Oshanswers/phys\\_agents/exposur\\_e\\_can.html](https://www.ccohs.ca/Oshanswers/phys_agents/exposur_e_can.html)
- [12] Regulation on preventive measures for health and safety at work regarding noise exposure. Off. J. RS. 2011, 96, pp. 10-12 and Off. J. RS. 2015, 78, p. 24
- [13] Directive 2003/10/EC of the European Parliament and of the Council of 6 February 2003 on the minimum health and safety requirements regarding the exposure

- of workers to the risks arising from physical agents (noise). Off. J. Eur. Commun. L 42, 15.2.2003, p. 38
- [14] M. R. Forrest “The effects of high intensity impulsive noise on hearing”, *M.Sc. Dissertation, University of Southampton*, 1967.
- [15] W. Burns and D. W. Robinson “Hearing and Noise in Industry”. *London: Her Majesty's Stationery Office*, 1970.
- [16] ISO R1999:1971. Assessment of occupational noise exposure for hearing conservation purposes.
- [17] G. R. C. Atherley and A. M. Martin “Equivalent-continuous noise level as a measure of injury from impact and impulse noise”, *Annals of Occupational Hygiene* 14, 11-28, 1971.
- [18] C. G. Rice and A. M. Martin “Impulse Noise Damage Risk Criteria”, *Journal of Sound and Vibration* 28(3), 359-367, 1973.
- [19] ISO 1999:1990 Acoustics - Determination of occupational noise exposure and estimation of noise-induced hearing impairment
- [20] ISO 1999:2013 Acoustics — Estimation of noise-induced hearing loss
- [21] V. H. E. Gierke, D. Robinson and S. J. Karmy “Results of the workshop on impulse noise and auditory hazard”, *Institute of Sound and Vibration Research, Southampton, U.K., ISVR Memorandum 618 October 1981. J. Sound Vibrat.* 83 pp. 579–584, 1982.
- [22] Noise-induced hearing loss, in: *Noise and Military Service: Implications for Hearing Loss and Tinnitus*, *Institute of Medicine, Washington, DC, The National Academies Press* (2006)
- [23] A. Lie et al. “Occupational noise exposure and hearing: a systematic review”, *Int Arch Occup Environ Health* 89:351–372, 2016.
- [24] R.E. Clifford and R.A. Rogers “Impulse noise: theoretical solutions to the quandary of cochlear protection”, *Ann Otol Rhinol Laryngol* 118(6):417–427, 2009.
- [25] J. Erdreich “Distribution based definition of impulse noise,” *J. Acoust. Soc. Am.* 77, S19–S19, 1985.
- [26] G. Steven Goley, Won Joon Song and Jay H. Kim “Kurtosis corrected sound pressure level as a noise metric for risk assessment of occupational noises”, *J. Acoust. Soc. Am.* 129 (3), March 2011.
- [27] R. P. Hamernik, W. Qiu and B. Davis “The effects of the amplitude distribution of equal energy exposures on noise-induced hearing loss: The kurtosis metric”, *J. Acoust. Soc. Am.* 114, 386–395, 2003.

**WE PARTICIPATE  
IN**



**SENVIBE**

**‘Strengthening Educational Capacities  
by Building Competences and Cooperation  
in the Field of Noise and Vibration Engineering’**



**ERAZMUS+ KA2 CBHE PROJECT**



## NOISE MONITORING ON THE TERRITORY OF THE CITY OF NIŠ - OVERVIEW OF THE METODOLOGIES AND THE RESULTS

Momir Prašćević<sup>1</sup>, Darko Mihajlov<sup>2</sup>, Marko Ličanin<sup>3</sup>

<sup>1</sup> University of Niš, Faculty of Occupational Safety, Serbia, momir.prascevic@znrfak.ni.ac.rs

<sup>2</sup> University of Niš, Faculty of Occupational Safety, Serbia, darko.mihajlov@znrfak.ni.ac.rs

<sup>3</sup> University of Niš, Faculty of Occupational Safety, Serbia, marko.licanin@znrfak.ni.ac.rs

**Abstract** - *Noise management and environmental protection is becoming increasing challenge in the world. Even though there are many of the hi-tech solutions higher investments into solving problems nowadays, this problem stays the same. In some cases, level of the noise pollution is even higher. Knowledge of the exact environmental noise level data is the first condition for the overview of the existing noise conditions and its impact on the environment, as well as for planning the corresponding actions and measures. Those actions can be predictive and corrective, in order to maintain the noise level below limit values, or to reduce noise in the areas where this represents a serious threat to the performance of human activities and creates a health issues. First environmental noise measurements in Serbia has been performed in 1957. The city of Niš as a local municipality started with systematic measurements in 1995., and since that date, with short interrupts, environmental noise monitoring has been performing every year. Methodologies of environmental noise monitoring have been changed and improved according to the new and modern technical capacities. Currently, in the city of Niš, a long term environmental noise monitoring is being done using latest generations of the equipment for continuous noise monitoring. After brief overview of the legal regulations and standards, this paper will be related to the methodologies that are used for noise level monitoring in Niš, as well as on measurement results with the special attention to those obtained by five-year long term noise monitoring.*

### 1. INTRODUCTION

Noise as one of the basic parameters of the living environment in urban areas, becomes very serious problem in cities all over the world. There are many factors that contributes to that fact. One of them is increasing density of human population which contributes to higher volume and intensity of the traffic. Additional load to the noise level is provided by communal activities, transport services and public transport, which are a necessity in those environments. Prediction of all of the negative scenarios in near future, implies that noise management and protection of the urban environment will pose as serious professional challenge. Even with significant effort invested, based on new technologies and investments, noise pollution is at the increasing rate.

Latest data on the condition of the environmental noise level, based on strategic noise mapping for agglomeration in

European Union obtained in first round noise mapping, shows that 54% of the population in urban areas (56,001,200 people) is exposed to the value  $L_{den}$  higher than 55 dB, while 15% of the population (56,754,200 people) is exposed above 65 dB of  $L_{den}$ . Besides that, additional 33,437,244 people lives in the areas outside agglomeration, where values of  $L_{den}$  are above 55 dB, and 7,657,1083 people in areas where  $L_{den}$  is higher than 65 dB. Total of the 89,438,444 people is exposed to  $L_{den}$  higher than 55 dB, where almost 89 million are affected by traffic noise [1].

Based on the already established reasons, monitoring of the environmental noise and noise assessment becomes necessity, especially when there is a need for noise control in areas highly affected by noise applying proper engineering and technical solutions, education and legislation.

In order to perform environmental noise monitoring, it is necessary to establish a proper measurement strategy that will include dynamic nature of the sound propagation, influence of the meteorological data on the sound propagation, as well as other factor that affects the precision of the annual values of noise indicators.

First noise measurements in Serbia were done in 1957 within diploma research of PhD Petar Pravica former student of the Faculty of Electrotechnical Engineering in Belgrade [2], nowadays retired full professor. Those were the first measurements done by General Radio Co sound level meter, which was a predecessor to the later more precisely sound level meters manufactured by Brüel&Kjær and other companies. In the following years, technical faculties in Belgrade, Novi Sad and Niš started performing environmental noise measurements [2].

After adopting the environment protection law [3], organized noise level monitoring in larger cities became a practice. City of Niš started environmental noise monitoring in 1995., and with short brakes, maintained these activities so far using advance measurement equipment. Tendencies in continues improvement in quality and services in environmental noise monitoring made the Laboratory for Noise and Vibration are very recognizable in this field.

### 2. OVERVIEW OF THE REGULATIONS AND STANDARDS IN ENVIRONMENTAL NOISE

First law regarding environmental protection has been adopted in 1991. [3]. This law has established system for management and improvement of the environment protection,

measures and procedures for protection of natural heritage, measures and procedures for protection of the environment influenced by harmful activities, method of financing and implementation organization for improvements in environment protection. Separate portion of the law was related to environmental noise. Articles in this law stated that each municipality is obliged to undergo noise protection measures, to define the acoustical zones and to perform environmental noise measurements. Noise measurements was regulated and entitled only to the certified institutions with proper measurement equipment and trained personnel.

Based on the previously mentioned law, the Regulation on the permissible environmental noise level [4] was adapted in 1992. The regulation defined determination of the rating noise level based on the measurements, permissible noise level in the living areas, method of the noise measurements, criteria that certified institutions must fulfil, as well as documentation of the noise sources that are sold and used, was explicitly defined. This regulation defined maximum permissible noise levels in indoor, while the noise levels in the outdoor living zones were defined by standard SRPS U.J6.205 [5]. The regulation determined that noise measurement method and correction of measured noise levels based on the noise type must be done as described in standard SRPS U.J6.090 [6]. Regulation also defined the choice of the measurement positions and measurement interval. In the case of the fluctuating noise, noise levels were measured at least three times during the day and two times during the night with measurement interval set to 15 min. Measurement interval was from 06:00 to 22:00 for day period and from 22:00 to 06:00 for night period

Standard SRPS U.J6.090 [6], based on the international standard ISO 1996-1:1982 [7] and ISO 1996-2:1987 [8], determined procedure for environmental noise measurements for the purpose of noise pollution assessment in communal environment and implementation of the noise control.

New Law on environment protection [9] adapted in 2004. This law determines the system of environmental protection that enables human development and existing in a healthy living environment and balanced relation between industrial development and living environment in Republic of Serbia. By adopting this law, previous legislations regarding noise protection has been inherited. In addition, all country's districts and municipalities are obliged within its jurisdiction to enable continual control and monitoring of the environmental conditions.

According to the Law [9] monitoring is being done by systematic monitoring the indicators values, i.e. monitoring the negative impacts on the environment, condition of the living environment, measures and activities to undertake in order to reduce those negative effects and improve the quality of the living environment. Only certified organizations according to SRPS ISO/IEC 17025 [10], with all of the necessary conditions fulfilled, in the context of trained personnel, equipment and facilities, are enabled to perform monitoring.

Operator in industry complex which is the source of emission and environmental pollution is obliged to perform the monitoring by certified institution or at his own under the assumption that his entity fulfils all conditions regulated by legislation.

In 2007, second edition of SRPS U.J6.205 [11] has been published. This standard defines noise level sampling with measurement interval of 15 min, in every hour, during the 24 h. Rating noise level is being calculated based on measured values.

First standalone law related to the environmental noise has been adopted in 2009, and then revised in 2010. [12]. This law regulates the subjects of the environmental noise protection, measures and conditions of protection, environmental noise measurements, noise information and data access and other important questions regarding environment protection and human health. Based on the articles in the Law [12], the additional by-laws are adopted that enabled more detailed and precise define the implementation of this Law [12]. Directive 2002/49/EC of the European Parliament and the Council relating to the assessment and management of environmental noise [13] is transpose by adopting Law and by-laws, which created compatibility of the national and European laws in this sector.

Noise indicators, limit values and noise indicator assessment methods are defined by regulation [14]. The regulation [15] defines the noise measurements methods, content and volume of the measurement reports. Environmental noise measurements are performed according to the SRPS ISO 1996-1 [16] and SRPS ISO 1996-2 [17], identical with ISO 1996-1 [18] and ISO 1996-2 [19], respectively.

Previously mentioned regulations and standards defined the obligation for environmental noise monitoring and determined basic procedures for noise measurements, but none of those defined the procedure for noise level monitoring in the longer time interval.

Meanwhile, a revision of the international standards has been done and the currently valid versions are ISO 1996-1 [20] and 1996-2 [21]. These standards, introduce the term of long-term measurement and monitoring, defines the necessary equipment, measurement procedure as well as a way of determining the long-term noise indicators. The same indicators were previously defined by directive [13], and national regulation [14].

### **3. OVERVIEW OF MEASUREMENT STRATEGIES AT THE TERRITORY OF CITY OF NIŠ**

Determination of the environmental noise pollution level assumes two measurement strategies for monitoring and determining noise indicators at the given location:

1. Strategy based on the short-term measurements;
2. Strategy based on the long term measurements.

#### **3.1 Short-term noise measurements**

First strategy includes the series of the short-term noise measurements of the equivalent noise levels undertaken under the specific noise source operating conditions and meteorological conditions. In this case, the annual values of noise indicators are determined by applying relevant methods of prediction, that is by calculation. The choice of the short-term measurement interval, as well as the number of the intervals during the year, is the most important factor for getting the most precise noise indicator values at the given location. The smallest time interval for short-term measurements is 10 minutes. The recommended time interval

is 30 minutes when variations in the meteorological condition during the measurement take into account. The choice of the length of the short-term time interval is an actual topic subjected by many papers written today [22]. Researchers chose different time intervals depend on the many factors and its contribution to the measurements results.

Environmental noise monitoring in Republic of Serbia is being done based on the actual regulations and standards at the territory of several cities. As those documents did not precisely described methodology for noise monitoring, these methodologies are different in the cities. This difference is related to the number and the manner of choice of measurement locations, number of measurements in the reference measurement intervals (day, evening, night) that defines the dynamic of the monitoring, measurement intervals as well as measurement parameters and noise indicators used for the noise assessment [23].

Application of the different measurement procedures is a result of many factors specific for different cities such as: terrain configuration, structure and type of the traffic roads, structure and volume of traffic, number and positions of the noise sensitive objects, contribution of the specific noise sources to the total noise level etc.

Ongoing practice of the noise monitoring in the cities in Serbia usually assumes strategy of the short term measurements of the  $L_{eq}$  in the 15 min. intervals, and counting traffic volume. Recently, in some cities time interval has been increased to 1 h, while in some (Novi Sad, Belgrade and Pančevo) noise monitoring is done as a series of short-term measurements with interval of 24 h.

At the territory of the city of Niš, noise monitoring has been done on a monthly basis since 1995, with the short interrupts. Monitoring methodology is defined by programmes for the communal noise level monitoring, that were created by Noise and vibration laboratory, hired by local municipality of Niš. Noise monitoring has been done according to the short-term monitoring measurements in the reference time intervals.

First programme was based on the 15-min measurements of the  $L_{eq}$ , as well as statistical noise parameters and noise frequency analysis in five day and two night intervals:

1. 06:00 - 08:00
2. 08:00 - 12:00
3. 12:00 - 15:00
4. 15:00 - 19:00
5. 19:00 - 22:00
6. 22:00 - 01:00
7. 01:00 - 06:00

Noise monitoring was done at 11 - 14 measurement locations, chosen to be especially sensitive to noise. Within those areas, measurement positions were chosen according to the national regulations, so the total measurement positions was 40 – 50 for one year. At all of these location, traffic volume and composition has been determined. Since 2001, noise monitoring was being done at 14 locations with a similar programme of the monitoring as in previous period. The difference was in the choice of the measurement intervals (4 intervals during the day and 2 intervals during the night):

1. 06:00 - 08:00
2. 08:00 - 13:00

3. 13:00 - 16:00
4. 16:00 - 22:00
5. 22:00 - 01:00
6. 01:00 - 06:00

After the 2005., after division of the city of Niš into municipalities, programme enveloped all of the municipalities within 15 measurement locations with the total of 60 measurement position. Number of time intervals was reduced to five:

1. 09:00 - 12:00
2. 13:00 - 16:00
3. 17:00 - 20:00
4. 22:00 - 01:00
5. 01:00 - 06:00

In 2007., number of locations was reduced to 11, and the number of measurement positions to 44, while in 2015., number of location was decreased to 7 (28 measurement positions). The reason being the introduction of the long-term monitoring procedures.

Based on the analysis of noise monitoring data until 2016, the standard deviations of the measured data and taking into concern the need for calculation of the annual noise indicators in accordance to the actual regulations, Noise and vibration laboratory has recommended to the city authorities, the procedure for noise monitoring based on the short-term measurements in six intervals.

1. 06:00 - 10:00
2. 10:00 - 14:00
3. 14:00 - 18:00
4. 18:00 - 22:00
5. 22:00 - 02:00
6. 02:00 - 06:00

New methodology is based on 15 min measurements in every 4h period, for each measurement position during first month. Those measurements are repeated at the same measurement positions during next three months by moving the measurement time interval in next hour within 4h measurement period. This procedure enables one 15 min sample for every hour (total of twenty-four 15 min intervals) for all measurement points during the first quarter. The complete procedure is then repeated for the next two quarters for the repeatability purpose.

Using this methodology, three 15 min. samples are being gathered for each hour during the day for each measurement position, during one year. This enables the precisely determination of the noise indicators using the following equations:

$$L_{day} = 10 \log \left[ \frac{1}{N} \sum_{i=1}^N 10^{\frac{\bar{L}_{Aeq,i}}{10}} \right] \quad (1)$$

$$L_{evening} = 10 \log \left[ \frac{1}{N} \sum_{i=1}^N 10^{\frac{\bar{L}_{Aeq,i}}{10}} \right] \quad (2)$$

$$L_{evening} = 10 \log \left[ \frac{1}{N} \sum_{i=1}^N 10^{\frac{\bar{L}_{Aeq,i}}{10}} \right] \quad (3)$$

where:  $\bar{L}_{A,eq,i}$  is the average value of three measured values of equivalent noise level for  $i$ -th hour during day, evening and night,  $i$  - is the order number of the hour during the day ( $i = 1 \div 24$ ), while  $N$  is the total number of measurements (24).

The recommended noise monitoring methodology based on short-term noise measurements was applied at the territory of the city of Niš from September 2017 to August 2018 and will be continue in the following period. Measurement results have not yet been publicly announced.

### 3.2 Long-term noise measurements

Second strategy of the noise monitoring is the long-term measurement of the equivalent noise level during period that is long enough to include all variations in the operating conditions of the noise sources, as well as all variations in meteorological conditions. Having in mind that composition and volume of the traffic is very unpredictable during different time intervals and that the connection of those events to the meteorological data seems to be randomized, a specific period within calendar year (a month, three, six or even entire year) should be considered for the noise monitoring interval.

Results of the long-term monitoring are in any aspect more precise and require less corrections than the short-term noise measurements.

Long-term noise measurements can be realized applying two concepts – permanent noise monitoring and semi-permanent noise monitoring.

Permanent noise monitoring represents continuous measurements of the equivalent noise level at fix position 24 hours per a day through entire year. For this purpose, permanent noise monitoring stations are used. Permanent noise monitoring enables the real time noise levels and precisely data that can be used for calibration of strategic noise maps.

Semi-permanent noise monitoring usually lasts between several days and up to the several weeks or months and it can be used for determination the annual noise indicator and for economic monitoring of environmental noise trend because it can be cover many measurement locations and still maintain data precision. Also, this kind of monitoring can be fairly used for determining compliance with limit values, public information, increasing knowledge about noise dose-effects, as well as for calibration of strategic noise maps. For this purpose, there are mobile noise monitoring stations, that are easy to disassemble and move between locations.

The adequate time interval for the semi-permanent noise monitoring, as well as the number of  $L_{eq}$  measurements at the same position during the year, that will enable representative data for precisely assessment of the annual noise indicators, are not defined by standards. In this way, as there are no exact regulations, researchers determine the length of the semi-permanent noise monitoring measurements intervals to reduce the need for corrections in noise indicators calculations, based on the experimental studies taking into account noise sources operation conditions (such as composition and volume of the traffic). If noise propagation and emission conditions are different for the different seasons, for example due to use of the winter tires, the snow layer on the road, the researchers usually choose the

measurement time intervals in different seasons in order to account as many meteorological conditions as possible.

Strategy of the semi-permanent and permanent noise monitoring apply in the limited scope in Serbia, at the territories of the cities of Niš [24] and Novi Sad [25].

Since 2013., Faculty of occupational safety in Niš, has the Brüel&Kjær's Environmental Noise Management System, intended for long-term noise monitoring. The system is composed of software type 7843 and two noise monitoring terminals - type 3639-B-203. For the meteorological data monitoring one noise monitoring terminal is equipped by meteorological station type Vaisala WXT 520. The metrological stations measure the atmospheric pressure, temperature, air moisture, speed and wind direction, as well as the amount of rain.

The central part of the system is software type 7843 that maintains real-time internet connection with noise monitoring terminals, enables continually data storage from both terminals, as well as the graphic representation of the real-time data. Software is running on the server that enables large data storage, data analysis, report creation, GPS location tracking etc. This system constantly generates 15 - minutes reports based on the  $L_{eq}$  with the sampling of 0.5 s, as well as four periodic reports:

1. One hour reports based on  $L_{eq}$  using 0.5 s sampling;
2. Daily report based in the hourly noise indicators;
3. Monthly report based on the daily noise indicators;
4. Annual report based on the monthly noise indicators.

Beside mentioned, system enables additional twelve custom reports. For the need of this research, additional reports have been selected and defined as:

1. Monday to Friday report (working days);
2. Saturday and Sunday report (weekend);
3. Monday to Sunday (whole week).

## 4. OVERVIEW OF THE RESULTS OF NOISE MONITORING AT THE TERRITORY OF THE CITY OF NIŠ

### 4.1 Short-term noise measurements

Programmes of the noise level monitoring at the territory of the city of Niš for the period 2009 - 2016 enveloped all of the municipalities, where short term measurements have been undertaken at 27 measurements positions (biggest municipality - Medijana), 9 measurement positions (Crveni Krst), 11 measurement positions (Palilula), 9 measurement positions (Pantelej), and 6 measurement positions (Niška banja). Based on those short term measurements, by applying the defined methodologies, annual noise indicators have been calculated for all measurement positions. Values of the indicator  $L_{den}$  during the period 2009 - 2016. are presented in figure 1. Measurement positions where  $L_{den}$  is higher than 65 dB is specially marked in the figure. It can be easily observed that majority of the values presented in figure 1 is higher than the maximum permissible values, which easily points to the problem of the increasing environmental noise level at the observed location/

## 4.2 Long-term noise measurements

Procedure of the long-term measurements is realized in 10 measurement locations until to the time of writing this paper. Measurements locations has been chosen in accordance to the population density, locations of the residential objects, as well as structure of the nearby traffic roads. The measurement locations are shown in the figure 2.

At the measurement location NMT1.1, environmental noise has been monitored two years, at NMT1.2 - 18 months, at NMT1.3, NMT2.6 and NMT2.7 - one year, at NMT2.2 - nine months, at NMT2.1 , NMT2.4 and NMT2.5 - six months, at

NMT2.3 - three months. At all of these locations, microphone was placed in the free field, except at the NMT2.3 and NMT2.4, where it was mounted on the facade of the object. In all of the locations, dominant noise source was road traffic, except at the location NMT2.4, where railway traffic was the dominant noise source.

Daily noise indicators for all measurement locations, with 24-hour profiles can be found in the application "Continuous noise monitoring" at the following hyperlink: <http://www.zrnfak.ni.ac.rs/BVLab-KMB/KMB-Home.html>.

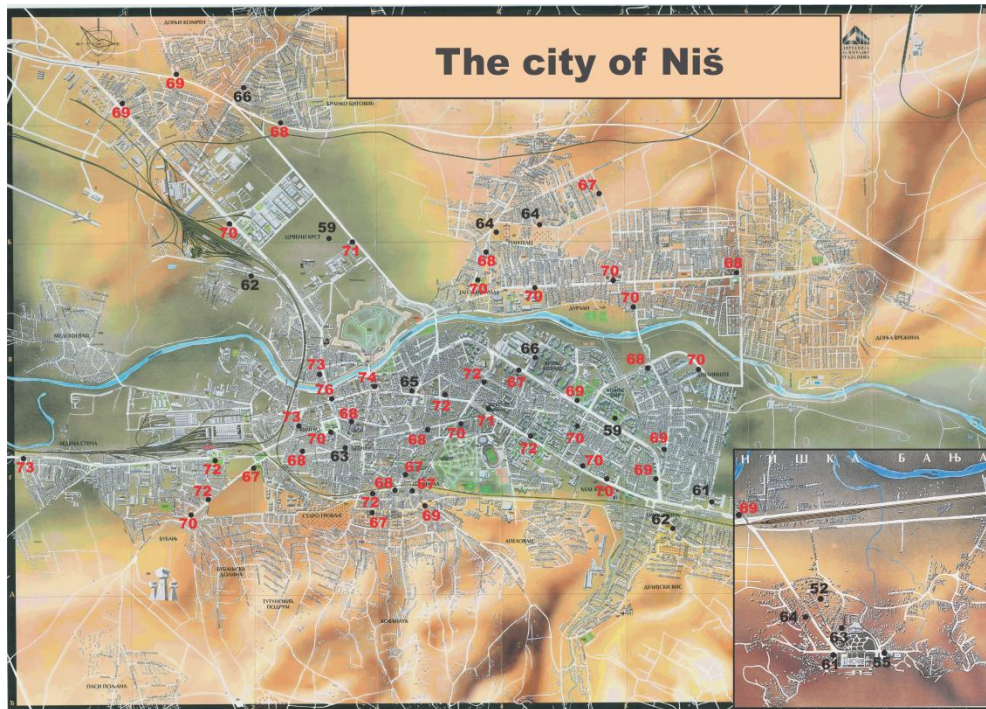


**Fig. 1** Values  $L_{den}$  for the measurement positions in the city of Niš, as a results of measurements during period 2009 - 2016. Red coloured values represent the positions where  $L_{den}$  is higher than 65 dB

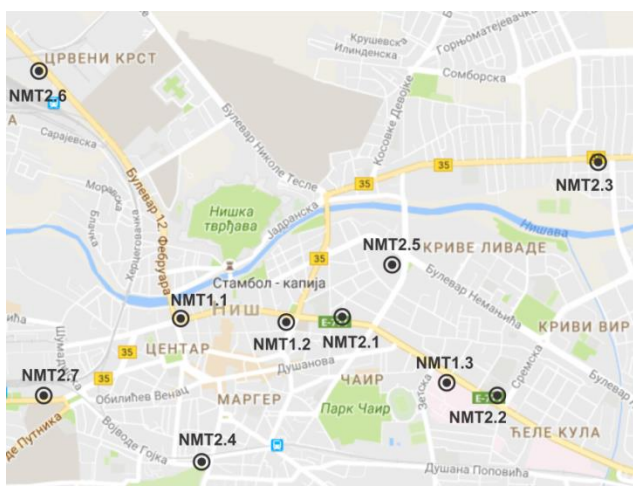


**Fig. 2** Distribution of the measurement locations for long-term noise monitoring

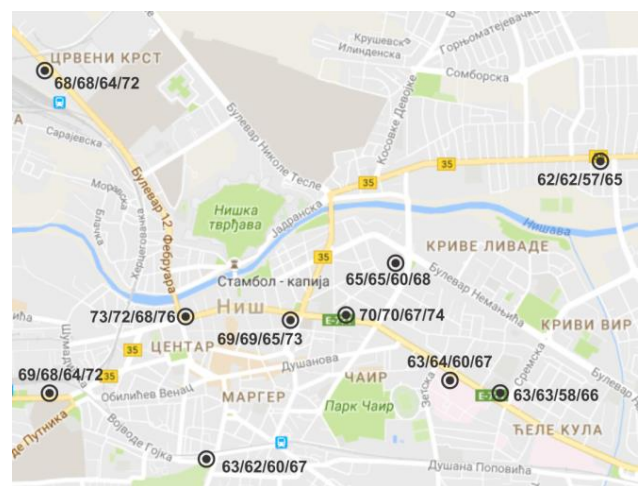


**Fig. 3** Values of  $L_{day}/L_{evening}/L_{night}/L_{den}$  in dB

Besides that, in application is given a description of the measurement locations, as well as reports extracted for the need of city of Niš municipality authorities within realization of the communal noise monitoring programme. Figure 3 represents measured, that is evaluated annual noise indicators.

Graphical representation of the monthly noise indicators, for all measurement locations, where measurement interval was longer than six months, are represented in figures 4-13.

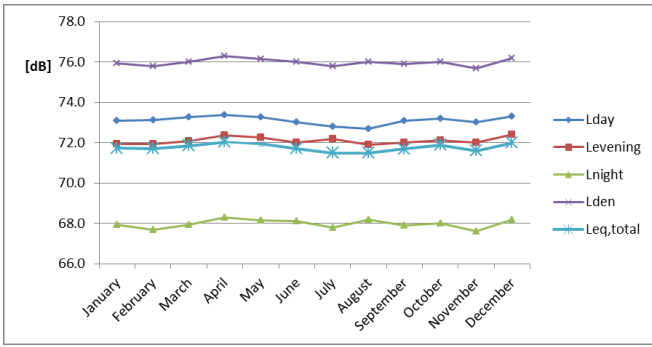


**Fig. 4** The monthly noise indicator values in 2014 for measurement location NMT1.1

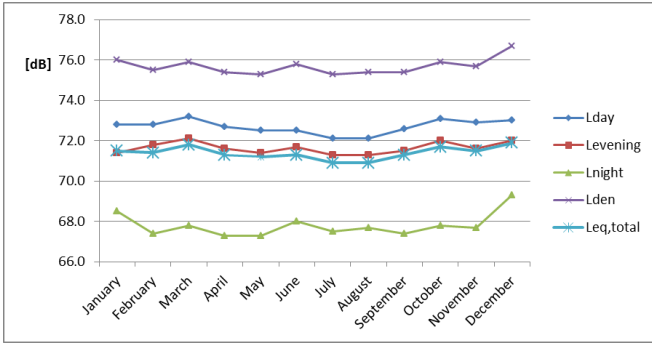


**Fig. 5** The monthly noise indicator values in 2015 for measurement location NMT1.1

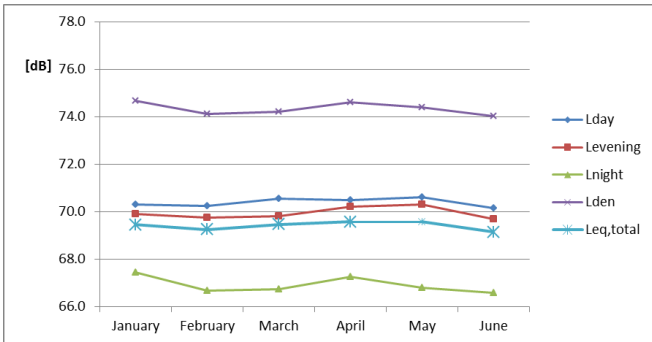


**Fig. 6** The monthly noise indicator values in 2014 for measurement location NMT2.1

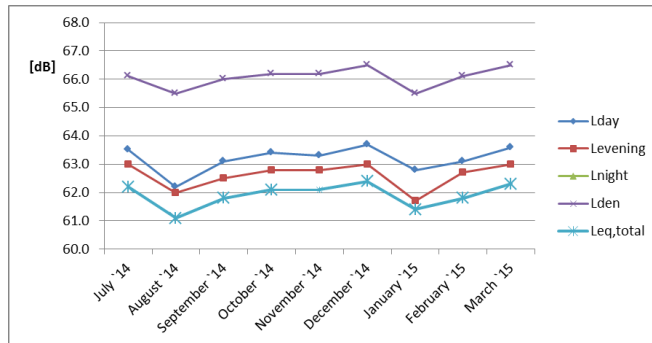


**Fig. 7** The monthly noise indicator values in 2015/2016 for measurement location NMT2.2

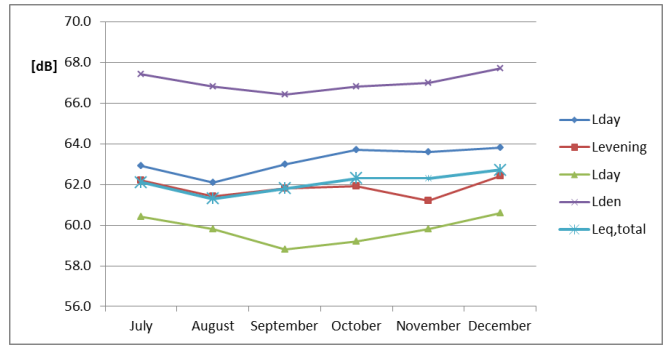


**Fig. 8** The monthly noise indicator values in 2015 for measurement location NMT2.4

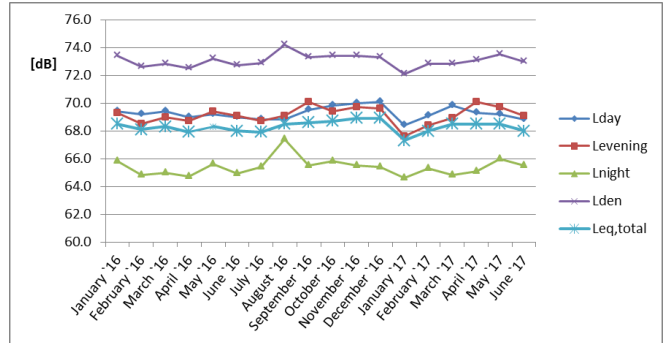


**Fig. 9** The monthly noise indicator values in 2016/2017 for measurement location NMT1.2

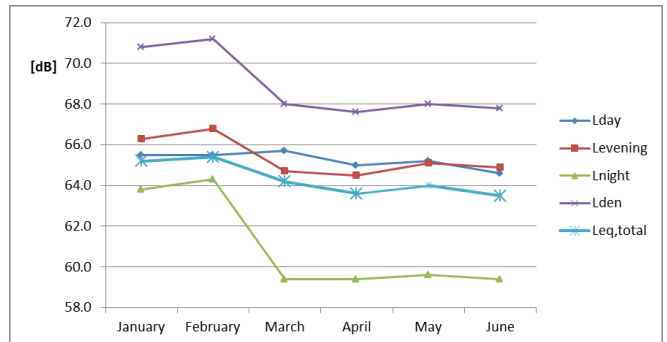


**Fig. 10** The monthly noise indicator values in 2016 for measurement location NMT2.5

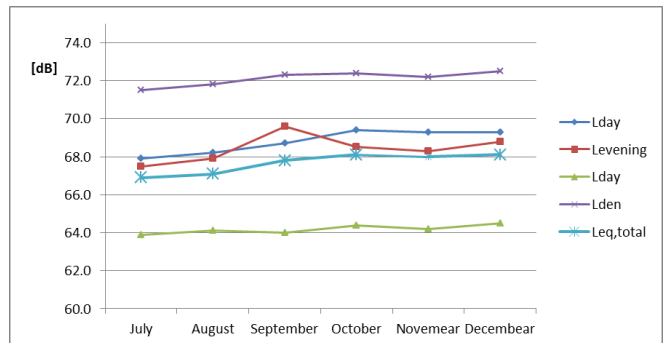


**Fig. 11** The monthly noise indicator values in 2016 for measurement location NMT2.6

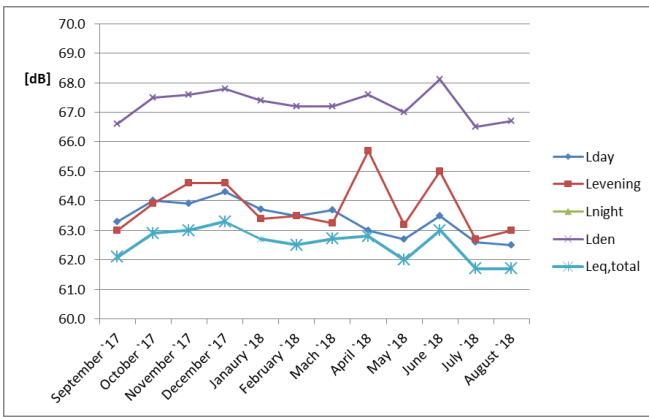


**Fig. 12** The monthly noise indicator values in 2017/2018 for measurement location NMT1.3

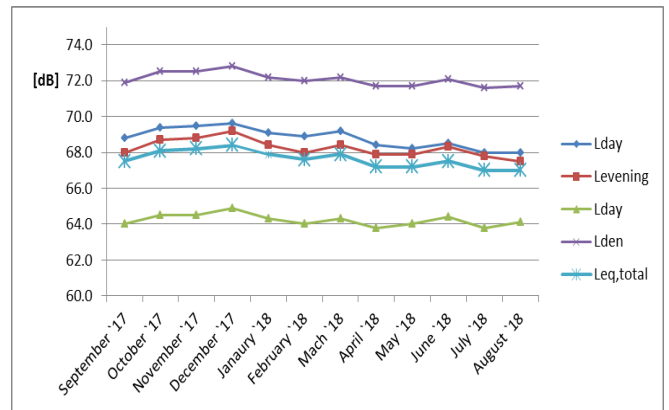


**Fig. 13** The monthly noise indicator values in 2017/2018 for measurement location NMT2.7

Besides standard monthly reports, shorter reports have been defined: Monday-Friday (working days), Saturday-Sunday (weekend), Monday-Sunday (whole week). In figure 14 and 15, changes in noise indicators for working days has been shown. This representation is done for the data gathered in 2017/2018 at measurement location NMT1.3 and NMT2.7

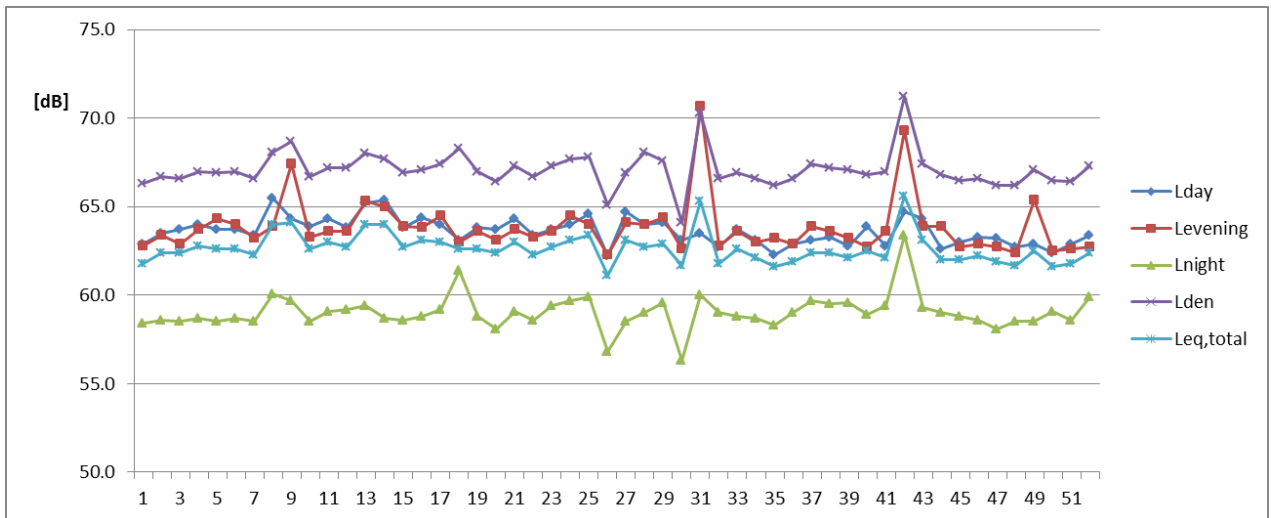


**Fig. 14** The work days' noise indicator values in 2017/2018 for measurement location NMT1.3

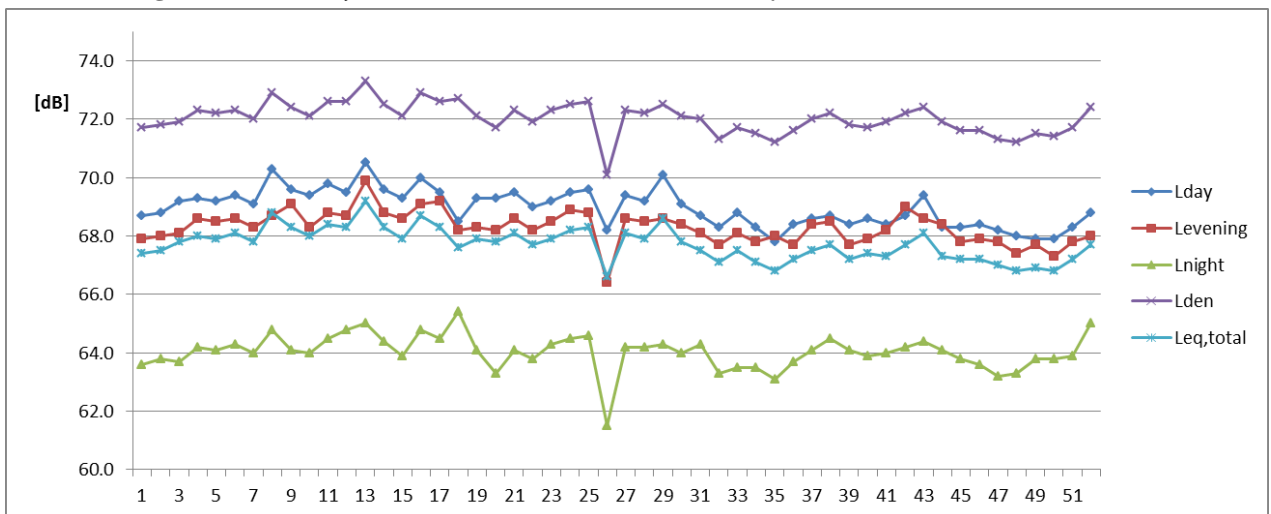


**Fig. 15** The work days' noise indicator values in 2017/2018 for measurement location NMT2.7

## CONCLUSION

This paper contains the overview of the regulations in Republic of Serbia and standards in the area of environmental noise measurements and points to the fact that noise monitoring procedure in urban areas is not yet precisely defined. This leads to the problem, where results of the noise monitoring undertaken in different cities are inconsistent, thus, often incomparable and unsuitable for the environmental information system that needs the standardized data of the environmental noise level.

It is suggested to specify the methodology for noise monitoring in urban areas based on the new series of ISO standards [20] and [21] and long-term noise monitoring with the defined measurement time interval.

The basis for defining the necessary time interval for noise monitoring in order to provide representative data for determining the annual noise indicators values, the long-term noise monitoring data at the territory of the city of Niš can be used. Analysis of the results of the long-term noise monitoring for the period 2014-2018, shows that monthly noise indicators can be taken as representative values for determining annual noise indicator values. If there are no significant noise sources, other than road traffic, even a five days long interval can serve as a representative data.

## ACKNOWLEDGMENT

This paper is presented as a part of the projects "Development of the methodology and means for noise protection in urban areas" (No. TR - 037020) and "Improvement of the monitoring system and evaluation of the long-term exposure of the population to sustenance in the environment using neural networks" (No. III - 43014). Authors would like to express gratitude to the Ministry of education, science and technological development of Republic of Serbia, for the financing support in these research

## REFERENCES

- [1] Licitra G. 2012. *Noise mapping in EU: Models and Procedures*. CRC Press, USA. 442 p.
- [2] Pravica P. 2012 *Invited lecture*, The Serbian Noise Congress "Sharing Sound in Serbia", Belgrade
- [3] Law on Environmental Protection, "Gazette RS" No. 66/91 (in Serbian)
- [4] Regulation on the permissible environmental noise level, "Gazette RS" No. 66/91 (in Serbian)
- [5] SRPS U.J6.205:1992, Acoustics in building – Acoustical zoning of space (in Serbian)
- [6] SRPS U.J6.090:1992, Acoustics in building – Measurement of communal noise (in Serbian)
- [7] ISO 1996-1:1982, Acoustics - Description and measurement of environmental noise - Part 1: Basic quantities and procedures
- [8] ISO 1996-1:1987, Acoustics - Description and measurement of environmental noise - Part 2: Acquisition of data pertinent to land use
- [9] Law on Environmental Protection, "Gazette RS" No. 135/04 (in Serbian)
- [10] SRPS ISO/IEC 17025:2005, General requirements for the competence of testing and calibration laboratories (in Serbian)
- [11] SRPS U.J6.205:2007, Acoustics in building – Acoustical zoning of areas (in Serbian)
- [12] Law on environmental noise protection, "Gazette RS" No. 36/2009 and 88/2010 (in Serbian)
- [13] Directive 2002/49/EC of the European Parliament and the Council relating to the assessment and management of environmental noise, Official Journal of the European Communities, L 189, 45, (on-line) available at: <http://eur-lex.europa.eu/legalcontent/EN/TXT/?uri=CELEX:32002L0049>, 2002
- [14] Regulation on noise indicators, limit values, methods for assessing noise indicators, disturbance and harmful effects of environmental noise, "Gazette RS" No. 75/2010 (in Serbian)
- [15] Regulation on noise measurement methods, content and scope of noise measurement report, "Gazette RS" No. 72/2010 (in Serbian)
- [16] SRPS ISO 1996-1:2010, Acoustics – Description, measurement and assessment of environmental noise - Part 1: Basic quantities and assessment procedures (in Serbian)
- [17] SRPS ISO 1996-2:2010, Acoustics – Description, measurement and assessment of environmental noise - Part 2: Determination of sound pressure levels (in Serbian)
- [18] ISO 1996-1:2003, Acoustics – Description, measurement and assessment of environmental noise - Part 1: Basic quantities and assessment procedures
- [19] ISO 1996-2:2007, Acoustics – Description, measurement and assessment of environmental noise - Part 2: Determination of sound pressure levels
- [20] ISO 1996-1:2016, Acoustics – Description, measurement and assessment of environmental noise - Part 1: Basic quantities and assessment procedures
- [21] ISO 1996-2:2017, Acoustics – Description, measurement and assessment of environmental noise - Part 2: Determination of sound pressure levels
- [22] Abbaspour M., Golmohammadi R., Nassiri P., Mahjub H. 2006. An investigation on time-interval optimisation of traffic noise measurement, Research note, Journal of Low Frequency Noise, Vibration and Active Control 25(4): 267–273.
- [23] Pljakić M., Radičević B., Tomić J., Petrović Z. (2012). Analysis of systematic measurements of noise in cities. 23rd Conference with International Conference "Noise and Vibration", 59–62.
- [24] Mihajlov D., Praščević M. 2015. Permanent and Semi-permanent Road Traffic Noise Monitoring in the City of Nis (Serbia), Journal of Low Frequency Noise, Vibration and Active Control 34(3): 251-268.
- [25] Milošević S., Bijelović S., Živadinović E., Jevtić M., Popović M. (2010). Continuous environmental noise measurement in the city of Novi Sad in April 2010. 22nd Conference with International Conference "Noise and Vibration", 49–52.
- [26] Praščević M., Cvetković D., Mihajlov D. 2014. Measurement and evaluation of the environmental noise levels in the urban areas of the city of Niš (Serbia), Environmental Monitoring and Assessment, 186(2): 1157–1165

## ANALYSIS OF ACOUSTIC PARAMETERS IN SERBIAN ORTHODOX CHURCHES

Violeta Stojanović<sup>1</sup>, Zoran Milivojević<sup>2</sup>

<sup>1</sup> College of Applied Technical Sciences of Nis, Serbia, e-mail: violeta.stojanovic@vtsnis.edu.rs

<sup>2</sup> College of Applied Technical Sciences of Nis, Serbia

**Abstract** - This paper represents the analysis of acoustic parameters in Serbian Orthodox churches "St George" in Žitni potok and „St Prokopije" in Katun. The first part of the paper includes the description of the results of the experiment in which practical measurements of acoustic impulse responses were performed, as well as the results of the calculated acoustic parameters presented in graphs. The second part of the paper includes the analysis of the results in relation to ISO standards, as well as the conclusion.

### 1. INTRODUCTION

The beginnings of researches of Serbian Orthodox churches concerning acoustics of church spaces are related to [1]: a) the cultural heritage of the people, which implies the historical and cultural significance of the church and church objects, implying the research of churches as they are, and b) the aesthetics of sound, aesthetically optimal acoustic response to the space during Orthodox church services. Acoustic research of church spaces is also accompanied by an engineering dimension that indicates the ways of achieving optimal acoustic conditions within the framework of construction or electroacoustic methods.

In Orthodox churches, both in large cathedrals and in small local churches, three characteristic forms of sound information are reported: a) the priest's singing, b) polyphonic singing of priests solely or priests and quires, and c) preaching [1]. The acoustic design of the church must include the requirements of all three sound forms, where the most important parameter is the time of reverberation  $RT$ .

Space reverberation and noise level are two important parameters in the process of recognizing the content of communication, referring to the comprehensibility of speech and the clarity of speech and music.

This paper presents the performed analysis of the mean values of the following acoustic parameters in two Serbian Orthodox churches: Reverberation Time  $RT$ , Speech Transmission Index  $STI$ , the Articulation Loss of Consonants  $Al_{cons}$ , Clarity of speech  $C_{50}$  and music  $C_{80}$  and Definition  $D$  [2]. The values of the acoustic parameters were determined according to the acoustic impulse response and the EASERA program package. The statistical analysis was performed using the Matlab software package. The obtained values of the parameters were analyzed in relation to the standard values [3] and certain conclusions were obtained.

The paper is organized as follows: Section 2 explains the experiment and presents the experimental results. Section 3 provides the analysis of the results for acoustically processed churches. Section 4 is the Conclusion.

### 2. EXPERIMENT

The process of measuring impulse response was carried out in two Serbian Orthodox churches: 1) the church "St. George" in Žitni potok (Figure 1) and 2) the church "St Prokopije" in Katun (Figure 2).



Fig. 1 The church St George in Žitni Potok.

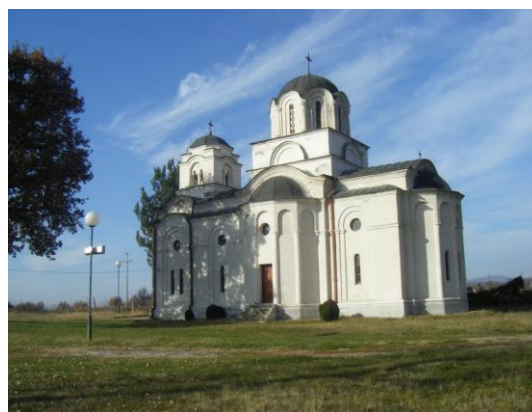


Fig. 2 The church St Prokopije in Katun.

The analysis of the mean values of acoustic parameters in churches was performed for: a) every measuring position  $MP(j)$ :  $RT_{30j}$ ,  $STI_j$ ,  $Al_{consj}$ ,  $C_{50j}$ ,  $C_{80j}$  and  $D_j$ , b) all measuring positions  $MP$ :  $\overline{RT}_{30}$ ,  $\overline{STI}$ ,  $\overline{Al}_{cons}$ ,  $\overline{C}_{50}$ ,  $\overline{C}_{80}$  and  $\overline{D}$ , c) all measuring positions at the central frequencies defined by

octaves  $f_c = \{125, 250, 500, 1000, 2000, 4000\}$  Hz:  $RT_{30f}$ ,  $C_{50f}$ ,  $C_{80f}$  and  $D_f$  and d) all measured positions at the central frequencies  $f_c = \{500, 2000\}$  Hz:  $STI_f$ . The quality of speech comprehension in churches was determined by the correlation between the  $STI$  parameter value and the quality of speech intelligibility. (Table 1) [4]. The conclusion was reached by comparing the obtained values of acoustic parameters for both churches with the recommended values given by ISO 3382 [3].

**Table 1** Correlation between the values of the  $STI$  parameter and the quality intelligibility of speech.

$STI$	$0 \div 0.3$	$0.3 \div 0.45$	$0.45 \div 0.6$	$0.6 \div 0.7$	$0.75 \div 1$
	3			5	
Rating	bad	poor	fair	good	excell.

1) The church St George in Žitni Potok (church 1) has a volume of  $V = 2163 \text{ m}^3$  and inner area is  $S = 167 \text{ m}^2$ . The interior walls and the ceilings covered with plaster (the coefficient of absorption  $\alpha = 0.02$ ). The floor with the ceramic tiles (the coefficient of absorption  $\alpha = 0.015$ ). Measurements were performed at a temperature  $t = 25 \text{ }^\circ\text{C}$ .

112 wav files are a database. They were obtained by recording acoustic impulse responses in  $MP = 16$  measuring positions (Fig. 3) 7 times, using the EASERA software package. The position of the sound source,  $LS$  is located near the altar.

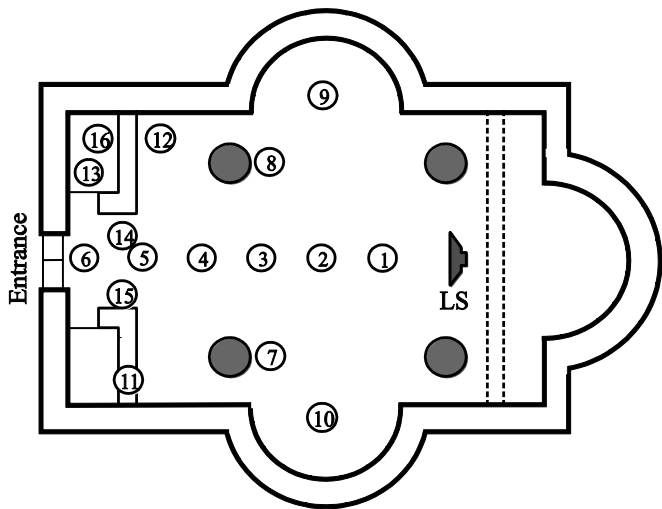


**Fig. 3** The church St George in Žitni Potok where the impulse response is measured:  $LS$  the location of the sound source, 1-16-measured points.

2) The church St Procopije in Katun (church 2) has a volume of  $V = 1659.68 \text{ m}^3$  and inner area is  $S = 646.68 \text{ m}^2$ . The interior walls and the ceilings covered with plaster (the coefficient of absorption  $\alpha = 0.02$ ). The floor with the ceramic tiles (the coefficient of absorption  $\alpha = 0.015$ ). Measurements were performed at a temperature  $t = 11 \text{ }^\circ\text{C}$ .

The database includes 63 wav files that were obtained by recording the acoustic impulse response using the software package EASERA. Recordings were made at 9 measuring point  $MP$ , which is shown in Fig. 4. For each measuring

point, 7 measurements were made. Sound source  $LS$  is placed near the altar.

The equipment used for the experiment as follows: (a) an omnidirectional microphone (PCB 130D20), having a

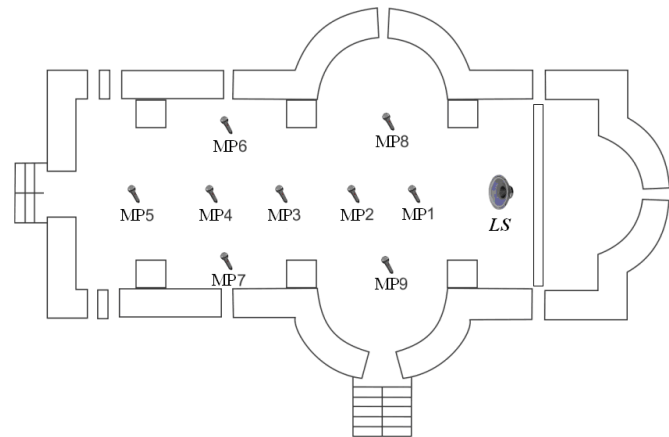


**Fig. 4** The position of measuring point  $MP$  and sound source  $LS$  in the church St Procopije in Katun during the recording impulse response.

diaphragm diameter of 7mm; (b) a B&K omnidirectional sound source type 4295 (dodecahedron loudspeaker); (c) a B&K audio power amplifier, rated at 100W RMS, stereo, type 2716-C; (d) a laptop, incorporating a Soundmax Integrated Digital Audio sound card from Analog Devices. Measuring of the impulse response is carried out using incentive log sweep signal with the duration of 5 s sampling frequency is  $f_s = 44.1 \text{ kHz}$ . The procedure for recording and calculation of acoustic parameters was performed in accordance with ISO 3382.

## 2.1 Rezultats of the exsperiment

Tables 2, 6, 8, and 10, for church 1, present the following values: a)  $RT_{30}$ ,  $RT_{30j}$ ,  $RT_{30f}$  and  $\overline{RT}_{30}$ , b)  $C_{50}$ ,  $C_{50j}$ ,  $C_{50f}$  and  $\overline{C}_{50}$  c)  $C_{80}$ ,  $C_{80j}$ ,  $C_{80f}$  and  $\overline{C}_{80}$  and d)  $D$ ,  $D_j$ ,  $D_f$  and  $\overline{D}$ , respectively. The same values for church 2 are presented in Tables 3, 7, 9 and 11. Tables 4 and 5 present the values  $STI$  (500 Hz, 2 kHz),  $STI_f$ ,  $STI_j$ ,  $\overline{STI}$ ,  $Al_{consj}$  and  $\overline{Al}_{cons}$  for church 1 and church 2, respectively. Figures 5 – 8 present comparative graphs of the dependence of acoustic parameters  $RT_{30f}$ ,  $C_{50f}$ ,  $C_{80f}$ , and  $D_f$  from frequency  $f_c$  for the analyzed churches.

## 3. THE RESULTS ANALYSIS

Based on the results shown in the Tables (2 - 11) and the Figures (5 – 8) the following can be concluded:

a) the values of the parameter  $\overline{RT}_{30}$  for both churches are approximate values of 2s. Namely, the difference in the values of this parameter is  $\Delta \overline{RT}_{30} = 0.11 \text{ s}$  ( $\overline{RT}_{30} = \{1.99 \text{ s}, 2.1 \text{ s}\}$ ). At the analyzed frequencies, the mean values of the reverberation time in churches 1 and 2 are in the range of the following values:  $RT_{30-1} = 1.86 \text{ s} \div 2.63 \text{ s}$ , and  $RT_{30-2} = 1.22 \text{ s} \div 2.99 \text{ s}$ , respectively. This parameter has a slightly lower value at higher frequencies. At  $f_c = \{500 \text{ Hz}, 1\text{kHz}\}$  it is  $RT_{30f} = 1.82\text{s} \div 2.35 \text{ s}$ .

**Table 2** Values:  $RT_{30}$ ,  $RT_{30j}$ ,  $RT_{30f}$  and  $\overline{RT}_{30}$  for the church 1.

$f$ (Hz)	$RT_{30}$ (s)																$RT_{30f}$ (s)
	MP (j)																
	1	2	3	4	5	6	7	8	9	10	11	12	13	14	15	16	
125	2.38	2.7	2.39	2.58	2.76	2.84	2.88	2.88	2.80	2.41	2.96	2.71	1.34	2.60	2.31	3.50	2.63
250	1.71	2.27	2.44	2.62	2.16	2.49	2.20	2.21	2.67	2.43	2.46	2.68	3.07	2.92	3.41	2.16	2.49
500	2.7	2.54	2.36	1.90	2.33	2.28	2.16	2.17	2.30	2.36	2.63	1.88	2.85	2.16	2.66	2.38	2.35
1000	2.65	2.36	2.29	2.25	2.25	2.23	2.12	2.13	2.29	2.46	2.51	2.54	2.22	2.44	2.45	2.25	2.34
2000	2.29	2.26	2.12	2.12	2.08	2.06	2.05	2.05	2.11	2.23	2.21	2.13	2.13	2.02	2.07	2.03	2.12
4000	1.96	1.92	1.91	1.91	1.85	1.78	1.81	1.81	1.82	1.88	1.90	1.86	1.91	1.78	1.87	1.80	1.86
$RT_{30j}$ (s)	2.07	2.05	2.04	2.06	2.04	1.92	1.94	1.94	1.91	2.04	2.05	1.97	2.04	1.82	2.01	1.97	
$\overline{RT}_{30}$ (s)	1.99																

**Table 3** Values:  $RT_{30}$ ,  $RT_{30j}$ ,  $RT_{30f}$  and  $\overline{RT}_{30}$  for the church 2.

$f$ (Hz)	$RT_{30}$ (s)									$RT_{30f}$ (s)
	MP (j)									
	1	2	3	4	5	6	7	8	9	
125	3.24	3.16	2.68	3.06	2.64	2.75	2.90	2.83	3.61	2.99
250	3.23	2.67	2.52	2.55	2.17	2.49	1.46	2.01	3.29	2.49
500	2.76	2.04	1.99	1.29	1.60	2.03	2.08	1.99	2.82	2.07
1000	2.24	1.64	1.56	1.46	1.61	1.88	1.80	1.90	2.32	1.82
2000	1.66	1.49	1.41	1.47	1.41	1.53	1.49	1.65	1.67	1.53
4000	1.25	1.22	1.20	1.22	1.20	1.19	1.21	1.23	1.23	1.22
$RT_{30j}$ (s)	2.52	1.94	1.89	1.64	1.74	1.99	2.00	2.51	2.66	
$\overline{RT}_{30}$ (s)	2.1									

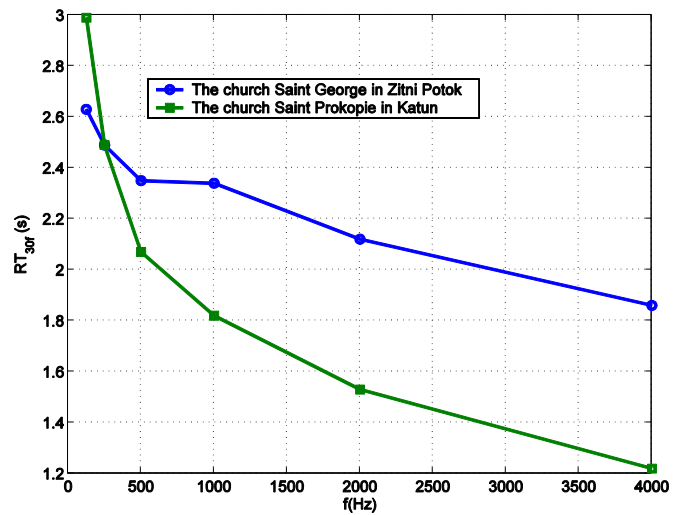


**Fig. 5** Dependence  $RT_{30f}$  from frequency in analyzed churches.

**Table 4** Values:  $STI$  (500 Hz, 2 kHz),  $STI_f$ ,  $STI_j$ ,  $\overline{STI}$ ,  $Al_{consj}$  and  $\overline{Al}_{cons}$  for the church 1.

		MP (j)																$STI_f$
		1	2	3	4	5	6	7	8	9	10	11	12	13	14	15	16	
$STI$	500 Hz	0.66	0.53	0.51	0.4	0.38	0.35	0.34	0.37	0.37	0.45	0.47	0.39	0.54	0.41	0.56	0.33	0.44
	2 kHz	0.77	0.62	0.50	0.46	0.40	0.35	0.35	0.37	0.39	0.58	0.57	0.41	0.46	0.38	0.47	0.36	0.46
$STI_j$ rating		0.79 excell.	0.65 good	0.51 fair	0.49 fair	0.45 fair	0.42 poor	0.39 poor	0.41 poor	0.42 poor	0.54 fair	0.53 fair	0.47 fair	0.53 fair	0.44 poor	0.55 fair	0.38 poor	
$\overline{STI}$ rating		0.5 fair																
$Al_{consj}$ (%)		2.41	5.03	10.47	12.21	14.86	17.52	20.13	18.11	17.37	9.27	9.84	13.44	9.83	15.61	8.59	21.35	
$\overline{Al}_{cons}$ (%)		12.88																

**Table 5** Values:  $STI$  (500 Hz, 2 kHz),  $STI_f$ ,  $STI_j$ ,  $\overline{STI}$ ,  $Al_{consj}$  and  $\overline{Al}_{cons}$  for the church 2.

		MP (j)									$STI_f$
		1	2	3	4	5	6	7	8	9	
$STI$	500 Hz	0.57	0.49	0.44	0.38	0.37	0.42	0.43	0.44	0.48	0.45
	2 kHz	0.69	0.55	0.54	0.52	0.53	0.57	0.57	0.58	0.56	0.57
$STI_j$	rating	0.64	0.54	0.5	0.5	0.53	0.53	0.53	0.55	0.56	fair
$\overline{STI}$	rating	0.54 fair									
$Al_{consj}$	(%)	5.25	9.29	11.3	11.4	9.65	9.41	9.78	8.53	8.12	
$\overline{Al}_{cons}$	(%)	9.2									

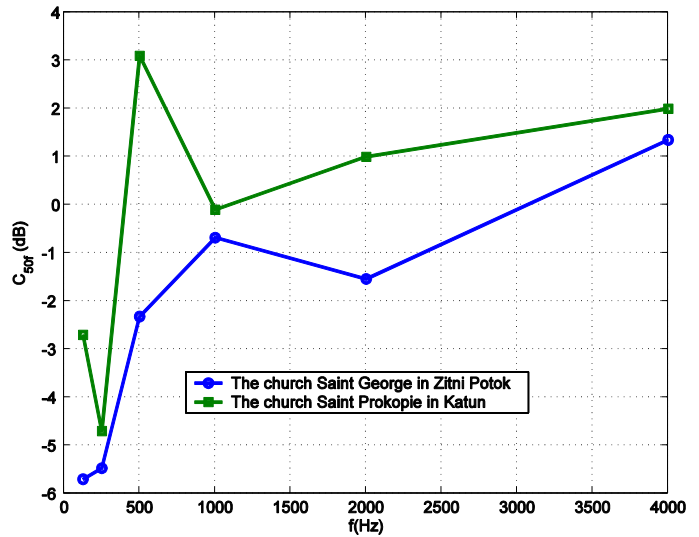


**Fig. 6** Dependence from  $C_{50f}$  from frequency in analyzed churches.

**Table 6** Values:  $C_{50}$ ,  $C_{50j}$ ,  $C_{50f}$  and  $\overline{C}_{50}$  for the church 1.

$f$ (Hz)	$C_{50}$ (dB)																$C_{50f}$ (dB)
	MP (j)																
	1	2	3	4	5	6	7	8	9	10	11	12	13	14	15	16	
125	4.1	-1.7	-6.1	-7.7	-7.2	-10.6	-7.8	-8.6	-10.4	-6.1	-6	-1.7	-3	-4.3	-3	-11.1	-5.7
250	4.6	0.1	-1.3	-4.5	-7.1	-11.6	-12.5	-10.6	-11.8	-6.1	-7.3	-7.8	0.1	-6.9	0.5	-5.3	-5.47
500	4.9	0.9	0	-3.1	-3.9	-5.1	-6.8	-5.1	-5.1	-1.6	-1.2	-4.4	1.1	-2.8	2.1	-7	-2.32
1000	7.5	2.5	-1.3	-1.7	-3.1	-5.4	-5.4	-4.9	-5	2.1	2.2	0.7	1.7	0.2	4	-5	-0.68
2000	8.1	3.7	-0.4	-1.6	-3.9	-5.6	-5.2	-4.9	-4.1	2.3	2.3	-3.1	-1.9	-3.8	-1.3	-5.3	-1.54
4000	13.4	9	1.3	1.2	-0.1	0.6	-3.2	-0.6	-1.3	4.1	2.6	-0.5	-0.1	-1.5	1	-4.3	1.35
$C_{50f}$ (dB)	13.9	9.9	1.6	1.8	-0.3	1.3	-2.1	-0.1	-0.9	4.3	3.4	0.1	0.9	-1.0	1.9	-3.8	
$\overline{C}_{50}$ (dB)	1.93																

**Table 7** Values:  $C_{50}$ ,  $C_{50j}$ ,  $C_{50f}$  and  $\overline{C}_{50}$  for the church 2.

$f$ (Hz)	$C_{50}$ (dB)									$C_{50f}$ (dB)
	MP (j)									
	1	2	3	4	5	6	7	8	9	
125	-1.8	-1.8	-3.7	-4.4	-1.5	-4.1	-5.2	-1.4	-0.8	-2.7
250	-0.6	4.1	-6.9	-2.9	-3.5	-4.9	-6.2	-8.4	-5.3	-4.7
500	1.7	1.3	-2.7	-6.4	-5.6	-3	-2.8	-3	-1.5	3.1
1000	4.5	1	-2.1	-1	-0.5	-0.2	-0.5	-2.6	0.1	-0.1
2000	5.3	0.2	0.2	-0.5	-0.6	1.5	1.3	0.8	1	1
4000	6.7	1.1	0.4	-0.7	1.8	3.3	3.1	4.3	4.3	2
$C_{50f}$ (dB)	5.6	1.3	0.1	1.10	1.4	3.0	3.0	5.1	4.6	
$\overline{C}_{50}$ (dB)	2.8									

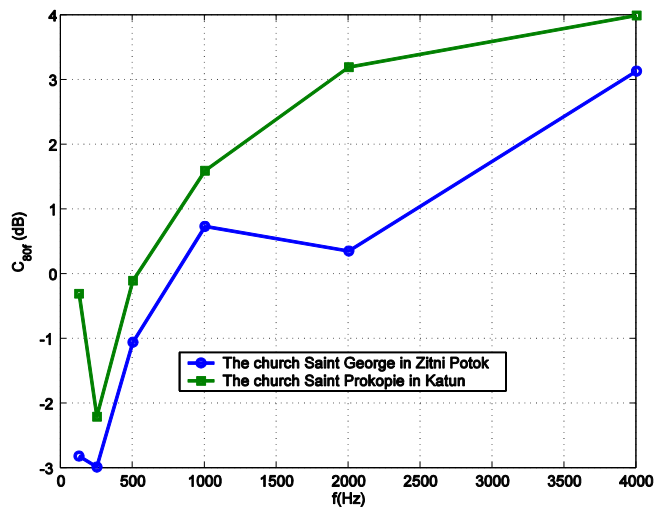


**Fig. 7** Dependence from  $C_{80f}$  from frequency in analyzed churches.

**Table 8** Values:  $C_{80}$ ,  $C_{80j}$ ,  $C_{80f}$  and  $\overline{C}_{80}$  for the church 1.

$f$ (Hz)	$C_{80}$ (dB)																$C_{80f}$ (dB)
	MP (j)																
	1	2	3	4	5	6	7	8	9	10	11	12	13	14	15	16	
125	5.6	0.4	-2.6	-2.1	-1.6	-6.6	-6	-5.3	-6.8	-3.6	-4.4	-0.5	-1.2	-2.1	-1.2	-7	-2.81
250	5.2	0.6	-0.3	-2.6	-3.6	-9.7	-5	-7.1	-7	-4.2	-4.3	-4	0.8	-4	2	-4.5	-2.98
500	5.4	1.7	0.7	-1.7	-2.5	-3.6	-4.9	-3.6	-3.9	-0.6	-0.5	-2.1	2	-1.3	3.1	-5	-1.05
1000	8.2	3.4	0.2	-0.8	-1.3	-2.9	-3.5	-3.1	-2.7	3.1	3	1.6	2.9	1.4	5	-2.7	0.74
2000	8.8	4.8	1.5	0.2	-1.2	-2.7	-2.9	-2.6	-1.8	3.5	3.3	-1.3	0.1	-1.5	0.5	-3	0.36
4000	14.3	10.2	3.3	2.7	1.9	2.1	-1.1	0.9	0.8	5.4	4.1	1.4	2.7	0.5	2.5	-1.5	3.14
$C_{80j}$ (dB)	13.9	9.9	1.6	1.8	-0.3	1.3	-2.1	-0.1	-0.9	4.3	3.4	1.9	3.2	1.0	3.5	-1.3	
$\overline{C}_{80}$ (dB)	2.57																

**Table 9** Values:  $C_{80}$ ,  $C_{80j}$ ,  $C_{80f}$  and  $\overline{C}_{80}$  for the church 2.

$f$ (Hz)	$C_{80}$ (dB)									$C_{80f}$ (dB)
	MP (j)									
	1	2	3	4	5	6	7	8	9	
125	0	-2	-2.4	-1.5	1.2	-0.3	-1.9	1.3	0.6	-0.3
250	1.7	-0.3	-3.1	-0.6	-1.7	-2.1	-3.8	-4.2	-3.6	-2.2
500	3	0.2	-1.4	-2.7	-3.4	-1.8	-1.6	-1	-0.4	-0.1
1000	5.8	2.3	-0.9	0.9	1.1	0.9	0.8	-0.5	1.3	1.6
2000	6.6	2.5	1.9	4.8	1.3	3.1	3.2	2.9	2.7	3.2
4000	8.4	3.3	2.7	2.3	3.7	5.1	4.9	6	6	4
$C_{80j}$ (dB)	7.1	3.2	1.9	1.71	3.3	4.7	4.5	6.8	6.1	
$\overline{C}_{80}$ (dB)	4.37									

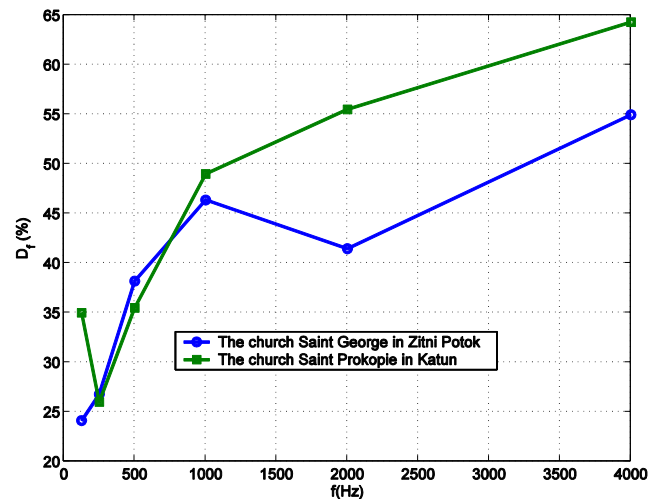


**Fig. 8** Dependence from  $D_f$  from frequency in analyzed churches.

**Table 10** Values:  $D_{80}$ ,  $D_{80j}$ ,  $D_{80f}$  and  $\overline{D}_{80}$  for the church 1.

$f$ (Hz)	$D$ (%)																$D_f$ (%)
	MP (j)																
	1	2	3	4	5	6	7	8	9	10	11	12	13	14	15	16	
125	72	40.4	19.9	14.4	15.9	8.1	14.1	12.1	8.4	19.6	20	40.3	33.2	27.1	33.3	7.3	24.13
250	74.3	50.5	42.7	26.3	16.4	6.5	5.4	7.9	6.2	19.6	15.6	14.3	50.4	17	52.6	22.8	26.78
500	75.6	55.4	49.8	32.7	29.2	23.8	17.4	23.4	23.5	40.6	43.1	26.8	56.4	34.6	62.1	16.7	38.19
1000	84.9	63.9	42.5	40.1	33	22.2	22.4	24.3	24.2	61.6	62.7	54	59.5	50.9	71.6	24.2	46.37
2000	86.5	69.9	47.7	40.6	28.9	21.5	23.2	24.4	28	63	62.8	32.8	39.2	29.6	42.5	22.7	41.46
4000	95.6	88.9	57.4	56.6	49.3	53.2	32.5	46.4	42.7	71.9	64.5	46.9	49.4	41.7	55.5	26.9	54.96
$D_j$ (%)	96.1	90.8	59.1	60.1	48.0	57.3	38.3	49.6	45.0	72.9	68.9	50.3	55	44.5	60.9	29.4	
$\overline{D}$ (%)	57.89																

**Table 11** Values:  $D_{80}$ ,  $D_{80j}$ ,  $D_{80f}$  and  $\overline{D}_{80}$  for the church 2.

$f$ (Hz)	$D$ (%)									$D_f$ (%)
	MP ( $j$ )									
	1	2	3	4	5	6	7	8	9	
125	39.7	38.7	30	26.5	41.5	28.8	23.4	42.3	45.2	35
250	46.7	26.7	16.9	33.7	30.9	24.3	19.3	12.6	22.7	26
500	59.6	41.4	35.1	18.7	21.6	33.4	34.6	33.6	41.6	35.5
1000	73.9	56	38	44.5	47.1	49.1	47.3	35.6	50.7	49
2000	77.1	51.3	51.2	47.2	46.3	58.8	57.3	54.8	55.8	55.5
4000	82.6	55.8	52.4	46.2	60.4	68.2	67.2	72.8	73.1	64.3
$D_j$ (%)	78.4	57.3	50.3	43.6	58.0	66.8	66.6	76.7	74.2	
$\overline{D}$ (%)	63.5									

The time of reverberation in an Orthodox church should not be longer than 3 s, and the aesthetic optimum should be near 2 s [1]. This means that the mean values of this parameter in the analyzed churches meet these requirements.

b) the mean values of the speech transfer index in both churches ( $\overline{STI}_1 = 0.5$ ,  $\overline{STI}_2 = 0.54$ ) show that intelligibility speech quality is acceptable. The difference in the values of this parameter is  $\overline{\Delta STI} = 0.04$ . For the acceptable intelligibility of the speech, the values of this parameter are  $STI = 0.45 \div 0.6$  [4]. At  $f_c = \{500 \text{ Hz}, 2\text{kHz}\}$  it is  $STI_{f,1} = \{0.44, 0.45\}$  and  $STI_{f,2} = \{0.45, 0.57\}$ . Thus, a slightly decreased intelligibility of speech occurs in church 1 only at  $f = 500 \text{ Hz}$ .

c) the average values representing the percentage of incomprehension of consonants (articulation loss of consonants) in the analyzed churches are acceptable. They are in the recommended range of the values:  $Al_{cons} = 7 \% \div 15 \%$ . Namely:  $\overline{Al}_{cons1} = 12.88 \%$  and  $\overline{Al}_{cons2} = 9.2 \%$ , or  $\overline{\Delta Al}_{cons} = 3.68 \%$ .

d) the acceptable values representing the speech clarity index parameter for the analyzed spaces are  $C_{50} > -2 \text{ dB}$ . The mean values of this parameter for church 1 satisfy this criterion only at  $f = 4 \text{ kHz}$  ( $C_{50,4\text{kHz}} = 1.35 \text{ dB}$ ) and at  $f = 500 \text{ Hz}$  the value is approximately acceptable ( $C_{50,500\text{Hz}} = -2.32 \text{ dB}$ ). In church 2, this parameter at  $f_c = \{500 \text{ Hz}, 1\text{kHz}, 2\text{kHz}, 4\text{kHz}\}$  has values in the range of allowed values for the given spaces:  $C_{50f} = -0.1 \div 2 \text{ dB}$ . However, in general, for all measuring positions, the mean values of this parameter meet the established criteria:  $\overline{C}_{501} = 1.93 \text{ dB}$ ,  $\overline{C}_{502} = 2.8 \text{ dB}$ , or  $\overline{\Delta C}_{50} = 0.87 \text{ dB}$ .

e) the allowed values of the clarity index parameter for music for the analyzed spaces are  $C_{80} = 1 \div 5 \text{ dB}$ . The mean values of this parameter for all measuring positions for both churches meet this criterion:  $\overline{C}_{801} = 2.57 \text{ dB}$ ,  $\overline{C}_{802} = 4.37 \text{ dB}$ .

( $\overline{\Delta C}_{80} = 1.8 \text{ dB}$ ). For church 1 this criterion is fulfilled by the value of this parameter only at  $f = 4\text{kHz}$ ,  $C_{80,4\text{kHz}} = 3.14 \text{ dB}$ . Church 2 has higher values of this parameter at  $f_c = \{1\text{kHz}, 2\text{kHz}, 4\text{kHz}\}$ ,  $C_{80f} = \{1.6 \text{ dB}, 3.2 \text{ dB}, 4 \text{ dB}\}$ .

f) the difference between the mean values of definition for all measuring positions for church 2 and church 1 is  $\overline{\Delta D} = 5.61 \%$ . Namely  $\overline{D}_1 = 57.89 \%$  and  $\overline{D}_2 = 63.5 \%$ . These values are in the range of optimal values:  $D = 30 \div 70 \%$ . Also, in the range of these values are those at  $f_c = \{500 \text{ Hz}, 1\text{kHz}, 2\text{kHz}, 4\text{kHz}\}$ :  $D_{f,1} = 38.19 \div 54.96 \%$  and  $D_{f,2} = 35 \div 64.3 \%$ .

#### 4. CONCLUSION

The paper presents an acoustic analysis of the results of experiments performed in Serbian Orthodox churches "St. George" in Žitni Potok and "St. Prokopije" in Katun. According to the measured impulse responses in churches a) the elementary acoustic parameters were determined: Reverberation Time  $RT$ , Speech Transmission Index  $STI$ , Articulation Loss of Consonants  $Al_{cons}$ , Clarity of speech  $C_{50}$ , Clarity of music  $C_{80}$  and Definition  $D$ , b) their mean values were compared and c) the mean values of acoustic parameters were analyzed in relation to the standard values defined by the standard ISO 3382.

It has been concluded that the mean values of all analyzed acoustic parameters of both churches ( $\overline{RT}_{30} = \{1.99 \text{ s}, 2.1 \text{ s}\}$ ,  $\overline{STI} = \{0.5, 0.54\}$ ,  $\overline{Al}_{cons} = \{12.88 \%, 9.2 \%\}$ ,  $\overline{C}_{50} = \{1.93 \text{ dB}, 2.8 \text{ dB}\}$ ,  $\overline{C}_{80} = \{2.57 \text{ dB}, 4.37 \text{ dB}\}$ ,  $\overline{D} = \{57.89 \%, 63.5 \%\}$ ) meet the criteria according to the standard ISO 3382. . Based on the classification of the objective acoustic parameter ratio  $STI$  (Standard IEC 60268-16 [4]), and the quality of speech intelligibility, it has been demonstrated that speech intelligibility in acoustically examined churches is acceptable.

#### REFERENCES

- [1] M. Mijić, D. Šumarac Pavlović, Acoustical characteristics of old wooden churches in Serbia, *The Journal of the Acoustical Society of America*, 108 (5), pp. 2648 – 2648, 2000.
- [2] H. Kuttruff, Room Acoustics, *E&FN Spon, London*, 2000.
- [3] ISO 3382: *Acoustic - Measurement of the Reverberation Time of Rooms with Reference to Other Acoustical Parameters*, 1997.
- [4] International Electrotechnical Commission IEC 60268 - 16 - International Standard: Sound system equipment - Part 16, *Objective rating of speech intelligibility by speech transmission index*, Switzerland: IEC, 2011.



## DEFINING THE ENVIRONMENTAL NOISE INDICATORS MEASUREMENT TIME INTERVAL USING MULTI-CRITERIA OPTIMIZATION

Darko Mihajlov,<sup>1</sup> Momir Prašćević<sup>1</sup>, Marko Ličanin<sup>1</sup>

<sup>1</sup> University of Niš, Faculty of Occupational Safety, Serbia; darko.mihajlov@znrfak.ni.ac.rs

**Abstract** - Annual values of the environmental noise indicators represents the state of noise pollution and potential impact on the health of the people living and working in the noise affected areas. Assessment of the value of this indicator is being done using different software packages, together with large number of data related to the noise sources, and terrain topography. Software solutions are usually used for development of the strategic noise maps. Absolutely precise and correct values of the noise indicator in the environment is only possible to determine through permanent noise monitoring, which represents very demanding operation form a standpoint of many aspects. In the cases where dominant noise source is a road traffic of a large frequency and volume, it is possible to perform the monitoring using a semi-permanent in order to extract the high accuracy noise indicators data. This approach represents far more acceptable way of collecting the relevant noise data, as it requires significantly less resources. The main problem that occurs in using this method is the choice of the length of the measurement interval. This paper describes the process of choosing the correct interval using multi-criteria optimization based on the PROMETHEE method. Experimental data of the one year permanent noise measurements confirms the results and conclusions described in this paper.

### 1. INTRODUCTION

In the past twenty years, surface of the cities in Europe increased by 20 %, while people count raised by 6 % [1]. Noise in such environment, caused by intensive traffic, construction industry and recreational activities, becomes serious and in some cases main local problem of the environmental condition. Latest data on the environmental noise pollution [2] gathered after the first run of the strategic mapping in the living areas in EU shows that 54 % of the population (56 million) in urban areas is exposed to the noise levels  $L_{den}$  higher than 55 dB and the 15 % of the population (around 15.5 million) in urban areas to a noise level  $L_{den}$  higher than 65 dB. Besides that, around 33.5 million of people outside agglomeration lives in the neighborhood where  $L_{den}$  is over 55 dB, while 7.6 million of people is in the similar areas are exposed to the  $L_{den}$  of more than 65 dB. Latest researches shows that in total 89.5 million people are living in the areas where  $L_{den}$  is more than 55 dB, where 89 million in environment where dominant noise source is traffic [2]. Results of these statistical data, inspired researcher from all over the world to pay more attention into studying and defining the problems of the traffic noise as a dominant

environmental noise sources [3 - 10]. For the mentioned reasons, assessment, evaluation and monitoring of the environmental noise becomes the necessity, especially if there is a need to recover highly affected areas with specific activities.

Overview of the existing state of the noise level specific territory is obtained by development of the strategic noise maps, which serves as a starting points in the process of defining the scope of the problem and preventing the increase of the emission of noise into environment. Noise maps intuitively visually explains the mechanism of noise propagation from the emission source, as well as influence of magnitude and purpose of the areas on the noise emission. This gives clear distribution of the "loud and quiet areas", which is very important information for urban planning.

The essential element for calibration of the strategic maps, as a base document on the environmental noise, are values of the noise indicators determined by applying different strategies. One the most important is the equivalent noise level  $L_{eq}$  for the chosen location, where the observation time interval is one year. Having in mind the change of the traffic volume during 24h period, especially observable between day and night, as well as influence of the human activities in different periods of the day, it is necessary, in addition to one year observation, to have the values of the noise indicators during the entire day, on the day, evening and night basis. During the day, there are three intervals, thus there are three noise indicators:  $L_{day}$ ,  $L_{evening}$  and  $L_{night}$ , equivalent noise levels during the day, evening and night respectively.

Yearly (annual) indicator of the noise describes the noise disturbance during the day, through the entire year, and it is defined as:

$$L_{den} = 10 \log \left[ \frac{1}{24} \left( 12 \cdot 10^{\frac{L_{day}}{10}} + 4 \cdot 10^{\frac{L_{evening}+5}{10}} + 8 \cdot 10^{\frac{L_{night}+10}{10}} \right) \right] \text{ [dB]} \quad (1)$$

where:

$L_{day}$  - A-curve weighted long-term average noise level for all of days throughout the year;

$L_{evening}$  - A-curve weighted long-term average noise level for all of evenings throughout the year;

$L_{night}$  - A-curve weighted long-term average noise level for all of nights throughout the year.

Applying the values of correction for different day interval is regulated by current laws and regulations [11], as a consequence of subjective feeling of noise impact on the people during the specific time periods of the day or during

the week. Taking into concern that people spend more time at home during the weekend, the decisions of the authorities to regulate noise levels is positive action as people can experience better conform, rest and recovery at home [12].

A-frequency weighted long-term noise level for the separate interval within one year, from the equation (1), are determined by following expressions:

$$L_{day} = 10 \log \left[ \frac{1}{N} \sum_{i=1}^N 10^{\frac{L_{day,i}}{10}} \right] \quad (2)$$

$$L_{evening} = 10 \log \left[ \frac{1}{N} \sum_{i=1}^N 10^{\frac{L_{evening,i}}{10}} \right] \quad (3)$$

$$L_{night} = 10 \log \left[ \frac{1}{N} \sum_{i=1}^N 10^{\frac{L_{night,i}}{10}} \right] \quad (4)$$

where:

$i$  - order number of a day within a year;

$N$  - Total number of days in a year.

In the previous equation, the term "Year" is related to the relevant year in the context of noise emission and average of the meteorological conditions.

Values of basic noise indicator can be determined by evaluation or measurement. For prediction of the noise, software is used in most cases. Determination of the annual parameters can be done using two strategies. First strategy represents long-term measurement of the equivalent noise level during long enough interval, that can envelope all of the changes in meteorological conditions. In addition, weather conditions influence the traffic flow, which will result in a noise emission change. Some periods of the year, such as holidays and events, have higher communal activities, which must be included in long-term noise monitoring.

Second strategy represents the series of short-term measurements of the equivalent noise level, that are undertaken under the specific conditions of the noise sources. The determination of the annual noise indicators is in this case done by applying the relevant method of prediction. The choice of the time interval of the short term measurement, as well as the number of those measurements are very important for determination of the noise indicators at the given location.

The shortest time interval is 10 min, but if the influence of the meteorological conditions are necessary, recommended interval is 30 min. The choice of the time intervals is the popular topic among the scientist in this area, and the inspiration for the many recent papers [13]. Because of the different conditions and factors, researches chose different measurement intervals for their noise study.

The results of the long-term measurements are by all means more precise than short-term and less corrections are needed. Permanent noise monitoring represents non-stop noise measurement, 24 hrs a day, 365 days per year. This gives the realistic overview of the noise conditions at the given location, as well as most precise results for the calibration of strategic noise maps.

Semi-permanent noise monitoring, usually continuously during one or several days, weeks, or even months. This method can be used for determination of the annual noise indicators, and is particularly useful because of its economical reasons. Monitoring equipment is expensive, and

if there is a chance for covering more location than one during the annual noise tracking, usage of the equipment becomes more efficient.

Adequate time interval of measurements using semi-permanent method of noise monitoring as well as the number measurements of the equivalent noise level, are not yet defined by standards. In this context, there is a very high level of experimentations, as researchers tend to chose those time intervals as they see it best fits to their conditions and factors. In using this method, it is very important to take into concern the volume of the traffic, change of the meteorological data, time during the year with specific communal activities etc. In order to get better precision data, measurements should be organized in such a way, to envelope of all the mentioned specifics, if the goal is to assess the annual noise indicators based on the semi-permanent measurements.

## 2. RESEARCH METHODOLOGY

This paper is based on the assumption that by using the results obtained from long-term noise monitoring, it is possible to determine optimal length of the measurement interval. It is assumed that, using optimized intervals, assessment of the annual noise indicators at the given location, mostly influenced by traffic noise, will be with an accuracy of 1.5 dB and precision 1.0 dB.

Required accuracy implies that values of any measured noise indicators, obtained with some of the semi-permanent strategies, do not differ more than 1.5 dB from a data taken using a permanent monitoring. This requirement of 1.0 dB assumes that value of standard deviation of measurement results of any indicators by semi-permanent monitoring, should not cross that value.

Defined values of the accuracy of 1.5 dB and precision of 1.0 dB, as control parameters of considered measurement solutions, are defined by Directive 2002/49/EC, which is related to the development of strategic noise mapping. Resolution is 5 dB.

Process of solving a problem related to the application of multi-criteria optimization is dissolved into four phases.

- Setting up base of the problem;
- Determination of the relative importance (weighting) of the criteria;
- Choice of the adequate method of multi-criteria optimization to be applied on specific problem;
- A study of the stability of the solution.

### 2.1 Phase 1

According to the defined goal of the research, that is, finding the minimal measurement time interval that will satisfy the established criteria, following alternatives setup has been made:

- **Alternative  $a_1$**  - Measurement strategy with a one week interval (Monday 00:00 - Sunday 24:00 );
- **Alternative  $a_2$**  - Measurement strategy with one month interval (1st day in month 00:00 - last day in month 24:00);
- **Alternative  $a_3$**  - Measurement strategy with six month interval;

- **Alternative  $a_4$**  - Measurement strategy with a interval of one year (1st of January 00:00 - 31st of December 24:00).

Preference towards certain alternatives of a mentioned order ( $a_1 \rightarrow a_2 \rightarrow a_3 \rightarrow a_4$ ), comes from the defined goal of the research, that is, to find the shortest possible time interval (shortest use of the monitoring equipment) with a satisfied precision of the results on the given measurement location, comparable to those obtained by long-term monitoring. The essence of the problem is the fact that in case of the long-term permanent monitoring (alternative  $a_4$ ), station is mounted only at one location throughout the year with a minimal usability.

In this paper, for the choice of optimal measurement strategy using multi-criteria optimization, a set of nine criteria is considered. Chosen criteria are divided into three categories, where category  $f_1 \div f_4$  are related to the standard deviation of the measured noise indicators, as a measure of deviation of all data from the average value within given data set in measurement interval. Second category is composed of criteria  $f_5 \div f_8$ , that represents maximum deviation of the noise indicators for a certain time interval from the six month or one year long acquisition obtained data set. Third category is only criteria  $f_9$ , that defines the level of the usability of the measurement equipment. Being different from the other criteria,  $f_9$  is described by qualitative attributes because of its nature. Method of quantification of the qualitative attributes is represented in table 1, where Saaty scale for pairs relation quantification has been used.

**Table 1** Quantification of qualitative attributes according to criterion goal for the defined alternatives

Criteria $f_9$		
Goal of criteria: max		
	Qualitative mark	Quantitative mark
$a_1$	Very good	9
$a_2$	Average	4
$a_3$	Fair	2
$a_4$	Bad	1

## 2.2 Phase 2

Having in mind that defined criteria are not of the same importance, it is necessary to define the factors of importance of the certain criteria using the weighting coefficients. Determination of the relative weights of the criteria is done using Delphi methods [18], by considering suggested weight criterias from the survey taken by ten experts in the field (authors, that is examiners did not participated).

## 2.3 Phase 3

Problem of the choice of the optimal measurement strategy of the multi-criteria optimization can be solved using the PROMETHEE. From the aspect of mutual comparison and ranking of the alternatives, based on the nature and values of the certain alternative by choice of the adequate types of the preference function, as well as defining the values of the preference and indifference parameters, this method is more than acceptable. Applying a PROMETHEE method as a solution of the addressed problem is done in five steps:

1. Definition of the type of general criteria and the parameters of indifference and preference, for each individual criteria;

2. Determination of the preference function for all alternative pairs, towards each criteria order;
3. Determination of the preference index for every alternative pair and formation of the preference index table;
4. Calculation of the values of the input and output flow, for each alternative, and forming of the partial order of the compared alternative (PROMETHEE I);
5. Calculation of the clear flows values for all alternatives and formation of the complete rank of the alternatives (PROMETHEE II).

## 3. RESULTS OF THE RESEARCH

For the purpose of this research, a permanent noise monitoring of the road traffic has been done at the characteristic location at the territory of the city of Niš - The crossroad of the street Milojka Lešjanina and Knjeginje Ljubice (measurement location MM1). Reason for the choice of this measurement location is as following:

- Very intensive road traffic through the crossroad of two busy streets during the entire day;
- Existence of the residential objects of the high population density, business related objects, as well as research and educational object in the close proximity.

The results of the noise indicators measurements are given in period 01. 01. 2014 - 31. 12. 2014. and period 01. 01. 2015 - 31. 12. 2015. This is shown in tables 2 through 8:

**Table 2** Weekly reports (Monday - Sunday)

	$L_{day}$		$L_{evening}$		$L_{night}$		$L_{den}$	
	2014	2015	2014	2015	2014	2015	2014	2015
avr	73.1	72.7	72.1	71.6	68.0	67.7	76.0	75.7
$\sigma.s$	0.32	0.45	0.31	0.37	0.37	0.94	0.27	0.63
$\sigma.p$	0.32	0.44	0.31	0.36	0.37	0.93	0.27	0.62
max	74.0	73.6	73.0	72.6	69.1	72.5	76.8	78.8
min	72.6	71.4	71.5	70.9	67.2	66.7	75.4	75.0

**Table 3** Monthly reports

	$L_{day}$		$L_{evening}$		$L_{night}$		$L_{den}$	
	2014	2015	2014	2015	2014	2015	2014	2015
avr	73.1	72.7	72.1	71.6	68.0	67.8	76.0	75.7
$\sigma.s$	0.20	0.35	0.17	0.28	0.22	0.58	0.17	0.41
$\sigma.p$	0.19	0.34	0.17	0.27	0.21	0.56	0.17	0.39
max	73.4	73.2	72.4	72.1	68.3	69.3	76.3	76.7
min	72.7	72.1	71.9	71.3	67.6	67.3	75.7	75.3

**Table 4** Half year reports

	$L_{day}$		$L_{evening}$		$L_{night}$		$L_{den}$	
	2014	2015	2014	2015	2014	2015	2014	2015
avr	73.1	72.7	72.1	71.7	68.0	67.8	76.0	75.7
$\sigma.s$	0.1	0.1	0	0	0	0.1	0	0
max	73.2	72.8	72.1	71.7	68.0	67.9	76.0	75.7
min	73.0	72.6	72.1	71.7	68.0	67.7	76.0	75.7

**Table 5** Annual reports

	$L_{day}$		$L_{evening}$		$L_{night}$		$L_{den}$	
	2014	2015	2014	2015	2014	2015	2014	2015
	73.1	72.7	72.1	71.7	68.0	67.8	76.0	75.7

**Table 6** Deviations of the weekly from annual results

	$L_{day}$		$L_{evening}$		$L_{night}$		$L_{den}$	
	2014	2015	2014	2015	2014	2015	2014	2015
max	0.9	0.9	0.9	0.9	1.1	1.0	0.8	0.8

**Table 7** Deviations of the monthly from annual results

	$L_{day}$		$L_{evening}$		$L_{night}$		$L_{den}$	
	2014	2015	2014	2015	2014	2015	2014	2015
max	0.4	0.6	0.3	0.4	0.4	1.5	0.3	1.0

**Table 8** Deviations of the half-year from annual results

	$L_{day}$		$L_{evening}$		$L_{night}$		$L_{den}$	
	2014	2015	2014	2015	2014	2015	2014	2015
max	0.1	0.1	0	0	0	0.1	0	0

By applying the program package PROMETHEE [16], at first, verification of the results for choice of the optimal measurement strategy, obtained by calculation, is verified. This has been done for measurement location MM1 (scenario 1). In order to validate the obtained results, changes in the preference functions and parameters values has been done, for the same values of criteria (scenario 2). By choosing the

preference functions with linear preference and the area of indifference for all of the criteria, and considering smaller values of preference parameter in comparison to scenario 1, a more strict conditions has been set for alternative ranking in scenario 2.

For criteria  $f_1 \div f_4$ , in the case of scenario 2, unless the difference in results standards deviation of the measurements, per alternative is equal or higher than 1 dB, there is strict preference of the alternative with lower standard deviation. On the other hand, if the difference is lower than 0.1 dB, two compared alternative are considered to be equally important.

Conclusion for criteria  $f_5 \div f_8$  is that in scenario 2, unless the difference in maximum absolute deviations of the measurement results per alternative, is equal or higher than 2 dB, there is a strict preference towards alternative with smaller deviations. If the difference is smaller than 0.5 dB, alternative are considered as equally important. The graphic representation of the software Visual PROMETHEE, for the problem of choosing optimal measurement strategy, for measurement location MM1, based on scenario 1 and 2, is given in figures 1 and 2.

Visual PROMETHEE Academic - MM1.vpg (sačuvano)										
Datoteka Uredi Model Kontrola PROMETHEE-GAIA GDSS GIS Prilagodeni Pomocnici Trenutni snimci Opcije Pomoc										
<input checked="" type="checkbox"/>	<input checked="" type="checkbox"/>	<input checked="" type="checkbox"/>	<input checked="" type="checkbox"/>	<input checked="" type="checkbox"/>	<input checked="" type="checkbox"/>	<input checked="" type="checkbox"/>	<input checked="" type="checkbox"/>	<input checked="" type="checkbox"/>	<input checked="" type="checkbox"/>	<input checked="" type="checkbox"/>
<input checked="" type="checkbox"/> Scenario1	criteron1	criteron2	criteron3	criteron4	criteron5	criteron6	criteron7	criteron8	criteron9	
Jedinica	dB	1-9								
Klaster/Grupa	◆	◆	◆	◆	◆	◆	◆	◆	◆	◆
<b>Preferencije</b>										
Min/Max	min	max								
Težina	0,05	0,05	0,05	0,10	0,05	0,05	0,05	0,05	0,10	0,50
Preferentna Fun.	V-oblik	V-oblik	V-oblik	V-oblik	Linearna	Linearna	Linearna	Linearna	Linearna	V-oblik
Granice	apsolutan									
- Q: Indiferentnost	n/d	n/d	n/d	n/d	n/d	0,50	0,50	0,50	0,50	n/d
- P: Preferencija	2,00	2,00	2,00	2,00	3,00	3,00	3,00	3,00	3,00	10,00
- S: Gausova	n/d									
<b>Statistika</b>										
Minimum	0,00	0,00	0,00	0,00	0,00	0,00	0,00	0,00	0,00	1,00
Maksimum	0,32	0,31	0,37	0,27	0,90	0,90	1,10	0,80	0,80	9,00
Prosek	0,15	0,12	0,14	0,11	0,35	0,30	0,38	0,28	0,28	4,00
Standardno odstupanje	0,12	0,13	0,16	0,12	0,35	0,37	0,45	0,33	0,33	3,08
<b>Vrednovanja</b>										
<input checked="" type="checkbox"/> action1	0,32	0,31	0,37	0,27	0,90	0,90	1,10	0,80	0,80	9,00
<input checked="" type="checkbox"/> action2	0,19	0,17	0,21	0,17	0,40	0,30	0,40	0,30	0,30	4,00
<input checked="" type="checkbox"/> action3	0,10	0,00	0,00	0,00	0,10	0,00	0,00	0,00	0,00	2,00
<input checked="" type="checkbox"/> action4	0,00	0,00	0,00	0,00	0,00	0,00	0,00	0,00	0,00	1,00

**Fig. 1** Decision matrix for measurement location MM1 – scenario 1

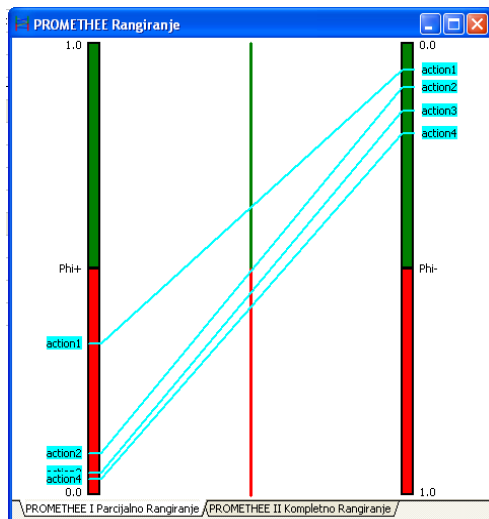
Visual PROMETHEE Academic - MM1.vpg (sačuvano)										
Datoteka Uredi Model Kontrola PROMETHEE-GAIA GDSS GIS Prilagodni Pomocnici Trenutni snimci Opcije Pomoc										
[Icons]										
<input checked="" type="checkbox"/>	<input checked="" type="checkbox"/>	<input checked="" type="checkbox"/>	<input checked="" type="checkbox"/>	<input checked="" type="checkbox"/>	<input checked="" type="checkbox"/>	<input checked="" type="checkbox"/>	<input checked="" type="checkbox"/>	<input checked="" type="checkbox"/>	<input checked="" type="checkbox"/>	<input checked="" type="checkbox"/>
<input checked="" type="checkbox"/> Scenario2	criteron1	criteron2	criteron3	criteron4	criteron5	criteron6	criteron7	criteron8	criteron9	
Jedinica	dB	1-9								
Klaster/Grupa	◆	◆	◆	◆	◆	◆	◆	◆	◆	◆
<b>Preferencije</b>										
Min/Max	min	max								
Težina	0,05	0,05	0,05	0,05	0,05	0,05	0,05	0,05	0,10	0,50
Preferentna Fun.	Linearna									
Granice	apsolutan									
- Q: Indiferentnost	0,10	0,10	0,10	0,10	0,50	0,50	0,50	0,50	0,50	1,00
- P: Preferencija	1,00	1,00	1,00	1,00	2,00	2,00	2,00	2,00	2,00	8,00
- S: Gausova	n/d									
<b>Statistika</b>										
Minimum	0,00	0,00	0,00	0,00	0,00	0,00	0,00	0,00	0,00	1,00
Maksimum	0,32	0,31	0,37	0,27	0,90	0,90	1,10	0,80	0,80	9,00
Prosek	0,15	0,12	0,14	0,11	0,35	0,30	0,38	0,28	0,28	4,00
Standardno odstupanje	0,12	0,13	0,16	0,12	0,35	0,37	0,45	0,33	0,33	3,08
<b>Vrednovanja</b>										
<input checked="" type="checkbox"/> action1	0,32	0,31	0,37	0,27	0,90	0,90	1,10	0,80	0,80	9,00
<input checked="" type="checkbox"/> action2	0,19	0,17	0,21	0,17	0,40	0,30	0,40	0,30	0,30	4,00
<input checked="" type="checkbox"/> action3	0,10	0,00	0,00	0,00	0,10	0,00	0,00	0,00	0,00	2,00
<input checked="" type="checkbox"/> action4	0,00	0,00	0,00	0,00	0,00	0,00	0,00	0,00	0,00	1,00

Fig. 2 Decision matrix for measurement location MM1 - scenario 2

Results of the optimization in some specific cases are given in figure 3 and 4. Figure 3.a shows partial ranking of the alternatives towards the output (left) and input (right) flow of the alternative. The alternative  $a_1$  (action 1) is dominant by both criteria, which confirms the complete ranking of the alternatives by method PROMETHEE (figure 3.b) for both scenario cases. PROMETHEE table of flow (figure 4) shows

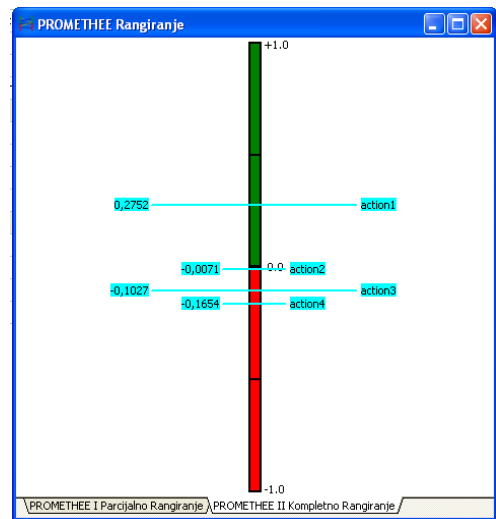
the results of the output, input and the clear flows of all alternatives, and based on this, their complete ranking by method PROMETHEE II.

PROMETHEE table of flow (figure 4) shows the results of the output, input and the clear flows of all alternatives, and based on this, their complete ranking by method PROMETHEE II.



a1

Scenario 1



b1

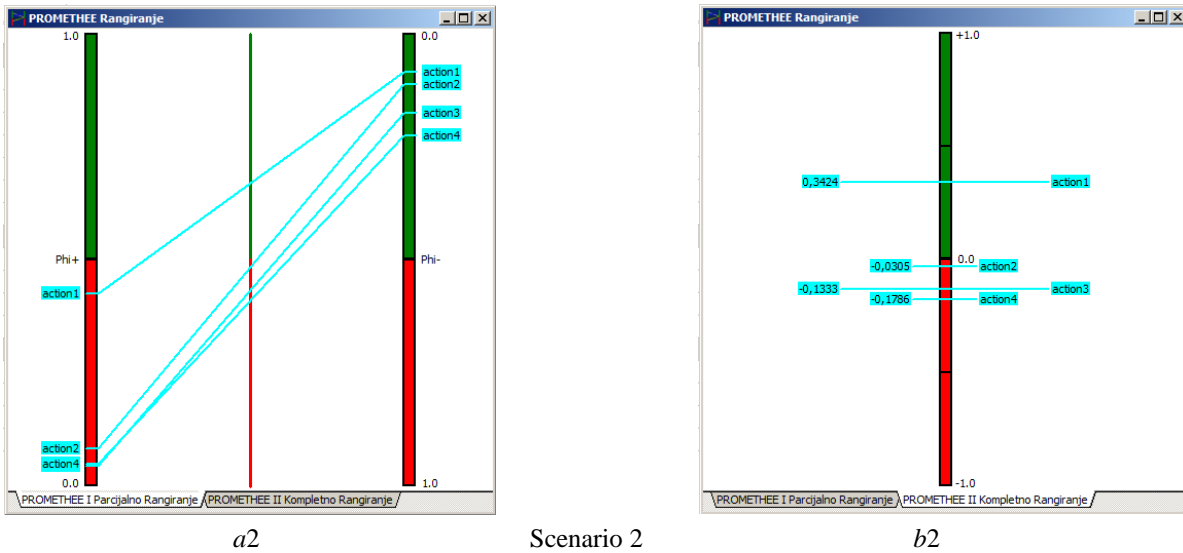


**Fig. 3** Partial (a) and complete (b) ranking of the alternative by PROMETHEE I and PROMETHEE II methods, for measurement location MM1, under to scenario 1 and 2

PROMETHEE Tabela Toka				
Rank	akcija	Phi	Phi+	Phi-
1	action1	0,2752	0,3333	0,0581
2	action2	-0,0071	0,0906	0,0977
3	action3	-0,1027	0,0481	0,1508
4	action4	-0,1654	0,0346	0,2000

Scenario 1

PROMETHEE Tabela Toka				
Rank	akcija	Phi	Phi+	Phi-
1	action1	0,3424	0,4261	0,0836
2	action2	-0,0305	0,0812	0,1118
3	action3	-0,1333	0,0421	0,1754
4	action4	-0,1786	0,0470	0,2256

Scenario 2

**Fig. 4** Complete ranking of the alternatives by PROMETHEE II method, for measurement location MM1 under the scenario 1 and 2, based on the values of clear(net) alternative flow

Figure 5 represents two dimensional result of the joint ranking of the alternatives by methods PROMETHEE I and

PROMETHEE II, for measurement location MM1, under the scenarios 1 and 2. Square represents areas  $\Phi^+$  and  $\Phi^-$  planes, where each of the alternative is represented by point. Plane is tilted at the  $45^\circ$  angle, so that vertical dimension gives Phi net flow of the alternative. Output  $\Phi^+$  flow increase the angle from the left side towards the peak, while input  $\Phi^-$  increase angle from the right side towards the bottom. For each of the actions, a cone shape is generated inside the plane.

Especially applicable way of representing the multi-criteria optimization from the PROMETHEE software is the Rainbow (figure 6), which gives broad spectrum of views on the PROMETHEE II method. In this way, advantages and disadvantages of the certain alternatives, based on which the ranking of the solution has been done, are easily shown. Comparable graphical representation of the ranking alternatives by PROMETHEE II method under scenarios 1 and 2, is given in figure 7.

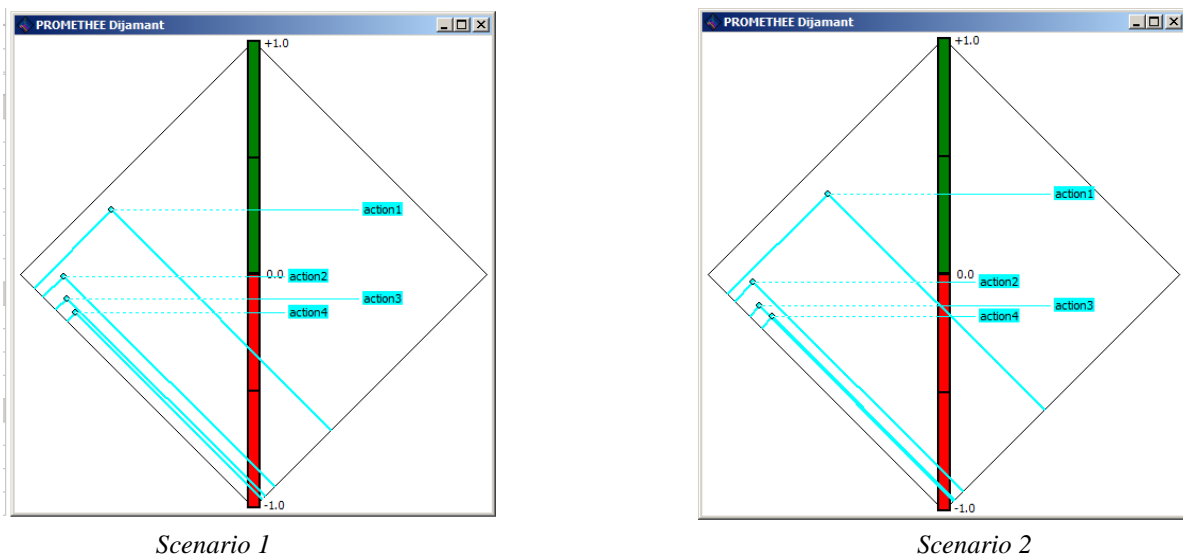
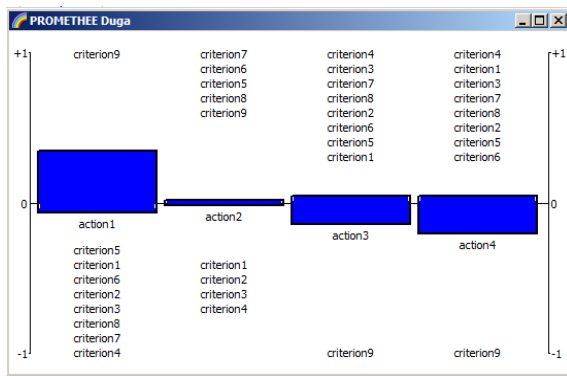
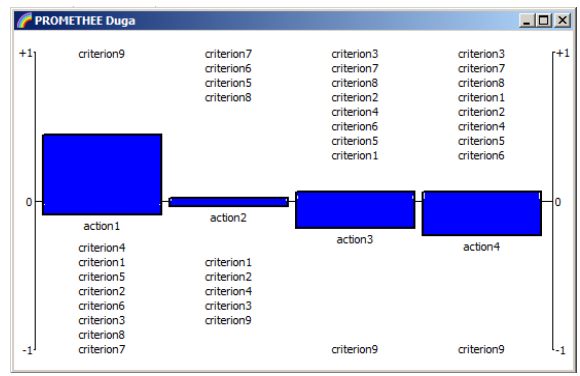


**Fig. 5** View of the PROMETHEE window Diamond - ranking of the alternatives for measurement location MM1, under the scenarios 1 and 2



Scenario 1



Scenario 2

**Fig. 6** View of the PROMETHEE window Rainbow - ranking of the alternatives for measurement location MM1, under the scenarios 1 and 2

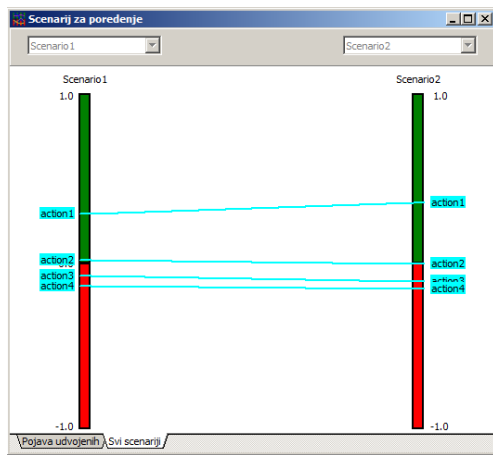


**Fig. 7** Comparison of the ranked alternative by PROMETHEE II method for measurement location MM1, under the scenarios 1 and 2

Procedure of the choice of the optimal measurement interval length that has been done for the measurement location MM1 emphasis the alternative  $a_1$  (one week measurement interval) as the most acceptable from the standpoint of the given criteria. Final order of the alternatives is:

$$a_1 \rightarrow a_2 \rightarrow a_3 \rightarrow a_4$$

Resulted solution entirely corresponds to the goal of the research that has been set, which is minimization of the measurement time interval with achievement of the satisfactory accuracy and precision, which enables maximum exploitation level of the measurement equipment.

## CONCLUSION

By applying multi-criteria optimization for solving the problem described in this paper, based on the results of this research, following conclusion can be drawn:

1. Application of this method represents a improvement step in making a decision on the length of the measurement time interval when environmental noise indicators are monitored. If this is based on the input criteria and noise limits, conditions for maximum exploitation of the measurement equipment are satisfied.
2. The choice of the optimal solution is affected by following factors:
  - Choice of the method itself is an important decision for the purpose multi-criteria optimization of the

denoted problem, in the context of the sensitivity of the method on the given criteria and expected results. By applying PROMETHEE method for the multi-criteria optimization on the available base of experimental data, with a possibility of defining conditions and parameters that additionally affect the choice of the optimal measurement strategies, represents a fully acceptable solution from the aspect of defining goals and expected research results.

- Subjective choices of the researchers in decision making during the process of the multi criteria optimization is very common. It is expressed through personal attitude and preference towards certain variation of solutions. Objective approach in choice of the optimal measurement strategy has been searched through opinions and attitudes of the experts in the field, by defining an importance of some criterias by each expert individually approaching the given problem.
3. The choice in the measurement strategy with a weekly intervals satisfied the established hypothesis at the beginning of the research, that with shorter time intervals of the noise indicators measurements than annual interval length, it is possible to get indicators values that do not differs from the values obtained by entire year interval length measurements. This variations stays within defined accuracy of 1.5 dB, and precision 1 dB.
  4. Measurement strategy for assessing the annual noise level indicators, with a weekly time intervals of measurements, obtained as a optimal solution, is related to the "noisy" locations in the city where traffic noise is the dominant noise source and the main factor of crossing the permissible noise level, with a traffic volume of more than 1000 vehicle per hour.
  5. Meteorological conditions in which long-term noise monitoring has been done, that does not change extremely during measurements, have no significant impact on the change of the noise indicators, which is why any week can be chosen for the monitoring during the year.
  6. Limits during the choice of the correct week in which measurements will be done, are related to holidays and events, where significant acoustical activities are expected.

## REFERENCES

- [1] Murphy E., King E.A.: „Strategic environmental noise mapping: methodological issues concerning the implementation of the EU Environmental Noise Directive and their policy implications”, *Environment International journal*, 36(5), 290–298, 2010
- [2] Vos P. and Licitra G.: „Noise maps in the European Union: An overview”, In G. Licitra (Ed.), „Noise mapping in EU: Models and Procedures”, 1<sup>st</sup> edition, CRC Press, USA, 2012
- [3] Bengtsson J. and Waye P.K.: „Assessments of low frequency noise complaints among the local Environmental Health Authorities and a follow-up study 14 years later”, *Journal of Low Frequency Noise, Vibration and Active Control*, 22(1), 9–16, 2003
- [4] Doygum H. and Gurun D.K.: „Analysing and mapping spatial and temporal dynamics of urban traffic noise pollution: a case study in Kahramanmaraş, Turkey”, *Environmental Monitoring and Assessment*, 142(1-3), 65–72, 2008
- [5] Georgiadou E., Kourtidis K. and Ziomas I.: „Exploratory traffic noise measurements at five main streets of Thessaloniki, Greece”, *Global Nest I International Journal*, 6(1), 53–61, 2004
- [6] Jamrah A., Al-Omari A. and Sharabi R.: „Evaluation of traffic noise pollution in Amman, Jordan”, *Environmental Monitoring and Assessment*, 120(1-3), 499–525, 2006
- [7] Korfali S.I. and Massoud M.: „Assessment of community noise problem in greater Beirut area, Lebanon”, *Environmental Monitoring and Assessment*, 84(3), 203–218, 2003
- [8] Mortensen F.R. and Poulsen T.: „Annoyance of low frequency noise and traffic noise”, *Research Note, Journal of Low Frequency Noise, Vibration and Active Control*, 20(3), 193–196, 2001
- [9] Omokhodion F.O., Ekanem S.U. and Uchendu O.C.: „Noise levels and hearing impairment in an urban community in Ibadan, Southwest Nigeria”, *Journal of Public Health*, 16(6), 399–402, 2008
- [10] Pandya G.H.: „Urban noise - A need for acoustic planning”, *Environmental Monitoring and Assessment*, 67(3), 379–388, 2001
- [11] Directive 2002/49/EC of the European Parliament and the Council relating to the assessment and management of environmental noise, *Official Journal of the European Communities*, L 189, 45, 2002
- [12] SRPS ISO 1996-1:2010: „Akustika – Opisivanje, merenje i ocenjivanje buke u životnoj sredini – Deo 1: Osnovne veličine i procedure ocenjivanja”, Institut za standardizaciju Srbije, 2010
- [13] Abbaspour M., Golmohammadi R., Nassiri P. and Mahjub H.: „An investigation on time-interval optimisation of traffic noise measurement”, *Research note, Journal of Low Frequency Noise, Vibration and Active Control*, 25(4), 267–273, 2006
- [14] Mihajlov D., Prašević M.: „Permanent and Semi-permanent Road Traffic Noise Monitoring in the City of Nis (Serbia)”, *Journal of Low Frequency Noise, Vibration and Active Control*, Vol. 34, Issue 3, pp. 251–268, doi: 10.1260/0263-0923.34.3.251, 2015
- [15] Prašević M., Mihajlov D., Cvetković D.: „Permanent and semi-permanent noise monitoring – first results in the city of Niš“, in *Proc. of 24<sup>th</sup> International Conference „Noise and Vibration“*, ISBN: 978-86-6093-062-2, pp. 33-40, Niš, 2014
- [16] Nikolić I., Borović S.: „Višekriterijumska optimizacija”, *Medija centar Odbrana, Beograd*, 1996
- [17] Saaty, T.L.: „Analytic hierarchy process”, *McGrawHill, New York*, 1980
- [18] Hsu C., Sandford B.: “The Delphi Technique: Making Sense Of Consensus”, *Practical Assessment, Research & Evaluation*, Vol. 12, No. 10, 2007
- [19] <http://www.promethee-gaia.net/software.html>



## PROBLEM OF EXCESSIVE NOISE GENERATED BY INDUSTRIAL MACHINERY

Ana Đorđević<sup>1</sup>, Dejan Ćirić<sup>2</sup>

<sup>1</sup> University of Niš, Faculty of Electronic Engineering, Serbia, ana.djordjevic@elfak.rs

<sup>2</sup> University of Niš, Faculty of Electronic Engineering, Serbia

**Abstract** - *One of serious problems in working environment is noise. This problem is of special significance in production halls under industrial conditions with heavy machines generating rather high noise levels, such as production plants in metal industry. Noise emitted by industrial machinery as well as treatments how to reduce the excessive noise are presented and analysed in this paper. This is done by providing some characteristic examples of radiated machine noise. The measurement results of equivalent noise level and levels in third-octave bands are given. Various alternatives how to reduce the noise are discussed from a general point of view, and some particular solutions are considered in more detail.*

### 1. INTRODUCTION

Noise defined as any unwanted, unpleasant or injurious sound [1] is generated as a by-product of almost any machine [2,3], and it is considered as a form of “invisible pollution” [4]. Often, noise generated by industrial machinery has levels that are rather high meaning that they can jeopardize human hearing [5-7]. How large this problem is can be illustrated by the fact that 34% of plants out of 3236 noise emitting objects exceeded the allowable noise level in the period between 2012 and 2015 [1]. The effects of noise on human organism depend on noise characteristics such as intensity, frequency, time distribution and content, but also on person exposed to noise. Noise-induced hearing loss is one of the most common occupational illnesses, and it is present in about one third of all work-related diseases [1]. Negative effects of noise also include disturbance of the physiological and psychological balance, reduction of working performance as well as mental, physical and psychosomatic disorders [3,5,6,8,9].

The workplaces known as the most exposed to noise are: metal industry, timber industry, base metal industry, paper industry and constructions [4]. In metal industry, there are a number of machines and machines' parts that can produce extremely high and protracted volumes of noise [2,6]. For example, lathes, milling and drilling machines generate noise up to 104 dB(A), metal cutting saws up to 115 dB(A), and grinders up to 134 dB(A) [1]. Noise levels in other industries can also be high, e.g., the levels of machinery used in the paper making sector is 94 dB(A) for paper guillotine, 95 dB(A) for box gluing machine and 100.5 dB(A) for a paper rotary press factory [5].

Permissible levels of noise are defined in several standards. Internationally accepted noise level not causing temporary or permanent hearing loss is 75 dB(A) [9]. The most common allowable noise exposure level applicable to an 8-hour working day is 85 dB(A) determined by the International Labor Organization [5] as well as Occupational Safety and Health Administration [2]. Maximum permissible noise exposure is 115 dB(A) for a period that does not exceed 2 minutes per 24 hours [4].

To assess the noise pollution in an adequate way, noise measurements play an essential role [3]. The aim of noise measurements is either to get an expression of the acoustical output from a specific source or to determine the noise at a specific point [10]. Measurements of noise emission and methods used to investigate noise levels are topics of several standards including ISO 230-5 and ISO 3740.

According to the rules for health protection, the machinery noise emission has to be reduced to levels allowed by corresponding standard(s). In the hierarchical approach, the noise reduction ranges from physical removal, replacement and isolation from hazard to personal protective equipment. Noise control can be broadly categorized into three types: source treatment, path treatment and receiver treatment [11]. Whenever is possible, the noise reduction should be done as close to the noise source as possible [8].

This paper presents the measured noise levels generated by various machines in the metal industry production hall. Nine machines are included in this research. The generated noise is analysed focusing on equivalent A-weighted levels as well as frequency distribution of noise in third-octave bands. In order to reduce the excessive noise, different alternatives for noise control are considered. Special attention is paid to noise reduction close to the source. Some particular solutions for noise reduction are discussed and the effects of their application.

### 2. INDUSTRIAL NOISE ANALYSIS

In industrial production plants, there are a number of different machines including those that contain pumps, conveyor belt chains, sorting drums, drying chambers, metal carts, etc. These machines can generate rather high noise level, which depends on the machine itself and its construction, but also on working condition (full operation or idle condition). Regarding construction, especially in machines of older

design, there can be a number of openings, slits and holes where most of noise is radiated from.

Generated noise also depends on parts that are processed on a particular machine. For example, a machine whose main purpose is to sort the metal elements (shells, rotors, etc.) vibrates creating the movement of the metal parts, see Fig. 1. If these parts are made of metal, then the situation regarding noise is made even worse. Impulsive and structural noise is generated by mutual collisions of metal pieces that hit each other and also the machine walls. Simulated noise levels at the surface of the container (drum) of such sorting machine are presented in Fig. 2.

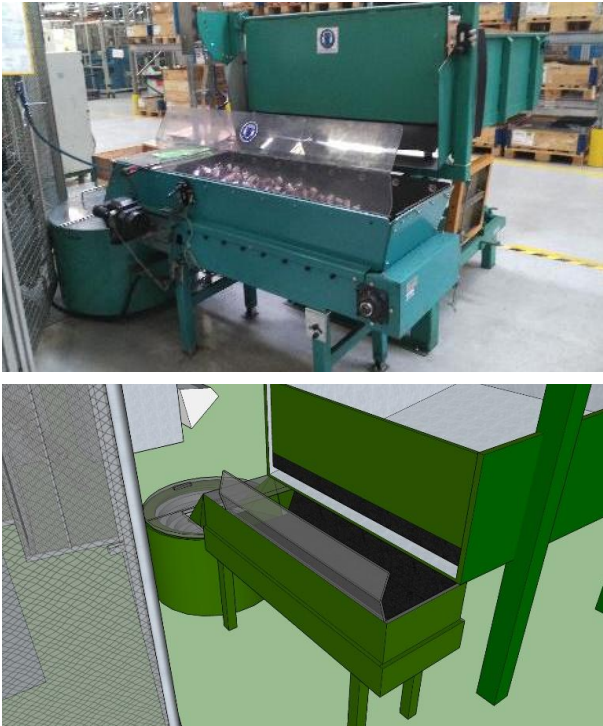


**Fig. 1** Machine with vibrating sorting mechanism: photo (above) and 3D model (below)

If the metal parts are heavier, there will be high velocity impacts of two metal pieces, and the noise levels will be higher. Besides, spectrum of generated noise will be somewhat different, where heavier parts typically lead to increase of components at lower frequencies. Collision of lighter metal pieces typically results in more significant contribution at higher frequencies. High frequency noise is specific, since this noise will create discomfort and decrease productivity during the 8 hours shift as a consequence of human hearing sensitivity to such type of noise. Such a problem should not be overlooked.

In many cases, machines are rather complex consisting of more other machines or devices. An example is illustrated in Fig. 3. Due to that, it is often hard to distinguish which part of a particular machine generates most of noise. Besides, it is also not easy to detect all important noise sources, since they can be masked by other sources.

Noise sources are often located at close proximity to operator's work areas, and combined sources rise the overall noise level. Typically, produced noise has broad-band spectrum, although in some cases there are dominant frequency components.

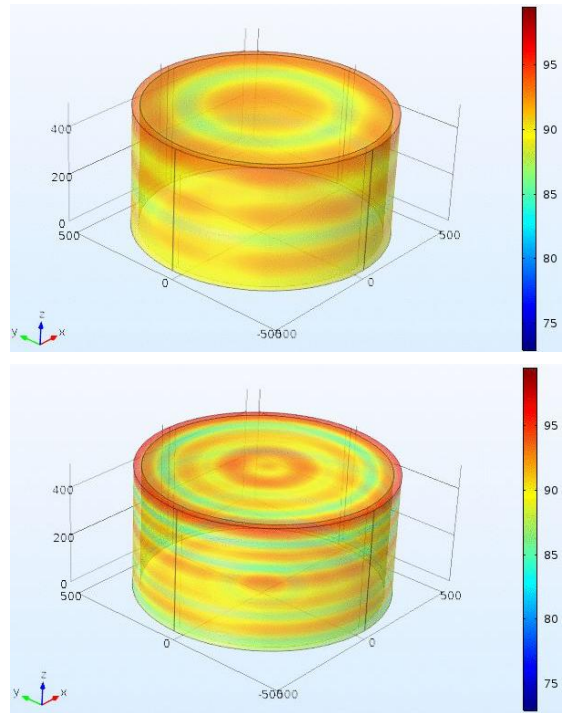


**Fig. 2** Noise levels at the surface of container of sorting machine obtained by simulations at 1 kHz (above) and 2 kHz (below)

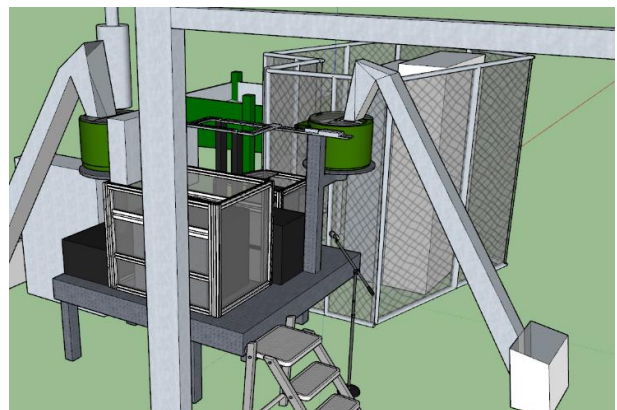


**Fig. 3** Model of complex machine consisting of several machines, devices and constructions

### 3. MEASUREMENT METHOD

Noise levels of most of machines detected as dominant noise sources were measured with standard sound level analyzer of class 1 - Norsonic Nor140. Minority of machines were measured by the sound level meter with frequency analyzer of class 2 - Pulsar Model 96. The measurements were performed in close proximity of the machines, at distances not smaller than 1 m.

Whenever it was possible, the measurements were carried out during the cycle when the machine of interest was dominant noise source. This means that other machines surrounding the measured one were not in operation. The sound level meter was placed at height of approximately 1.2 m, and directed toward the tested machine. Noise was measured for 1 minute using fast averaging.

#### 4. MEASURED NOISE LEVELS

Equivalent noise levels in time generated by one of the machines with sorting mechanism based on vibrations similar to the one given in Fig. 1 are presented in Fig. 4. Frequency characteristic of this noise in third-octave bands is shown in Fig. 5. This noise has broad-band spectrum, with dominant component at 50 Hz.

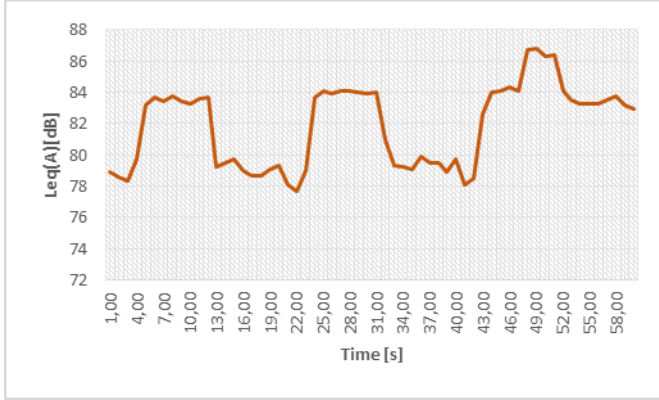


**Fig. 4** Equivalent noise levels in time generated by the machine with vibrating sorting mechanism

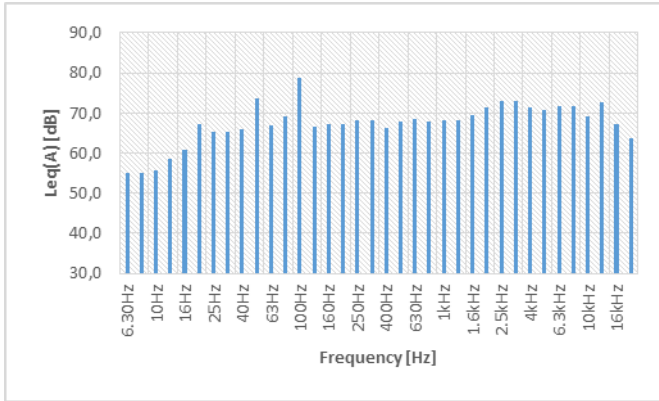


**Fig. 5** Frequency characteristic of noise from Fig. 4 in third-octave bands

Equivalent A-weighted noise levels measured in vicinity of six different machines located within the same production line are summarized in Table 1. Third-octave frequency analysis is performed for noise generated by each machine and presented in Figs. 6 and 7. It is observed that noise exists throughout entire frequency range. For all of the machines other than the machine 2 and 6, there are significant high frequency components, while the machines 2 and 6 produce noise with most energy at mid frequencies.

**Table 1** Noise levels measured in vicinity of 6 machines

Machine	$L_{min}$ , dB(A)	$L_{Aeq}$ , dB(A)	$L_{max}$ , dB(A)
Machine 1	43.8	94.9	101.1
Machine 2	59.7	105.5	112.2
Machine 3	62.1	86.7	91.1
Machine 4	57.7	93.8	102.8
Machine 5	41.9	93.8	100.7
Machine 6	62.8	85.5	97.1

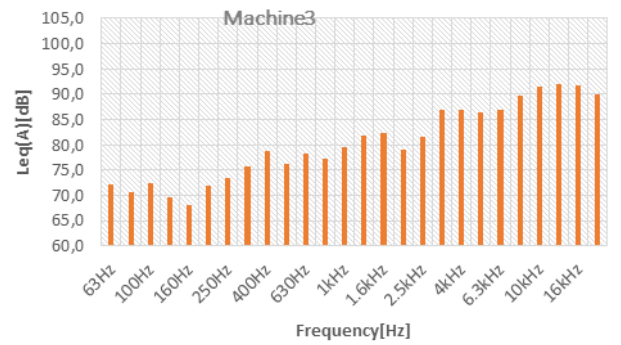
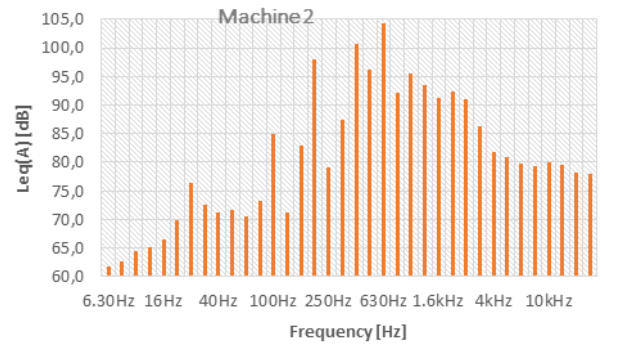
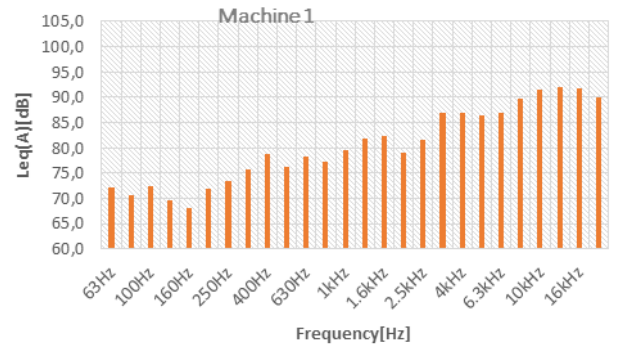


**Fig. 6** Frequency characteristics of noise measured in vicinity of the machines 1 to 3 in third-octave bands

The results of noise level measurements performed on another machine (machine 7, located within another production line in the same production hall) in two points are summarized in Table 2 and 3. The measurements 1 and 2 were done at two different times with the gap of almost two months. The measurement 3 was done under somewhat changed conditions since the rubber dumper at the bottom of the container of sorter had been removed. The measurement 4 was carried out after installation of the acoustic treatment applied to reduce the noise levels.

**Table 2** Minimum, A-weighted equivalent and maximum noise levels measured in vicinity of the machine 7 at different times, in the measurement point 1

Machine 7	$L_{min}$ , dB(A)	$L_{Aeq}$ , dB(A)	$L_{max}$ , dB(A)
Measurement 1	42.2	92.3	97.5
Measurement 2	88.7	91.2	93.8
Measurement 3	80.7	98.6	102.4
Measurement 4 after treatment	77.9	82.3	84.8

**Table 3** Minimum, A-weighted equivalent and maximum noise levels measured in vicinity of the machine 7 at different times, in the measurement point 2

Machine 7	$L_{min}$ , dB(A)	$L_{Aeq}$ , dB(A)	$L_{max}$ , dB(A)
Measurement 1	74.7	87.5	91.9
Measurement 2	87.2	89.1	90.3
Measurement 3	74.7	96.0	104.4
Measurement 4 after treatment	76.8	79.5	82.0

treatment reduces the noise levels from 8 dB to more than 16 dB.

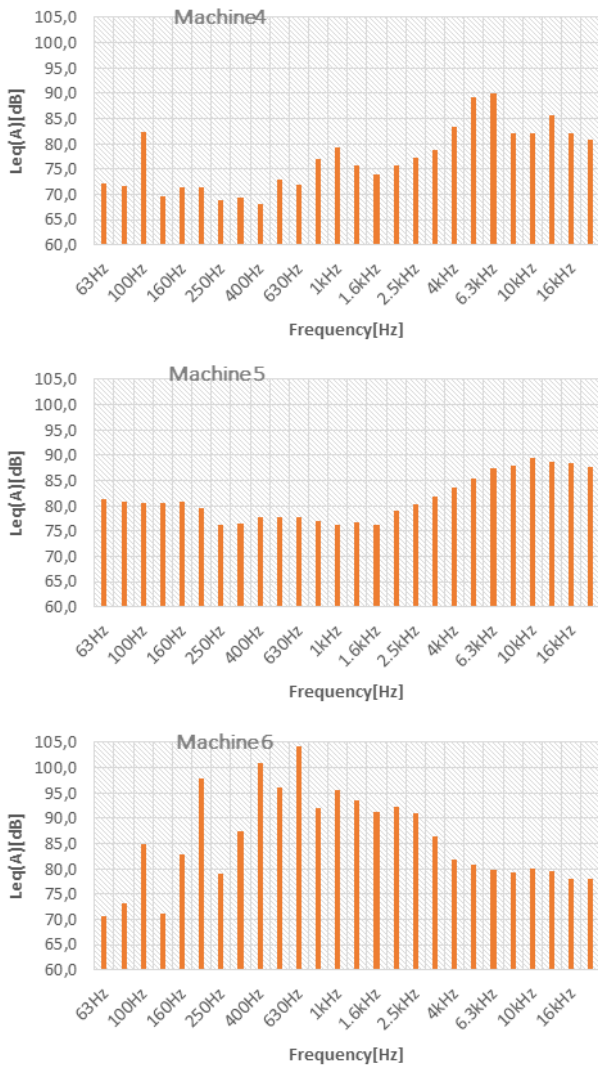


**Fig. 7** Frequency characteristics of noise measured in vicinity of the machines 4 to 6 in third-octave bands

Frequency characteristics of noise measured in vicinity of the machine 7 before and after installation of the noise reduction are given in Fig. 8 and 9. It is interesting to note that there is a dominant component at 100 Hz. This component was even more dominant before the noise reduction. Although the noise reduction treatment contains the resonator at about 100 Hz, noise in the frequency band at 100 Hz is still about 10 dB greater than at other frequencies. The given levels are the worst case scenario measured when the container was full of metal parts. In a situation when the container was half-full, the noise levels were for about 3 dB lower. Depending on measurement point and working conditions, the noise

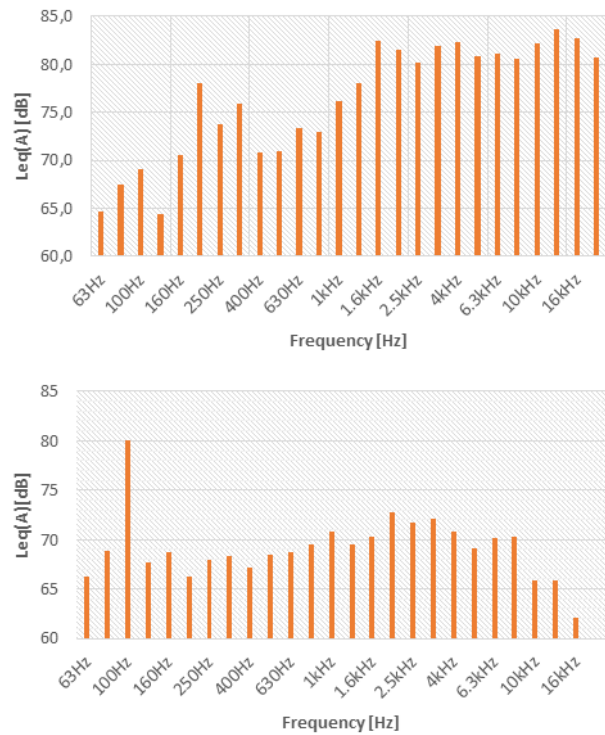


**Fig. 8** Frequency characteristics of noise measured in vicinity of machine 7 in third-octave bands in measurement point 1 before the treatment, measurement 2 (above) and after the noise reduction treatment, measurement 4 (below)

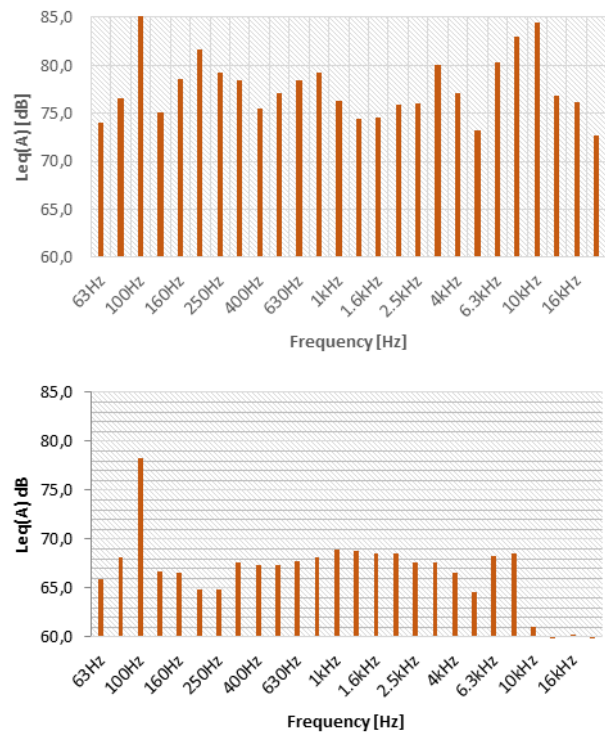


**Fig. 9** Frequency characteristics of noise measured in vicinity of machine 7 in third-octave bands in measurement point 2 before the treatment, measurement 2 (above) and after the noise reduction treatment, measurement 4 (below)

The noise levels measured in vicinity of the machine 8 within the same production line as the machine 7 are given in Table 4 and 5 for two measurement points. Frequency characteristics of this noise before and after the noise reduction treatment are presented in Fig. 10. Dominant component is again at 100 Hz. The acoustic treatment reduces noise especially at higher frequencies, but it is not that efficient for the dominant component of 100 Hz. It could be the case that this component is not even generated in this machine.

**Table 4** Minimum, A-weighted equivalent and maximum noise levels measured in vicinity of the machine 8 at different times, in the measurement point 1

Machine 8	$L_{min}$ , dB(A)	$L_{Aeq}$ , dB(A)	$L_{max}$ , dB(A)
Measurement 1	90.6	95.4	108.8
Measurement 2	87.3	90.4	105.6
Measurement 3 after treatment	76.7	78.9	81.0

**Table 5** Minimum, A-weighted equivalent and maximum noise levels measured in vicinity of the machine 8 at different times, in the measurement point 2

Machine 8	$L_{min}$ , dB(A)	$L_{Aeq}$ , dB(A)	$L_{max}$ , dB(A)
Measurement 1	76.8	81.1	86.5
Measurement 2	79.1	81.8	85.5
Measurement 3 after treatment	77.3	79.0	81.1

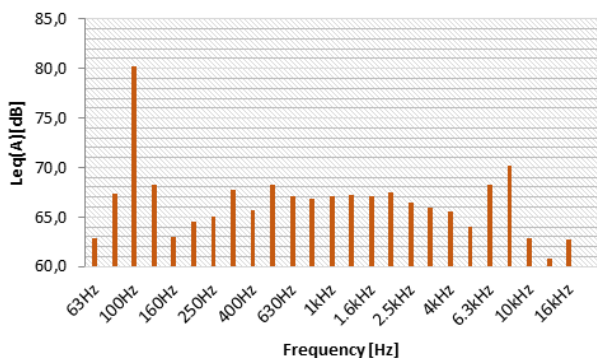
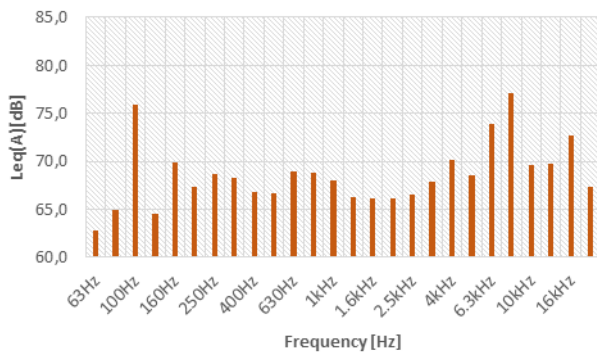


**Fig. 10** Frequency characteristics of noise measured in vicinity of machine 8 in third-octave bands in measurement point 1 before the treatment, measurement 1 (above) and after the noise reduction treatment, measurement 3 (below)

The measurement results of noise levels for the machine 9 in the same production line as the machines 7 and 8 are given in Table 6 and 7 as well as in Fig. 11. Here, the components at low frequencies about 100 Hz are greater than other frequency components for about 7 dB to 9 dB.

**Table 6** Minimum, A-weighted equivalent and maximum noise levels measured in vicinity of the machine 9 at different times, in the measurement point 1

Machine 9	$L_{min}$ , dB(A)	$L_{Aeq}$ , dB(A)	$L_{max}$ , dB(A)
Measurement 1	79.5	83.2	88.6
Measurement 2	87.2	89.1	90.3
Measurement 3 after treatment	78.7	79.4	80.5

**Table 7** Minimum, A-weighted equivalent and maximum noise levels measured in vicinity of the machine 9 at different times, in the measurement point 2

Machine 9	$L_{min}$ , dB(A)	$L_{Aeq}$ , dB(A)	$L_{max}$ , dB(A)
Measurement 1	80.0	84.8	88.7
Measurement 2	88.7	91.2	93.8
Measurement 3 after treatment	72.1	78.2	80.0

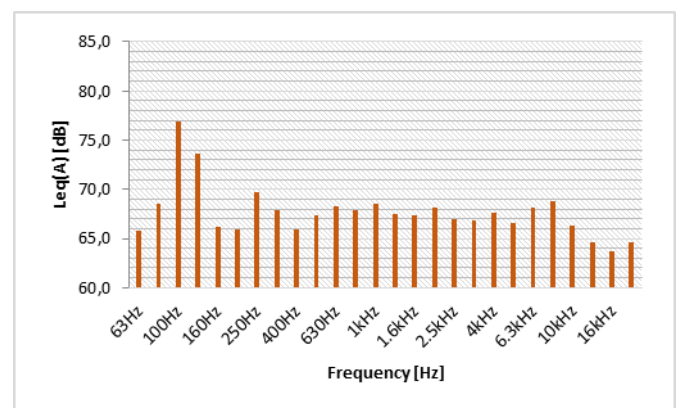
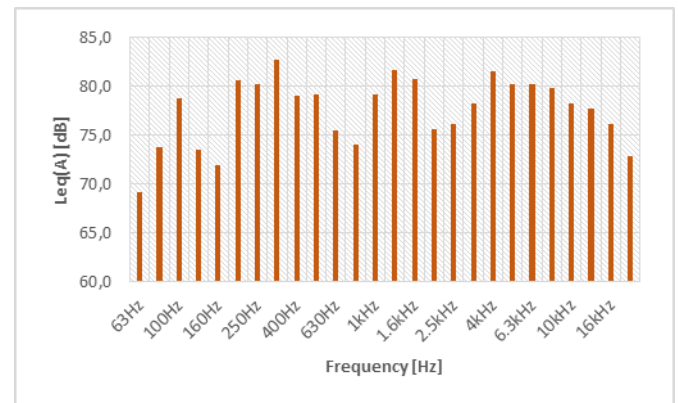


**Fig. 11** Frequency characteristics of noise measured in vicinity of machine 9 in third-octave bands in measurement point 2 before the treatment, measurement 2 (above) and after the noise reduction treatment, measurement 3 (below)

## 5. APPLICATION OF NOISE REDUCTION

Reduction of noise levels of machines in a production line is a rather challenging task. Machines whose noise should be attenuated are of different construction. They often work all the time, and they should be easily accessible by both the operators and maintenance personnel.

Noise generated by industrial machinery can be reduced in different ways, where treatments on the source are often considered as the most efficient ones. However, in industry it is not easy to apply noise reduction treatments on the source.

Requirements related to reduction of noise levels can include: target noise level after the noise control treatment should be less than 80 dB at the place of treatment, installed noise reduction elements must not interfere with the normal operation of the machine, and installed noise reduction elements must not interfere with machine maintenance.

Noise treatment on the source can be realized by applying various alternatives. One of them is related to treatment that is applied only to some parts of the machine, see Figs 12 and 13. This includes covering some metal walls with material of high insertion loss (damping factor) to reduce impact noise, but also preventing the noise leakage. The leakage can be prevented by fixing and replacement of old and damaged insulating material, covering holes, gaps, slits and openings, adding partial covers, absorptive elements, specialized acoustic reinforced rubber, etc. Depending on the extent of preventing the noise leakage, this solution will reduce the noise level at particular frequency range and the total noise level will drop from about 3 dB to about 9 dB or typically around 5 to 6 dB.

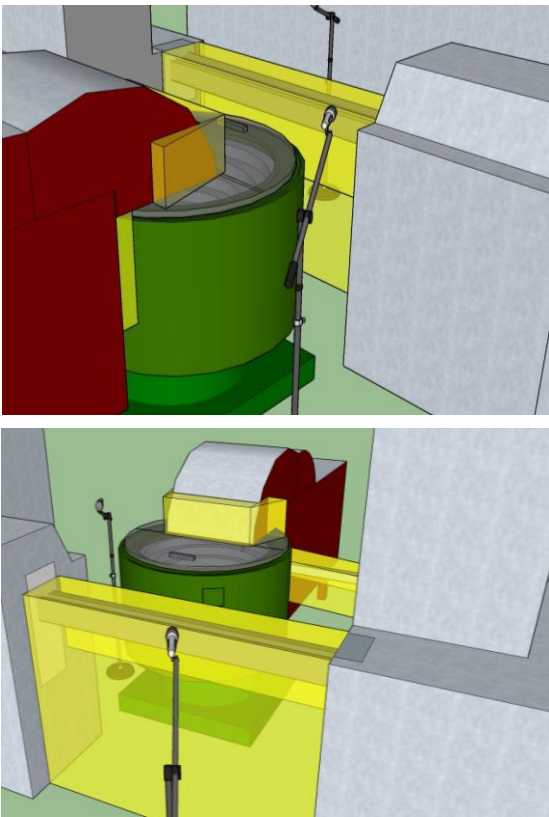


**Fig. 12** Noise reduction treatment by preventing noise leakage (noise treatment is denoted by yellow colour)

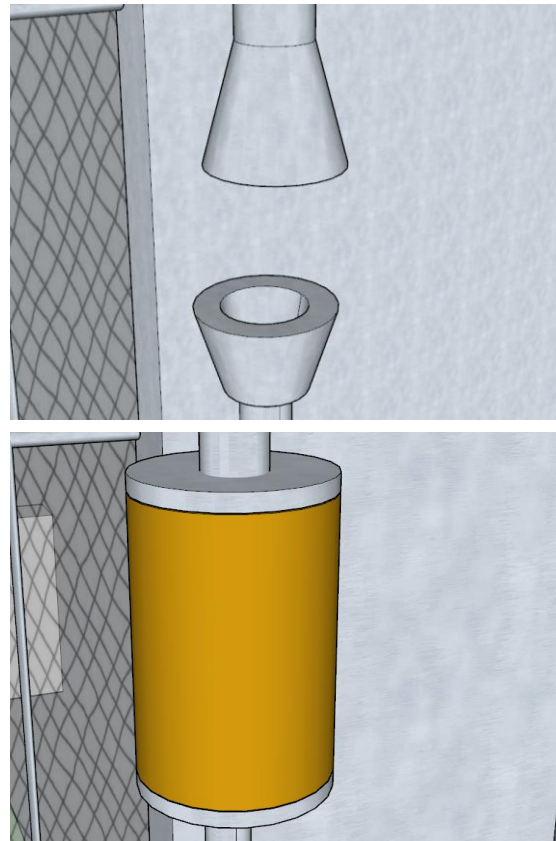


**Fig. 13** Noise reduction treatment by enclosing the exhaust hot air vent (treatment is denoted by dark yellow colour)

Noisy part(s) of a machine can be treated separately by placing an acoustic enclosure or acoustic cage around these parts, see Figs. 14 and 15. This solution is not always possible to be applied, since it disturbs the easy working environment. However, it enables noise reduction higher than 10 dB depending on the available space and requirements. Another alternative is the usage of acoustic ceiling to control noise inside a production line. This ceiling can be engineered not only to serve as a sound absorber, but also as a resonator type of sound absorber.

If the noise level generated by the machine is to be reduced to acceptable level of 80 dB, depending on working conditions and other factors, noise should be attenuated by even more than 10 dB. Thus, the approach based on hole fitting, gap fixing and rubber tight sealing will not lead to attenuation of this magnitude. Engineering approach in this case must be different, and based on placing an acoustic enclosure around the target machine, see Fig. 15.

The enclosure is designed in such a way that it is easy to demount and put together when necessary. Besides, the enclosure typically has transparent or non-transparent doors and windows. Walls of the enclosure can represent a sandwich insulation construction consisting of metal (facing outside), viscoelastic acoustic membrane for increasing acoustic mass and specially designed perforated absorber, fine-tuned to the noise spectrum produced by that particular machine. Vibro-insulation material will be applied below the drum, reducing transmission of noise through structural elements. In this way, depending on the used materials and construction, noise can be reduced by more than 15 dB.

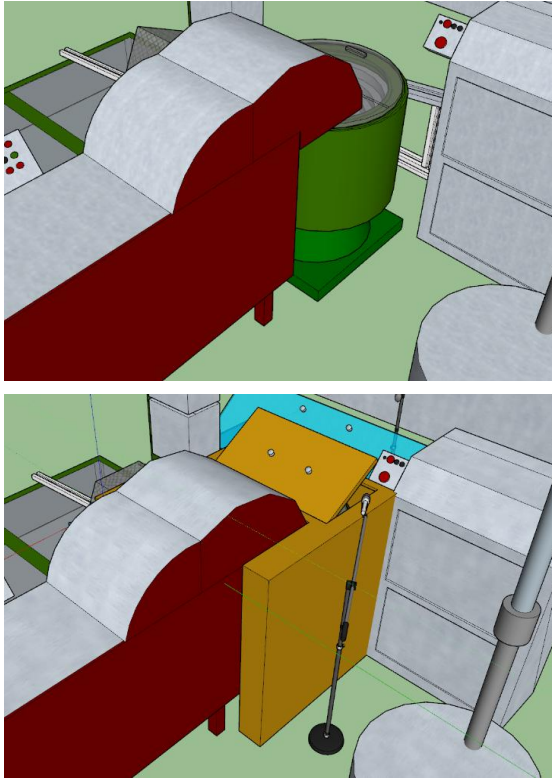


**Fig. 14** Noise reduction treatment by enclosing noisy part of machine (sorting drum) in acoustic cage (treatment is denoted by dark yellow colour)

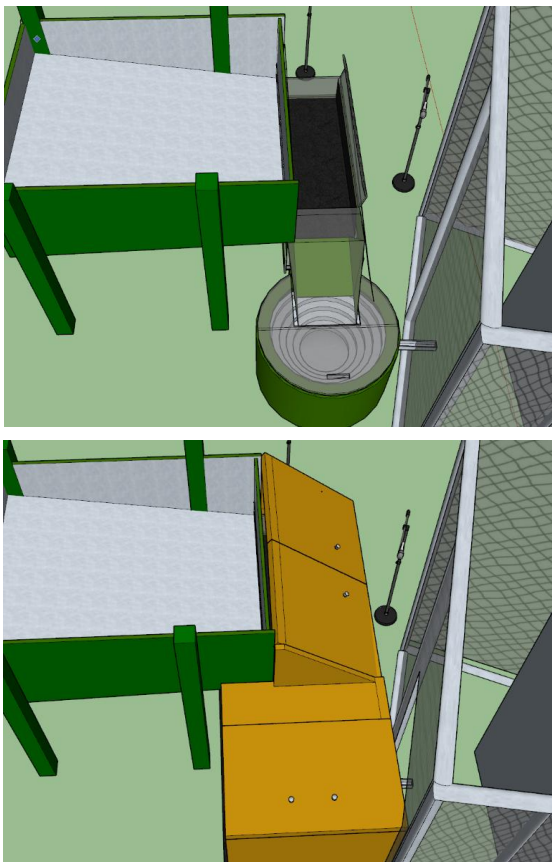


**Fig. 15** Noise reduction treatment by applying acoustic enclosure around the target machine: before the intervention (above), after the intervention (in the middle and below), yellow color represents the enclosure

In some situations, different solutions for noise treatment can be applied, as shown in Fig. 16. Here, one solution is related to partial treatment of only some parts of the machine detected as dominant noise sources. Another solution is related to applying a sort of acoustic cage around the machine, that can either be open or closed. When needed, e.g., in order to reach higher sound insulation, these solutions can be combined.

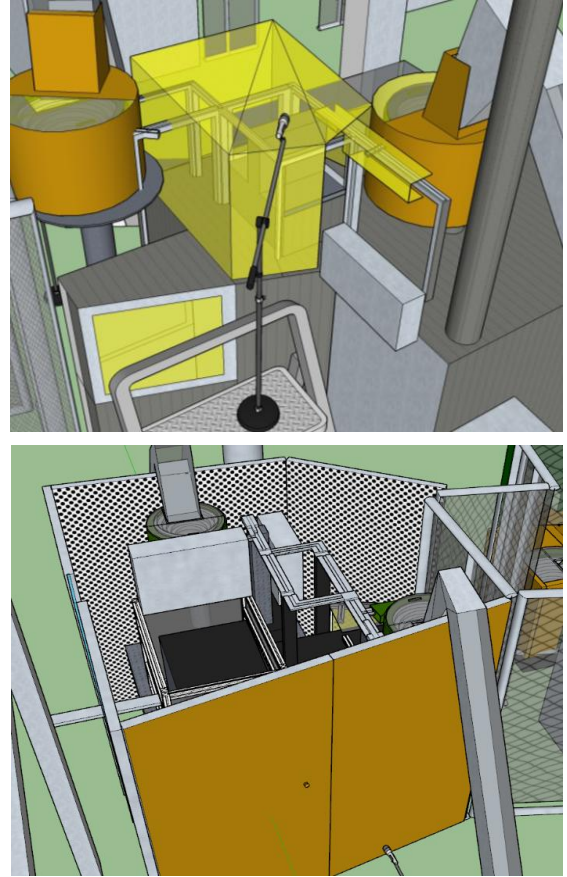


**Fig. 16** Alternatives for noise reduction treatments: intervention on some parts of machine indicated as the strongest noise sources (above), applying acoustic cage around the whole machine (below)

The solution of enclosing the treated machine in a closed or open cage is based on using non-transparent metal perforated panels. They can be designed to provide high enough insulation and fine-tuned to provide the best absorption in the frequency range where the machine produces the most noise. This is why such panels are one of the best solutions in noise insulation of the heating, ventilation and air conditioning (HVAC) systems. The acoustic enclosure typically has panel-door(s), so the machine located inside the enclosure can be easily reached. Often, the panels are demountable, for example for maintenance purposes. With such an enclosure, sound insulation of more than 12 dB can be achieved.

## 6. DISCUSSION AND CONCLUSION

It is very important to emphasize that conditions during measurements in a particular production hall typically differ from time to time. In many cases, machines have some modes of operations. Thus, the machine is active for some time, then it goes to idle mode or part-operation mode and the cycle is

repeated. The load of the machine is also not constant all the time.

The obtained results show that the measured noise levels at operator's workstations exceed the levels allowed by the standard. Based on the frequency analysis, it can be concluded that the spectrum of noise generated by industrial machinery is generally broadband. In some cases, dominant frequency components are observed.

Regarding the noise reduction treatment, there are some general guidelines that should be followed. However, especially in industrial environment, every machine requires special care to be paid in order to find an optimal solution for noise control among different available alternatives. Some partial treatments enable noise level to be reduced for about 5 dB to 6 dB. On the other hand, enclosing the machine within an acoustic cage can provide a larger noise reduction of even above 15 dB.

## REFERENCES

- [1] J. Józwiak, A. Wac-Włodarczyk, J. Michałowska, M. Kłoczko, "Monitoring of the noise emitted by machine tools in industrial conditions", *Journal of Ecological Engineering*, vol. 19, no. 1, pp. 83-93, January 2018.
- [2] S. A. Anjorin, A. O. Jemiluyi, T. C. Akintayo, "Evaluation of industrial noise: A case study of two Nigerian industries", *European Journal of Engineering and Technology*, vol. 3, no. 6, pp. 1-16, 2015.
- [3] T. M. Tersoo, O. M. Dawodu, N. Babakatcha, "Assessment of the level of noise produced by sound generating machines in Lapai, Northern Nigeria", *Advances in Applied Science Research*, vol. 2, no. 6, pp. 520-531, 2011.
- [4] V. Dimou, "Noise measurements in timber industries", *Drvna Industrija*, vol. 65, no. 3, pp. 243-249, 2014.
- [5] H. Serin, "Analysis of noise levels in corrugated board factories", *International Journal of Physical Sciences*, vol. 7, no. 11, pp. 1857-1861, March 2012.
- [6] B. H. M. Al-Dosky, "Noise level and annoyance of industrial factories in Duhok city", *IOSR Journal of Environmental Science, Toxicology and Food Technology*, vol. 8, no. 5, ver. I, pp. 1-8, May 2014.
- [7] O. Sharma, V. Mohanan, M. Singh, "Noise emission levels in coal industry", *Applied Acoustics*, vol. 54, no. 1, pp. 1-7, 1998.
- [8] H. Pettersson, "Environmental noise control in the pulp and paper industry", in *Proc. Forum Acusticum Congress*, Sevilla, Spain, 2002, paper ENV-Gen-002.
- [9] S. Grujić, A. Mihailović, J. Kiurski, S. Adamović, D. Adamović, "Noise level investigation in printing industry in Novi Sad, Serbia", *International Journal of Environmental and Ecological Engineering*, vol. 5, no. 4, pp. 224-226, 2011.
- [10] B. Dirdal, K. Gjaevanes, "Noise from compressors and pneumatic equipment", *Applied Acoustics*, vol. 4, no. 1, pp. 23-34, 1971.
- [11] S. S. Jayawardana, M. Y. A. Perera, G. H. D. Wijesena, "Analysis and control of noise in a textile factory", *International Journal of Scientific and Research Publications*, vol. 4, no. 12, pp. 1-7, December 2014.



# COMPARISON OF FREQUENCY CHARACTERISTICS OF SOUND GENERATED BY INTERNAL COMBUSTION ENGINES DEPENDING ON FUEL

Marko Milivojčević<sup>1</sup>, Filip Pantelić<sup>2</sup>, Dejan Ćirić<sup>3</sup>

<sup>1</sup>The School of Electrical and Computer Engineering of Applied Studies, Belgrade, Serbia, markomilivojcevic@gmail.com

<sup>2</sup>The School of Electrical and Computer Engineering of Applied Studies, Belgrade, Serbia

<sup>3</sup>University of Nis, Faculty of Electronic Engineering, Serbia

**Abstract** - This paper presents the process and results of measuring the sounds generated by internal combustion engines (ICE) in different operating modes depending on the type of the fuel. The measurements were made taking into account whether the bonnet is open or closed. Recorded audio sequences are shown as averaged spectra that are analyzed separately, and then they are compared in order to detect the difference that is heard with ears.

## 1. INTRODUCTION

Current and improved environmental standards in traffic have been used as the motive for measurement and analysis described in this paper, bearing in mind a clear difference between vehicles that use diesel or gasoline fuel [1]. The previous research on the acoustic analysis of internal combustion engines was primarily focused on the diagnosis of anomalies in the work [2], [3], [4], [5], [6], where, in addition to acoustic measurements, other types of data acquisition are taken and then correlated to get the most accurate results. However, a number of papers use exclusively the acoustic analysis of the internal combustion engine performance, primarily for testing insulation materials in the engine compartment [7], or for the acoustic characterization of certain engine elements [8], while for the needs of ecological standards it is necessary to identify the engine propellant fuel [1].

Taking into account the acquired experience of the authors regarding vehicles as well as the possibility of perceptual identification of these vehicle types by hearing sense, there was a need to perform acoustic analysis of the sounds (sound signals) generated by internal combustion engines used in vehicles powered by different propellant fuels. The measurements were carried out in a simple manner described in Chapter 2 and after collecting sound recordings a spectral analysis of the given signals was performed. The results of the analysis showed some differences in the signal spectra regardless of the engine operating mode, which opens up the possibility of acoustic identification of the fuel without the prior experience of the listener.

## 2. METHODOLOGY

The recording of sounds (audio signals) generated by internal combustion engines driven on different fuels was realized with two passenger cars. The chosen passenger cars were of approximate engine volume, design generation (age) and body dimensions. As perceptually it can be determined that

the number of inlet or exhaust valves per cylinder influences the color of the sound generated by the engine itself, it is taken into account that both vehicles have the same number of valves per cylinder. One vehicle uses gasoline, while the other one uses diesel fuel. Detailed vehicle characteristics are given in Table 1.

As can be seen in Table 1, the only essential difference between these two engines, other than the propellant fuel, is that the vehicle that uses diesel consumes a turbocharger that forcibly supplies additional air to the engine, however, under the conditions of the measurement that has been carried out, which involves engine running without load, the mentioned difference should not have an impact on the received sound recording. The load-free operation of the engine is achieved by letting the car rest and setting the gearbox to neutral position.

**Table 1.** Vehicle characteristics [9] [10]

	Vehicle 1	Vehicle 2
Car brand and type	Renault Clio 1.2 16v	Opel Corsa 1.3 CDTI
Fuel	gasoline	diesel
Engine displacement (cm <sup>3</sup> )	1149	1248
Number of valves per cylinder	4	4
Number of cylinders	4	4
Gearbox type	Manual	Manual
Injection	Multipoint	Multipoint
Engine type	Naturally aspirated	Turbo
Power (kW)	55	55
Vehicle dimensions LxWxH (mm)	3773x1639x 1417	4021x1736x 1479

A DBX RTA-M microphone was used to record sounds with the sampling frequency  $f_s = 44\ 100$  Hz, and a dynamic resolution of 16 bit. The signals were recorded with the

Behringer UMC404HD audio interface. The absolute level of ambient noise was monitored during the recording with the measuring device NTI Audio XL2. The recorded level was in the range of 44.8-51dB. The noise impact on the measurement results is negligible, since the noise levels produced by the engines are significantly higher. The lowest engine noise levels were achieved in the idle mode, 76.4dB for the gasoline engine and 76.7dB for the diesel engine.

The input gain of the audio interface during all measurements is kept at the same level so that the recorded signals can be subsequently compared regarding the level. In the case of a diesel engine with an open bonnet, there was a distortion of the signal (clipping), due to the high sound pressure level. For this reason, the measurement was repeated for this case by activating the attenuation (pad key) on the audio interface. By activating this key, the signal level is reduced by 16 dB.

While recording, the cars were placed on solid, concrete base, enclosed by three side walls. The nearest side wall was about 2 m away from the car body. The space in front of and above the car was open.

While recording, the measuring microphone was positioned at a distance of 1 m from the engine (see Fig. 1 and 2). The measurements were made separately for each vehicle in nine cases. Eight cases included the mentioned position of the measured microphone, while in one case the microphone was positioned on the ground directly below the engine, in order to avoid the possible impact of reflections from the solid ground and thus eliminate the comb filter effect.

Each measuring microphone position assumed four measurements: in idle mode, 1500 rpm, 2500 rpm and 3000 rpm with open or closed bonnet for each of the modes; the rpm refers to the number of engine crankshaft revolutions in one minute. In the case of a microphone positioned directly below the vehicle, the signals were recorded in idle mode.



**Fig. 1** Vehicle with petrol engine



**Fig. 2** Vehicle with diesel engine

The first step in the analysis of the recorded audio sequences was the spectral analysis. For this purpose, the software package SpectraLab was used, primarily chosen because of its simplicity. Spectral analysis was initially performed over the entire recorded audio sequence for 30 seconds in each case, however, as the time form of the signal is constantly repeating (Fig. 3), due to the speed of the spectrum calculation, the analysis was then continued at intervals of 5 seconds.

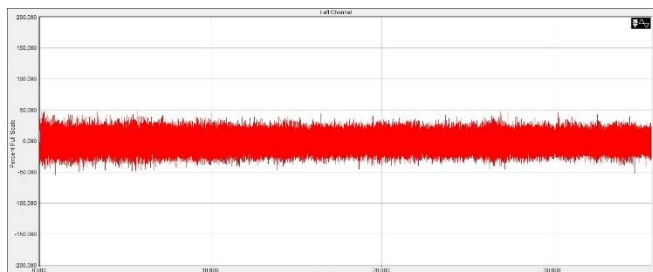


**Fig. 3** Petrol engine sound record in time domain

By selecting the "Compute and display average spectrum" option, the averaged spectrum for a given signal was observed in order to eliminate short-term ambient sounds that were not the subject of analysis such as speech, tram passage, etc. which could be heard during the measurement, but it was not possible to recognize them in the signal time domain. Settings used to calculate spectrum within the program SpectraLab are FFT size: 16384 pts and Hamming's window function. These settings were selected as per the minimum value required to make a visually clear spectrum on one hand, and so that all spectral components could be identified, on the other.

After the spectral analysis, whose results are given in the Chapter 3, a perceptual analysis of the processed audio signals was performed in order to determine the exact part of the signal spectrum that carries the most information regarding the identification of the engine type, based on the previous experience of the listeners. SpectraLayers pro 5.0 software was used for this procedure, as it required an effective removal of certain parts of the spectrum and then listening to the newly created audio track.

### 3. SPECTRAL ANALYSIS OF RECORDED SOUNDS

Spectrum analysis in Spectralab was performed in case of four engine operating modes (at idle mode at approx. 750 rpm, at 1500 rpm, at 2500 rpm and at 3000 rpm of the engine crankshaft), applying the procedure of open and closed hood for each one of them. The obtained comparative spectra for these two vehicles are shown in Figs. 4-11.

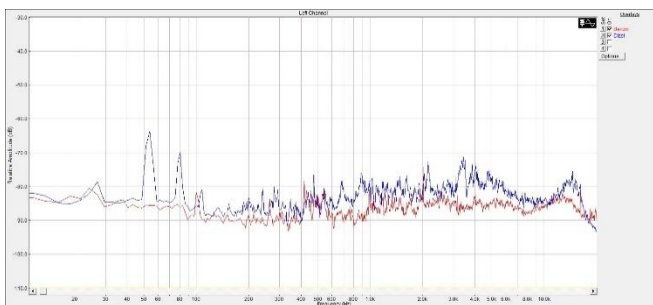


**Fig. 4** Sound spectrum for idle mode with closed bonnet

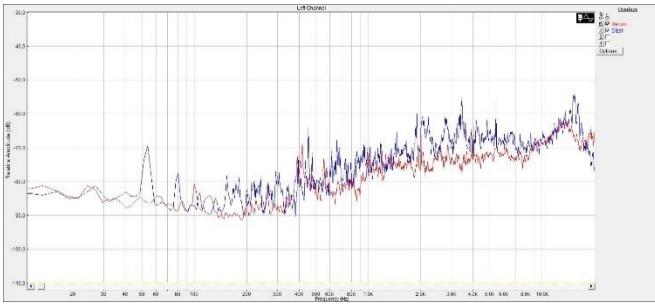


**Fig. 5** Sound spectrum for idle mode with open bonnet

While analyzing and comparing the spectrum of audio recordings of the engine working in the idle mode (Figs. 4 and 5), a pronounced "natural motor frequency" can be observed in case of a diesel vehicle, regardless of the bonnet position (open or closed) [11]. The natural motor frequency can be calculated directly from the revolutions of the engine crankshaft per minute, the number of engine cylinders and the engine type, that is the number of engine strokes per full cycle. The calculation method is as follows:

$$\text{crankshaft revs per sec} = \frac{\text{crankshaft revs per min}}{60} \quad (1)$$

$$\text{expansions per sec} = \frac{\text{crankshaft revs per sec}}{2} \quad (2)$$

$$\text{engine natural frequency} = \frac{\text{expansions per sec} \cdot \text{number of cylinders}}{\text{number of cylinders}} \quad (3)$$

Formula 2 is valid in the case of a four-stroke engine, because for each expansion in the engine it takes 2 crankshaft revolutions. In the engine idling case where the crankshaft speed is about 750 rpm, calculated natural frequency of the engine is 25 Hz. In the diesel engine audio spectrum, the harmonics of this frequency can be clearly observed due to the limitation or characteristics of the recording device. At higher rpm, the natural frequency is clearly observed, regardless of whether the bonnet is open or closed (Figs. 6-11).

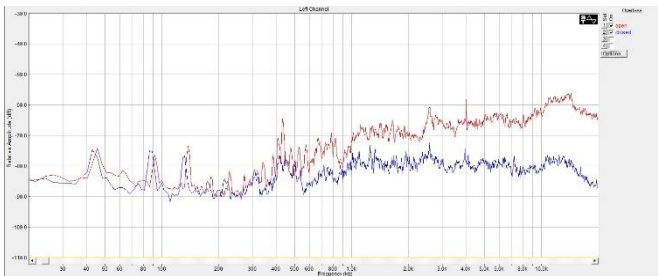


**Fig. 6 a)** Sound spectrum for petrol engine 1500 rpm mode with bonnet open/closed

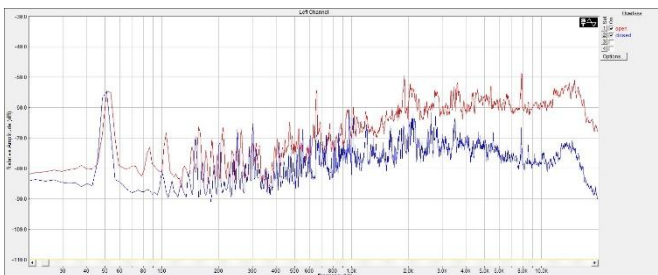


**Fig. 6 b)** Sound spectrum for diesel engine 1500 rpm mode with bonnet open/closed

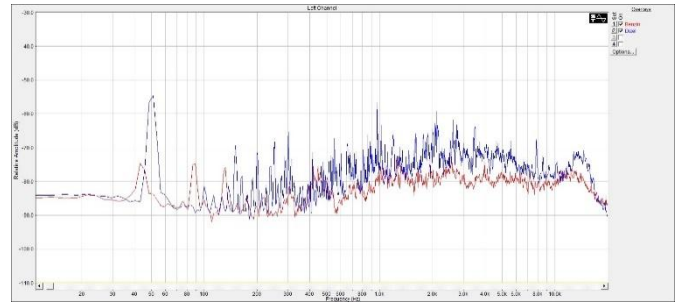


**Fig. 7** Sound spectrum for 1500 rpm mode with closed bonnet

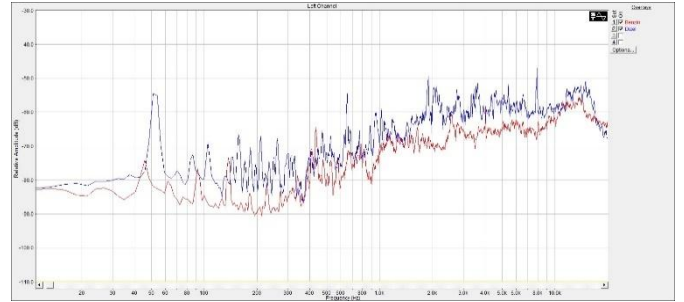


**Fig. 8** Sound spectrum for 1500 rpm mode with open bonnet

The sound spectrum of the analyzed engines for the 1500 rpm mode is given in Figs. 7 and 8. A clear natural engine frequency at approximately 50 Hz can be observed in these figures, matching the calculation (see Eqs. 1-3). The sound level at the engine natural frequency of a diesel-fueled vehicle is considerably higher than that of a gasoline-fueled vehicle, which can also be perceptually determined. Differences in the natural frequency that can be detected are caused by different methods of achieving the operating mode at 1500 rpm, that is by the imprecision of the scale on instrument cluster to show the number of rpms, as well as by the variations of the throttle pedal due to the human factor.

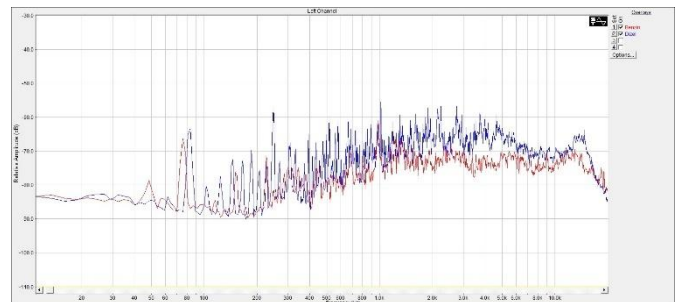


**Fig. 9** Sound spectrum for 2500 rpm mode with closed bonnet

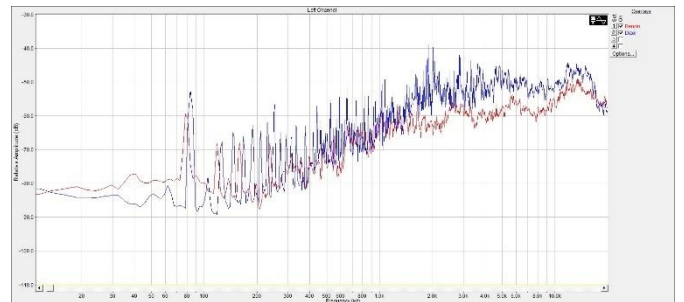


**Fig. 10** Sound spectrum for 2500 rpm mode with open bonnet

By observing the results for the operating mode at 2500 rpm (Figs. 9 and 10), one can notice the ever-weaker impact of the bonnet on the shape of the audio signal spectrum, i.e. the attenuation of higher frequencies in the spectrum. However, with diesel fuel vehicles, the natural-frequency harmonics of the engine have become even more pronounced than in the previous case.

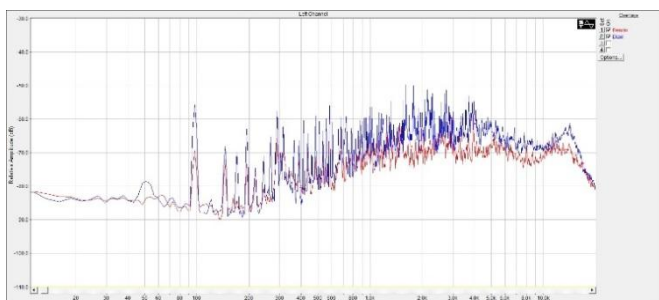


**Fig. 11** Sound spectrum for 3000 rpm mode with closed bonnet

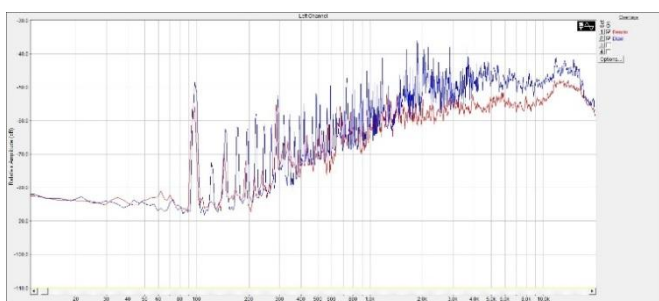


**Fig. 12** Sound spectrum for 3000 rpm mode with open bonnet

In the operation mode at 3000 rpm it becomes difficult to distinguish perceptually between diesel and gasoline-fueled vehicles, as shown in Figs. 11 and 12. In this mode, the bonnet almost has no effect on the shape of the audio signal spectrum, and the harmonics of the natural frequency of the gasoline engine become significant.

The results obtained by changing the position of the measuring microphone to the ground just below the motor, in order to eliminate the impact of reflection and other additional engine components, are shown in Fig. 13.

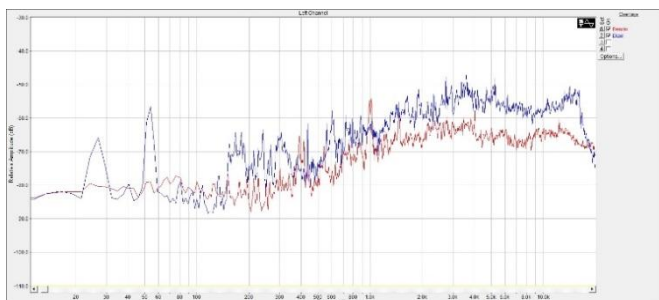


**Fig. 13** Sound spectrum for idle mode with measurement microphone on the ground for petrol and diesel engines

By analyzing the comparative review of spectra, a prominent natural frequency of diesel engines and the overall higher signal level across the entire range of spectrum are noticed.

As described in the methodology chapter, after analyzing the entire signal spectrum, individual parts of the spectrum are eliminated by usage of SpectraLayers Pro 5.0. These newly modified signals are continuously listened. In this way, it has

been determined that the awareness of the engine type, based on the previous experience of the listener, is in the range of 1.2-3.5 kHz, after which the signals are spectrally compared for each mode (Figs. 14-17).

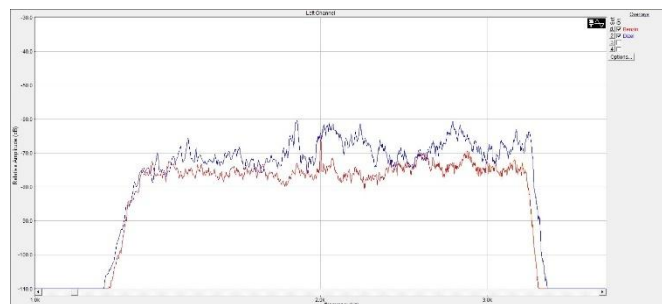


**Fig. 14** Sound spectrum for idle mode for the frequency range 1-4 kHz

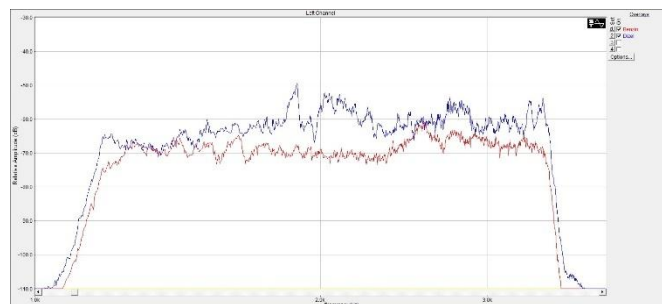


**Fig. 15** Sound spectrum for 1500 rpm mode for the frequency range 1-4 kHz

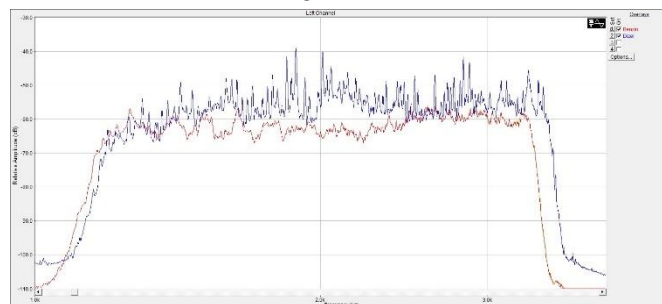


**Fig. 16** Sound spectrum for 2500rpm mode for the frequency range 1-4 kHz

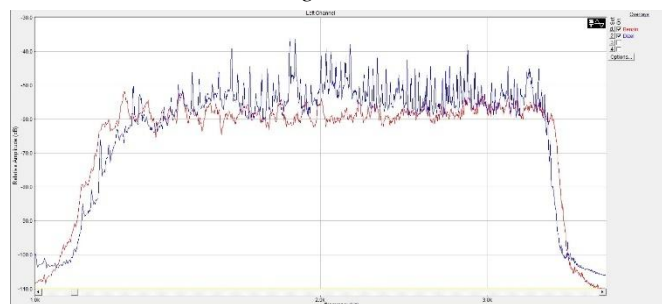


**Fig. 17** Sound spectrum for 3000rpm mode for the frequency range 1-4 kHz

By analyzing the signal spectra for the range 1-4 kHz through all the operating modes of engines, it can be concluded that the signal spectrum generated by the diesel-fueled vehicle in the range of 2-2.2 kHz always has a higher energy level, i.e. signal level, than the gasoline one. When carrying out the perceptual analysis of lower frequencies of the recorded sounds, despite the prominent natural frequency of diesel engines, it was not possible to identify the engine type. The inability to identify a motor type when taking into account

only the part of spectrum that goes below a frequency of 1 kHz, can be attributed to the isofonic characteristics of the human ear, i.e. lower sensitivity of the human ear to low frequencies.

#### 4. CONCLUSION

A comparative frequency analysis of sounds (audio signals) generated by internal combustion engines driven by different propulsion fuels has shown that, when it comes to lower engine revolutions (up to 2500 rpm), it is possible to clearly determine which type of propellant is operating, while for the engine operating mode over 2500 rpm the engine type can be hardly identified on the signal spectrum. However, a detailed analysis of the part of the spectrum in the 1-4 kHz range in all operating modes shows a clear difference, especially in the frequency range 2-2.2 kHz, where the diesel-fueled engine always has a higher signal level.

The inability to identify the engine type when taking into account only the part of spectrum that goes below a frequency of 1 kHz, despite the prominent natural frequency of diesel engines and numerous listenings, can be attributed to the limitation of human hearing sense.

#### 5. FUTURE WORK

Further elaboration of the topic of acoustic identification of engine types depending on the propellant fuel involves an even more detailed analysis of the audio signal spectrum, and further more, a comparison of a larger number of vehicles. The next step would be to measure the engine with 2 valves per cylinder, as it is expected to have a less smooth engine operation than the measurement of the motor of a larger displacement, as well as the measurement of the sound signals generated by engines under real load. In addition to the aforementioned plans, there are plans of the measurements based on engine mount types, which can be carried out in many ways. The continuation of the research implies the inclusion of other parameters, i.e. features, in order to enable autonomous engine recognition by artificial intelligence at a later stage.

#### REFERENCES

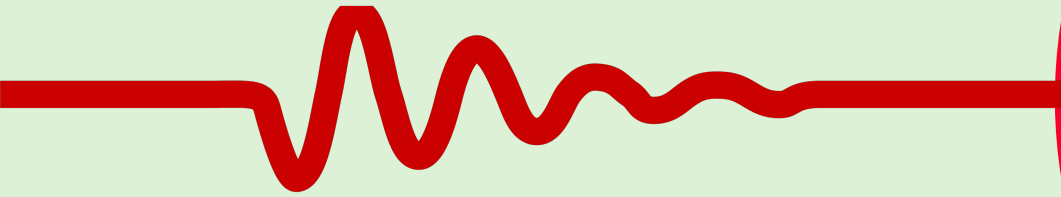
[1] G.P. Chossière, R.Malina, F. Allroggen, S. D. Eastham, R.L. Speth, S.R.H. Barrett, "Country- and manufacturer-level attribution of air quality impacts due to excess NO<sub>x</sub> emissions from diesel passenger vehicles

in Europe", *Atmospheric Environment*, vol. 189, pp. 89-97, September 2018.

- [2] P.M. Diéguez, J.C. Urroz, D. Sáinz, J. Machin, M. Arana, L.M. Gandía, "Characterization of combustion anomalies in a hydrogen-fueled 1.4 L commercial spark-ignition engine by means of in-cylinder pressure, block-engine vibration, and acoustic measurements", *Energy Conversion and Management*, vol. 172, pp. 67-80, September 2018.
- [3] S. Ji, X. Lan, J. Lian, H. Wang, M.Li, Y. Cheng, W. Yin, "Combustion parameter estimation for ICE from surface vibration using frequency spectrum analysis", *Measurement*, vol. 128, pp. 485-494, November 2018.
- [4] N. Dayong, S. Changle, G. Yongjun, Z. Zengmeng, H. Jiaoyi, "Extraction of fault component from abnormal sound in diesel engines using acoustic signals", *Mechanical Systems and Signal Processing*, vol. 75, pp. 544-555, June 2016.
- [5] O. Bondarenko, T. Fukuda, "Potential of acoustic emission in unsupervised monitoring of gas-fuelled engines", *IFAC-PapersOnLine*, vol. 49, no. 23, pp. 329-334, 2016.
- [6] S. Delvecchio, P. Bonfiglio, F.Pompoli, "Vibro-acoustic condition monitoring of internal combustion engines: A critical review of existing techniques", *Mechanical Systems and Signal Processing*, vol. 99, pp. 661-683, January 2018.
- [7] D. Siano, M.Viscardi, M.A.Panza, "Automotive materials: An experimental investigation of an engine bay acoustic performances", *Energy Procedia*, vol.101, pp. 598-605, November 2016.
- [8] A. Rynell, G. Efraimsson, M. Chevalier, M. Abom, "Acoustic characteristics of a heavy duty vehicle cooling module", *Applied Acoustics*, vol. 111, pp. 67-76, October 2016.
- [9] <https://www.auto-data.net/en/renault-clio-ii-1.2-i-16v-75hp-10418>, Accessed date: 12 November 2018
- [10] <https://www.auto-data.net/en/opel-corsa-e-3-door-1.3-cdti-ecotec-75hp-start-stop-22259>, Accessed date: 12 November 2018
- [11] S.Raynor, R.H.Haas, "Natural frequencies of multicylinder engines", *International Journal of Mechanical Sciences*, vol. 5, no. 1, pp. 69-75, January-February 1963.

# Building Acoustics

- **Type 2250 and 2270  
have it all!**

- 
- **Complete hand-held building acoustics analyzers**
  - **Complete systems – including airborne and impact sound sources**
  - **Single- or dual-channel measurements**
  - **Sound recording, voice commentary**
  - **Colour touch screen user interface**
  - **Wireless control  
– freedom to move**
  - **Integrated camera**
  - **Provides flexibility,  
ease of use and  
confidence in results**

Brüel & Kjær 





## HEALTH EFFECTS OF INDUSTRIAL NOISE

Jovica Jovanović<sup>1</sup>, Jovana Jovanović

<sup>1</sup> University of Nis, Faculty of Medicine, Serbia, e-mail: jovica.jovanovic@medfak.ni.ac.rs

**Abstract** - High levels of noise were associated with noise-induced hearing loss, which can be a occupational disease. The most investigated non-auditory health endpoints for noise exposure are perceived disturbance and annoyance, cognitive impairment, sleep disturbance, and cardiovascular health disturbances. The preventive measures includes efforts to reduce noise exposure (ideally at the source), educational campaigns in aim to promote both noise-avoiding and noise-reducing behaviours, personal protective means, recreations and adequate nutrition.

### 1. INTRODUCTION

Noise is unwanted sound judged to be unpleasant, loud or disruptive to hearing. From a physics standpoint, noise is indistinguishable from sound, as both are vibrations through a medium, such as air or water. The difference arises when the brain receives and perceives a sound. Noise sources expose millions of people to noise pollution that creates not only annoyance, but also significant health consequences such as elevated incidence of hearing loss and cardiovascular disease. There are a variety of mitigation strategies and controls available to reduce sound levels including source intensity reduction, land-use planning strategies, noise barriers and sound baffles, time of day use regimens, vehicle operational controls and architectural acoustics design measures.

### 2. HEALTH EFFECTS

Health effects were first recognised in occupational settings, such as weaving mills, where high levels of noise were associated with noise-induced hearing loss [1]. Occupational noise is the most frequently studied type of noise exposure. Research focus has broadened to social noise (eg, heard in bars or through personal music players) and environmental noise (eg, noise from road, rail, and air traffic, and industrial construction). These noise exposures have been linked to a range of non-auditory health effects including annoyance, sleep disturbance, cardiovascular disease and impairment of cognitive performance in children. The health effects of noise from entertainment venues and from neighbours are elusive, but nevertheless, cause many complaints to local authorities [2]. Noise is pervasive in urban environments and the availability of quiet places is decreasing [3].

#### 2.1 Noise-induced hearing loss

Noise is the major preventable cause of hearing loss. Noise induced hearing loss can be caused by a one time exposure to an intense impulse sound (such as gunfire), or by steady state

long-term exposure with sound pressure levels higher than  $L_A$  75–85 dB, in industrial settings. The characteristic pathological feature of noise induced hearing loss is the loss of auditory sensory cells in the cochlea. Because these hair cells cannot regenerate in mammals, no remission can occur, prevention of noise-induced hearing loss is the only option to preserve hearing. Hearing loss leading to the inability to understand speech in everyday situations can have a severe social effect. It can also affect cognitive performance and decrease attention to tasks. Accidents and falls are also associated with undiagnosed hearing loss, with excess mortality of 10–20 % in 20 years. Noise induced hearing loss is a public health problem. WHO estimates that 10 % of the world population is exposed to sound pressure levels that could potentially cause noise-induced hearing loss. In about half of these people, auditory damage can be attributed to exposure to intense noise.

Tinnitus, change in sound perception, such as ringing, that cannot be attributed to an external source often follows acute and chronic noise exposure, and persists in a high proportion of affected individuals for extended periods. Tinnitus can affect quality of life in several ways, including through sleep disturbance, depression, or the inability to sustain attention. The fact that hearing loss and tinnitus are reported in combination suggests that both symptoms share common pathophysiological pathways. Despite the introduction of standards for hearing protection, reduction in occupational noise exposure in developed countries, and extensive public health efforts, hearing loss induced by exposure to occupational noise remains a dilemma. Noise-induced hearing is the most common occupational disease in the are exposed to hazardous noise levels at work [4]. Noise induced hearing loss is determined by noise exposure and life course events, all age groups can be affected. Exposure to different types of noise from early childhood might have cumulative effects on hearing impairment in adulthood. Evidence is increasing that early social and biological factors might affect hearing in middle age (eg, a study of patients assessed at age 45 years). Prevalence of hearing loss is highly related to age. How noise and age interact is a major gap in the specialty's knowledge. Data suggest that pathological but sublethal changes from early noise exposure substantially increase risk of inner ear ageing and related hearing loss. In addition to noise, factors such as alcohol and tobacco use and hyperglycaemia are associated with age-related hearing loss. Smoking may increase the risk of noise-induced hearing loss [5]. The development of otoacoustic emission testing has been an important technological advance in audiological assessment.

Otoacoustic emissions are a release of acoustic energy from the cochlea that can be recorded in the ear canal. Otoacoustic emission testing is used to identify hearing defects in newborn babies and young children. A longitudinal study also suggested that otoacoustic emissions could indicate noise-induced changes in the inner ear undetected by audiometric tests. Otoacoustic emissions might therefore be a superior diagnostic predictor for noise-induced hearing loss, but further longitudinal studies are needed to show whether otoacoustic emission testing can replace standard audiometry or whether the two techniques have complementary roles.

### 3. NON-AUDITORY HEALTH EFFECTS

The most investigated non-auditory health endpoints for noise exposure are perceived disturbance and annoyance, cognitive impairment (mainly in children), sleep disturbance, and cardiovascular health.

#### 3.1 Annoyance

Annoyance is the most prevalent community response in a population exposed to environmental noise. Noise annoyance can result from noise interfering with daily activities, feelings, thoughts, sleep, or rest, and might be accompanied by negative responses, such as anger, displeasure, exhaustion, and by stress-related symptoms. In severe forms, it could be thought to affect wellbeing and health, and because of the high number of people affected, annoyance substantially contributes to the burden of disease from environmental noise. Investigators have proposed standardised questions about residents' long-term annoyance in their home for use in surveys. Additionally, investigators have gathered substantial data for community annoyance in residents exposed to noise in their home, based on which exposure response relationships were derived (eg, for wind turbines). These relations can be used in strategic or health impact assessments for estimating long term annoyance in fairly stable situations. Although the overall community response depends on societal values and is most relevant to the guidance of policy, several personal (eg, age and noise sensitivity) and situational characteristics (eg, dwelling insulation) might affect the individual degree of annoyance.

#### 3.2 Cardiovascular disease

Both short-term laboratory studies of human beings and long-term studies of animals have provided biological mechanisms and plausibility for the theory that long-term exposure to environmental noise affects the cardiovascular system and causes manifest diseases (including hypertension, ischaemic heart diseases, and stroke)[6]. Acute exposure to different kinds of noise is associated with arousals of the autonomic nervous system and endocrine system. Investigators have repeatedly noted that noise exposure increases systolic and diastolic blood pressure, changes heart rate, and causes the release of stress hormones (including catecholamines and glucocorticoids). The general stress model is the rationale behind these reactions. Potential mechanisms are emotional stress reactions due to perceived discomfort (indirect pathway), and non-conscious physiological stress from interactions between the central auditory system and other regions of the CNS (direct pathway). The direct pathway might be the predominant mechanism in sleeping individuals,

even at low noise levels. Chronic exposure can cause an imbalance in an organism's homeostasis (allostatic load), which affects metabolism and the cardiovascular system, with increases in established cardiovascular disease risk factors such as blood pressure, blood lipid concentrations, blood viscosity, and blood glucose concentrations[7]. These changes increase the risk of hypertension, arteriosclerosis, and are related to severe events, such as myocardial infarction and stroke. Studies of occupational and environmental epidemiology have shown a higher prevalence and incidence of cardiovascular diseases and mortality in highly noise exposed groups. The risk estimates for occupational noise at ear damaging intensities tend to be higher than are those for environmental noise (at lower noise levels). Because of different acoustic characteristics for different noise sources (sound level, frequency spectrum, time course, sound level rise time, and psycho acoustic measures) noise levels from different noise sources cannot be merged into one indicator of decibels. Different exposure response curves are needed for different noise sources. Meta analyses were done to quantitatively assess the exposure response link for transportation noise (exposure to road traffic and aircraft noise) and health effects (hypertension and ischaemic heart diseases, including myocardial infarction).

#### 3.3 Cognitive performance

Postulated mechanisms for noise effects on children's cognition include communication difficulties, impaired attention, increased arousal, learned helplessness, frustration, noise annoyance, and consequences of sleep disturbance on performance. Investigators have also suggested psychological stress responses as a mechanism because children are poor at appraising threats from stressors and have less well developed coping strategies than do adults. Areas with high levels of environmental noise are often socially deprived, and children from areas with high social deprivation do worse on tests of cognition than do children not exposed to social deprivation. Therefore, measures of socioeconomic position should be taken into account in the assessment of associations between noise exposure and health and cognition.

Many studies have shown environmental noise exposure has a negative effect on children's learning outcomes and cognitive performance, and that children with chronic aircraft, road traffic, or rail noise exposure at school have poorer reading ability, memory, and performance on national standardised tests than do children who are not exposed to noise at school. Investigators have examined exposure effect links between noise exposure and cognition to identify the exposure level at which noise effects begin. These investigations suggest that there is no threshold for effects and any reduction in noise level at school should improve a child's cognition.

#### 3.4 Sleep disturbance

Sleep disturbance is thought to be the most deleterious non-auditory effect of environmental noise exposure, because undisturbed sleep of a sufficient length is needed for daytime alertness and performance, quality of life, and health. Human beings perceive, evaluate, and react to environmental sounds, even while asleep. Maximum sound pressure levels as low as  $L_{Amax}$  33 dB can induce physiological reactions during sleep including autonomic, motor, and cortical arousals (eg,

tachycardia, body movements, and awakenings). Whether noise will induce arousals depends not only on the number of noise events and their acoustical properties, but also on situational moderators (such as momentary sleep stage) and individual noise susceptibility. Elderly people, children, shift workers, and people with a pre-existing (sleep) disorder are thought of as at-risk groups for noise-induced sleep disturbance. Repeated noise-induced arousals interfere with sleep quality through changes in sleep structure, which include delayed sleep onset and early awakenings, reduced deep (slow-wave) and rapid eye movement sleep, and an increase in time spent awake and in superficial sleep stages. However, these effects are not specific for noise, and generally less severe than those in clinical sleep disorders such as obstructive sleep apnoea. Short term effects of noise induced sleep disturbance include impaired mood, subjectively and objectively increased daytime sleepiness, and impaired cognitive performance. Results of epidemiological studies indicate that nocturnal noise exposure might be more relevant for the creation of long term health outcomes such as cardiovascular disease than is daytime noise exposure, probably because of repeated autonomic arousals that have been shown to habituate to a much lesser degree to noise than other, cortical arousals. In 2009, WHO published the Night Noise Guidelines for Europe, an expert consensus mapping four noise exposure groups to negative health outcomes ranging from no substantial biological effects to increased risk of cardiovascular disease. WHO regards average nocturnal noise levels of less than  $L_{Aeq}$ , outside 55 dB to be an interim goal and 40 dB a long term goal for the prevention of noise induced health effects.

### 3.5 Hospital noise

Although most environmental noise guidelines list hospitals as noise sensitive facilities, studies of external (eg, traffic) noise effects on hospital environments are very rare. However, research on the understanding and prevention of indoor hospital noise effects on patients and staff has been increasing. An extensive meta-analysis of hospital sound levels indicated that hospital noise has increased by about  $L_{Aeq}$  10 dB since the 1960s. Noise levels in hospitals are now typically more than  $L_{Aeq}$  15–20 dB higher than those recommended by WHO. Hospital noise could therefore be an increasing threat to patient rehabilitation and staff performance.

The sound environment in hospitals, especially in intensive care units, can be characterised by irregularly occurring noises from sources such as medical devices (eg, alarms), telephones or pagers, conversations, door sounds, and nursing activities. Such noise worsens patient health outcomes through factors such as increased cardiovascular stress, longer healing times, increases in doses of pain-relief drugs, and increased patient readmission rates. Neonates, long-term patients, and elderly people are thought to be particularly at risk to the effects of noise. Sleep disruption is the most common noise related patient complaint. Researchers of a sleep laboratory study developed arousal probability curves for 14 noises typically encountered in hospitals. The most disturbing noises were intravenous pump alarms and telephone rings, which are intentionally designed to alert staff members. Evidence of negative effects of noise on hospital

staff is increasing, particularly for nurses, with noise-induced stress linked to burnout, diminished wellbeing, and reduced work performance. Substantial proportions of staff report annoyance, irritation, fatigue, and tension headaches, which they assign to the noisy workplace environment. Noise also affects speech intelligibility and could therefore lead to misunderstandings that result in medical errors. Improved acoustics such as sound-absorbing ceilings are relevant factors for staff performance and reduced work strain, and have been associated with a decrease in rates of patients being readmitted to hospital. Reduction of background sound levels and ringtone volume of telephones is recommended to improve patient recovery at night. Researchers noted promise in reductions of rates of false alarms of medical devices and modification of staff behaviour to avoid unnecessary noise.

## CONCLUSIONS

Hearing loss caused by occupational or recreational noise exposure is highly prevalent and constitutes a public health threat needing preventive and therapeutic strategies. Non auditory health effects of environmental noise are manifold, serious and, because of the widespread exposure, very prevalent. These factors stress the need to regulate and reduce environmental noise exposure (ideally at the source) and to enforce exposure limits to mitigate negative health consequences of chronic exposure to environmental noise. Educational campaigns for children and adults can promote both noise-avoiding and noise-reducing behaviours, rewarded by lower amounts of annoyance, improved learning environments for children, improved and thus, mitigate negative health consequences. Efforts to reduce noise exposure will eventually be sleep, lower prevalence of cardiovascular disease, and, in the case of noise exposure in hospitals, improved patient outcomes and shorter hospital stays.

## REFERENCES

- [1] Alimohammadi I, Ahmadi Kanrash F, Abolghasemi J, Afrazandeh H, Rahmani K., Effect of Chronic Noise Exposure on Aggressive Behavior of Automotive Industry Workers. *Int J Occup Environ Med.* 2018; 9(4):170-175
- [2] Pyko A, Lind T, Mitkovskaya N, Ögren M, Östenson CG, Wallas A, Pershagen G, Eriksson C., Transportation noise and incidence of hypertension. *Int J Hyg Environ Health.* 2018; 221(8):1133-1141
- [3] Luo L, Jiang J, Huang SL, He J, Li JM, Analysis on characteristics of hearing loss in occupational noise-exposed workers in automotive manufacturing industry. *Zhonghua Lao Dong Wei Sheng Zhi Ye Bing Za Zhi.* 2018;20;36(6):445-448
- [4] Tran NR, Manchaiah V. Outcomes of Direct-to-Consumer Hearing Devices for People with Hearing Loss: A Review. *J Audiol Otol.* 2018; 22(4):178-188.
- [5] Yu P, Jiao J, Gu G, Chen G, Zhang H, Zhou W, Wu H, Li Y, Zheng Y, Yu S. Relationship between GR7 gene polymorphisms and the susceptibility to noise-induced hearing loss. *Wei Sheng Yan Jiu.* 2018; 47(2): 218-227

- [6] Nserat S, Al-Musa A, Khader YS, Abu Slaih A, Iblan I. Blood Pressure of Jordanian Workers Chronically Exposed to Noise in Industrial Plants. *Int J Occup Environ Med.* 2017; 8(4):217-223
- [7] Yadav MK, Yadav KS, Etiology of Noise-Induced Hearing Loss (NIHL) and its Symptomatic Correlation with Audiometry Observations in Type II Diabetes. *Indian J Otolaryngol Head Neck Surg.* 2018; 70(1):137-144



## CONTROL OF NOISE LEVEL IN THE PRIMARY SCHOOLS IN PODGORICA

Mladenka Vujošević<sup>1</sup>, Ivana Joksimović<sup>2</sup>

<sup>1</sup> Institut of public health Podgorica, Montenegro, mladenka.vujosevic@ijzcg.me

<sup>2</sup> Institut of public health Podgorica, Montenegro

**Abstract** - For understanding speech in the educational process in schools, it is especially important to have a range of 300 to 3000 Hz (voice zone). The noise interferes with a speech engagement by masking, or covering the voice of the teacher with the sound energy of another sound source. That is especially because children spend at least 3 to 6 hours in classes in primary schools. In addition to good hygienic conditions, microclimate conditions and noise levels in classes is important part of good conditions for school children. Primary schools are located in urban area in Podgorica, accept about 6000 children, in six objects, aged second 6 -15 years. This year the Institute of Public Health conducted the measurement of noise levels in classrooms and playgrounds of these educational units. The results show that the noise level has is in the limits of statutory value in classrooms, also in the measured noise level on the playgrounds of primary schools.

### 1. INTRODUCTION

Noise is an important public health issue. It has negative impacts on human health and well-being and is a growing concern [9]. The noise interferes with a speech engagement by masking, or covering the voice of the teacher with the sound energy of another sound source. The stronger the masked sound, the greater the number of words will be incomprehensible to the students. Noise is also a related factor associated with headaches and migraines in school children. The masking effect, noise in proces of learning have affect on mental brain filter [8]. Noise interferes with voice communication or voice teachers covering acoustic energy of another audio source. What is a masking sound stronger, the greater the number of words students to be incomprehensible. Traffic noise around schools reduces the student 'ability to read, short and long term memory, often causes headaches and migraine in schoolchildren[3].

The main objective of this paper is to determine and monitor the noise levels in classrooms in primary schools, protect children health and improvement of residence conditions. Primary schools are located in Podgorica, covered by measurement accept about 6000 children, in six objects, aged second 6 -15 years. In the framework of the public health control primary schools in Montenegro, measured the noise in six schools and theirs playgrounds in Podgorica.

### 2. METODOLOGY

During the control of sanitary and hygienic conditions in primary schools, was done and control of noise levels in classrooms and a playgrounds of schools. Measurement was done in six primary schools and playgrounds. Six units are located in residential areas, three in the mixed.

It was measured precision modular analyzer Brüel & Kjaer Model 2250 which meets the prescribed standard of IEC60804. Measurements were done in accordance with standard [4] and the requirements of legislation[7]. Before the measurements was performed calibration, used the wind protector for the outside during the measurements. The minimum duration of measurement interval is 10 minutes. In the classrooms were measured, temperature, humidity, and outside temperature, humidity, air pressure and velocity. Meteorological conditions were a favorable measurement. Determination of the equivalent noise level in the environment- outside of schools, was done according to the prescribed methodology, and results were compared with the Regulations on limit values for environmental noise, the method of determining the noise indicators and acoustic zones and assessment methods adverse effects [1].

The measured noise levels in primary schools is done in empty classrooms, in accordance with the recommendations of standard [4]. We could not compare with the current legislation in Montenegro, because it does not currently exist, so the results for the purposes of scientific research, commented in relation to the current legislation of Serbia [2], where the prescribed limit value of identical noise levels prescribed by law in other countries of the region. Table 1. date limit values for noise indicators indoors under Regulation [2].

**Table 1.** Limit values for noise indicators indoors [2]

	Room purpose	Noise level in dB			
		Day	Night		
1.	Residence rooms (bedroom and living room) in a building with windows closed	35	30		
2.	The public and other buildings, with windows closed:	35	30		
2.1	Health institutions and private practice, and in them:				
	a) hospital room			40	40
	b) Clinics			35	35
	v) the operational block without medical devices and equipment	35	30		
2.2.	Rooms in facilities for children and students, and a bedroom homes, facilities in facilities for children and students home, and bedroom homes for a stay of elderly and pensioners	35	30		
2.3.	Rooms for educational work (classrooms, lecture hall, classrooms, etc.), Movie theaters and reading rooms in libraries	40	40		
2.4.	Theater and concert hall	30	30		
2.5.	Hotel rooms	35	30		

### 3.RESULTS

Analising obtained value of equivalent noise level, which were measured in primary schools in Podgorica, we are trying to demonstrate the real case: does equivalent noise level exceed the law limitation for noise in environment, if it exceeds, we will try to answer the question what causes that. All measurements were done in day interval of measurements, during the regular activities in schools because the purpose was to find out the real state on site.

In Table 2. are shown the results of measures of equivalent noise level  $L_{eq}$  in duration of 10 minutes in accordance with the guidelines MEST EN ISO 1996-1,1996-2, in primary schools during 2018., in six classes and playgrounds of primary schools.

As shown in Table 2. the equivalent noise level measured in all classrooms no exceed the regulations limits for rooms in facilities for children in accordance with limit by Guidelines [2]. The measured values were from 35.5 dB to 39.4 dB below the provided by law limit of 40 dB.

Law predicted limits for noise levels from environment, were exceed only for one playground of school „Vuk Karadžić“. This value is the result of intensive road traffic near the school. Other values are the result of the position of the schools located in a residential zone. Facilities in the residential zone are far from the local road, with large yards where there is only the influence of the usual activities in residential zones.

**Table 2.** The results of measures taken in primary schools in Podgorica in 2018.

Name of schools	Class $L_{Aeq}$ [dB]	Allowed *	Outside of school $L_{Aeq}$ [dB]	Allowed
“Vuk Karadžić”	39.4	40	58.3	55
“Oktoih”	38.1	40	49.9	55
“Vlado Milić”	35.5	40	48.4	55
“Pavle Rovinski”	37.1	40	50.3	55
“Marko Miljanov”	37.9	40	48.6	55
“Branko Božovic”	35.6	40	43.6	55
“Sjutjeska”	38.8	40	50.5	60

### 4.CONCLUSION

The results of measurements of noise levels in classrooms in primary schools in Podgorica show that levels do not exceed the legally defined noise levels. The results of measurements of noise levels on playgrounds of primary schools show that levels do not exceed the legally defined noise levels in the environment except in one school. These results indicates that children who reside in primary schools are not exposed to increased level of noise from the environment, conditions are in accordance with the recommendations[5] and no negative impact on their activities in classes, growth and development. These indicates that children staying in schools not exposed to an increased level of noise from the environment and that there is no negative impact on their growth and development, dont exist negative impact of high level of noise.

### REFERENCES

- [1] Low on Environmental Noise Protection (Off. Gazette of Montenegro no. 28/2011).
- [2] Rulebook on limit values for environmental noise, the method of determining the noise indicators and acoustic zones and methods of assessment of harmful effects ("Off. Gazette of Montenegro", no. 60/11)
- [3] Regulation on noise indicators , limit values, methods for assessing indicators of noise , disturbance and adverse effects of environmental noise ( "Off. Gazette of the RS ", no . 75/2010 ).
- [4] World Health Organization. “Guidelines for community noise”, WHO, Geneva, 2018.
- [5] World Health Organization, Regional Office for Europe and JRC European Commission., “Burden of disease from environmental noise”. Quantification of healthy life years lost in Europe. WHO, Copenhagen, 2011.
- [6] J.Jorga, Hygiene with medical ecology, Faculty of Medicine, Belgrade, 2014, p.68-69.
- [7] MEST EN ISO 1996-1(2003), MEST EN 1996-2 (2007)
- [8] G. Belojevic, Hygiene, University of Montenegro, Podgorica, 2013
- [9] World Health Organization, Regional Office for Europe, “Environmental Noise Guidelines for the European Region,WHO, Copenhagen, 2018



## STRATEGIC NOISE MAPPING COMBINED WITH DEDICATED LONG AND SHORT TERM NOISE MONITORING. EXPERIENCE, OUTPUT

Boris Mihaylov<sup>1</sup>

<sup>1</sup> SPECTRI LTD, Bulgaria, [boris@spectri.net](mailto:boris@spectri.net)

**Abstract** - Based on EU Noise Directive (END – Directive 2002/49/EC) since 2005 started an intensive noise mapping process in EU member states. Some of the countries had a significant tradition in creating noise maps in the past. The END set a new path, and aimed a harmonized global strategic approach to reduce the increasing environmental noise from major sources (causing heavy health impact to EU population).

The author has a broad experience in last more than 9 years – creating noise maps and strategic noise plans, mainly in Bulgaria (both first, and second round). In the recent paper is presented a short overview of obtained experience and related practical conclusions.

The final aim is to determine exact dedicated action plans - based on the strategic noise management (restriction and reduction of the environmental noise impact), and applying set of measures and acoustical planning in short, middle and long terms.

The need of a publically open and accessible tool (as a result of EU Noise Directive (END – Directive 2002/49/EC) lead to implementing of stationary on-line cloud based monitoring systems – such as WEBNOISE.eu, or advanced Sentinel. It is with a major importance the opportunity given in such a web based open platform to the public – presenting the citizens a real, not adjusted actual information re. environmental protection status in largest agglomerations. Also having an enhanced system with opportunity to monitor further environmental parameters would give the option of dedicated environmental action plans.

Given overview of main components, features and conclusions from using the solution.

### 1. INTRODUCTION

The END defines EU Member States obligations towards overall strategic approach on Environmental Noise Protection.

The aim of END is “to determine the exposure to environmental noise, through noise mapping, by methods of assessment common to the Member States, and to ensure that information on environmental noise and its effects is made available to the public, and to adopt action plans based upon noise mapping results, with a view to preventing and reducing environmental noise where necessary and particularly where exposure levels can induce harmful effects on human health,

and to preserving environmental noise quality where it is good.

Europe is acting to determine the exposure to environmental noise through strategic noise mapping and elaborate action plans to reduce noise pollution. Since June 2007, EU countries are obliged to produce strategic noise maps for all major roads, railways, airports and agglomerations, on a 5-year basis. These noise maps are used by national competent authorities to identify priorities for action planning and by the European Commission to globally assess noise exposure across the EU. This information also serves to inform the general public about the levels of noise to which they are exposed, and about actions undertaken to reduce noise pollution to a level not harmful to public health and the environment. The action plans shall be aligned with other environmental actions too.

An interesting quote from the official World Health Organization paper “Burden of disease from environmental noise”

DALYs (disability-adjusted life-years) lost from environmental noise are 61 000 years for ischemic heart disease, 45 000 years for cognitive impairment of children, 903 000 years for sleep disturbance, 22 000 years for tinnitus and 654 000 years for annoyance in the European Union Member States and other western European countries. These results indicate that at least one million healthy life years are lost every year from traffic related noise in the western part of Europe.

The last more than **10 years** the author of recent paper, through company SPECTRI Ltd. – Bulgaria successfully finalized directly and indirectly 8 (eight) SNM (Strategic Noise Maps), and 10 (ten) AP (Action Plans) – see Fig. 1. Thus we collected vast experience not only re. the process of END noise mapping, but as well re. the ongoing process of sustainable follow up, and expected publicly available strategic approach for reducing the environment noise impact, combined with dedicated protection of quiet zones in the agglomerations.

### 2. METHODOLOGY, EXPERIENCE

Until 2022 shall be used the recommended by END harmonized assessment methods (see Appendix II - 2.2., recommended methods). From 2022 is mandatory to generate next stage SNM via the defined by CNOSSOS-EU New Noise Assessment Methods. Based on his experience

SPECTRI Ltd. can recommend and advise the total project's algorithm, shown in Fig. 1.

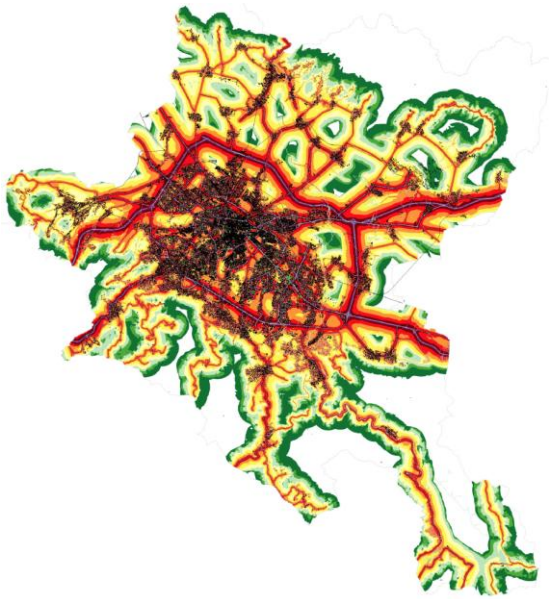


**Fig. 1.** SNM from SPECTRI extract from Sofia city, 2<sup>nd</sup> round (2018)

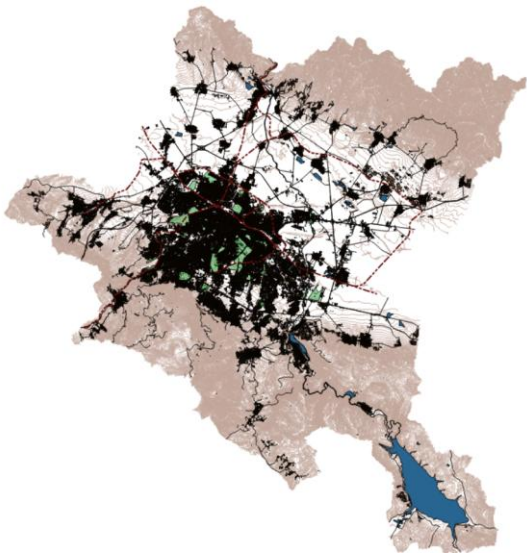


**Fig 2** GIS model overview of Sofia city, 2018. example of dedicated gis model - Sofia city

### 2.1. SNM (Strategic Noise Maps):

The quality of SNM is defined by several main requisites:

- quality of input GIS model, and its subsequent dedicated adaptation – see Fig. 2;
- data for main sources (own collection required)
- verification procedure (procedure needed)
- Used toolkits from EC Good Practice Guide (EC expert noise group paper – WG-AEN)
- Reverse engineering based, both on dedicated attended, and unattended noise measurement
- Using real traffic data for air traffic noise – made possible via “EMS Brüel&Kjær Noise Desk” – see Fig. 3.
- Good quality model for rail traffic – see Fig. 4.

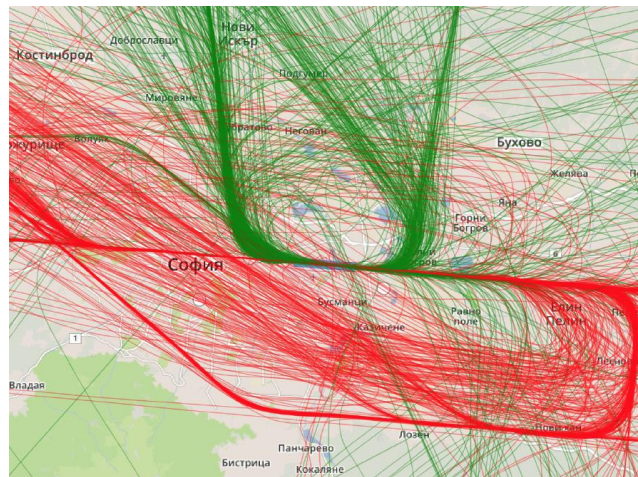


**Fig. 3.** Realized airport track usage Airport Sofia. Example of real adopted flight tracks – from Sofia airport monitoring system

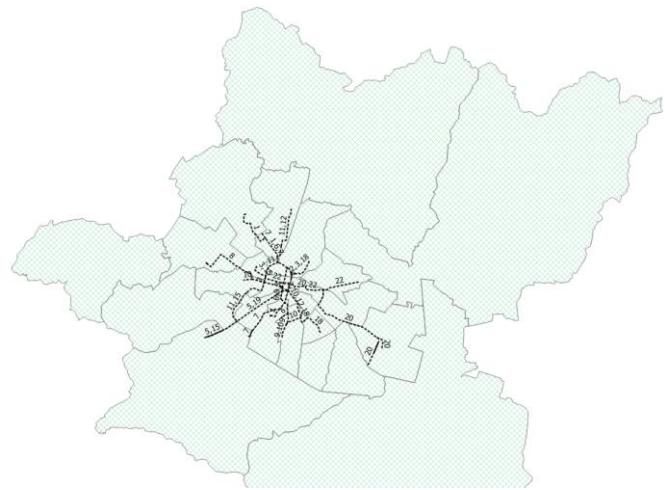


**Fig. 4.** Tram lines model, Sofia city, 2018. Example of trams model - Sofia city:

The model used for strategic noise mapping (by the author – powered and property of SPECTRI Ltd. is shown in Fig. 5.

Special attention shall be taken re. methodology of using existing, or organizing new measurements and/or monitoring of noise. An ISO1996-2:2017 measurement and/or monitoring results cannot be implemented in SNM process directly, without careful consideration and undertaken corrections.

From author experience a proper unattended measurement shall be a valid one, made by ISO17020/17025 accredited body, with EA traceability.

Also implementing results from 12 months, 24 hours dedicated noise monitoring system is the best practice for strategic noise mapping – see Fig. 6.

The attended measurements for agglomerations with traffic fluctuation in the different parts of the year shall be performed at least twice (example – see resort cities have different traffic flows in summer, and winter periods). Proper location of verification measurement points is a must – see Fig. 7-b.

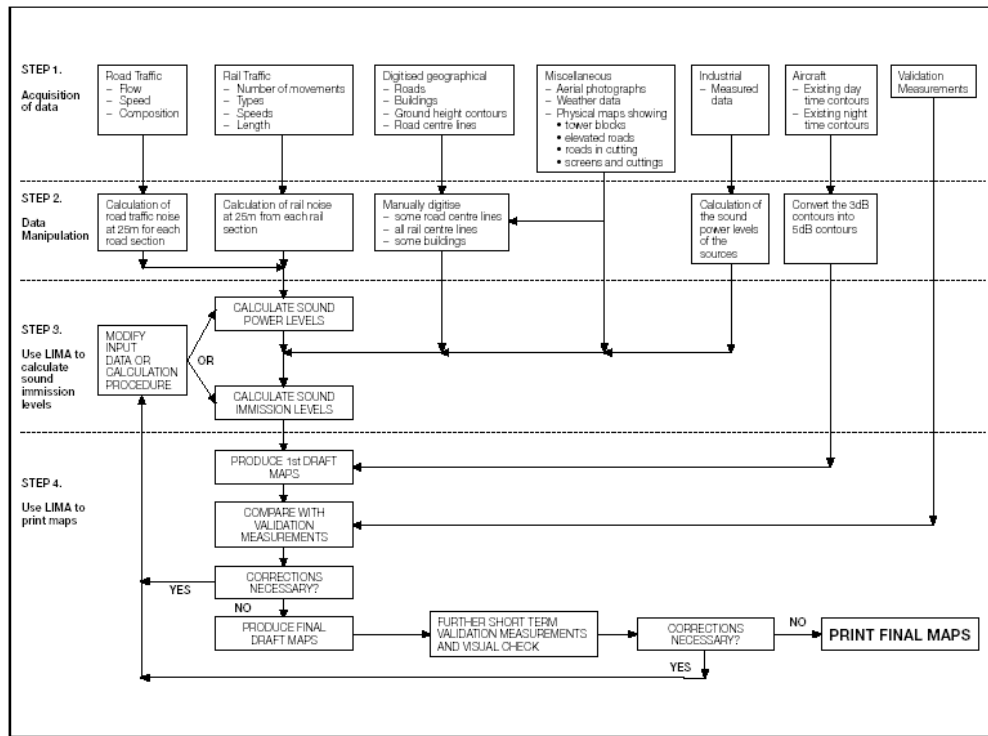


Fig. 5. Main steps re. Strategic noise mapping



Fig.6. Overview of Burgas city WEBNOISE noise monitoring system – web interface (see burgas.webnoise.eu)

After having imported in the model of the attended, and non-attended noise measurements, the acoustics model shall be corrected by the method called “reverse engineering”. At the end a final model verification is mandatory – see Fig. 7-a.

Some of the commercially available calculation tools for SNM are offering the so-called “reverse engineering” (correcting the acoustical model with introduced real noise level results). This tool is recommended to use rarely and with big care.

Choosing attended measurements measuring points, and there exact location is of a crucial importance for the quality of the model. See measurement points overview for Sofia City, 2018 (see Fig. 7-a, b).

SNM performer has to provide, even for verification purposes own argument methodology for obtaining main END indexes – Lden & Lnight.

$$L_{den} = 10 \cdot \log \frac{1}{24} \left( 12 \cdot 10^{\frac{L_{day}}{10}} + 4 \cdot 10^{\frac{L_{evening} + 5}{10}} + 8 \cdot 10^{\frac{L_{night} + 10}{10}} \right) \quad (1)$$

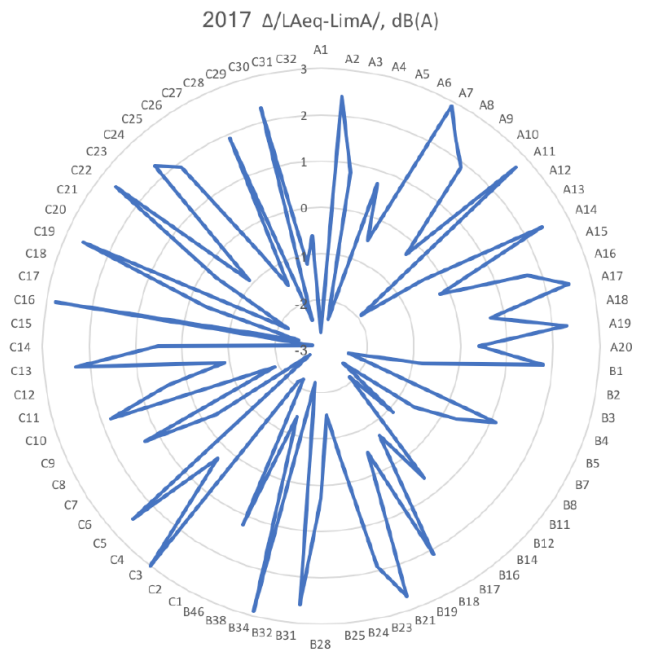


Fig. 7-a Example for final verification results (after applying of reverse engineering) – for Sofia city, 2018

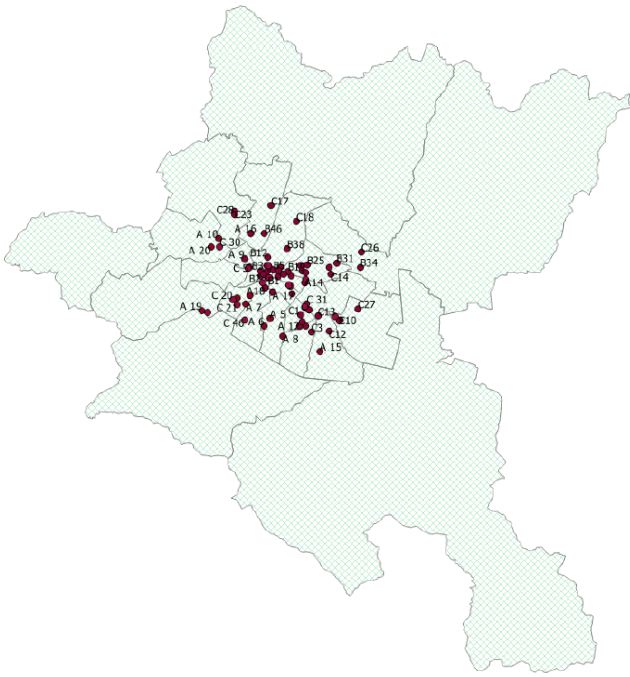


Fig. 7-b Example for verification locations - Sofia city, 2018

2.2. AP (Action Plans):

For all direct and concrete noise reduction measures shall be provided calculation of prognostic effect – using the recommended by END harmonized assessment methods (see Appendix II - 2.2., recommended methods)., and from 2022 the defined by CNOSSOS-EU New Noise Assessment Methods.

Proposed measures shall be accessed with the same noise calculation methods used for the original SNM – see Fig. 8.

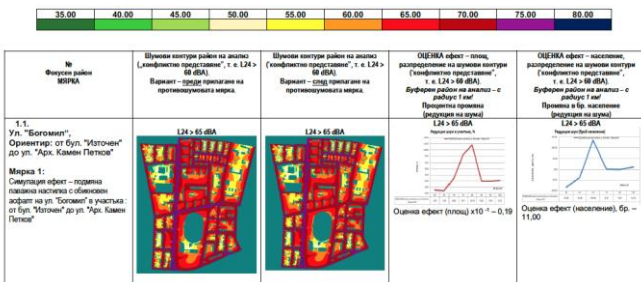


Fig. 8 Real action measure calculation quote

In a final AP document, one shall include variety of measures, i. e.:

- organizational global measures, with overall acoustical impact
- investment environmental projects, with overall acoustical impact
- public campaigns and measures with indirect acoustical impact
- measures on state and even cross border measures - with direct and indirect acoustical impact
- measures with direct acoustical impact (such as barriers, large green zones, traffic improvement, etc.) – see Fig. 8, and Fig. 9.
- alignment with the other environmental measures

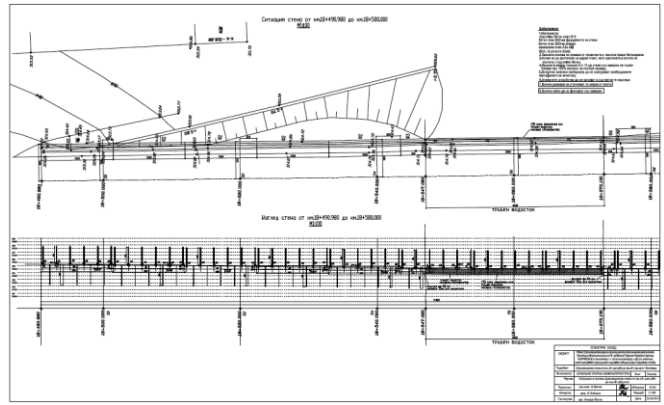


Fig. 9 Acoustical measure – noise barrier, design phase – made possible by SPECTRI Ltd.



Fig. 10 Acoustical measure – noise barrier, design phase, real set-up – made possible by SPECTRI Ltd.

2.3. Dedicated long and short term noise monitoring

It is of an comparable value the possibility to implement in a strategic noise mapping project of 12 months results of permanent noise monitoring. Having such a system, even open to public, would secure the trustworthy of the used data, and directly correspond to EN Directive spirit of open communication with the society.

Good example is a system like WEBNOISE.EU (see Fig. 11) – a customized system, made with the following main visualization features: Main screen Google maps API v3.0 based window with applied measuring locations, on a real map. Each points is with attached LAeq actual reading, displayed in respective color scheme. Secondary screen with LAeq measurement readings – for a defined time interval. The interval can be chosen either by pressing a button (hour, day, week, month), or via customized plots selecting interval. Self-refreshing plot. Each 5 min. passed interval is respectively added on the overall result. Additionally for each day period, there is an overview for the integral noise. Available on request service sections with possibility to download user defined reports.

The use of a dedicated Data Logger (communication, calculations, software, outputs) is a must: Supporting of encrypted protocols for data exchange between the server, and the client. Supports of protocols for communication between the noise measurement terminals and the logger. Subsequent mathematical processing of acquired data.

Algorithm for data flow maintenance. When a communication connection is down, the data are stored in the internal data logger memory – for later on restoring in the web server data base.



Fig. 11 SPECTRI WEBNOISE.eu portal

## 2.4. Correlation with other environmental parameters

Correlation mostly with dust particles (PM10), building vibrations, etc.

Need of on-line monitoring tool for simultaneous collection of different environmental data.

Example is shown in Fig. 12.

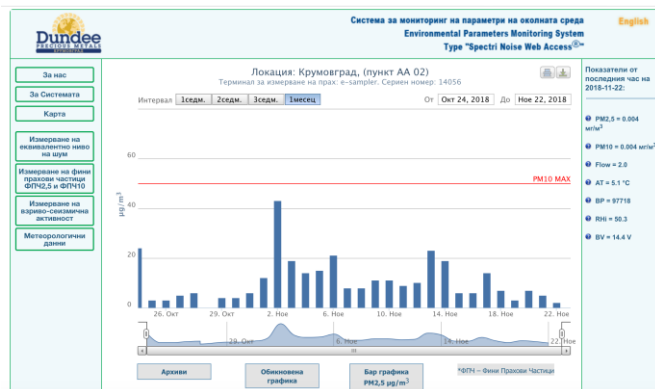


Fig. 12 SPECTRI WEBNOISE.eu portal– dust monitoring

It is of a comparable value the possibility to implement in a strategic noise mapping project of 12 months results of permanent noise monitoring. Having such a system, even open to public, would secure the trustworthiness of the used data, and directly correspond to EN Directive spirit of open communication with the society.

## CONCLUSION

Main practical advises, and conclusions from SPECTRI experience and Non Governmental involvement in Environmental Prediction process (through Bulgarian Acoustical Association) - experience from last 2 rounds of strategic noise mapping, and corresponding action planning:

3.1. A need of a publically open and accessible tool (as a result of EU Noise Directive (END – Directive 2002/49/EC) - on-line cloud based monitoring systems (such as WEBNOISE.eu, or advanced Sentinel). It is with a major importance the opportunity given in such a web based open platform to the public – presenting the citizens a real, not adjusted actual information re. environmental protection status in largest agglomerations. Also having an enhanced system with opportunity to monitor further environmental

parameters would give the option of dedicated environmental action plans.

3.2. Usage of measurement and monitoring data (available ones), and further arrangement of own measurements and traffic counts. Needed own argued methodology for introducing measurement data into SNM process, and for verification procedure.

3.3. Producing reliable, accurate and trustful tool for professional strategic noise impact reduction and noise protection – the END defined Action Plans, organized and created with care – from experience, and accredited team.

3.4. Collection of maximum possibly correct input data is achieved either through available sources, or collecting via different institutions' collaboration, or using own collective procedure and argued methodology.

3.5. Important practical conclusion is that the SNM and AP are to be created with same methodology, and possibly by the same performer.

3.6. Action planning with respect of correlations of other environmental parameters (dust particles, building vibrations, etc.).

## REFERENCES

- [1] European Noise Directive (END) 2002/49/EC;
- [2] EC Good practice guide for strategic noise mapping (EC expert noise group paper – WG-AEN);
- [3] Commission Directive (EU) 2015/996 of 19 May 2015 establishing common noise assessment methods according to Directive 2002/49/EC of the European Parliament and of the Council
- [4] Environmental dedicated monitoring, available for the public – real example, SPECTRI Ltd.: [http://krumovgrad.webnoise.eu/index\\_en.php](http://krumovgrad.webnoise.eu/index_en.php)
- [5] Environmental advanced noise monitoring, EMS Brüel&Kjær: <https://emsbk.com/sentinel/>
- [6] Environmental aircraft noise monitoring, and flights tracking, EMS Brüel&Kjær: <https://emsbk.com/noisedesk/>
- [7] ISO 1996-2: 2017 Acoustics – Description, measurement and assessment of environmental noise – Part 2: Determination of sound pressure levels
- [8] World Health Organization paper “Burden of disease from environmental noise”
- [9] Strategic Noise Map of Sofia City (project by SPECTRI Ltd.), 2009, 2018 – see city’s official web page.
- [10] Action Plan on Environmental Noise of Sofia City (project by SPECTRI Ltd.), 2010, 2018 – see city’s official web page.
- [11] Strategic Noise Map of Plovdiv City (project by SPECTRI Ltd.), 2009, 2017 – see city’s official web page.
- [12] Action Plan on Environmental Noise of Plovdiv City (project by SPECTRI Ltd.), 2010, 2018 – see city’s official web page.

- [13] Strategic Noise Map of Burgas City (project by SPECTRI Ltd.), 2012, **2017** – see city’s official web page.
- [14] Action Plan on Environmental Noise of Burgas City (project by SPECTRI Ltd.), 2013, **2018** – see city’s official web page.
- [15] Strategic Noise Map of Rousse City (project by SPECTRI Ltd.), 2012, **2017** – see city’s official web page.
- [16] Action Plan on Environmental Noise of Rousse City (project by SPECTRI Ltd.), 2013, **2017** – see city’s official web page.
- [17] Strategic Noise Map of Pleven City (project by SPECTRI Ltd.), 2012, **2017** – see city’s official web page.
- [18] Action Plan on Environmental Noise of Pleven City (project by SPECTRI Ltd.), 2013, **2018** – see city’s official web page.
- [19] Strategic Noise Map of Major Roads (project by SPECTRI Ltd.), 2009-2011, **2018** – see official Roads’ Agency web page.
- [20] Action Plan on Environmental Noise of Major Roads (project by SPECTRI Ltd.), 2010-2012 – see Roads’ Agency official web page.
- [21] Guidelines for the use of traffic models for noise mapping and noise action planning, EU-FP6 project.



## REALIZATION OF THE LOW-COST NOISE MEASUREMENT MONITORING STATION USING MEMS MICROPHONE TECHNOLOGY AND MICRO PC

Marko Ličanin<sup>1</sup>, Momir Prašćević<sup>1</sup>, Darko Mihajlov<sup>1</sup>

<sup>1</sup>University of Nis, Faculty of Occupational Safety, Serbia, marko.licanin@znrfak.ni.ac.rs

**Abstract** - Noise monitoring is a powerful tool for understanding its impact on the environment and human health. With an increasing density of the population and traffic load in cities, noise is becoming one of the most prominent problem influencing daily activities of the people. Since this problem is recognized in the past, many methods of its evaluation has been developed. Those methods in most occasions includes the use of the sophisticated equipment of a high cost, which as an result enabled only certain number of scientist or groups to be eligible for this task. Even with the proper equipment, the long-term noise monitoring, as one of the most precise method, reduces the number of possible monitoring locations, due to its high cost. This results in low efficiency of the monitoring process. In recent years, small factor PC hardware has advanced significantly, which opened a door to a new types of the low cost devices, that can although in lower sampling precision, perform certain sensing tasks. This paper addresses the possibility of the use of small portable system, that can act as an small noise monitoring station. The process of composing the hardware and software is explained as well as the initial results of long-term planned project.

### 1. INTRODUCTION

In Europe, long-term environmental noise monitoring is specified by the acting laws and regulations [1]. The output data of the noise monitoring is represented as an annual noise indicators, which are used for prediction and evaluation of the noise affected areas as well as for development of the noise control solutions. One of the assessment method is the creation of the strategic noise maps that intuitively explains the propagation of the noise in urban areas [2]. Those maps are based on the results gathered through the process of noise monitoring, which in most cases require expensive equipment. If long-term monitoring is used (measurement interval is one year) this equipment can be utilized in only one location which results in measurement inefficiency [3]. Another downside of the use of this equipment is the limitation of access to many people due to the high costs.

Development of the new hardware platforms, small factor sensors, and IoT (Internet of Things) technologies, significantly changed the accessibility of large number of people to hi-tech devices of the considerable processing power. This enables the students and enthusiasts to develop complicated hardware solutions, that was available only to the high educated engineers and industry in the past. One of the

fastest advancing technologies are Smart Homes and Smart Cities [4] with a very strong community, examples and solutions available on the internet.

The low-cost hardware platforms are now capable of processing huge number of data very fast, which enables them to perform a real-time operations as a data acquisition units. This can be exploited for the noise monitoring, as one of the requirement for the determination of the annual noise indicators is continuously tracking of the noise level data throughout the year. This has been a topic of several recent papers, where authors exploits the ability of individually developed systems to acts as small monitoring stations [5], [6]. Since there are no regulations on the topic of using such systems for noise monitoring, researchers are developing solutions according to the individual needs, goals of research and available hardware and sensor equipment. Hardware can be based on microcontrollers, small factor PCs or Field Programmable Arrays (FPGAs). Microphones as a sound pressure sensing units can be used in analog or digital representation, and structured as single or in an array distribution.

This paper describes the setup process of the small monitoring station based on Micro-Electro-Mechanical-Sensor (MEMS) microphone technology and Raspberry Pi as an micro PC acquisition unit. An overview of the technology is given, as well as a setup process and initial results.

### 2. MEMS MICROPHONE AND MICRO PC

There are two types of the microphones realized in MEMS technology, an digital and analog microphone. Digital microphones are then divided into PDM (Pulse Density Modulation) and I2S category, which describes the format of its digital data output. For the purpose of the portable monitoring station, an I2S digital microphone has been used by the manufacturer Adafruit [7].

The I2S protocol is an multiplexed serial data interface that enables audio signal data from a stereo pair of microphones to be sent by a single data line. In the past, this interface has been extensively used in transfer the serial data between a CD and read/write electronic hardware. Nowadays it is very useful when combined to the MEMS technology for getting the data from the microphones in very convenient way. This protocol contains several data and control lines:

- CKL (Base Clock) – Main rectangular clocking signal with a duty cycle at the frequency 64 times higher than

the sampling frequency of the audio data. This signal is used to drive the sigma-delta AD converter that oversamples data from the analog part of the MEMS microphone (See figure 1);

- WS (word select) – Control rectangular clocking signal with the frequency of duty cycle the same as the sampling frequency of the audio data. Typically it is 22.050 Hz, 24.000 Hz, 44.100 Hz, or 48.000 Hz;
- SELECT – left or right channels audio data selection;
- VDD/GND – Voltage and ground connection line;
- DATA – stereo data line as an output from the MEMS microphone, that goes to the acquisition hardware.

Block diagram of the digital MEMS microphone is shown in figure 1.

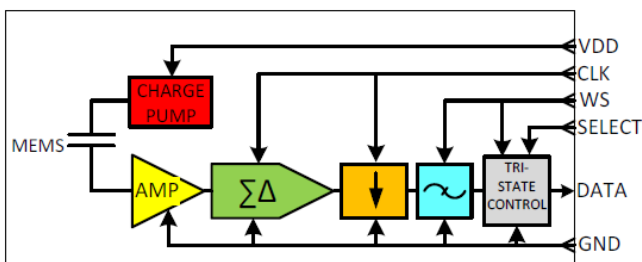


**Fig. 1** Block diagram of the digital MEMS microphone

Sound pressure is converted at the analog part of the MEMS, amplified, then oversampled to digital in sigma-delta AD convertor (green block) in the decimator stage (orange block) the frequency of the signal is reduced to the  $F_s$  (audio data sampling frequency) and filter via low-pass filter (blue block). At the end, there is a three-state-control block (gray) which compare data with a WS. When a WS is high (Logical 1) a microphone which has SELECT connected to VDD, pass the 24 bit (3 bytes) sample word to the DATA line, followed by 8 bit (1 byte) high impedance state (circuit recovery). After 32 bits, WS changes to low (logical 0), and microphone that have SELECT connected to the GND pass the 3 bytes of sample data, followed by 1 byte of the high impedance pause. The process is then repeated, and as a results on data lines there is a time division multiplex of left-right stereo audio data.

Raspberry pi 3B+ (Rpi) is the latest version of small factor very powerful micro PC that runs on a Raspbian Linux (Debian distribution based). The hardware has following specification [8], [9]:

- Processor: Broadcom Cortex - A53 64-bit SoC @ 1.4 GHz (figure 2 – Blue rectangle).
- Memory: 1 GB DDR2 SDRAM
- Connectivity: 2.4 GHz and 5 GHz 802.11.b/g/n/ac wireless LAN, Bluetooth 4.2, BLE (figure 2 – green rectangle).; Gigabit Ethernet (figure 2 – yellow rectangle).; 4x USB 2.0 (figure 2 – red rectangle).; 40-pin GPIO connection (figure 2 – orange rectangle).
- SD card: Micro SD card for loading the operation system.

Programming of the RPi is done using Python programming language, very suitable for engineering different solutions and

signal processing. Using Python with its large community and libraries, programming the GPIO pins can be done easily and communication between outside world (sensors, actuators, machines etc.) established. The overview of the hardware board is presented in figure 2.

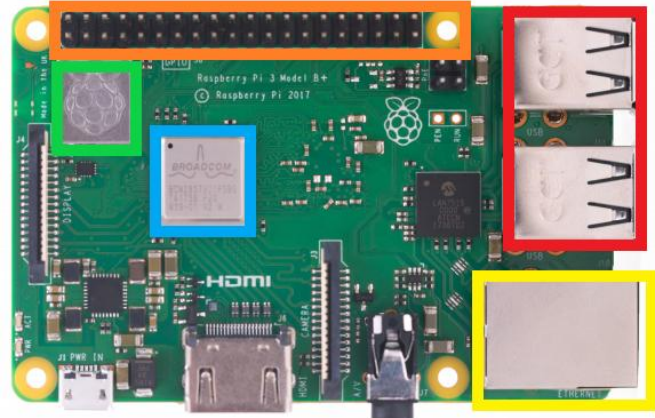


**Fig. 2** Top view of the Raspberry Pi 3B+

### 3. SYSTEM SETUP

The complete solution is based on the hardware setup, that is, physical connection between Rpi and MEMS microphone, and software setup that contains the logic. Devices are connected through wiring at the specific GPIO pins, while software solution is composed of I2S software implemented protocol, server side and client side of the transmission.

#### 3.1 Hardware solution

Connection between Rpi and MEMS microphone has been done using the development bread-board. Wiring has been made as shown in figure 3.

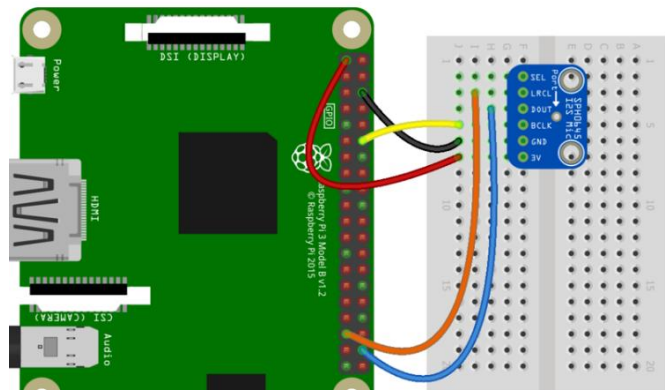


**Fig. 3** Wiring of the Raspberry Pi 3B+ and MEMS microphone

The corresponding pins connections are as following:

- MEMS VDD 3 V - RPi VDD 3.3 V
- MEMS GND - RPi GND
- MEMS LRCL (SELECT) - RPi VDD 3.3 V (this is used for channel selection.)
- MEMS BCLK (CKL) – RPi BCM 18 (GPIO pin 12)
- MEMS SEL (WS) – RPi BCM 19 (GPIO pin 35)
- MEMS DOUT (DATA) – Rpi BCM 20 (GPIO pin 38)

For the purpose of this setup, both left and right MEMS microphones are connected. This means that SELECT is

connected to the VDD for left channel MEMS, while for the right channel, SELECT is connected to the GND. For the purpose of simplification, figure 3 shows only one MEMS microphone. In software realization, data has been separated to a left and right channel, but initially only one channel used.

### 3.2 Software solution

Connection to the raspberry pi is done via SSH (simple command based terminal – Secure Shell) terminal and VNC (Virtual Network Computing). This has been performed using standard PC to connect through mentioned terminals via commands (SSH) or as visual desktop (VNC). The connection itself is based on IP protocol, which enables Raspberry Pi to be controlled and programed remotely. This is very important for the realization of monitoring station, as bugs and problems, as well as reconfiguration can be done from afar. Once this connection is established, PC can send commands, view RPi desktop and control installed application.

To program the device, certain Python packages has to be installed and libraries for I2S included. There are two separate pieces software written in Python. One is being run at the PC, and handles the received data. It is intended to have more advance graphical interfaces and representation of data, to store and in more complex way perform complex data manipulation. Even that RPi is being very powerful, average PC (desktop or laptop) is still much more complex device capable of handling more complex tasks, especially graphics of the software user interfaces.

Second piece of software is realized on the Raspberry Pi itself, again using Python. I2S libraries has been installed and Linux kernel recompiled to enable the use of the I2S protocol. This is an necessary step, as the hardware inside the RPi needs to produce adequate clocking frequency in order for MEMS microphone to perform correctly. If those clocking signals are not stable, or not in sync, it will create a problem during sampling of the audio data rendering them unusable.

Raspberry Pi has been program to perform a small server task, while python code on the PC side acts as a client application issuing a request for data feed. Once run, Python code will issue the command to listen a request from a client. Within this code, important parameters has been set:

- Sampling frequency (Fs) – As the noise data are not usually observed above 10 KHz, for this purpose, this parameter is set to 22 KHz.
- Chunk size – This parameter describes the amount of data that are taken and processed at the single take. It is related to the buffer size that continuously fills with data from microphone, as a chunk batch, and placed them into frames. This parameter is set to 2200 samples which 6600 bytes of data.
- Format type – Int 24 is a three byte integer containing 24 bits per sample of data, that is very common in recording instrumentation.
- Number of channels – Set to 2 channels (stereo MEMS microphone pair) but for the initial testing, only one channel data has been sent from RPi to PC.

On the client side (PC), two important parameters has been set, and IP address of the RPi (192.168.1.115) and the port

for sending data (22000). Once the server code is run, it will listen the request from the client for connection (status “LISTENING”). At that point, Python code on the PC can be started. This sends the control messages to the server and outputs the status “CONNECTING”. Server performs the “handshake” and returns the status “CONNECTED”, while client acknowledges the same status. At that point data acquisition starts.

At the RPi server side, Chunks of data starts to arrive and are being processed. First, there is a function written that separates data channel, taking only one of them for processing. Data format is converted to floating point 32, and RMS value of the entire chunk calculated. This value is then used into another function to calculate the SPL, which is the averaged sampled data of the Chunk. Result is then sent to the client PC in the form of ASCII message. If chunk size is set to 0.5 s, this mean that there are two samples of the noise per second, which is sufficient enough compared to the resolution that noise monitoring stations provide.

On the PC side, data has been received, and plotted in graphic window for observation. It is important to note that chunk size has to be chosen adequately. If this size is too small (i.e. 50 ms), the changes of data in RPi buffer will be very fast, resulting in buffer overflow (a condition where buffer is not emptied yet, while new data arrives). This will stop the data transfer. If chunk size is very large (i.e. few seconds), the RPi will not be able to process the chunk data, before new arrives, which will have the same effect (buffer overflow).

## 4. RESULTS

The measurement setup has been done according to figure 4. Small anechoic chamber has been used to provide a better measurement conditions. Adafruit MEMS microphone has been attached to RPi in the described configuration, and using loudspeaker, noisy signal reproduced. Signal has been composed of the noisy speech with an several impact noises of an objects hitting the floor and table.



**Fig. 4** Measurement setup inside small size anechoic chamber

Using the developed software solution, data was recorded with RPi and sent to PC using the same wireless network. This was interned to demonstrate the capability of the monitoring station to send data to PC that is at the distance location. The fine tuning of the chunk size has been done iteratively, until buffer overflow was not present, and the data

could be sent safely. In figure 5. The results of the transmission is shown, the high peaks present in the graph corresponds to the waveform file played from the loudspeaker. The Y axis shows the amplitude in energy, while for the correct noise level representation in dB, an additional work on the software side is necessary. It has been realized during the work on this projects, that digital MEMS microphones corresponds to sound pressure differently than the analog electret or condenser microphone. The correspondence is not entirely oriented as mPa/V (micro Pascal per Volt) conversion and it will be a topic for a further research

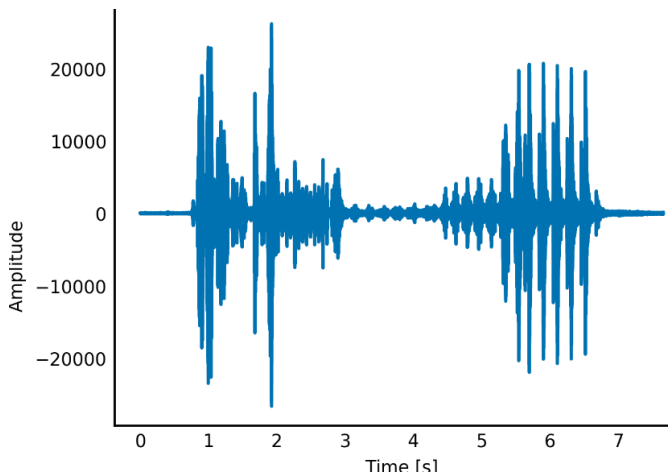


**Fig. 5** Received data on the client side (PC) sent from the server side (RPi)

## CONCLUSION

MEMS technology combined with a small factor PC is a very promising technology. These systems, as powerful as they are, did not existed in the past, and represents the dawn of an new kind of industry. This has been often recently called "Industry 4.0". IoT, Smart Homes and Smart Cities, are becoming attractive fields of study and application of the rising new technologies. This is especially true, as these device are nowadays available to large number of people, even students. Although not precise enough, in comparison to the expensive measurement equipment, in future it is to expected that technology of the low-cost devices will improve significantly, bringing them much closer to the measurement equipment. This paper exploits the use of the MEMS microphone and Raspberry Pi, as an small noise monitoring station. This is intended to be a long term applied science research, where initial conclusion and results are presented. Hardware has been successfully connected, server and client communication developed and first noise transfer protocol

established. Future research includes solving the problem for the correct SPL determination, adding more sensors (such as meteorological data), and creating the multiple nodes that will feed the central system with noise and other data. On the programming side, full development of the application is intended, that will be able to abstract data in different way, store into database and perform noise predictions using machine learning algorithms.

## REFERENCES

- [1] Directive 2002/49/EC of the European Parliament and the Council relating to the assessment and management of environmental noise, Official Journal of the European Communities, L189,45, <http://eur-lex.ropa.eu/legalcontent/EN/TXT/?uri=CELEX:32002L0049>, 2002
- [2] Vos P. and Licitra G.: „Noise maps in the European Union: An overview”, In G. Licitra (Ed.), „Noise mapping in EU: Models and Procedures”, 1st edition., CRC Press, USA, 2012
- [3] Mihajlov D., Prašćević M. 2015. Permanent and Semi-permanent Road Traffic Noise Monitoring in the City of Nis (Serbia), Journal of Low Frequency Noise, Vibration and Active Control 34(3): 251-268.
- [4] C. Asensio, “Acoustic in smart cities”, in Proc. Applied Acoustic, Volume 117, Part B, February 2017, pp. 191-192
- [5] P. Belluci, L. Peruzzi, and G. Zambon, “Life dyna map project: The case study of Rome”, in Proc. Applied Acoustic, Volume 117, Part B, February 2017, pp. 193-206.
- [6] C. Mydlarz, J. Salamon, and J.P. Bello, “The implementation of low-cost urban acoustic monitoring devices”, in Proc. Applied Acoustic, Volume 117, Part B, February 2017, pp. 207-218.
- [7] M. Barela, Getting started with Adafruit circuit playground express : O-Reilli, 1st edition, septembar 2018.
- [8] <https://static.raspberrypi.org/files/product-briefs/Raspberry-Pi-Model-Bplus-Product-Brief.pdf>
- [9] <https://www.raspberrypi.org/products/raspberrypi-3-model-b-plus/>

University of Nis  
Faculty of Occupational Safety

„Politehnica“ University of Timisoara  
Faculty of Mechanical Engineering



26<sup>th</sup> International Conference

**NOISE AND VIBRATION**

Niš, 6 - 7. 12. 2018.

# 3<sup>th</sup> SESSION

# VIBRATION



## CONTROL SIGNAL GENERATION FOR RANDOM VIBRATION TESTS

Karoly Menyhardt<sup>1</sup>, Ramona Nagy<sup>1</sup>, Remus Stefan Maruta<sup>1</sup>

<sup>1</sup> Politehnica University Timisoara, Faculty of Mechanical Engineering  
karoly.menyhardt@upt.ro, ramona.nagy@upt.ro, remus.maruta@upt.ro

**Abstract** - Fatigue tests are used to determine a material's ability to withstand cyclic loading conditions. Cyclic fatigue tests produce repeated loading and unloading in tension, compression, bending, torsion or combinations of these stresses. Unfortunately, real life conditions are unpredictable and thus, unexpected conditions are met. For this reason, often, variable load-frequency control signals must be generated instead of sine waves for control purposes.

Random vibration signal is non-deterministic, as in future behavior cannot be predicted. The randomness of the test is a characteristic of the excitation or input and the inertia of the system. Starting from an imposed acceleration spectral density (ASD) chart a suitable acceleration-time signal must be generated as random vibration control signal.

A solution to this problem is presented throughout the paper, in generating a kurtosis signal from a restrictive frequency domain to a usable time domain signal.

### 1. INTRODUCTION

Ground vehicle transportation encounters a variety of pavements and ground conditions, such as highway, a country road, unpaved road. The vibration spectrum from the road loading is typically of a random noise distribution due to sudden changes in velocity. On top of this, there are harmonic components from the engine and tires.

Products shipped with such loading conditions must survive and not suffer any defects during transit. Fatigue tests are used to determine the product's ability to withstand loading conditions. Real life conditions are unpredictable and thus, unexpected conditions are met. For this reason, often, variable load-frequency control signals must be generated in order to better replicate road irregularities.

Random vibration signal is non-deterministic, as in future behavior cannot be predicted. The randomness of the test is a characteristic of the excitation or input and the inertia of the system. Starting from an imposed acceleration spectral density (ASD) chart, taken from a previous record of the track, a suitable acceleration-time signal must be generated as random vibration control signal [1,2].

A vibration response investigation to determine the resonance frequencies offer essential information about the test specimen - shaker interaction. This investigation can reveal excessive test fixture vibration amplification or coincident resonance between fixture and specimen.

The control algorithm of the random vibration involves a compromise between control accuracy and control loop time [3].

A high control accuracy requires more input data and offers a slower response to dynamic changes in the actual acceleration spectral density. A narrow resolution bandwidth yields a higher control accuracy but a longer control loop time. In order to minimize the deviation between the true and the indicated acceleration spectral density at the specimen, optimization of the mentioned test parameters is required [4].

### 2. DATA ACQUISITION FOR RANDOM VIBRATION TEST

A generic electronic product was presented to us for vibration testing due to high failure occurrence in post-sale/warranty phase.

In order to replicate transportation conditions, an in-depth vibration measurement was conducted on the package during shipment from the fabrication plant to the local warehouse.

Instead of using of AC accelerometer which would have involved a larger setup, we opted for a low weight, low size, autonomous DC accelerometer. Data was logged with an acquisition system based on Arduino as parser and MPU9250 as a Microelectromechanical systems (MEMS) accelerometer (Fig. 1).

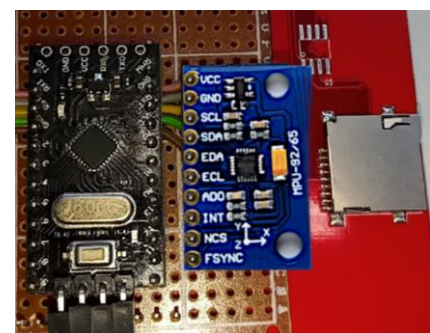
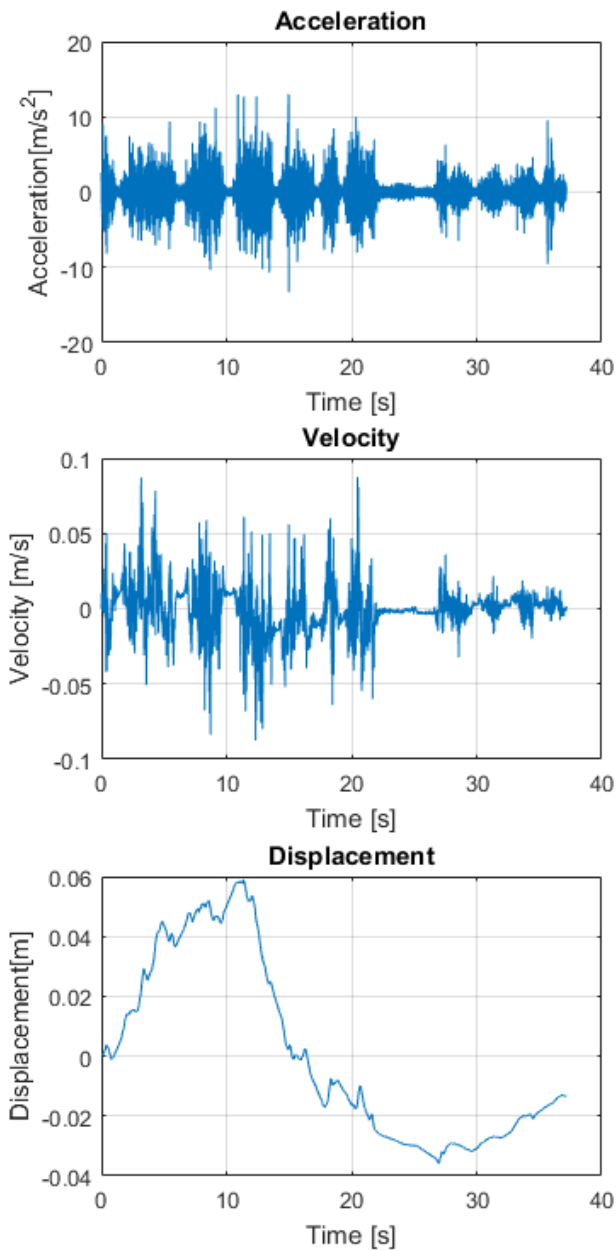


Fig. 1 Arduino Data logger

As the frequencies in road vehicles do not exceed 500Hz, the MPU9250 is able to read accelerations up to 16g at a sampling rate of 8 kHz. This theoretical value in practice is difficult to reach, but a sampling rate of 1 kHz, upper limit for frequencies found on road vehicles, is slow enough for the Arduino to read it from the accelerometer and record it on an SDcard.

Data was logged for over 4 hours, but for the purpose of this article, without breaching the terms of the Non-Disclosure Agreement a fraction of it is shown in Fig 2:



**Fig. 2** Sample measurement of kinematical parameters

Analyzing this data in the time domain (acceleration amplitude plotted against time) there are just a few parameters that quantify the strength of a vibration profile: amplitude, peak-to-peak value, and root mean square (RMS). From these values the acceleration is usually below 1g, having a RMS value of 1.59 m/s<sup>2</sup>. The amplitude of the acceleration can offer some insight into the shock events, but there is no information on the duration or energy involved.

Thus, there is the real need to transform this time domain into frequency. The simplest way to achieve this is through a Fourier transform, and mainly with a Fast Fourier Transform (FFT). A Discrete Fourier Transform needs N<sup>2</sup> operations while a FFT needs only N\*log<sub>2</sub>(N) operations [5].

In Fig3 the FFT of our sample acceleration data is presented:

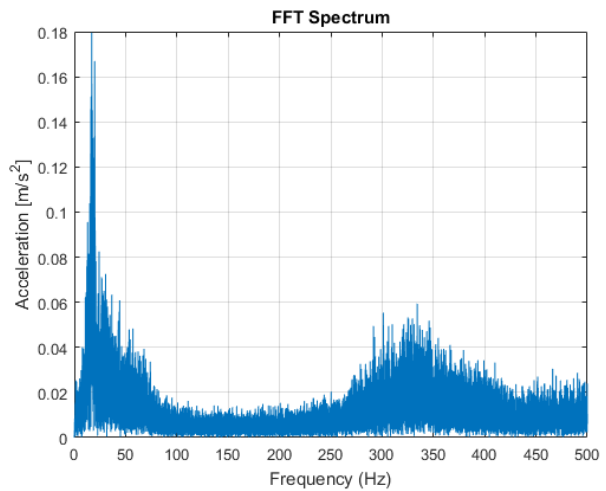


**Fig. 3** FFT of sample data

From the FFT data we can extrapolate the dominant frequencies at 17 Hz and 330 Hz, where there are peaks in the FFT. The use of a FFT vibration analysis can offer clues on what is causing the measured vibration.

FFT is a valuable tool in vibration analysis when there are a finite number of dominant frequency components; but ASD is used to characterize random vibration signals (Fig. 4). An ASD is computed by multiplying each frequency bin in an FFT by its complex conjugate which results in the real only spectrum of amplitude in g<sup>2</sup>.

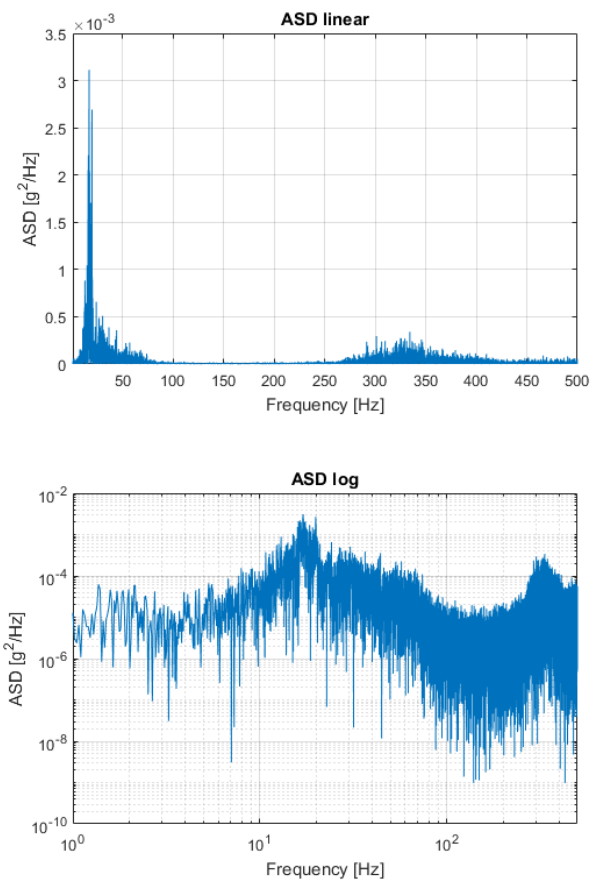


**Fig. 4** Sample ASD

The key aspect of ASD which makes it more useful than a FFT for random vibration analysis is that this amplitude value is then normalized to the frequency bin width to get units of  $g^2/Hz$  [6]. By normalizing the result, we get rid of the dependency on bin width so that we can compare vibration levels in signals of different lengths [7].

### 3. GENERATION OF RANDOM VIBRATION PROFILE FOR TESTING

A random spectrum is defined as a set of frequency and amplitude breakpoints, picked from the ASD graph (Fig. 4). Particularly, in our sample case this would be:

**Table 1** *Spectrum breakpoints*

Frequency [Hz]	ASD [ $g^2/Hz$ ]
10	0.0000344
17	0.000736
150	8.403E-07
330	0.00002583
500	0.00000291

The vibration profile is can be divided in subdomains, throughout which the amplitude varies linearly on a log-log graph. Thus, generating a set of log lines between these 5 sets of breakpoints ( $f, a$ ) can be achieved with:

$$a = offset \cdot f^{slope} \quad (1)$$

$$\text{with } slope = \frac{\log\left(\frac{a_2}{a_1}\right)}{\log\left(\frac{f_2}{f_1}\right)} \text{ and } offset = \frac{a_1}{f_1^{slope}},$$

or

$$a = a_1 \cdot \left(\frac{f}{f_1}\right)^{\frac{\log\left(\frac{a_2}{a_1}\right)}{\log\left(\frac{f_2}{f_1}\right)}} \quad (2)$$

where:

- $f$  – is the amplitude of the ASD control signal,
- $f_1$  – is the subdomain's left breakpoint's amplitude,
- $f_2$  – is the subdomain's right breakpoint's amplitude,
- $a$  – is the frequency of control signal,
- $a_1$  – is the subdomain's left breakpoint frequency,
- $a_2$  – is the subdomain's right breakpoint frequency.

Fig. 5 presents the calculated random vibration profile (red line) and it's accepted deviation of  $\pm 3$  dB (white dashed line). From this it is possible to calculate the root-mean-square acceleration ( $G_{rms}$ ), as just the square root of the area under the ASD vs. frequency curve.

Thus, the area can be calculated as:

$$area = \frac{offset}{slope + 1} \left( f_2^{slope+1} - f_1^{slope+1} \right) \quad (3)$$

if slope  $\neq -1$  or

$$area = offset \cdot \left( \log_{10} \frac{f_2}{f_1} \right) \quad (4)$$

if slope = -1.

In our case, from spectrum profile resulted a Grms of 0.1045g, in contrast with the density of every point 0.1146g.

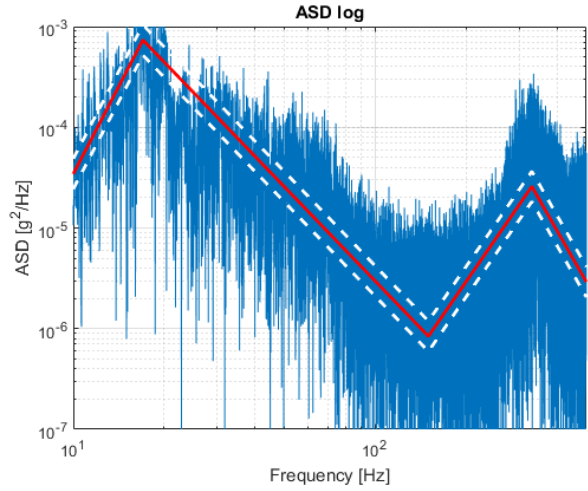


**Fig. 5** *Random vibration profile*

Mean-square acceleration could have been calculated also from the time domain as the average of the square of the acceleration over time.

### 4. CONTROL ALGORITHM

An automatic controller compares the process measurement to a desired "setpoint" value from the vibration profile and produces a "controller output" as response.

The error from the measurement must be within the accepted  $\pm 3$ dB band:

$$\varepsilon = setpoint - process\_measurement .$$

This error is used to calculate a change that will compensate the controller output, which when transmitted to the testing equipment (shaker) will change the acceleration (Fig. 6).

Having the vibration profile, independent from the linear or logarithmic parsing of the frequency domain, for each frequency the desired amplitude is sent to the shaker's controller. An accelerometer continuously monitors the response of the shaker-sample system and compares it with the desired curve. If its output value falls outside of our acceptable amplitude domain, steps are taken to redress the acceleration.

The shaker's acceleration is directly proportional with the frequency and amplitude of the displacement. This amplitude is controlled by limiting the input of the control signal's tension.

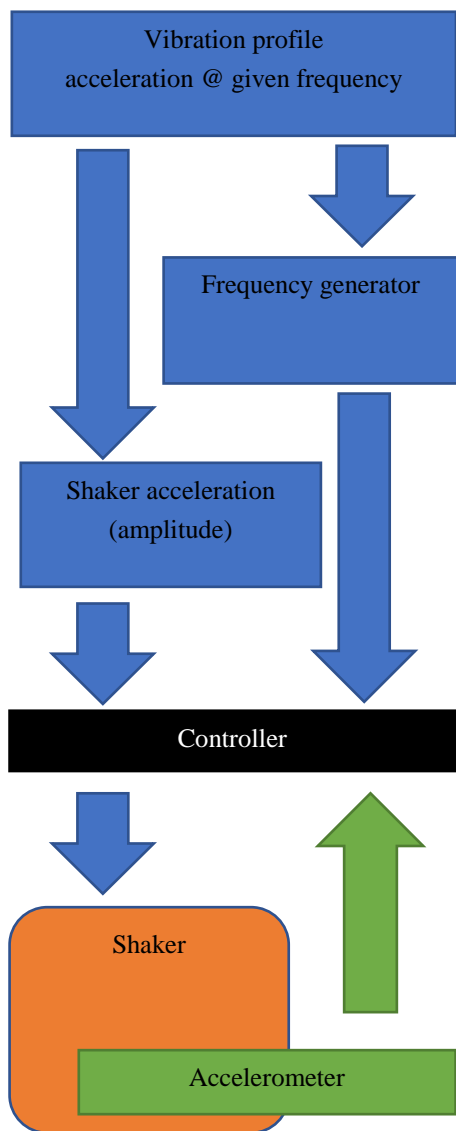


Fig. 6 - Auto control loop for vibration profile

## 5. CONCLUSIONS

Random vibration test are the *de facto* methods to prove the reliability or survivability of products from manufacturing, to shipping and throughout their normal usage. This method, if

correctly applied, can offer a valuable insight into the energy exchange of different samples being tested.

Control signal generation for random vibration tests, at a first glance, seems like a trivial operation. Unfortunately, there are plenty of factors that contribute to error prone results. Choosing the wrong sample frequency can lead to an overlook of some critical frequencies or having them all mashed up.

Numerical integration of acceleration in time do give us velocity and eventually displacement. But, these are functions that depend on initial conditions, which from simple numerical integration are unknown, and the resulted values are offset by an unknown factor. None the less, the curve gives us an idea about the overall variation of velocity and displacement.

Having the FFT spectrum of the acceleration, one has to carefully choose the breakpoints in order to obtain a realistic (minimum) amplitude for testing (vibration profile) and not overly exceed the acceleration in regions where it is minimum.

## REFERENCES

- [1] Tustin, Wayne, Random Vibration & Shock Testing, Equipment Reliability Institute, Santa Barbara, CA, 2005.
- [2] Connon, W. H., "Comments on Kurtosis of Military Vehicle Vibration Data," Journal of the Institute of Environmental Sciences, September/ October 1991, pp. 38-41.
- [3] Rao, S. S., ed., Mechanical Vibrations, Prentice Hall, 4th edition, March, 2003
- [4] Broch, J. T., Mechanical Vibration and Shock Measurements, Brüel & Kjær, 2nd Edition, April 1984, Denmark
- [5] Randall, R. B., Vibration-based Condition Monitoring: Industrial, Aerospace and Automotive Applications, Wiley, 2011
- [6] IEC EN 60068-2-64.
- [7] Midé Technology Corporation, <https://blog.mide.com/vibration-analysis-fft-psd-and-spectrogram> 2018/11/01

## APPLICATION OF FREQUENCY SIMULATION FOR DETECTING THE RISK OF EXTREME EVENTS ON TRANSPORT MACHINES

Miomir Jovanović<sup>1</sup>, Goran Radoičić<sup>2</sup>, Predrag Milić<sup>1</sup> and Taško Maneski<sup>3</sup>

<sup>1</sup> University of Nis, Faculty of Mechanical Engineering, Serbia, miomir@masfak.ni.ac.rs

<sup>2</sup> University of Nis, Faculty of Mechanical Engineering and PUC "Mediana" Niš, Serbia

<sup>3</sup> University of Belgrade, Faculty of Mechanical Engineering, Serbia,

**Abstract** - In order to investigate the dynamic maximums generated by the operation of interrupted and continuous transport machines, frequency simulation was used as one of the best methods for the analysis of resonance phenomena. As the vibration process (caused by overloading fine-grained material) can be numerically analyzed, a simulation model of forced vibration of a mechanical structure has been developed. By simulation model it is possible to determine extreme phenomena in the exploitation of equipment for receiving material streams. In addition to the theoretical basis of the model, an experimental tests with FFT analyzes on the loading systems have been provided. One study relates to overloading in intermittent transport and the second to the stecker in continuous transport at the Copper mine in Bor. The value of research is reflected in the developed model and mathematically modeled excitation functions defined on the basis of the flow and frequency. The research results can be used to monitoring and develop well-adapted protective equipment.

### 1. INTRODUCTION

In the exploitation of heavy machines, there are often emergent external excitation forces due to the circular movement of drive elements. These forces are usually of a harmonic character in the form of a sinus or cosine function, with the period of oscillation  $T = 2\pi / \omega$ . Observation of such stationary dynamic processes with frequency excitation has the advantage of being reduced to the observation of only one period of the wave in the continuous duration of excitation period and not for a long period as in the transient processes analysis. Such analyses forced by frequency-excitation are known as linear frequency response analysis or Steady-state response analysis. These analyses have engineering significance because they are studying the frequency domain of machine operations, the appearance of the resonance and the dynamic amplification factors [1, 2]. These analyses make a significant contribution to the study of the durability and reliability of large mining machines, as well as energy and industrial plants.

The study of the frequency response of the mining stacker (depositor) in Fig. 1 was performed numerically and experimentally. The capacity in the delivery of waste-rock of this large machine for continuous transportation is up to 4800 tons per hour [3]. The stacker's basic geometry is 55.90 m×16.88 m×7.87 m, and mass is 210680 kg. In Fig. 1 we can

see that the long and heavy frame structure of the boom relies on a relatively small rotating support of 1.5 m in diameter located on the stand. So, an important question about dynamic stability of the machine, vibration amplitude and dynamic amplification factor in the wider frequency domain can be asked. Linear frequency response analysis was performed by the FE method. The FE model in Fig. 2 consists of 2134 finite elements in the form of discrete masses and 1016 nodes. Such great number of masses makes modelling more realistic and implies advantages of discrete models.



Fig. 1 Stacker in work 4800 t/h (RTB Bor 2012)

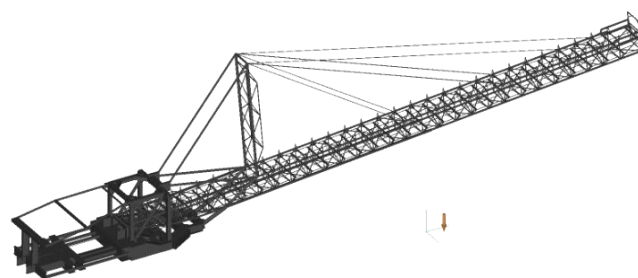


Fig. 2 FE model of the stacker in the Copper mine Bor

Frequency excitation in these machines makes more process:

1. Fast-eccentric masses on the rotating parts of the conveyor,
2. Fall of load (waste-rock) on the conveyor belt,
3. Weight on the bracket of the belt drive gearbox mounted,
4. Vertical harmonic movement of the material on the belt through equally spaced rollers of the conveyor,
5. The vibrating device excitation for filling (cleaning) the bunkers of the conveyor belt system,
6. Frequency of eccentric mass of propulsion conveyor motor.

The issue of falling material on the belt conveyor of large mining machines was discussed in the paper [4] and [5] from the aspect of possible damage and durability of the components of the transportation system. Also, in the study [6], a method for measuring the impact effect of the falling object on a horizontal surface (load cell) is shown, which can be applied in transportation systems, for example, in large mining machines such as a stacker.

## 2. THEORETICAL BASIS

Frequency response analysis is a method to determine structural response to steady-state vibratory excitation. In frequency response analysis, the excitation is explicitly defined in the frequency domain (forced frequency). The obtained responses have a complex form, with magnitude and phase (real and imaginary component). Two different numerical methods can be used in frequency response analysis. The first method is direct frequency response analysis and second method is modal frequency response analysis. Modal method uses the normal modes of the structure to uncouple the equations of motion, with the solution for a particular forced frequency, obtained through the summation of the individual modal responses. Equation of motion of damped forced vibration with harmonic excitation has coordinates  $\{x_{(t)}\}$  and form (1), with notation [2]. In Eq.(1),  $[M]$  is the mass matrix,  $[B]$  is the damping coefficient matrix,  $[K]$  is the global stiffness matrix of the structure and  $\{P(\omega)\}$  is an external vector of excitation with frequency  $\omega$ . Modal frequency response analysis uses the mode shapes of the structure to reduce the size, uncouple the equations of motion (when modal damping is used), and make the numerical solution more efficient. The first step in the formulation is transformation of the variables from physical coordinates  $\{u(\omega)\}$  to **modal coordinates**  $\{\xi(\omega)\}$  using a relationship (2) in which  $\{u(\omega)\}$  is one complex displacement vector with magnitude ( $u$ ) and phase angle ( $\theta$ ) as real and imaginary components of oscillation.

$$[M]\{\ddot{x}_{(t)}\} + [B]\{\dot{x}_{(t)}\} + [K]\{x_{(t)}\} = \{P_{(\omega)}\} \cdot e^{i\omega t} \quad (1)$$

$$\{x\} = \{u(\omega)\} \cdot e^{i\omega t} = [\Phi]\{\xi(\omega)\} \cdot e^{i\omega t} \quad (2)$$

Expression (2) represents an equality if all modes are used. The mode shapes  $[\Phi]$  are used to transform the problem in terms of the behavior of the modes as opposed to the behavior of the grid points. Number of used modes represents level of model approximation. In case that structural damping is used, the orthogonality property does not diagonalize the generalized stiffness matrix  $[\Phi]^T[K][\Phi] \neq \text{diagonal}$  because structural damping matrix has complex form (3). Where  $[K]$  is the global stiffness matrix,  $G$  is the overall structural damping coefficient,  $[K_E]$  is the elements stiffness matrices and  $G_E$  is element structural damping coefficient (in the material).

$$[B] = (1 + iG)[K] + i \cdot \sum G_E [K_E] \quad (3)$$

In this situation, the modal frequency approach [2, page 131] solves the coupled problem in terms of modal coordinates using the direct frequency approach. When Eq.(2) is substituted into Eq.(1), the following is obtained:

$$-\omega^2 [\Phi]^T [M] [\Phi] + i\omega [\Phi]^T [B] [\Phi] + [\Phi]^T [K] [\Phi] \{\xi_{(\omega)}\} = [\Phi]^T \{P_{(\omega)}\} \quad (4)$$

If damping is applied to each mode separately, the uncoupled equations of motion can be maintained. When modal damping is used, each mode has damping  $b_i = 2m_i\omega_i\zeta_i$ . The equations of motion remain uncoupled and have the form:

$$-\omega^2 m_i \xi_i(\omega) + i\omega b_i \xi_i(\omega) + k_i \xi_i(\omega) = p_i(\omega) \quad (5)$$

Then, each of the modal responses is computed with Eq. (6):

$$\xi_i(\omega) = \frac{p_i(\omega)}{-m_i\omega^2 + ib_i\omega + k_i} \quad (6)$$

At resonance the three types of damping are possible and they are defined by damping ratio  $\zeta_i$  and structural damping coefficient  $G_i$ , Eq. (7):

$$\zeta_i = \frac{b_i}{b_{cr}} = \frac{G_i}{2}; \quad b_{cr} = 2m_i\omega_i \quad (7)$$

The uncoupled equation of motion, for final solutions, are:

$$-\omega^2 m_i \xi_i(\omega) + [1 + iG(\omega)]k_i \xi_i(\omega) = p_i(\omega) \quad (8)$$

## 3. NUMERICAL SIMULATION

Dynamic modelling of Stacker is performed by forming discrete system of mass elements of the carrying structure and installed machine equipment. Masses are mutually connected by elastic connections of the structure. For more practical research, modelling can be performed by FEM model. For modelling, this paper uses real structure of the Stacker RBB [3]. Analysis is performed by the finite element method [2] by using FEMAP, PLM Siemens Software [7].

The rotatory platform and boom have a frame structure, so they are modelled by beam finite elements. Machine equipment, belts, drums and transported material on conveyor belt are modelled by dotted-mass finite elements. The base construction of Stacker is rigidly laid on the ground.

Modal analysis is carried out to determining whether the individual parts of the structure oscillate, by what frequencies, and with what type of damping. The damping can be viscous and structural. The viscous damping is proportional to the vibration speed while the structural damping is proportional to the size of displacement. Modal analysis is performed aimed to determine the speeds and processes of damping.

Figure 3 shows a modal shape of the free vibration of the rotary part of the stacker. The 28<sup>th</sup> modal shape at the eigenfrequency of 6.606 Hz is displayed. This vibration shape is characterized by vertical undulation of the main carrier [8-10]. After the modal analysis, two frequency-based excitations were selected. They were described and introduced in the **modal-frequency analysis**. Significant vibration of the structure were sought by the analysis in order to prevent extreme dynamic phenomena.

Dynamic forced action is determined from the conveying flow  $Q=4800 \text{ t/h} = 1333 \text{ kg/s}$ . Frequency of appearance of compact pieces is determined by average material granulation  $f=5-50 \text{ Hz}$ . The impulse force of the material pieces weight according to Figure 4 acting on  $n=16$  receiving rollers of the belt. The force on a roller of an entry of the conveyor is done by Eq.(9):

$$F_{2(f)} = \frac{Qg}{n} \cdot \frac{1}{f} = \frac{1333 \cdot 9.81}{16} \cdot \frac{1}{f} = \frac{817.5}{f} \text{ [N]} \quad (9)$$

By introducing this forces  $F_2(f)$  defined in the frequency domain in the dynamic equation of the structure (1) and solving it with a front exposed modal-frequency procedure, we obtain a dynamic response of any point of structure grid. Figure 5 shows the accelerations of the stacker boom in the node of the connection between the horizontal beam structure of the boom and first (shortest) tie rod. The picture shows three curves of acceleration components in the frequency

domain of 50 Hz. The smallest vibration of this point is seen at a frequency of 15 Hz. Vibrations between 6-8 Hz are due to the flow of material through the conveyor loading bunker. In the analysis it is possible to introduce the excitation of the electric motor drives. This effect can be seen in Figure 6-b as a single frequency of 25 Hz (corresponding to the speed of the motor).

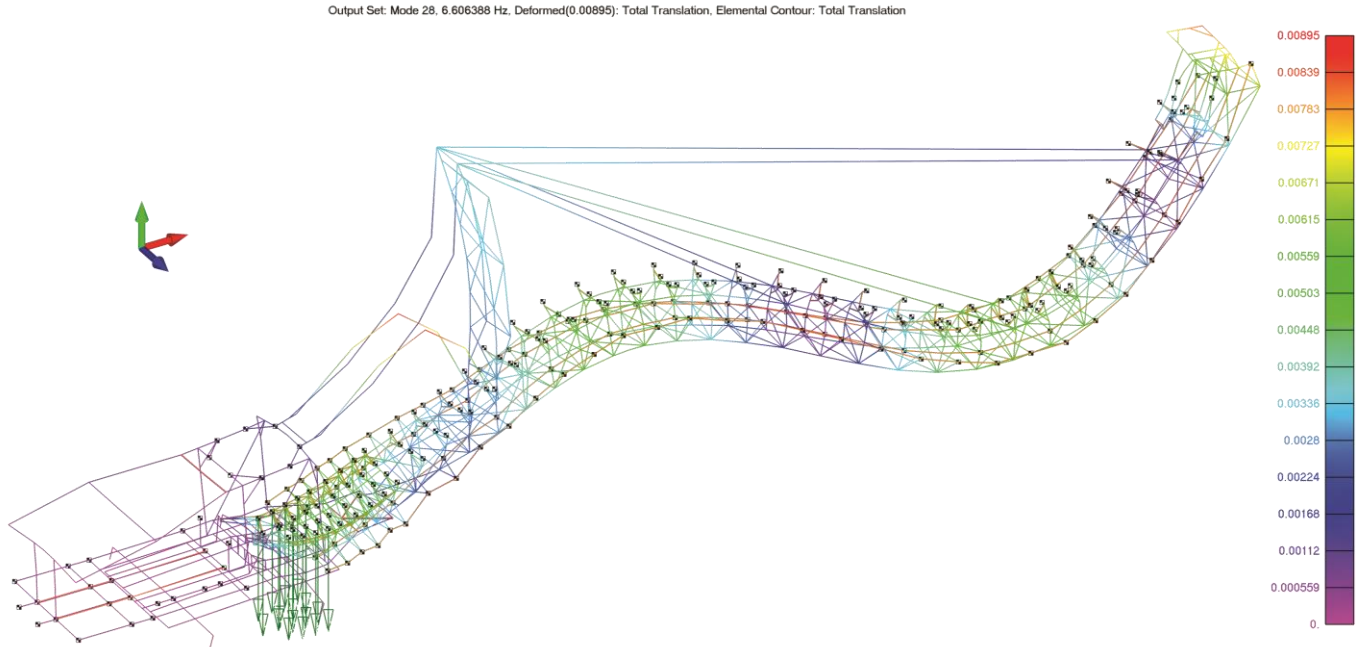


**Figure 3.** The first step in modal analysis - the eigenvalues of the structure; the Mod 28 at the eigenfrequency of 6.606 Hz (vertical sine wave of the boom)

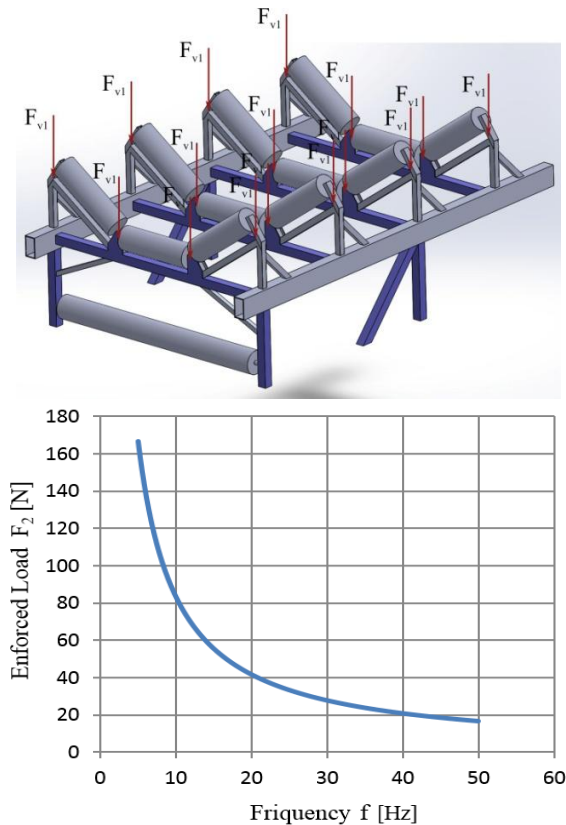


**Figure 4.** Dynamic forces  $F_{v1}=F_2$  due to the entry of material on the conveyor (flow/arrival of material with 5-50 compact pieces in every second)

#### 4. EXPERIMENT ON REAL STRUCTURE

Reality of investigated eigenvalue was checked experimentally by measuring the acceleration of the characteristic points of structure [8]. The three component acceleration with excitation caused by more positions on conveyor were measured in positions of the pylon, ROD-1, ROD-2, ROD-3 and the driving conveyor drum, Figure 6. A three-component piezo sensor ADXL-312 brand MEMS with integrated amplifier Analog Device AD-320 were used as the sensor. Record of measurements were analyzed by VIBRAREC software [11]. The acceleration and speed in the frequency-domain were identified using FFT transformations on the basis of measured accelerations in time-domain. They are clearly defined all the present dominant frequencies - caused by them themselves.

Figure 6a shows an experimental record of velocities in time-domain. The velocity is shown in the three component directions of the boom and relates to the position where the shortest tie rod connects the boom. Figure 6b shows the component accelerations in frequency domain up to 35 Hz, and that for acceleration in the vertical direction using the red curve ( $a_y$ ), acceleration in the lateral direction the blue curve ( $a_x$ ) and in the longitudinal direction black curve ( $a_z$ ). The component accelerations in Fig. 6b reach up to  $0.026 \text{ m/s}^2$  (at an eigenfrequency between 16-17 Hz). In the frequency domain of 0-20 Hz dominated the accumulation of eigenfrequencies. The drive motor excitation appears at 25 Hz (Figure 6-b, red curve). The maximum value of the component acceleration in frequency response analysis

obtained by the numerical method is  $0.14 \text{ m/s}^2$ , at the eigenfrequency of  $6.606 \text{ Hz}$  (Fig. 5), corresponding to value of  $\approx 0.15 \text{ m/s}^2$  in Fig. 6b which was obtained in an experimental analysis of frequency domain.

For theoretical investigations of mining and construction machines with similar geometry and structure, the results of experimental analyses [12-17] may also be helpful.

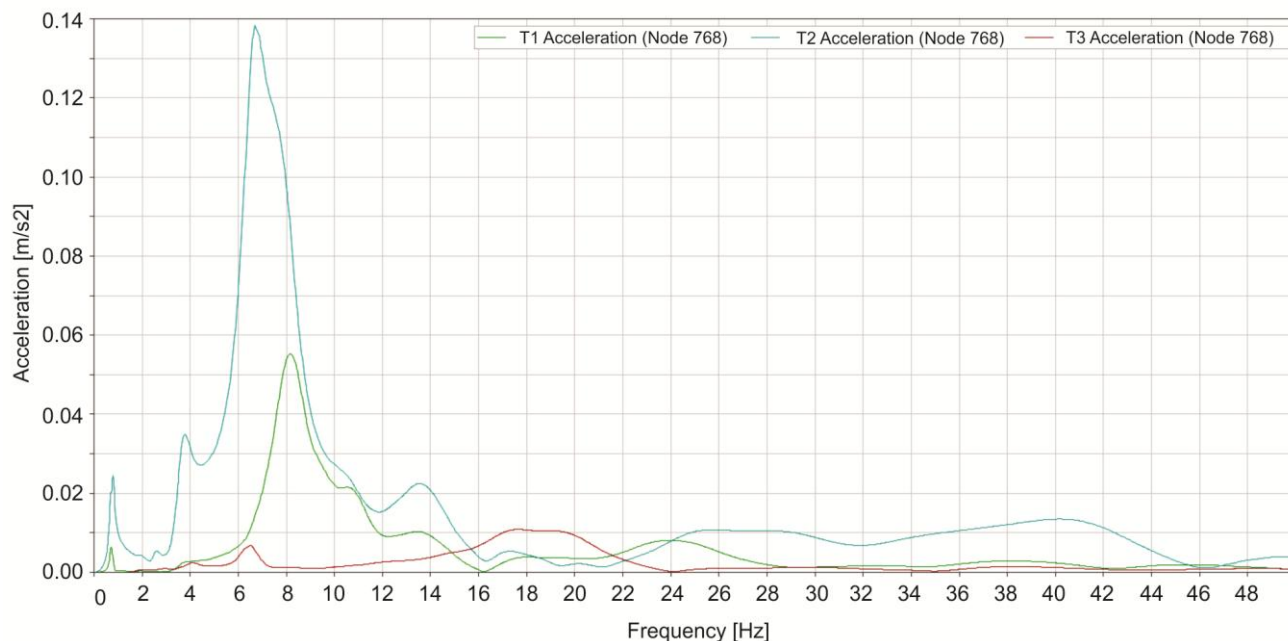


**Figure 5.** Numerical solution of frequency response analysis; calculated acceleration of the structure  $a_x, a_y, a_z$ ; the excitation in the point of connection between the boom and first tie rod caused by material flowing on the stacker conveyor (Node 768).

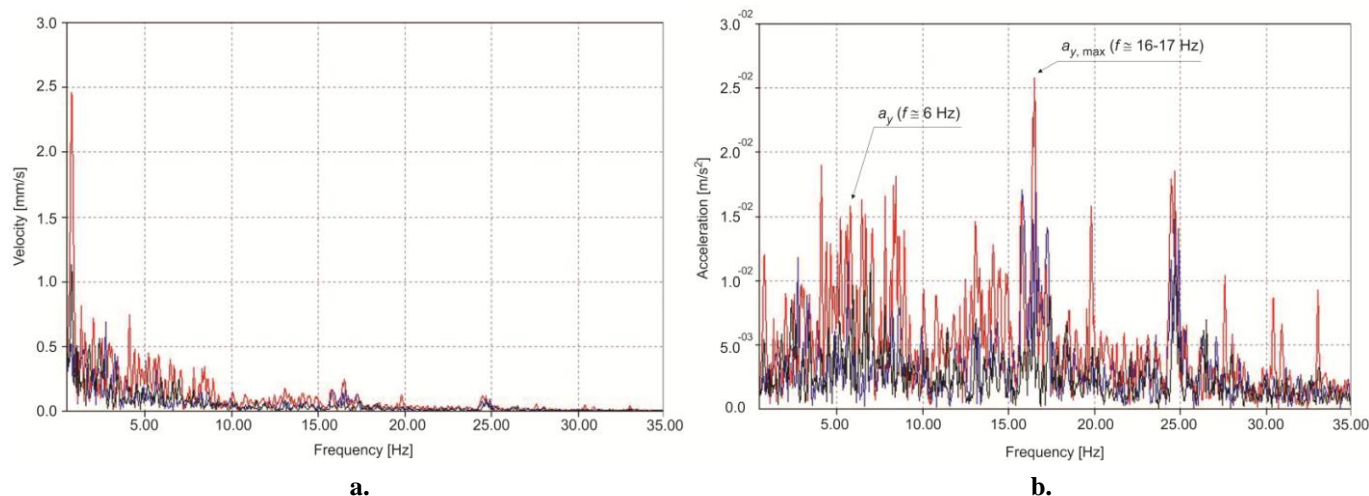


**Figure 6.** Experiment [8] – measurement in the frequency domain at the point of boom and connection of the first tie rod in Node 768 (measuring location according to the mark in Figure 7): **a.** Velocity; **b.** Acceleration.

## 5. CONCEPT OF MONITORING

The monitoring system starts from a number of previously made modal-frequency analyses which determine the level of amplitude of a large number of points of the structure and the resulting stresses by these displacements. The group of obtained points of a structure with significant results is firstly evaluated by the level of responsibility and then the reduction of number of points is performed. Figure 7 shows a scheme of location of the accelerometer sensor and a stress sensor, [18]. At the same time the scheme shows the necessary equipment and functions that must be performed by encoders and controllers. Since the stacker is working in different working regimes, it is necessary to introduce in the control of the structure - the active vibration setting in the domain of small amplitudes. This can be done by installing the movable mass

one on the lower side of boom structure (Figure 7, blue mass). By changing the position of weight the frequency-amplitude characteristics of the structure are changing. The outer natural effects have accidental nature (wind), the present control system can fine-tune the weight distribution that minimizes the amplitude. The adjustment should be manual and then autonomous. The development of an autonomous balancing system requires the introduction of a critical acceleration value when the setting starts ( $a_{\max}$ ) and the maximum acceleration when the operation stops. The measuring system requires amplifiers and equipment for monitoring and control, which is a typical control technique. Introducing a measuring system into a structure significantly increases the level of plant safety which ensures the planned and long exploitation of large machines. The first step towards the regulation system is to set up monitoring and introduce the stacker into the phase

of observing and registering phenomena. Modal-frequency analyses have the greatest significance for heavy machines that operate in shock regimes. These are bucket-wheel excavator and crushers.

## 6. CONCLUSIONS

1. The stacker is a large structure with model of thousands elements and several load sources inside the machine. For these conditions the modal method is recommended by the software manufacturer.
2. Comparison of numerical and experimentally determined acceleration in the frequency domain (Figure 5 and 6-b): There are visible differences in results. The differences are due to the various influences in the real system on which the measurement was performed. These are the effects of eccentric rotary drives, ambient influences (wind), impact of the drive motor
3. The defined model enables the simultaneous introduction of a number of frequency influence (frequency environments) in analysis, which

contributes to the approximation of amplitude-frequency characteristics.

4. Modal-frequency FEM analysis can also treat large carrying structures from the numerical aspect. The reason for efficiency is in non-coupled equations of oscillation in different modes, which has a simple algorithm for solving and a shorter period for obtaining a solution.
5. Modal-frequency FEM analysis allows to the obtaining basic dynamics data of the carrying structures. These are the data in the amplitude-frequency domain of the structure. These data are discrete and show the positions of construction points that have dynamic extremes. These points are crucial for the deployment of control and monitoring equipment.
6. The observed stacker has a low vibration level since it works with a loose, crushed material. However, these constructions also require amplitude checking due to the sensitivity of the bearing rotary part and swinging boom.

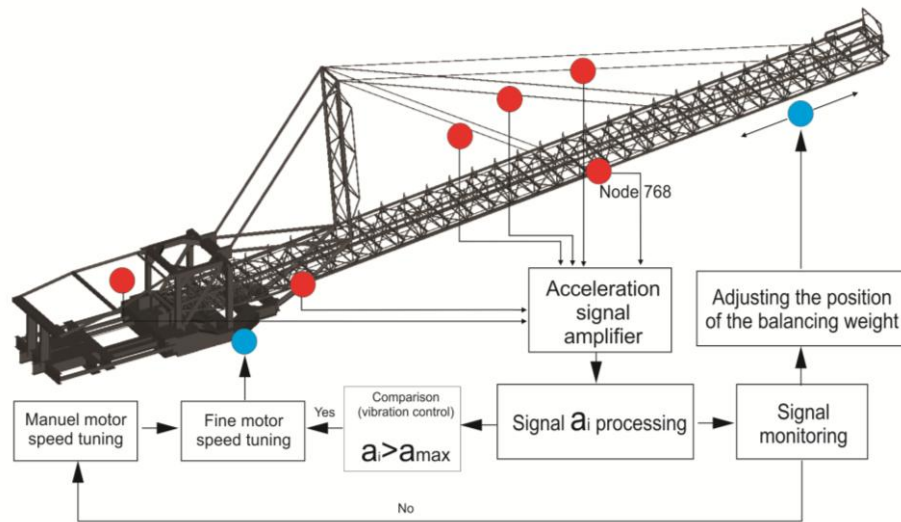


Figure 7. Monitoring algorithm and active vibration control structure

## Acknowledgment

This paper is part of the project TR-35049 at the University of Niš, Faculty of Mechanical Engineering, and was supported by the Ministry of Education, Science and Technological Development of the Republic of Serbia.

## REFERENCES

- [1] D. Rašković, *The theory of oscillations*, Building book, Belgrade, 1974.
- [2] MSC Nastran Corporation, *Basic Dynamic Analysis*, User documentation Ver. 68, Santa Ana, CA, 2004,
- [3] M. Jovanović, P. Milić, “Statical stacker-boom inspection on transportation system Veliki Krivelj – Bor”, Project No. 612-22-70/11, Faculty of Mechanical Engineering in Niš, 2011.
- [4] A. Grinčová and D. Marasová, “Experimental research and mathematical modelling as an effective tool of assessing failure of conveyor belts”, *Eksploatacja i Niezawodność – Maintenance and Reliability*, Vol. 16, No. 2, pp. 229–235, 2014.
- [5] L. Ambriško, K. Frydrýšek, D. Jelisivac-Erdeljan and D. Marasová, “Experimental research of a new generation of support systems for the transport of mineral raw materials”, *Acta Montanistica Slovaca*, Vol. 22, No. 4, pp. 377-385, 2017.
- [6] A. Gilman and D.G. Bailey, “High-speed weighing using impact on load cells”, Conference TENCON 2005, 0-7803-9312-0/05/S20.00©2005 IEEE.
- [7] FEMAP, *Siemens PLM Software, Plano*, <https://community.plm.automation.siemens.com/t5/Event-Collateral/FS13-07-Dynamic-Response-with-External-Superelements/ta-p/303701?attachment-id=22137> (accessed on March 2018)
- [8] T. Maneski, “Vibration measuring on trail supporting structure in Mining RBB Bor”, Industrial report, IC Faculty of Mechanical Engineering in Belgrade, 2010.
- [9] M. Jovanović and G. Radoičić, “Dynamical structural reliability based on the case study analysis”, *Facta Universitatis, Series: Working and Living Environmental Protection*, Vol. 12, No. 1, pp. 95-109, 2015.

- [10] M. Jovanović, G. Radoičić and T. Maneski, “Dynamical eigenvalue identification of heavy machine structures”, 7<sup>th</sup> International Conference Heavy Machinery, Vrnjačka Banja, Serbia, Proc. HM'2011, pp.73-78, 2011.
- [11] T. Maneski, *VIBRAREC – Structural Measurement and Analysis Software*, Faculty of Mechanical Engineering in Belgrade and MicroElektronik d.o.o, 2010, <https://www.mikroe.com/about> (accessed on March 2018).
- [12] M. Jovanović, J. Vladić and G. Radoičić, *Experimental research of transport machines*, Monography, Faculty of Mechanical Engineering in Niš, 2018.
- [13] M. Arsić and M. Jovanović, “System for measuring the export capacity of the pit mine of the Copper Mine in Bor”, Technical solution TR35049-2, Faculty of Mechanical Engineering in Niš, 2014.
- [14] G. Radoičić, M. Jovanović and M. Arsić, “Experience with one heavy vehicles on-board weighing system solution”, *ETRI Journal*, Vol. 38, No. 4, pp. 787-797, 2016.
- [15] M. Jovanović, G. Radoičić, B. Grigorov and R. Mitrev, “Special properties generation with transient structural simulation”, *Bulgarian Journal for Engineering Design* Vol. 18, pp.83-90, Sofia, 2013.
- [16] M. Jovanović, Z. Marinković, D. Živanović and S. Jovanović, “Logical concept of crane vibration control”, 15<sup>th</sup> EPCD International Conference on Material Handling and Warehousing, Mechanical Faculty, University of Belgrade, 1998.
- [17] M. Jovanović et al, “APD – Automatic Rack Crane”, Project of Ministry of the Government of Serbia I.5.1333, Faculty of Mechanical Engineering Niš, 1997.
- [18] M. Jovanović, G. Radoičić, P. Milić and T. Maneski, “With frequency simulation to design the monitoring of frame structures”, International Conference KOD 2018, Faculty of Technical Science Novi Sad, 2018.

## THE DISSIPATION AND THE DISSIPATION FUNCTION OF SEISMIC ENERGY

Slavko Zdravković<sup>1</sup>, Dragan Zlatkov<sup>2</sup>, Andrija Zorić<sup>3</sup>, Sandra Šaković<sup>4</sup>

<sup>1</sup> Dr, Full Professor, Academic of Serbian Royal Association of academics, innovators and scientists, Expert of the Federal Ministry of science, technology and development in the field: Civil engineering, Aseismic engineering, Bridge stability, University of Nis, Faculty of Civil Engineering and Architecture, Serbia, [slavko.zdravkovic@gaf.ni.ac.rs](mailto:slavko.zdravkovic@gaf.ni.ac.rs)

<sup>2</sup> Dr, Docent, University of Nis, Faculty of Civil Engineering and Architecture, Serbia, [dragan.zlatkov@gaf.ni.ac.rs](mailto:dragan.zlatkov@gaf.ni.ac.rs)

<sup>3</sup> M.C.Eng, PhD student, University of Nis, Faculty of Civil Engineering and Architecture, Serbia, [andrija.zoric@gaf.ni.ac.rs](mailto:andrija.zoric@gaf.ni.ac.rs)

<sup>4</sup> C.Eng, University of Nis, Faculty of Civil Engineering and Architecture, Serbia

**Abstract** - It is known that there is no oscillatory system without energy dissipation. Hysteresis damping is a very important mechanism of energy dissipation in vibrations in an inelastic region. In addition to the dissipative function, the paper focuses on dissipation of seismic energy. If the quantity of energy is considered to be known, the task is directed to determining the amount of absorbed energy. The damping coefficient is taken as a measure of energy loss.

### 1. INTRODUCTION

When it comes to earthquake load, the goal of the structural analysis is clear: it is necessary to justify the choice of design concepts and determine the level of resistance of the structure in such conditions.

It is very important that the behaviour of the structure can be traced both in elastic and in post-elastic stage, so it can be talked about dynamic analysis in two phases: a linear-elastic and elasto-plastic.

### 2. DAMPING TYPES

There are non-conservative forces that oppose the motion and reduce mechanical energy. These forces are called damping forces, and the occurrence of reduction of mechanical energy is called energy dissipation or damping. There are various types of damping that can be modelled in different ways.

External viscous damping occurs in construction vibrations in the water or air because of the resistance of water or air. This is negligible in comparison with other types of damping.

Internal viscous damping occurs due to the viscosity of the material. It is proportional to the relative velocity of vibration. It increases with the increase of vibration frequency. That type usually prevails at the vibration of structures in the elastic area and is easy to incorporate into a mathematical model. That is why it is the most commonly used in practice. Viscous damping model is often used for modelling of other types of loads, with the use of equivalent damping coefficients.

Energy dissipation occurs due to friction too. This type of damping doesn't depend on velocity and displacements. Friction can be significant in the case of construction vibrations, for example, when it comes to the filling walls after cracking.

Hysteresis damping is a very important mechanism of energy dissipation at the vibration in the non-elastic area. Dissipated energy is equal to the area of the loop in the load-deformation (area inside the hysteresis loop) diagram. Hysteresis damping depends on the amount of displacement. It can be modelled by a spring that has a non-linear relationship between the load and displacement. In that case, the problem becomes non-linear and for solving the equations of motion it is necessary to use nonlinear methods. Approximately linear analysis with viscous damping is sometimes used, with the provision of the use of an equivalent period and equivalent viscous damping coefficient. In the literature there are various methods for the determination of equivalent quantities. It should in fact be noted that the equivalent quantities depend on the vibration time course details and, therefore, they can not be determined in advance. In the case of the cycle as shown in Fig. 1, dissipated energy  $E_G$  is equal to the hatched surface. The equivalent viscous damping coefficient is calculated by the formula:

$$\xi = \frac{1}{4\pi} \frac{E_G}{E} \quad (1)$$

Where "E" is maximum potential energy ( $E = 0,5kumax$ ).

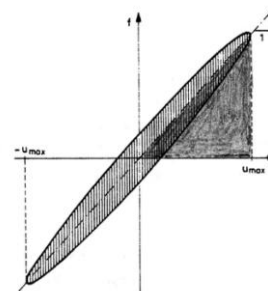


Fig. 1. Dissipated energy

The amount of energy dissipated by damping hysteresis can be very large for large non-elastic displacements or for wide loops. Hysteresis damping is one of the most important phenomenon that enables the structures to survive very strong earthquakes without demolition.

During construction vibrations, elastic waves spread throughout the half-space where the construction is funded. This way of energy dissipation is called radiation damping, which depends on the characteristics of the soil and the characteristics of the structure. Damping increases with increasing the stiffness of the structure, soil flexibility and the depth of foundation. During earthquake action, the damping acts preferably on the behavior of the structure because it reduces the amplitudes of the displacement [1].

When it comes to the real structures, a combination of different types of damping always appears. While vibrations are in the elastic range, viscous damping is prevailing. Nevertheless, hysteresis damping occurs even for minor deformations, which increases with increasing of deformation.

In order that task to be successfully solved, dynamic analysis sets it as an energy problem. It should be noted that this approach was initiated earlier (G. W. Housner, 1949) and later delivered as an energy method whose essential aim is determining the amount of energy ( $E_u$ ) which the building as a whole, not just the caring structure, can accept.

This amount of energy can be determined from the equation:

$$E_u = E_p + E_0 \quad (2)$$

where:

$E_p$  is the amount of energy absorbed by structure in the form of internal friction and damping;

$E_0$  - is currently accumulated amount of potential and kinetic energy in the building.

In practice, this problem is de facto reduced to the determination of the relationship between delivered and dissipated energy, as a fundamental indicator of the building resistance. In fact, the behaviour of the building depends on this relationship, or as it is usually said, response level. This means that if the amount of delivered energy greater than that the building can absorb, it will be greater response (greater response means, in short, larger displacement).

If it is considered that the amount of energy delivered to the building is known (for selected earthquake of known characteristics), the task is directed to determining the amount of the absorbed energy ( $E_p$ ). In this regard, the most important indicators are damping and ductility. As it is well known, every oscillatory system has the capability of damping. This can arise mainly from two sources: by inputting an external mechanism in the system (the absorber), or, what is here important, due to the internal resistance of the system as a consequence of the properties of its material. Furthermore, each damping essentially represent waste of energy introduced or already existing in the system. Therefore the damping coefficient is taken as a measure of energy loss.

When it comes to the amount of absorbed energy, it should be noted that the degree of the building damage is the most

significant indicator for it. This attitude can be explained by simple reasoning: the structure can accept an increasing load until it reach such an intensity to cause damage. During this period there is damping in the structure, but after appearance of damages, damping will be much smaller, which means that it has already been absorbed part of the input energy. Furthermore, the appearance of defects changes the stiffness of the structure, and that means the period of its free oscillations is changed, i.e. the dynamic coefficient ( $K_d$ ). is reduced. Then it follows that the seismic forces acting on the building will be smaller, and the damage will not increase.

The most of construction materials behave, in fact, non-linear, even at low deformation. For this reason, the damping is one of the factors that contributes to the uncertainty of data, and thus to the results of the earthquake analysis.

### 3. THE DISSIPATIVE FUNCTION

In any oscillating system there is energy dissipation, because there is no ideal system without friction and other similar resistances.

Because of the mathematical difficulties in one hand, and reliable matching of demonstration in the other, usually considered are dissipative forces proportional to speed:

$$D_i = -\gamma_i v_i \quad (3)$$

where  $\gamma_i$  is an experimentally determined coefficient of environmental resistance. Generalized resistance  $L_j$  is taken in the form:

$$L_j = -\sum_{(i)} D_i \frac{\partial s_i}{\partial \eta_j} \quad (4)$$

Drag force is represented by  $D_i$  and it is acting on mass  $m_i$ .

Observations show that the vibrations of the structure, which are not supplied with energy (for example in the form of external loads), the vibration amplitudes decrease with time. This means that the mechanical energy of the structure (kinetic and potential energy) is gradually reduced and converted into other forms of energy, especially heat.

While deriving the Lagrange equations of the second order, it is concluded that the velocity of the point is expressed by the generalized velocities as their linear function, i.e.:

$$\frac{\partial s_i}{\partial \eta_j} = \frac{\partial v_i}{\partial \dot{\eta}_j} \quad (5)$$

With this substitution it is:

$$L_j = -\sum_{(i)} \gamma_i v_i \frac{\partial v_i}{\partial \dot{\eta}_j} \quad (6)$$

that is:

$$L_j = -\frac{\partial}{\partial \dot{\eta}_j} \sum_{(i)} \frac{\gamma_i v_i v_i}{2} \quad (7)$$

Expression  $\sum_{(i)} \frac{\gamma_i v_i v_i}{2}$  is called the dissipative function. If the notation is introduced:

$$G = \sum_{(i)} \frac{\gamma_i v_i v_i}{2} \quad (8)$$

than it is:

$$L_j = -\frac{\partial G}{\partial \dot{\eta}_j} \quad (9)$$

The structure of the dissipative function is similar to the expression for the kinetic energy, and in the system with stationary connections it is positive definite quadratic form, which is expressed by generalized velocities in the form:

$$G = \frac{1}{2} \sum_{jk} c_{jk} \eta_j \dot{\eta}_k \quad (10)$$

where  $c_{jk} = c_{kj}$ .

After that the equation (9) will be:

$$L_j = -\frac{1}{2} \sum_{k=1}^j c_{jk} \dot{\eta}_k \quad (11)$$

The equations (9) and (11) show the relationship between energy, the resistance force, and the dissipative function. In fact, this function is one part of the mechanical energy, and its derivative with respect to the velocity is the resistance force. It can therefore be set relation:

$$d(E+V) = \sum_{j=1}^m L_j d\eta_j \quad (12)$$

$$\sum_{j=1}^m L_j d\eta_j = \sum_{j=1}^m \frac{\partial \eta_j}{\partial \dot{\eta}_j} d\eta_j = \sum_{j=1}^m \frac{\partial G}{\partial \dot{\eta}_j} \dot{\eta}_j dt = -2Gdt \quad (13)$$

and hence:

$$\frac{d}{dt}(E+V) = -2G \quad (14)$$

which means that the dissipative function represents the velocity of reduction of the mechanical energy of the system.

#### 4. CONCLUSION

The amplitudes of the structure vibration are reduced with time, which means that the mechanical energy (kinetic and potential) is gradually transformed into other forms of energy, especially in the heat. Conservative forces are opposing to the motion and these forces are called damping forces, while occurrence of mechanical energy reduction is called dissipation, or energy damping. The most of construction materials behave non-linear, even at low deformation. In earthquake analysis damping is one of the factors which causes the uncertainty of the data, as well as soil-structure interaction, which itself is unknown considering the location of its formation.

Dissipative function displays the velocity of mechanical energy reduction of a system, and its derivation with respect to the velocity is resistance force. This function expresses the kinetic energy of the system, and in the system with stationary connections it is positive definite quadratic form.

In the case of earthquake loads the most important indicators of the amount of energy absorbed are damping and ductility. Each damping is essentially the loss of introduced or already

existing energy in the system, and therefore the damping coefficient is taken as a measure of energy loss.

#### ACKNOWLEDGEMENT

This research is conducted at The Faculty of Civil Engineering and Architecture of University of Niš in the framework of the project in the field of technological development in the period 2011-2019, and titled "Experimental and theoretical investigation of frames and plates with semi-rigid connections from the view of the second order theory and stability analysis" (TR 36016), financed by the Ministry of Education, Science and Technological development of the Republic of Serbia.

#### REFERENCES

- [1] D. Cvetković, M. Prašćević, "Buka i vibracije", Univerziteta u Niš, Fakultet zaštite na radu, Niš, 2005, ISBN: 86-80261-45-9, 534.83(075.8), COBISS.SR-ID 127576332.
- [2] S. Zdravković, "Elementi za seizmičku izolaciju i apsopciju kod drumskih mostova", *Građevinski kalendar*, br. 45, 2013, Savez građevinskih inženjera Srbije, Beograd, ISSN 0352-2733, pp. 65-127.
- [3] V. Brčić, "Dinamika konstrukcija – (Metoda energije)", *Građevinska knjiga*, Beograd, 1978, pp. 261.
- [4] D. Antić, P. Fajfar, B. Petrović, A. Szavits-Nossan, M. Tomažević, "Zemljotresno inženjerstvo-visokogradnja", *Građevinska knjiga*, Beograd, 1990. D. Antić, P. Fajfar, B. Petrović, A. Szavits-Nossan, M. Tomažević, "Zemljotresno inženjerstvo-visokogradnja", *Građevinska knjiga*, Beograd, 1990.
- [5] T. Igić, S. Zdravković, B. Mladenović, P. Petronijević, S. Šaković, "Characteristic sources of seismic vibration", *23<sup>rd</sup> National Conference and 4<sup>th</sup> International conference "Noise and Vibration"*, University of Niš Faculty of Occupational Safty and "Polytechnica" University of Temisora Faculty of Mechanical Engineering Department of Mechanics and Vibration Noise andVibration Laboratory, Niš, 17-19 October, 2012, Serbia, 534.83(082), 62-752(082), 614.872(082), 628.517(082), ISBN 978-86-6093-042-4, COBISS-SR-ID 194076684 pp. 131-135.
- [6] S. Zdravković, D. Stojić, M. Spasojević-Šurdilović, D. Zlatkov, S. Šaković, "Experimental determination of damping of oscillation structural elements, whole buildings and structures", *XXVI Congress and international symposium on researsing and application of contemporary achievements in civil engineering in the filed of materials and structures*, Vrnjačka Banja, October 29-31, 2014, 624 (082) 666/9 (082), ISBN 978-86-87615-05-2, COBISS-SR-ID 210812172, pp. 417-423.

- [7] S. Zdravković, "Evaluation of earthquake intensity based on measured period and damping of buildings", *XXVI Congress and international symposium on researsing and application of contemporary achievements in civil engineering in the filed of materials and structures*, Vrnjačka Banja, October 29-31, 2014, 624 (082) 666/9 (082), ISBN 978-86-87615-05-2, COBISS-SR-ID 210812172, pp. 427-438.
- [8] V. Andrejev, "*Mehanika, III deo dinamika*", Tehnička knjiga, Zagreb, 1973.
- [9] S. Zdravković, "*Dinamika konstrukcija sa zemljotresnim inženjerstvom*", Građevinsko-arhitektonski fakultet Univerziteta u Nišu i AGM knjiga, Beograd, 2017.
- [10] E. Hadži-Musić, "*Aseizmičke konstrukcije u viskogradnji*", Svjetlost, Sarajevo, 1985.

## THE EVALUATION OF THE WHOLE-BODY VIBRATION EXPOSURE OF VIBRATORY ROLLER OPERATORS

Miljan Cvetković<sup>1</sup>, Boban Cvetanović<sup>2</sup>, Mário Fedatto Neto

<sup>1</sup> University of Nis, Faculty of Occupational Safety, Serbia, e-mail miljn.cvetkovic@znrfak.ni.ac.rs

<sup>2</sup> College of applied technical sciences Nis

<sup>3</sup> Universidade Federal do Rio Grande do Sul, Porto Alegre, Brazil

**Abstract** - When performing daily work operations, operators of heavy construction machinery are exposed, in addition to other damages, to the negative effects of vibrations. Vibrations are transmitted to the whole body of the driver and can be the cause of numerous health disorders of drivers and operators of construction machines. For most construction machines, vibrations are an undesirable consequence of the operation of engines and power generators, combined with the rough terrain. However, in addition to such harmful vibrations, vibratory rollers also produce desired vibrations with the function of material compaction. This paper aims to investigate the levels of daily exposure to vibrations that affect the operator of a vibratory roller.

**Keywords:** vibratory roller, whole-body vibrations, levels of daily exposure to vibrations.

### 1. INTRODUCTION

During their work activities, drivers and operators of heavy construction machinery are exposed to numerous negative influences which have complex harmful effects on humans. In addition to physical stress, atmospheric precipitation, adverse microclimate and temperature, various chemical pollution and noise, one of the significant negative factors is vibration.

These are whole body vibrations caused by the effects of uneven terrain in interaction with the operating conditions of the engine, as well as the work processes of the connecting tools and aggregates. The entire machine or vehicle, under working conditions, is exposed to complex oscillating processes that are transferred from the engine, through the transmission and chassis, to the cabin and further through the floor, seats and work controls, to the body of the driver or operator.

Even a short-term, but daily exposure to vibrations can cause abdominal and chest pain, shortness of breath, nausea, loss of balance, etc., while long-term and constant exposure can lead to a disorder of the psychomotor, physiological and psychological system of the driver and operator.

With the largest number of vehicles, vibrations are an unwanted and inevitable consequence of the operation of the engine and aggregate. However, there are also construction machines in which vibrations are necessary and the desired

factor in performing work operations. Vibratory rollers are such machines in which surface compaction of the material is carried out with vibrations, certain frequencies and amplitudes.

This paper provides information about the values of important vibration parameters in vibratory rollers and evaluates operator hazards due to the exposure to vibrations when working with a vibratory roller. The paper will present the measured values of vibrations on the operator's seat, in working conditions, and then the levels of the daily exposure of the driver to vibrations will also be analyzed and determined if they are within legally permitted limits.

### 2. VIBRATORY ROLLERS - OPERATION PRINCIPLES

The use of vibratory rollers (Figure 1) has begun in the 1950s, when it was understood that, due to dynamic action, the weight of these rollers could be considerably lower than the weight of rollers that only have a static effect.



Figure 1. Vibratory roller

The basic element of a vibratory roller is a vibrator which, depending on the design, can create circular or vertical vibrations. Vibratory rollers can be manual with one or two cylinders, self-propelled with two tandem cylinders and pulled with one or two cylinders. In tandem rollers, only one cylinder vibrates and operates dynamically, while the other operates statically and is used for steering. Vibratory rollers vibrate without bouncing, that is, they constantly stay in close contact with the compacting mass.

The vibration system is located in the roller chassis, which uses a diesel or gasoline engine. The weight of the vibratory

rollers ranges from 0.34 t for light rollers to up to 5 t for heavy rollers.

Vibratory rollers are primarily used for the compaction of unbound materials, although they also give good results when rolling incoherent materials. In relation to the mass, the use of vibrations increases the effects multiple times (5 to 7 times). Vibration should not be used at the very beginning of the compaction process and when turning the machine, since it creates waves on a still soft and freshly poured layer. The vibration frequency is from 20 to 75 Hz, and vibrations allow for the cohesion forces and friction to decrease in the poured material during vibration, so that the particles of the material are adjoined in the free spaces, creating the largest possible density in the poured material (Figure 2) [1,3].

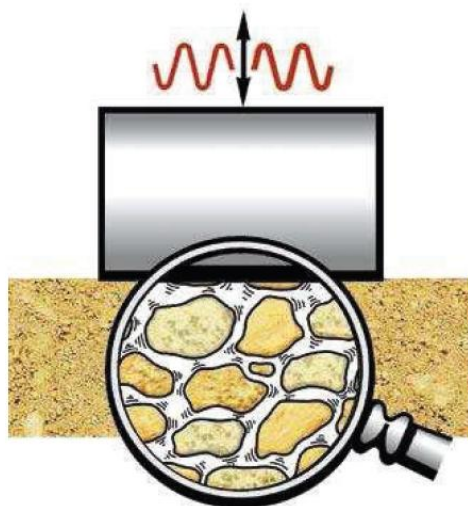


**Figure 2.** The effect of a vibratory roller on the surface [1]

The key parameters when compacting with the vibratory roller are the mass of the machine itself, which is significant due to the static linear load, and also the vibrational mass (the mass of the vibrating roller), as well as the amplitude and the frequency of vibration. The higher the vibrating mass, as well as the vibration amplitude, the higher the compaction depth (Figure 3).

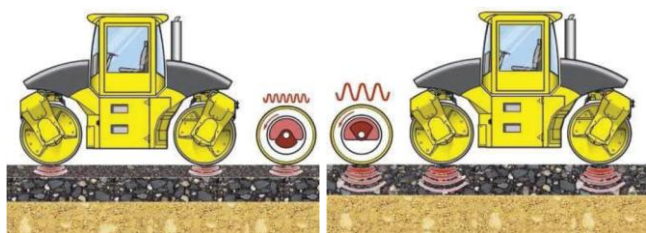


**Figure 3.** Relationship between the compaction depth and the vibration amplitude [1]

### 3. THE LEVEL OF DAILY EXPOSURE TO VIBRATIONS

The vibration values are measured on the seat of a Bomag BW 161 AD2 vibratory roller (Figure 4) during the compaction of freshly laid asphalt.



**Figure 4.** Bomag BW 161 AD2 vibratory roller

It is a tandem roller (two cylinders), weighing about 10 tons and having a power of 70 kW. The vehicle is not bogged down and the seat is mechanical.

The measurement lasted for 1 hour and 34 minutes. The measured values of vibration acceleration [2] are given in Table 1 for all three orthogonal measuring directions: z-direction (vertical – up / down), x-direction (longitudinal – forward / backward) and y-direction (transverse – left / right).

**Table 1.** Measured whole-body vibration values on the driver's seat [2]

Vibratory roller type	Duration [hr:min]	Average r.m.s. acceleration – equivalent value $A_{eq}$ [ $m/s^2$ ]		
		X	Y	Z
Bomag BW161 AD2	1:34	0.29	0.38	0.54
		Maximum acceleration values in the three directions [ $m/s^2$ ]		
		X	Y	Z
		3.30	5.39	14.00

Figure 5 presents the values obtained during the entire measurement period. It can be noted that the acceleration rates are critical only for the Z-axis, with a few high peaks that go up to  $14m/s^2$ .

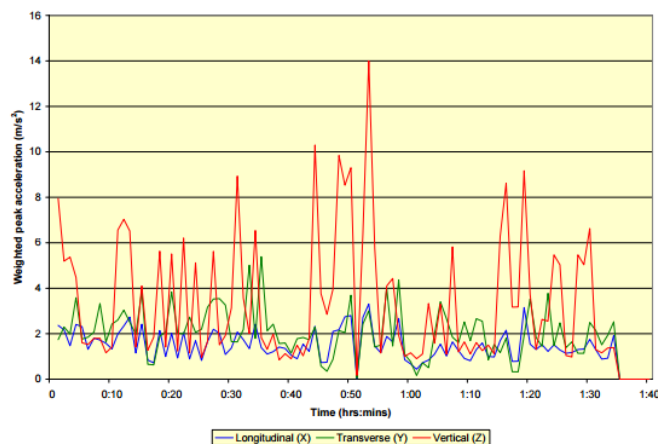


**Figure 5.** Time histories of weighted 1-minute peak seat accelerations (X, Y and Z-axes)

Using the measured values of vibration acceleration and with the help of the software (HSE whole body vibration calculator), the level of daily exposure of the driver to vibrations – A(8), obtained for the eight-hour working time (Table 2), was calculated. The values obtained were compared with the maximum permissible legal values in the European Union, prescribed by the Vibration Directive 2002/44/EC, and in the Republic of Serbia by the Rules and Regulations on Preventive Measures for Safe and Healthy Work during Exposure to Vibration.

In the case of the daily exposure to vibrations transmitted to the whole body, we listed the daily exposure limit value (ELV) which should not be exceeded in professional conditions and which is  $1.15 \text{ m/s}^2$ , as well as the daily exposure action value (EAV) above which employers are required to control the risks arising from vibrations and which is  $0.5 \text{ m/s}^2$ .

**Table 2.** *Determination of the daily exposure to the whole-body vibrations for the eight-hour working*

Vibratory roller type	Daily exposure levels by axes [ $\text{m/s}^2$ ]			Daily exposure level A(8) [ $\text{m/s}^2$ ]	Time to EAV [hr:min]	Time to ELV [hr:min]
	A(8) X-axis	A(8) Y-axis	A(8) Z-axis			
Bomag BW161 AD2	0.13	0.17	0.24	0.24	6:51	>24hr

#### 4. CONCLUSION

The obtained results of the daily exposure of  $0.24 \text{ m/s}^2$  show that, during the performance of the work activities, there are no negative vibration effects on the driver in case of the Bomag BW161 AD2 vibratory roller. Although it is a machine that, in addition to vibrations generated by the operation of the engine has additional vibrations generated by

the rollers themselves, the levels of exposure on the daily level have remained far below the legally permissible limits (even below the daily exposure action value (EAV) of  $0.5 \text{ m/s}^2$ ). However, it is recommended that the employer should control vibration risks in cases where the operator is working full-time for eight hours, since the time to reach the daily exposure action value is just under seven hours.

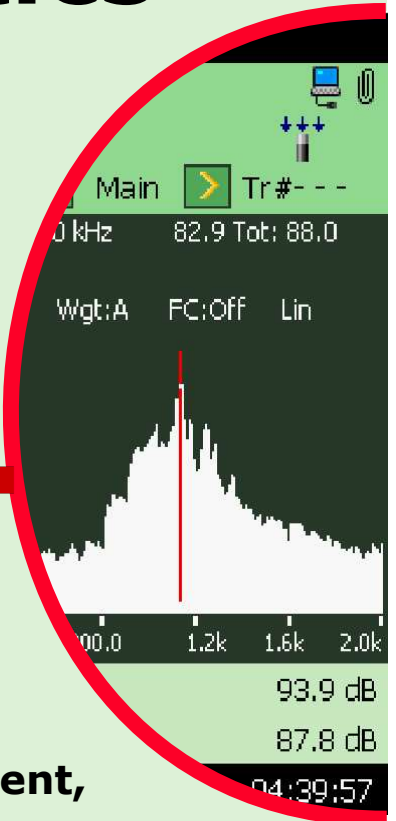
#### REFERENCES

- [1] Basic principles of asphalt compaction, 2009, Bomag. <http://www.bomag.com/world/media/pdf/PRE1090160901.pdf>
- [2] A.J.Scarlett, R.M.Stayner. Whole-body vibration on construction, mining and quarrying machines - Evaluation of emission and estimated exposure levels, Silsoe Research Institute for the Health and Safety Executive. 2005.
- [3] M.Horvat. Izbor i primjena strojeva i opreme za zbijanje zemljanih i kamenih gradiva, Sveučilište u Zagrebu, Geotehnički fakultet, 2010.

# Machine Diagnostics

## Type 2250/2270 **FFT**

### - **Frequency profiling!**



- **Single-channel FFT analysis of sound or vibration**
- **Machinery noise and vibration assessment, diagnostics and quality control**
- **Product development**
- **High frequency resolution, tap-and-drag operation and a wide dynamic range**
- **Tone assessment in accordance with ISO 1996-2 (optional)**
- **Simplified measurement process**
- **Transform size to match the job**
- **Analyse spectra and recordings in PULSE**

Brüel & Kjær 





## STRESSING ISSUE OF A PIEZOCERAMIC SECTIONAL CYLINDER WITH A CIRCULAR POLARIZATION

Igor Jovanović<sup>1</sup>, Ljubiša Perić<sup>2</sup>, Uglješa Jovanović<sup>1</sup>, Dragan Mančić<sup>1</sup>

<sup>1</sup>University of Niš, Faculty of Electronic Engineering in Niš, Serbia, igor.jovanovic@elfak.ni.ac.rs

<sup>2</sup>Regional Chamber of Economy Niš, Serbia

**Abstract** - This paper presents a general case of stressing a circular-ring cross-sectional cylinder with a circular type of polarization. Sectional cylinder is observed as electroelastic body consisted of separate prisms. It is assumed that the sectional cylinder is infinitely long in direction of the z-axis and that the component deformation in this direction is equal to zero. By applying the equations of electroelasticity in polar-cylindrical coordinates and satisfying electrical and mechanical conditions for the stress of a cylinder with a circular type of polarization, electric potential, componential displacements and mechanical stress in radial direction are determined for the sectional cylinder made from PZT4 piezoceramic material.

### 1. INTRODUCTION

The propagation of elastic waves in piezoceramic materials has many applications in various fields of science and technology such as electronics, navigation, biology etc. A piezoelectric material, such as lead zirconate titanate (PZT), can convert electrical energy into mechanical energy, and produce a small amount of mechanical strain proportional to the strength of an applied electric field [1]. This effect is employed in actuators, which produce displacements with fine resolution over small distance ranges [2], [3].

The optimal design characteristics and reliable behavior of piezoceramic actuators require deep understanding of wave propagation in these components. The theory of electroelastic waves in deformable piezoelectric structures is an intensively developed research area. The free vibration and dynamic characteristics of piezoelectric and composite structures such as beam, plate and cylinder have been extensively studied [4], [5].

Piezoceramic cylinders of circular or hollow cross-sections with axial, radial or circular type of polarization are frequently considered [6]. Due to their wide application as actuators, piezoelectric circular cylinders have attracted a considerable amount of research interest. In literature [7], the free vibration of piezoelectric cylinders with longitudinally and radially polarized transverse isotropy with one-dimensional theory (the wall thickness of the cylinder was assumed to be much less than the diameter), and three-dimensional theory (based on the general solution for coupled equations for piezoelectric cylinder) were analyzed. In literature [8], the circular cylinder is simplified to a two-dimensional model and then the voltage response of radially

polarized cylinders is analyzed when static and oscillating pressures are applied on the inside surface. Literature [9] proposes a linear theory of piezoelectric cylinder vibration, which can be simplified to account for spheres, cylinders and plates. In literature [10] an eigenfunction approach to determine the approximation response of radially polarized piezoelectric cylindrical shells of finite length subjected to electrical excitation is presented.

The main subject of this study is investigation of free vibration of a circular-ring cross-sectional cylinder with a circular type of polarization. Based on the general solution for coupled equations for piezoceramic material, applying the equations of electroelasticity and satisfying electrical and mechanical conditions for the stress of a cylinder, componential displacements, electric potential and mechanical stress are determined for the sectional cylinder.

### 2. FUNDAMENTAL EQUATIONS

Circular-ring cross-sectional cylinder with a circular polarization is observed as electroelastic body consisted of separate prisms. It is assumed that such sectional cylinder is infinite long and that dilatation in direction of z-axis is equal to zero ( $\varepsilon_z=0$ ). This is a case of plane strain state of infinitely long prisms.

AC generator performs excitation that induces occurrence of oscillatory process of sectional cylinder. Hence, on all prisms of the sectional cylinder is lead the same AC electric potential difference  $\pm U_0 e^{i\omega t}$ . In the absence of external mechanical loads, boundary problem of a cylinder is reduced to a boundary problem of a separate prism. If the internal and external radius of the cylinder are  $r_0$  and  $r_1$ , and lateral angle (angle of prism) of single prism is  $2\alpha$  (see Fig. 1), it is obvious that radial sections, on which electrodes are set, will not move in circular direction, due to the identity of the deformation condition of prisms. However, the points of these sections will move only in radial direction. The displacement vector  $\vec{s}$  in polar-cylindrical coordinate system is taken in the form of  $\vec{s} = u(r, \varphi, z)\vec{r}_0 + v(r, \varphi, z)\vec{c}_0 + w(r, \varphi, z)\vec{k}$ , wherein  $u$ ,  $v$ , and  $w$  are physical coordinates of the displacement vector (see Fig. 1). In given sections there are no shear stresses. Therefore, on the prism sides  $\varphi=\pm\alpha$  mechanical condition of conjugations of the tangential stresses ( $\tau_{\varphi r}$  and  $\tau_{\varphi z}$ ) should be satisfied:

$$v = 0, \quad \tau_{\varphi r} = \tau_{\varphi z} = 0. \quad (1)$$

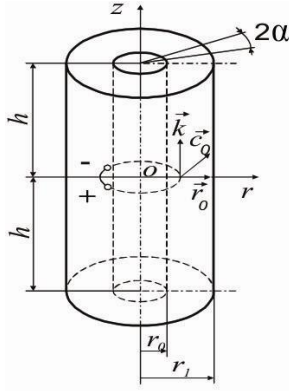


**Fig. 1** Sectional cylinder with circular polarization and electrodes on lateral sides of prism

These conditions are automatically fulfilled if points of piezoceramic material are moving in radial direction, that is  $\vec{s} = u(r, t)\vec{r}_0$ , not only in sections  $\varphi = \pm\alpha$ , but also in any other section  $\varphi = \text{const}$ . Electric potential depends upon a circular coordinate and time  $\psi = \psi(\varphi, t)$ . For this case of oscillation stand following relations [11] are:

$$\begin{aligned} u &= u(r, t), \\ \psi &= \psi(\varphi, t), \\ v &= 0, \quad w = 0. \end{aligned} \quad (2)$$

By substituting coordinates (2) into Cauchy's kinematic equations:

$$\begin{aligned} \varepsilon_r &= \frac{\partial u}{\partial r}, \quad \gamma_{rz} = 2\varepsilon_{rz} = \left( \frac{\partial u}{\partial z} + \frac{\partial w}{\partial r} \right), \\ \varepsilon_\phi &= \frac{1}{r} \frac{\partial v}{\partial \phi} + \frac{u}{r}, \quad \gamma_{r\phi} = 2\varepsilon_{r\phi} = \left( \frac{\partial v}{\partial r} - \frac{v}{r} + \frac{1}{r} \frac{\partial u}{\partial \phi} \right), \\ \varepsilon_z &= \frac{\partial w}{\partial z}, \quad \gamma_{z\phi} = 2\varepsilon_{z\phi} = \left( \frac{\partial v}{\partial z} + \frac{1}{r} \frac{\partial w}{\partial \phi} \right). \end{aligned} \quad (3)$$

and into the equations of electroelasticity [12]:

$$\vec{E} = -\text{grad}\psi, \quad (4)$$

one gets:

$$\begin{aligned} \varepsilon_r &= \frac{\partial u}{\partial r}, \quad \varepsilon_\phi = \frac{u}{r}, \quad E_\phi = -\frac{1}{r} \frac{\partial \psi}{\partial \phi}, \\ \varepsilon_z &= 0, \quad \gamma_{\phi z} = \gamma_{rz} = \gamma_{r\phi} = 0, \\ E_r &= E_\phi = 0. \end{aligned} \quad (5)$$

In deriving of the coupled equations of electroelasticity for piezoceramic cylinders with circular polarization, one must start from equations of piezoelectric effect:

$$\begin{aligned} \sigma_r &= c_{11}^E \varepsilon_r + c_{13}^E \varepsilon_\phi + c_{12}^E \varepsilon_z - e_{31} E_\phi, \\ \sigma_\phi &= c_{13}^E (\varepsilon_r + \varepsilon_z) + c_{33}^E \varepsilon_\phi - e_{33} E_\phi, \\ \sigma_z &= c_{12}^E \varepsilon_r + c_{13}^E \varepsilon_\phi + c_{11}^E \varepsilon_z - e_{31} E_\phi, \\ \tau_{r\phi} &= c_{44}^E \gamma_{r\phi} - e_{15} E_r, \end{aligned} \quad (6a)$$

$$\begin{aligned} \tau_{rz} &= \frac{1}{2} (c_{11}^E - c_{12}^E) \gamma_{rz}, \\ \tau_{\phi z} &= c_{44}^E \gamma_{\phi z} - e_{15} E_z, \\ D_r &= d_{11}^E E_r + e_{15} \gamma_{r\phi}, \\ D_\phi &= d_{33}^E E_\phi + e_{31} (\varepsilon_r + \varepsilon_z) + e_{33} \varepsilon_\phi, \\ D_z &= d_{11}^E E_r + e_{15} \gamma_{z\phi}. \end{aligned} \quad (6b)$$

By inserting the obtained expressions (5) into the equations of state for circular type of cylinder polarization (6a) and (6b), one gets expressions for componential mechanical stresses ( $\sigma$ ) and piezoelectric displacements ( $D$ ):

$$\begin{aligned} \sigma_r &= c_{11}^E \frac{\partial u}{\partial r} + c_{13}^E \frac{u}{r} + e_{31} \frac{1}{r} \frac{\partial \psi}{\partial \phi}, \\ \sigma_\phi &= c_{13}^E \frac{\partial u}{\partial r} + c_{33}^E \frac{u}{r} + e_{33} \frac{1}{r} \frac{\partial \psi}{\partial \phi}, \\ \sigma_z &= c_{12}^E \frac{\partial u}{\partial r} + c_{13}^E \frac{u}{r} + e_{31} \frac{1}{r} \frac{\partial \psi}{\partial \phi}, \\ D_\phi &= -d_{33}^E \frac{1}{r} \frac{\partial \psi}{\partial \phi} + e_{31} \frac{\partial u}{\partial r} + e_{33} \frac{u}{r}, \\ \tau_{\phi z} &= \tau_{rz} = \tau_{r\phi} = 0, \\ D_r &= D_z = 0. \end{aligned} \quad (7)$$

By substituting expression (7) into Navier's equations of motion:

$$\begin{aligned} \frac{\partial \sigma_r}{\partial r} + \frac{1}{r} \frac{\partial \tau_{r\phi}}{\partial \phi} + \frac{\partial \tau_{rz}}{\partial z} + \frac{\sigma_r - \sigma_\phi}{r} &= \rho \frac{\partial^2 u}{\partial t^2}, \\ \frac{\partial \tau_{r\phi}}{\partial r} + \frac{1}{r} \frac{\partial \sigma_\phi}{\partial \phi} + \frac{\partial \tau_{z\phi}}{\partial z} + \frac{2\tau_{r\phi}}{r} &= \rho \frac{\partial^2 v}{\partial t^2}, \\ \frac{\partial \tau_{rz}}{\partial r} + \frac{1}{r} \frac{\partial \tau_{z\phi}}{\partial \phi} \frac{\partial \sigma_z}{\partial z} + \frac{2\tau_{rz}}{r} &= \rho \frac{\partial^2 w}{\partial t^2}, \end{aligned} \quad (8)$$

and into the equation of electroelasticity [12]:

$$\vec{E} = -\frac{\partial \psi}{\partial r} \vec{r}_0 - \frac{1}{r} \frac{\partial \psi}{\partial \phi} \vec{c}_0 - \frac{\partial \psi}{\partial z} \vec{k}, \quad (9)$$

one gets system of two partial differential equations in form of [11]:

$$\begin{aligned} c_{11}^E \left( \frac{\partial^2 u}{\partial r^2} + \frac{1}{r} \frac{\partial u}{\partial r} \right) - c_{33}^E \frac{u}{r^2} &= \rho \frac{\partial^2 u}{\partial t^2} + \frac{e_{33}}{r^2} \frac{\partial \psi}{\partial \phi}, \\ -d_{33}^E \frac{1}{r^2} \frac{\partial^2 \psi}{\partial \phi^2} &= 0. \end{aligned} \quad (10)$$

In the observed case, all prisms of the sectional cylinder are in identical conditions of electric loading, and external loadings of surface forces are absent, therefore boundary problem for cylinder is reduced to boundary problem for individual prism. Electric boundary conditions, in case of

leading the electric voltage onto the electrodes of single prisms, are:

$$\psi \Big|_{\varphi=\pm\alpha} = \pm U_0 e^{i\omega t}. \quad (11)$$

Mechanical boundary conditions in the absence of external mechanical stresses on cylindrical surfaces  $r=r_0$  and  $r=r_1$ , give:

$$\sigma_r \Big|_{r=\{r_0, r_1\}} = \left( c_{11}^E \frac{\partial u}{\partial r} + c_{13}^E \frac{u}{r} + \frac{e_{31}}{r} \frac{\partial \psi}{\partial \varphi} \right) \Big|_{r=\{r_0, r_1\}} = 0. \quad (12)$$

Conditions of absence of shear stresses on the same surfaces are satisfied identically.

Solutions are assumed in form of product of two functions:

$$u = \hat{u}(r) e^{i\omega t}, \quad \psi = \hat{\psi}(\varphi) e^{i\omega t}, \quad (13)$$

wherein  $\hat{u}$  and  $\hat{\psi}$  represent amplitude of eigenfunction of componential displacement and electric potential, respectively.

After inserting assumed solutions (13) into the system of partial differential equations (10), they disintegrate into two common differential equations in form of:

$$r^2 \frac{d^2 \hat{u}}{dr^2} + r \frac{d\hat{u}}{dr} + (\lambda^2 r^2 - \nu_1^2) \hat{u} = \frac{e_{33}}{c_{11}^E} C_1, \quad (14)$$

$$\frac{d^2 \hat{\psi}}{d\varphi^2} = 0,$$

where:

$$\lambda = \omega \sqrt{\frac{\rho}{c_{11}^E}}, \quad \nu_1 = \sqrt{\frac{c_{33}^E}{c_{11}^E}}. \quad (15)$$

Solution of the second differential equation of the system (14) is:

$$\hat{\psi} = C_1 \varphi + C_2. \quad (16)$$

First equation of the system (14) represents nonhomogeneous Bessel's differential equation and its solution may be written in form of:

$$\begin{aligned} \hat{u}(r) = & AJ_\nu(\lambda r) + BY_\nu(\lambda r) + \\ & + \frac{\pi}{2} \frac{e_{33}}{c_{11}^E} C_1 \left\{ Y_\nu(\lambda r) \int_{r_0}^r J_\nu(\lambda r) \frac{dr}{r} + J_\nu(\lambda r) \int_r^{r_1} Y_\nu(\lambda r) \frac{dr}{r} \right\}. \end{aligned} \quad (17)$$

From the boundary conditions for electric potential (11), constants can be expressed as:

$$C_1 = \frac{U_0}{\alpha}, \quad C_2 = 0, \quad (18)$$

where the angle  $\alpha$  is determined depending on a number of single prisms  $n$ , from which is sectional cylinder consisted, that is  $\alpha = \pi/n$ .

$$\begin{aligned} \hat{E}_r &= 0, \\ \hat{E}_\varphi &= -\frac{1}{r} \left( \frac{U_0}{\alpha} \right), \\ \hat{E}_z &= 0. \end{aligned} \quad (19)$$

For determination of unknown integral constants  $A$  and  $B$ , which enter into the solution for amplitude eigenfunction of componential displacement (17), it is necessary to use boundary conditions (12). Therefore, developed expression for amplitude eigenfunction of mechanical stress in radial direction is:

$$\begin{aligned} \frac{\hat{\sigma}_r}{c_{11}^E} = & \frac{A}{r} \left[ \lambda r J_{\nu-1}(\lambda r) - \left( 1 - \frac{c_{13}^E}{c_{11}^E} \right) J_\nu(\lambda r) \right] + \\ & + \frac{B}{r} \left[ \lambda r Y_{\nu-1}(\lambda r) - \left( 1 - \frac{c_{13}^E}{c_{11}^E} \right) Y_\nu(\lambda r) \right] + \\ & + \frac{e_{33}}{c_{11}^E} \frac{U_0}{\alpha r} \left\{ \frac{e_{31}}{e_{33}} + \frac{\pi}{2} \left[ \left( \lambda r Y_{\nu-1}(\lambda r) - \right. \right. \right. \\ & \left. \left. \left. - \left( 1 - \frac{c_{13}^E}{c_{11}^E} \right) Y_\nu(\lambda r) \right) \int_{r_0}^r J_\nu(\lambda r) \frac{dr}{r} + \right. \right. \\ & \left. \left. \left. + \left( \lambda r J_{\nu-1}(\lambda r) - \left( 1 - \frac{c_{13}^E}{c_{11}^E} \right) J_\nu(\lambda r) \right) \int_r^{r_1} Y_\nu(\lambda r) \frac{dr}{r} \right] \right\}. \end{aligned} \quad (20)$$

By equaling this expression with zero for  $r=r_0$  and  $r=r_1$ , one gets algebraic equations for determination of unknown constants  $A$  and  $B$ .

### 3. NUMERICAL ANALYSIS AND DISCUSSION

Subject of observation in this paper is stressing of circular-cross-sectional PZT4 [13] cylinder with a circular type of polarization, with the following dimensions:  $r_0=7.5$  mm,  $r_1=19$  mm and density  $\rho=7500$  kg/m<sup>3</sup> (Fig. 1). Number of single prisms used in numerical analysis is  $n=30$ .

Based on the obtained solutions (16), (17) and (20), numerical analysis was performed using Matlab software package. Electric potential  $\psi$ , biparametric surfaces of spatial state for amplitude of componential displacement  $u$  and mechanical stress in radial direction  $\sigma_r$  were obtained.

Electric potential  $\psi(\varphi, n, U_0)$  in function of the circular coordinate  $\varphi$ , number of single prisms  $n$  and applied electric voltage  $U_0$  is presented on Fig. 2.

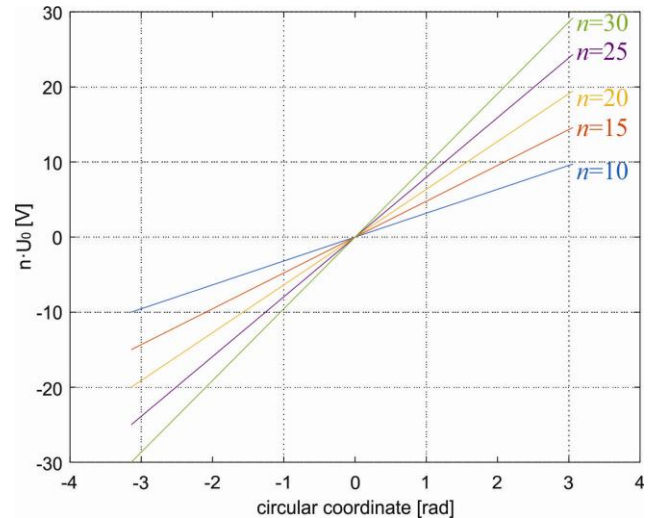


**Fig. 2** Electric potential  $\psi$  in function of the circular coordinate  $\varphi$ , applied electric voltage  $U_0$ , and number of single prisms  $n$

When electric voltage is applied to the cylinder, three resonant modes occur at frequencies up to 400 kHz. On Fig. 3, Fig. 4 and Fig. 5 biparametric surfaces of the amplitude of componential displacement  $u(r,f)$  in function of radial coordinate  $r$ , and frequency  $f$  are presented. Componential displacement for first resonant mode has maximum value on cylindrical surface for  $r=r_0$  (Fig. 3). For other two resonant mode componential displacement has extreme values on cylindrical surfaces for  $r=r_0$  and  $r=r_1$  (Fig. 4), and for  $r=r_0$ ,  $r=13.25$  mm, and  $r=r_1$  (Fig. 5), while in the points of  $r=13.25$  mm (Fig. 4), and of  $r=10.25$  mm and  $r=16.25$  mm (Fig. 5), its value is equal to zero.

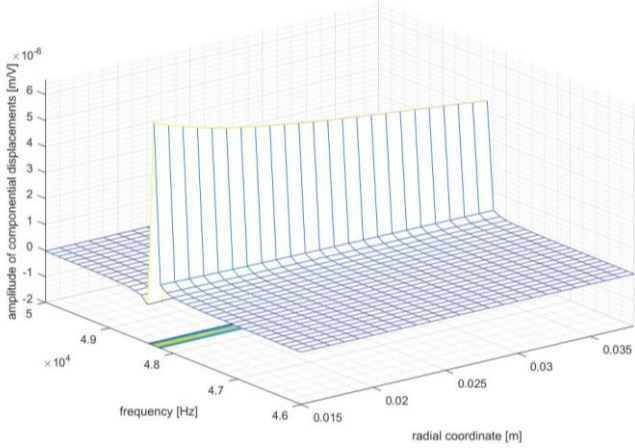


**Fig. 3** Amplitude of componential displacement  $u(r,f)$  in the vicinity of the first resonant mode

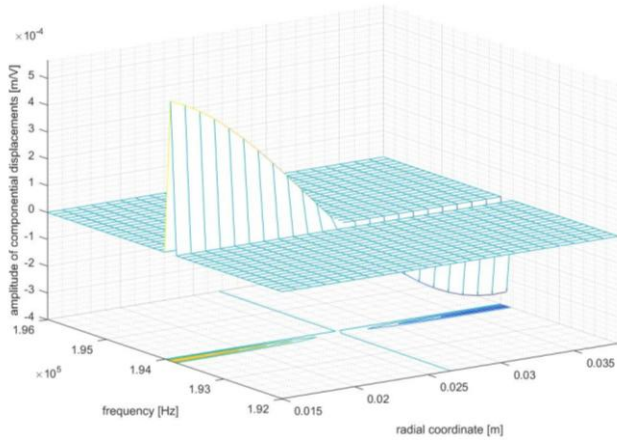


**Fig. 4** Amplitude of componential displacement  $u(r,f)$  in the vicinity of the second resonant mode

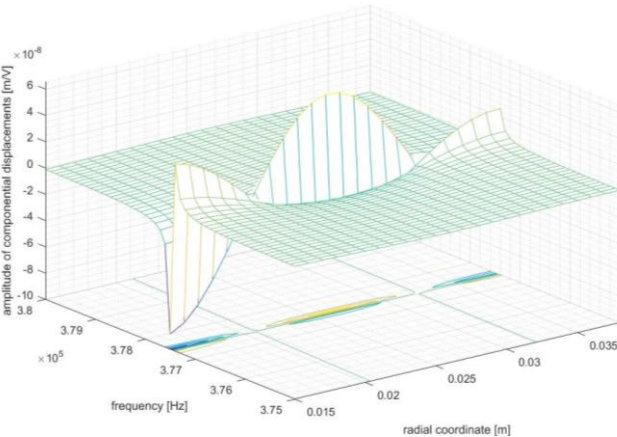


**Fig. 5** Amplitude of componential displacement  $u(r,f)$  in the vicinity of the third resonant mode

Mechanical boundary conditions, in the case of absence of external mechanical stresses on cylindrical surfaces (12), is confirmed as can be seen in Fig. 6, Fig. 7 and Fig. 8. On these figures, biparametric surfaces of the mechanical stress in radial direction  $\sigma_r(r,f)$  in function of radial coordinate  $r$ , and frequency  $f$  are presented. Mechanical stress has maximum value for  $r=11.5$  mm (Fig. 6),  $r=13.25$  mm (Fig. 7), and extreme values for  $r=10.25$  mm and  $r=16.25$  mm (Fig. 8), while on the cylindrical surfaces  $r=r_0$  and  $r=r_1$  its value is equal to zero, which was expected.

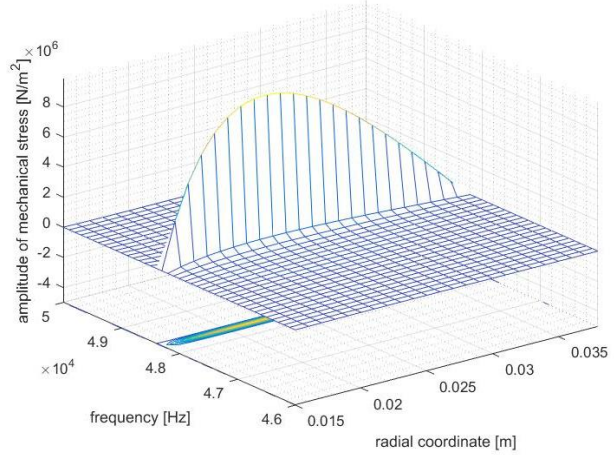


**Fig. 6** Mechanical stress in radial direction  $\sigma_r(r,f)$  in the vicinity of the first resonant mode

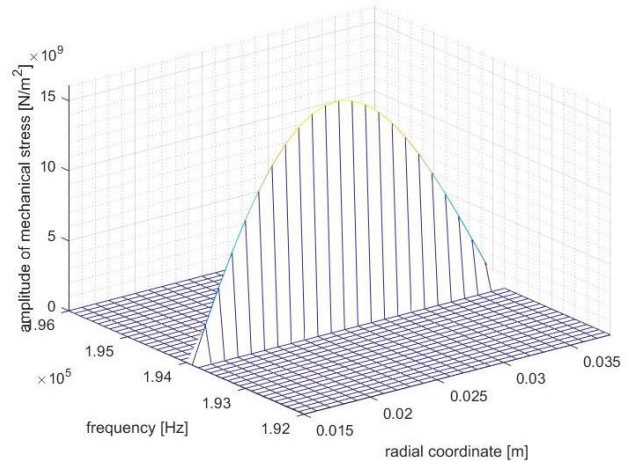


**Fig. 7** Mechanical stress in radial direction  $\sigma_r(r,f)$  in the vicinity of the second resonant mode

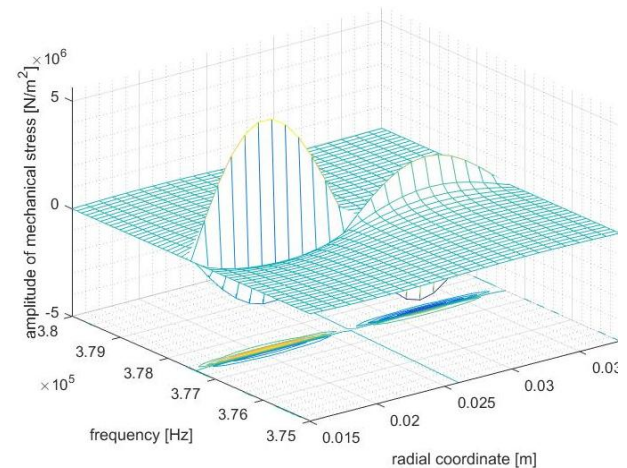


**Fig. 8** Mechanical stress in radial direction  $\sigma_r(r,f)$  in the vicinity of the third resonant mode

#### 4. CONCLUSION

In solving problems of the theory of electroelasticity, for a general case of electroelastic deformable solid-state body stressing, one is faced with great mathematical problems.

This paper presents a method of studying elastic wave propagation in circular-ring cross-sectional piezoceramic cylinder with a circular type of polarization. The observed cylinder has three resonant modes at the following frequencies: 48.3 kHz, 193.9 kHz, and 377.5 kHz. In the second mode, the cylinder acts as a half-wave resonator (Fig. 4 and Fig. 7), and in the third mode the cylinder acts as a full-wave resonator (Fig. 5 and Fig. 8).

This kind of analysis enables prediction of the characteristics of piezoceramic cylinders (as actuators or sensors) with analyzed configuration before their construction.

**Acknowledgements:** The research presented in this paper is financed by the Ministry of Education, Science and Technological Development of the Republic of Serbia under the project TR33035.

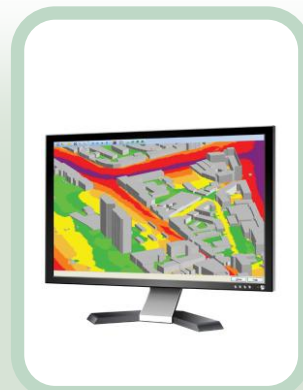
#### REFERENCES

- [1] K.F. Hii, R. Vallance, M.P. Mengüç, "Design, operation, and motion characteristics of a precise piezoelectric linear motor", *Precision Engineering*, vpl. 34, pp. 231-241 2010.
- [2] M.D. Bryant, R.B. Reeves, "Precise positioning problems using piezo-electric actuators with force transmission through mechanical contact", *Precision Engineering*, vol. 6, no. 3, pp.129-134, 1984.
- [3] Y. Peng, Y. Peng, X. Gu, J. Wang, H. Yu, "A review of long range piezoelectric motors using frequency leveraged method", *Sensors and Actuators A Physical*, vol. 235, pp. 240-255, 2015.
- [4] F. Ebrahimi, A. Rastgoo, "Free vibration analysis of smart annular FGM plates integrated with piezoelectric layers", *Smart Materials and Structures*, vol. 17, no. 1-015044, 2008.
- [5] M.T. Kamali, H.M. Shodja, "Three-dimensional free vibration analysis of multiphase piezocomposite structures", *ASCE Journal of Engineering Mechanics*, vol. 132, pp. 871-881, 2006.
- [6] V. Puzyrev, "Elastic waves in piezoceramic cylinders of sector cross-section", *International Journal of Solids and Structures*, vol. 47, no. 16, pp. 2115-2122, 2010.
- [7] H.J. Ding, R. Xu, W. Chen, "Free vibration of transversely isotropic piezoelectric circular cylindrical panels", *International Journal of Mechanical Sciences*, vol. 44, pp. 191-206, 2002.
- [8] J.A. Burt, "The electro-acoustic sensitivity of radially polarized ceramic cylinders as a function of frequency", *Journal of the Acoustical Society of America*, vol. 64, pp. 1640-1644, 1978.
- [9] H.S. Tzou, J.P. Zhong, "A linear theory of piezoelectric shell vibrations", *Journal of Sound and Vibration*, vol. 175, pp. 77-88, 1994.
- [10] D.D. Ebenezer, P. Abraham, "Eigenfunction analysis of radially polarized piezoelectric cylindrical shells of finite length", *Journal of the Acoustical Society of America*, vol. 102, pp. 1549-1558, 1997.
- [11] Lj. Perić, *Coupled Tensors of Piezoelectric Materials State and Applications*, Le Locle, Switzerland, 2005.
- [12] D. Rašković, *Teorija elastičnosti* (in serbian), Beograd: Naučna knjiga, 1985.
- [13] *Five piezoelectric ceramics*, Bulletin 66011/F, Vernitron Ltd., 1976.

# BRÜEL & KJÆR SOUND & VIBRATION MEASUREMENTS

We help our partners and customers  
measure and manage  
the quality of sound and vibration  
in products and environment

With more than 90 sales offices or local agents,  
we provide immediate and comprehensive  
customer support



Contact your local  
sales representative:

**RMS d.o.o.**  
Partizanske avijacije 12/3  
11070 Novi Beograd, Srbija  
Tel.: +381(0)11 2280 951  
Fax: +381(0)11 2280 751  
[www.rms.rs](http://www.rms.rs)

**Brüel & Kjær** 



## DESIGN OF SWITCHED QL QUANTIZER OF LAPLACIAN SOURCE WITH GR CODES FOR MEDIUM QUALITY OF RECONSTRUCTED SIGNAL

Nikola J. Vučić<sup>1</sup>, Zoran H. Perić<sup>1</sup>, Bojan D. Denić<sup>1</sup>

<sup>1</sup> University of Niš, Faculty of Electronic Engineering, Serbia, vucicnikola90@gmail.com

**Abstract** -This paper examines quasi-logarithmic (QL) quantizer for speech signal with variable length codes (VLC). In this research we use Laplacian distribution to depict speech signal's attributes. Switched quantizer, that assumes splitting variance range into separate quantizers and designing a separate quantizer for each of them, leads to the achievement of better performances. Within the variance range, every quantizer has own model with a two-stage code. Our approach uses Golomb-Rice (GR) coding technique, one among the many VLC, due to its simplicity. Performances, i.e. SQNR and average bit rate, are computed depending on various input parameters and optimal ones are found according to the specific criterion.

### 1. INTRODUCTION

Switched quantization is an important type of scalar quantization, where the choice of the desired quantizer among the set of quantizers is done using the predetermined rule. Specifically, scalar quantization refers to the technique where each discrete sample is individually processed [1].

The symmetrical distributions, such as Laplacian or Gaussian, are often used to model real signals, e.g. speech signal [1]. As the speech is non-stationary process whose frequency content varies slowly with time, it can be considered as a quasi-stationary over the short interval (frames). Therefore, it is suggested to be processed frame-by-frame.

Generally, when dealing with non-stationary signals (i.e. the ones whose variance changes within time), the goal is to ensure stable SQNR (robustness property) over the wide range of variances. Some efficient solutions based on switched quantization intended for non-stationary signal processing has been analyzed in [2], [3]. A solution that switches between 16 fixed rate  $\mu$ -law companding quantizers applied to Laplacian sources is given in [2]. Robustness is achieved by dividing the dynamic range of the signal into a number of subranges, with one  $\mu$ -law logarithmic quantizer designed for each subrange. The switching among quantizers is done according to the estimated frame variance. An adaptive switched quantization algorithms choosing between two fixed-rate forward adaptive  $\mu$ -law companding quantizers, restricted and unrestricted ones, for Laplacian source has been analyzed in [3].

In this paper, we focus on the switched quantization technique employing the set of piecewise uniform quantizers (PUQ) based on the piecewise linear approximation to the  $\mu$ -law compression function, followed by the Golomb-Rice encoder.

Particularly, Golomb-Rice code belongs to the group of variable length coding algorithms [1], [4], [5]. The reason of application a given coding technique instead of other one, e.g. Huffman code, can be found in its simplicity as well as in a better performance when large number of symbols is available. Some efficient quantizer solutions based on variable length coding has been proposed in [6]-[15]. Similarly as in [6]-[8], [12]-[14], we propose two stage coder, where the Golomb-Rice encoder is applied in the first quantization stage for coding of segments of the PUQ; in the second quantization stage we use a natural binary code (i.e. fixed length codewords) to encode the cells within the segments. Using the same approach as in [2], the robustness using the proposed switched quantizer is achieved by suitable designing of each of  $N_g$  available quantizers for a certain subrange, and the parameters of the corresponding  $N_g$ -th PUQ are optimized in terms of maximal SQNR. It is assumed frame-by-frame analysis of the signal, and switching among the quantizers is done according to frame variance. In addition, to the receiver is sent index of the employed quantizer.

The rest of the paper is organized as follows: in Section 2 we describe the PUQ and the proposed switched quantizer. In Section 3 we present the performances of this model with numerical results. In Section 4 we conclude the paper.

### 2. SWITCHED QUASI-LOGARITHMIC QUANTIZER OF LAPLACIAN SOURCE WITH GOLOMB-RICE CODING

The solution addressed in this paper is related to efficient coding of the non-stationary signals in a wide dynamic range of the signal variances, and is based on switched quantization model. According to it, the range of interest  $L$  from  $-20$ dB to  $20$ dB is covered by the  $N_g$  non-uniform PUQ based on the piecewise linear approximation of the  $\mu$ -compression law. In particular, the piecewise linear approximation of the compression function is performed due to the easier practical realization. The goal is to obtain almost stable SQNR in the established variance range. In following, we will describe the employed PUQ.

#### 2.1 Piecewise uniform quantizer based on the piecewise linear approximation of $\mu$ -compression law

Compression characteristic of proposed model has a piecewise linear approximation of the  $\mu$ -law characteristic,

where  $\mu+1$  marks a ratio between the biggest and the smallest quant for non-linear logarithmic quantizer [1], whereby applies:

$$\mu = 2^\alpha - 1, \alpha \in N. \quad (1)$$

The compression function with  $\mu$ -law of compression [1] is:

$$c(x) = x_{\max}^g \frac{\ln(1 + \mu|x|/x_{\max}^g)}{\ln(1 + \mu)} \text{sgn}(x). \quad (2)$$

It is very important to notice that parameters  $\mu$  and  $Ng$  are given for the entire range  $L$ , whereas support region is different for every quantizer and therefore we introduce the notation  $x_{\max}^g$ . In PUQ design, the support region  $[-x_{\max}, x_{\max}]$  of is divided into  $2l=16$  segments. As the observed quantizer is symmetric, only positive part of characteristic will be observed. The segment thresholds  $x_i$  can be determined as [1]:

$$x_i^g = \left[ (\mu+1)^{i/l} - 1 \right] \frac{x_{\max}^g}{\mu}, i = 0, \dots, l. \quad (3)$$

The step size within the particular segment is constant (i.e. uniform quantization is assumed) and is given by:

$$\Delta_i^g = \frac{x_{i+1} - x_i}{t} = 2^{i\alpha/l} (2^{\alpha/l} - 1) \frac{x_{\max}^g}{t\mu}, i = 0, \dots, l-1, \quad (4)$$

whereby  $t$  is the number of uniform cells in the particular segment.

Step sizes of consecutive segments have the following ratio:

$$\frac{\Delta_{i+1}^g}{\Delta_i^g} = 2^{\alpha/l} = \sqrt[l]{\mu+1}. \quad (5)$$

Decision levels  $x_{i,j}^g$  which are equally distanced within  $i$ -th segment can be calculated in this way:

$$x_{i,j}^g = x_i + j\Delta_i^g, i = 0, \dots, l-1, j = 1, \dots, t-1. \quad (6)$$

The borderline cases are defined as well:

$$x_{i,0}^g = x_i^g, x_{i,t}^g = x_{i+1}^g. \quad (7)$$

All the samples between  $x_{i,j-t}^g$  and  $x_{i,j}^g$  are represented with the representation level  $y_{i,j}^g$ .

$$y_{i,j}^g = x_i^g + \frac{(2j-1)}{2} \Delta_i^g, i = 0, \dots, l-1, j = 1, \dots, t. \quad (8)$$

The quantizer will be designed for the memoryless Laplacian source, which is accepted as a good model for speech signal:

$$p(x, \sigma) = \frac{1}{\sqrt{2}\sigma} \exp\left(-\frac{|x|\sqrt{2}}{\sigma}\right), \quad (9)$$

where  $\sigma$  is standard deviation.

The measure of signal's quality is distortion. It is consisted from granular  $D_g$  and overload  $D_{ov}$  distortion whose sum is total distortion  $D = D_g + D_{ov}$ . Signal to Quantization Noise Ratio (SQNR) is defined as:

$$\text{SQNR}(\sigma) = 10 \log(\sigma^2/D). \quad (10)$$

The measure of error inserted during quantization is mean-squared error (MSE) distortion. It is usually consisted of component introduced in granular part  $[-x_{\max}, x_{\max}]$ , called

granular distortion  $D_g$ , and the one introduced in the overload part  $[-\infty, -x_{\max},) \cup [x_{\max}, \infty)$ , called overload distortion  $D_{ov}$ . In a case of PUQ and high bit rate (asymptotic quantization) granular distortion is given by [1]:

$$D_g(\sigma) = \int_{-x_{\max}^g}^{x_{\max}^g} \frac{\Delta^2(x, \sigma) p(x, \sigma)}{12} dx, \quad (11)$$

where  $\Delta(x, \sigma)$  represents cell width defined in Eq. (4). We can further derive it as in [1]:

$$D_g(\sigma) = \frac{1}{12} \sum_{i=0}^{l-1} \Delta_i^2(\sigma) P_i(\sigma), \quad (12)$$

whereas  $P_i$  is probability of  $i$ -th segment:

$$P_i(\sigma) = \int_{x_i}^{x_{i+1}} p(x, \sigma) dx = \frac{1}{2} \left[ \exp\left(-\frac{x_i \sqrt{2}}{\sigma}\right) - \exp\left(-\frac{x_{i+1} \sqrt{2}}{\sigma}\right) \right] \quad (13)$$

On the other side, overload distortion is calculated as [1]:

$$D_{ov}(\sigma) = 2 \int_{x_{\max}^g}^{\infty} (x - y_{l-1,t})^2 p(x, \sigma) dx, \quad (14)$$

$$D_{ov} = \exp\left(-\frac{\sqrt{2}x_{\max}^g}{\sigma}\right) \times \left( \left( x_{\max}^g - y_{l-1,t} + \frac{\sigma}{\sqrt{2}} \right)^2 + \left( \frac{\sigma}{\sqrt{2}} \right)^2 \right). \quad (15)$$

## 2.2 Encoding procedure

Having in mind that the support region is split into  $2l = 16$  segments and each segment is split into  $t = N/2l$  cells, we need to find an efficient way to code this information. The G.711 coder [16] has the average bit rate equal to  $\log_2 N$  bits per sample, and our goal is to find a solution that requires lower bit rate.

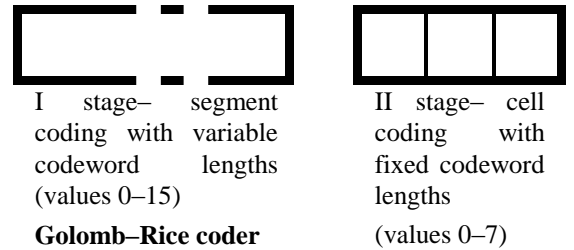


**Fig. 1** Proposed two-stage speech signal coding scheme ( $N=128$ )

Therefore we propose the coder with  $N=128$  levels, and implemented as a two stages coder, as depicted in Fig. 1. In first stage we split whole support region into  $2l = 16$  segments and try to code them with code words of variable length. The segments are labeled from left to right on the axis one after the another with numeral  $i=1, \dots, 2l$  where  $i=1$  marks the furthest segment to the left on the axis, i.e. the segment bounding  $-x_{\max}^g$ , and  $i=16$  marks the furthest segment to the right on axis, i.e. segment next to the  $x_{\max}^g$ . In this way with a proper technique we could achieve better bit usage than the G.711 standard. Here we use a Golomb-Rice coder where

values of  $n$  from 0 to 15 are coded with code words of various lengths, as seen in Table 1. In order to have the most efficient results we must try to designate shorter codes to the segments with higher probability of appearance and longer codes to the segments with lower probability of appearance. Therefore we developed a rule for this designation, as shown in the last column of Table 1. In this way we conclude the first stage of proposed coder. In second stage we code each of  $t = N/2l$  cells naturally with  $\log_2 t$  bits.

**Table 1** Golomb–Rice code,  $k = 2, m = 4$ ; Designating segments  $i = 1, \dots, 2l$  with proper codes  $n = 0, \dots, 15$

$n$	$Si$	$li$	$i$	$n$	$Si$	$li$	$i$
0	000	3	9	8	11000	5	13
1	001	3	8	9	11001	5	4
2	010	3	10	10	11010	5	14
3	011	3	7	11	11011	5	3
4	1000	4	11	12	111000	6	15
5	1001	4	6	13	111001	6	2
6	1010	4	12	14	111010	6	16
7	1011	4	5	15	111011	6	1

The Golomb-Rice (GR) coding technique uses code words of variable length and was created by combining Golomb's (Solomon W. Golomb) and Rice's (Robert F. Rice) coding techniques [4], [5]. This coding technique is well known in literature, hence its detail description is omitted here.

### 2.3 The proposed switched quantization model

The model of switched quantizer we propose is composed of  $N_g$  PUQs described in subsection 2.1 and switching among them is done using the predefined rule. As stated before, the variance range of interest is divided into  $N_g$  equal ranges, and for each range the corresponding PUQ is designed. Let us define signal variance  $\sigma^2 [dB] = 10 \log(\sigma^2 / \sigma_{ref}^2)$ , whereby  $\sigma_{ref}^2 = 1$ .

Also, let us introduce the subrange borders, i.e. lower  $(\sigma_{max}^g)^2 [dB]$  and upper  $(\sigma_{min}^g)^2 [dB]$ ,  $g = 1, \dots, N_g$ . For particular range, the PUQ will be designed for the centered variance, i.e. for  $(\sigma_{ref}^g)^2 [dB] = ((\sigma_{max}^g)^2 [dB] + (\sigma_{min}^g)^2 [dB]) / 2$ .

Specifically, we propose frame-by-frame analysis of the input signal, where frame is composed of  $M$  samples, and for each frame the variance is calculated as:

$$\sigma_j^2 = \frac{1}{M} \sum_{n=1}^M x(n)^2, \quad (16)$$

Further, it is necessary to check in which of  $N_g$  available subranges the estimated variance belongs. With known signal's variance  $\sigma^2$  the matching quantizer  $g$  is unambiguously determined. After that, the suitable PUQ is used for its efficient procession. Additional information about the quantizer, for a frame of size  $M$ , is transmitted to the receiver via  $\log_2 N_g$  bits per frame with  $M$  samples, where  $M$  has values of 120, 180 and 240.

The crucial parameters for the switched quantizer design are: parameter of compression law  $\mu$ , support region  $x_{max}^g$  and  $N_g$  -

the number of PUQ quantizers included by the switched quantizer. Support region  $x_{max}^g$  is defined as:

$$x_{max}^g = \varphi \sigma_{ref}^g, \quad (17)$$

whereby  $\varphi$  is the parameter whose optimal value will be searched for in the range  $[\varphi_{min}, \varphi_{max}]$  for each quantizer. Hence, given  $\mu$  and  $N_g$ , within the  $g$ -th subrange, the goal is to determine the optimal value of  $x_{max}^g$ . It will be selected according to the maximal SQNR criterion, without taking care about the average bit rate. In particular, by setting  $\varphi_{min} = 5$  and  $\varphi_{max} = 50$ , SQNR will be computed, and  $x_{max}^g$  value for which the maximal SQNR is achieved will be adopted as optimal.

## 3. PERFORMANCES

### 3.1 Signal to Quantization Noise Ratio – SQNR

On the range  $L$ , whereby  $\sigma_s^2 = 10^{\sigma_s^2 [dB] / 10}$ , we calculate the average SQNR in a large number of points  $p$  as following:

$$SQNR_{av} = \frac{1}{p} \sum_{s=1}^p SQNR(\sigma_s). \quad (18)$$

### 3.2 Bit rate

The first stage's average bit rate for a particular standard deviation  $\sigma$  is equal to:

$$\bar{R}_l(\sigma) = 2 \sum_{i=1}^l l_i P_i(\sigma), \quad (19)$$

whereas  $l_i$  is the code word's length, defined in Table 1, and  $P_i$  is defined in Eq. (13). We calculate the average bit rate of the first stage on the variance range  $L$  in a large number of points  $p$  as:

$$\bar{R}_l = \frac{1}{p} \sum_{s=1}^p \bar{R}_l(\sigma_s). \quad (20)$$

The bit rate of second stage is constant:

$$R_{II} = \log_2 t. \quad (21)$$

The total average bit rate of the proposed quasi-logarithmic quantizer, with additional information about quantizer, is:

$$\bar{R} = \bar{R}_l + R_{II} + \frac{\log_2 N_g}{M}. \quad (22)$$

### 3.3 Numerical results

The values for  $SQNR_{av}$  and  $\bar{R}$  are shown in Tables 2-4, whereby computations are made for different values of parameters  $N_g$  and  $\mu$ , and for the frame size  $M=240$ .

In Fig. 2 is shown how  $SQNR_{av}$  depends on parameter  $\alpha$ . In all examined cases the maximal  $SQNR_{av}$  is achieved for  $\mu=31$  ( $\alpha=5$ ) and  $N_g=16$ . These values are bolded in Tables 2-4.

We should also find the optimal values. The criterion for choosing the optimal quantizer can be presented as [15]:

$$\psi_z = [SQNR_z - SQNR^*] - [R_z - R^*] \times 6 \frac{dB}{bit}, \quad (23)$$

whereas performances marked with \* refer to the ones with maximal reached  $SQNR_{av}$ , and index  $z$  refers to the currently observed ones. The maximal parameter  $\psi$  would give us the optimally designed quantizer.

**Table 2** Quantizer performances calculated for  $N=64$

$N=64$		$SQNR_{av}$ [dB]		$\bar{R}$ [bit/ sample]	
$\alpha$	$\mu$	$Ng=16$	$Ng=8$	$Ng=16$	$Ng=8$
2	3	24.2373	24.1257	5.2030	5.1656
3	7	26.2759	25.9235	5.2927	5.2502
4	15	<u>27.3216</u>	26.7527	<u>5.4141</u>	5.4106
5	31	<b>27.3257</b>	27.1424	<b>5.6129</b>	5.5586
6	63	26.9270	26.7989	5.7790	5.7258
7	127	26.0900	26.0208	6.0012	5.9462
8	255	25.1573	25.1195	6.1682	6.1178

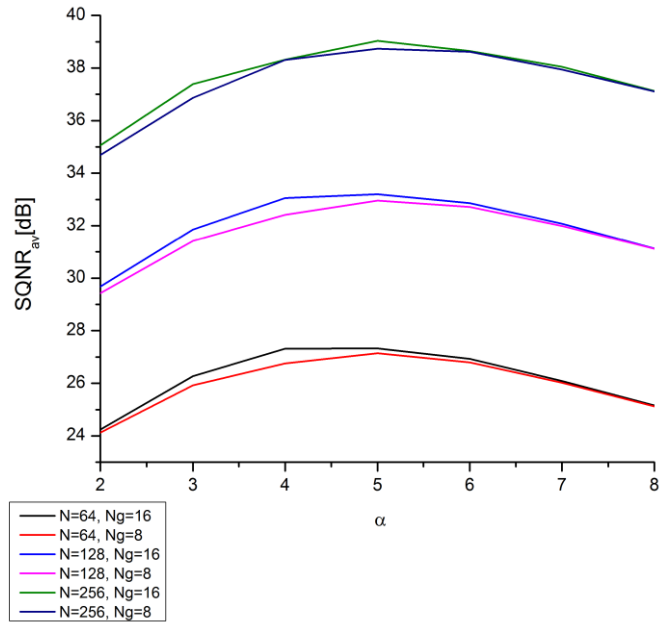


**Fig. 2**  $SQNR_{av}$  calculated for different values of parameter  $\alpha$

**Table 3** Quantizer performances calculated for  $N=128$

$N=128$		$SQNR_{av}$ [dB]		$\bar{R}$ [bit/ sample]	
$\alpha$	$\mu$	$Ng=16$	$Ng=8$	$Ng=16$	$Ng=8$
2	3	29.6819	29.4260	6.1671	6.1372
3	7	31.8579	31.4155	6.2525	6.2169
4	15	<u>33.0518</u>	32.4125	<u>6.3711</u>	6.3678
5	31	<b>33.2000</b>	32.9624	<b>6.5632</b>	6.5149
6	63	32.8660	32.7189	6.7314	6.6830
7	127	32.0763	31.9918	6.9526	6.9020
8	255	31.1325	31.1163	7.1682	7.0777

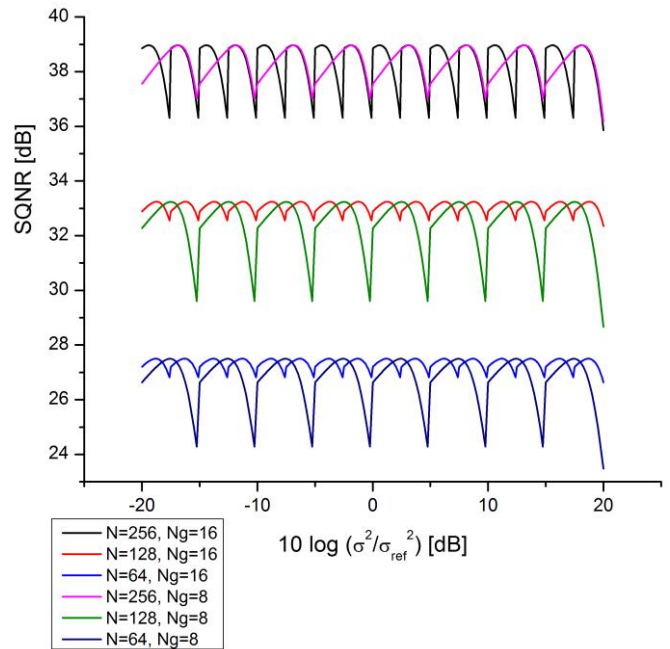


**Fig. 3** Quantizer performances-  $SQNR$ [dB] for  $\mu = 15$

**Table 4** Quantizer performances calculated for  $N=256$

$N=256$		$SQNR_{av}$ [dB]		$\bar{R}$ [bit/ sample]	
$\alpha$	$\mu$	$Ng=16$	$Ng=8$	$Ng=16$	$Ng=8$
2	3	35.0596	34.6920	7.1386	7.1145
3	7	37.3875	36.8672	7.2190	7.1888
4	15	38.3235	<u>38.3072</u>	7.3711	<u>7.2983</u>
5	31	<b>39.0315</b>	38.7387	<b>7.5193</b>	7.4759
6	63	38.6505	38.6195	7.7314	7.6441
7	127	38.0486	37.9453	7.9083	7.8614
8	255	37.1302	37.1075	8.1247	8.0404

#### 4. CONCLUSION

Switched quantizers' performances for different values of  $\mu$ ,  $N$  and  $Ng$  are calculated, whereas we apply the criterion of maximal  $SQNR$ .

The highest average  $SQNR$  is reached parameter  $\mu=31$ , but the optimal quantizer is achieved for  $\mu=15$ , as described above.

Comparing to the improved G.711 quantizer for  $N=256$ , here proposed optimal solution (underlined values in Tables 2-4) has better performances, namely about 6 dB higher average  $SQNR$ . There is also reduction of average bit rate equal to 0.7142 bit/sample.

According to this criterion optimal quantizers are: for  $N=64$  with parameters  $\mu=15$  and  $Ng=16$ , for  $N=128$  with parameters  $\mu=15$  and  $Ng=16$ , and for  $N=256$  with parameters  $\mu=15$  and  $Ng=8$ . These values are underlined in Tables 2-4. Therefore, we decided to show on Fig. 3 ( $SQNR_{av}$ ) and Fig. 4 ( $\bar{R}$ ) the performances for analyzed quantizers (different values for  $N$  and  $Ng$ ) and  $\mu = 15$ .

Another advantage of this solution is implementation of Golomb-Rice code, as it is simpler than other mostly used VLC, e.g. Huffman's code.

In future researches we are looking forward to improving this quantization method and reaching better performances.

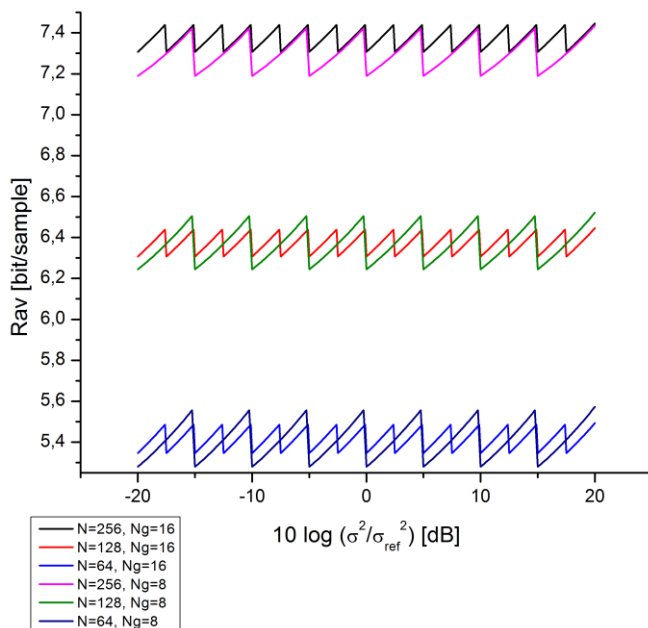


Fig. 4 Quantizer performances- $\bar{R}$  [bit/sample] for  $\mu = 15$

## ACKNOWLEDGMENT

This work was supported in part by the Ministry of Education and Science of the Republic of Serbia, grant no. TR32035 and TR32051 within the Technological Development Program.

## REFERENCES

[1] N. S. Jayant, P. Noll, *Digital coding of waveforms, principles and applications to speech and video*, Prentice Hall, pp. 115–251, 1984.

[2] Z. Perić, A. Mosić and S. Panić, “Coding Algorithm Based on Loss Compression using Scalar Quantization Switching Technique and Logarithmic Companding,” *J. of Information Science and Engineering*, vol. 26, 2010, pp. 967-976.

[3] Z. Perić, J. Nikolić, “High-quality Laplacian source quantisation using a combination of restricted and unrestricted logarithmic quantisers”, *IET Signal Processing*, vol. 6, no. 7, pp. 633 640, 2012.

[4] D. Solomon, *A concise introduction to data compression*, Springer-Verlag, London, pp. 36–38, 2008.

[5] S. W. Golomb, “Run-length encodings”, *IEEE Transactions on Information Theory*, IT-12(3), pp. 399–401, 1966.

[6] Z. Perić, J. Nikolić, J. Lukić, D. Denić: “Two-stage quantizer with Huffman coding based on G.711 standard”, *Przeglad Elektrotechniczny (Electrical Review)*, vol. 88, no. 09a, pp. 300–302, 2012.

[7] N. Vučić, Z. Perić, N. Simić, “Two-stage quantizer with Golomb-Rice coding”, *Book of Abstracts Third International Conference Taktons*, pp. 34–35, Novi Sad, Serbia, 2015.

[8] N. Vučić, Z. Perić, “Quasi-logarithmic quantizer with Golomb-Rice coding”, *XIII International Conference SAUM*, ISBN: 978-86-6125-170-2, pp. 124–127, Niš, Serbia, 2016.

[9] Z. Perić, M. Dinčić, D. Denić, A. Jocić, “Forward adaptive logarithmic quantizer with new lossless coding method for Laplacian source”, *Wireless Personal Communications*, vol. 59, no. 4, pp. 625–641, 2011

[10] Z. Perić, M. Dinčić, M. Petković, “Design of a Hybrid Quantizer with Variable Length Code”, *Fundamenta Informaticae*, vol. 98, no. 2-3, pp. 233-256, 2010

[11] Z. Perić, M. Dinčić, D. Denić, A. Jocić, “Forward adaptive logarithmic quantizer with new lossless coding method for Laplacian source”, *Wireless Personal Communications*, vol. 59, no. 4, pp. 625–641, 2011.

[12] N. Vučić, Z. Perić, M. Dinčić, “Switched Quasi-Logarithmic Quantizer with Golomb–Rice Coding”, *Elektronika ir elektrotehnika*, vol. 23, no. 4, 2017.

[13] N. Vučić, Z. Perić, M. Dinčić, “Design of Switched Quasi-Logarithmic Quantizer for Gaussian Source with Variable Length Codes”, *13<sup>th</sup> International Conference TELSIKS*, pp. 203–206, Niš, Serbia, 2017.

[14] N. Vučić, Z. Perić, “Quasi-logarithmic quantizer with Golomb-Rice coding”, *XIII International Conference Systems, Automatic Control and Measurements- SAUM*, pp. 124–127, Niš, Serbia, 2016.

[15] Z. Perić, J. Nikolić, “An adaptive waveform coding algorithm and its application in speech coding”, *Digital Signal Processing*, vol. 22(1), pp. 199-209, 2012.

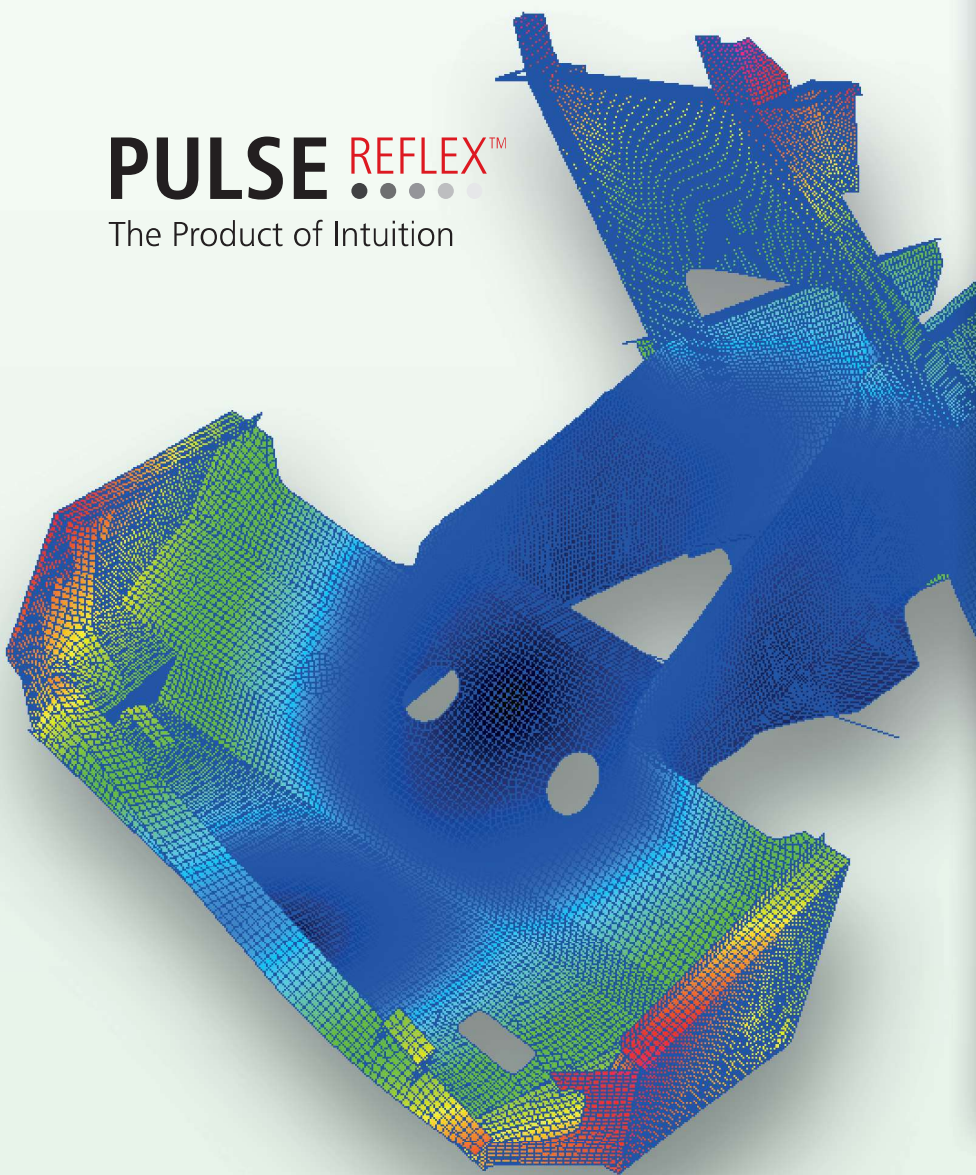
[16] Recommendation G.711, *Pulse code modulation of voice frequencies*, ITU-T, (1972).

PULSE Reflex Structural Dynamics

# Make decisions based on results you can trust

**PULSE** REFLEX™

The Product of Intuition



## A LONG-TERM BUSINESS PARTNER

Brüel & Kjær delivers innovative solutions that create sustainable value for customers in a diverse number of industries

[www.bksv.com/StructuralDynamics](http://www.bksv.com/StructuralDynamics)

Brüel & Kjær 

## VIBRODIAGNOSTIC METHODS FOR DETECTION OF STRUCTURAL AND FUNCTIONAL FAILURE OF MACHINES

Dragan Jovanović<sup>1</sup>, Milena Mančić<sup>2</sup>, Miomir Raos<sup>2</sup>, Slobodan Jovanović<sup>1</sup>, Milan Banić<sup>1</sup>, Marko Mančić<sup>1</sup>

<sup>1</sup>University of Niš, Faculty of Mechanical Engineering, Serbia, dragan.jovanovic@masfak.ni.ac.rs

<sup>2</sup>University of Nis, Faculty of Occupational Safety, Serbia

**Abstract** - The machines operate in a design mode which can be with more or less pronounced oscillatory effect on the machine as well as on the construction or on the environment. One of the most important method in detecting the cause of the failure in machine operation mode is a vibrodiagnostic analysis. The paper will present some of the classic examples and analysis of the FFT spectrum, but also examples from the practice that deviate from the classic vibrodiagnostic methods and require a different approach. The degree of complexity of the used method depends on the type and size of the machine, as well as its interaction with the environment. In complex vibration systems it is not possible to use only simpler methods, but it is necessary to create simple dynamic models that are checked by simulation of software for continuum analysis such as ANSYS, as shown in one example in this paper.

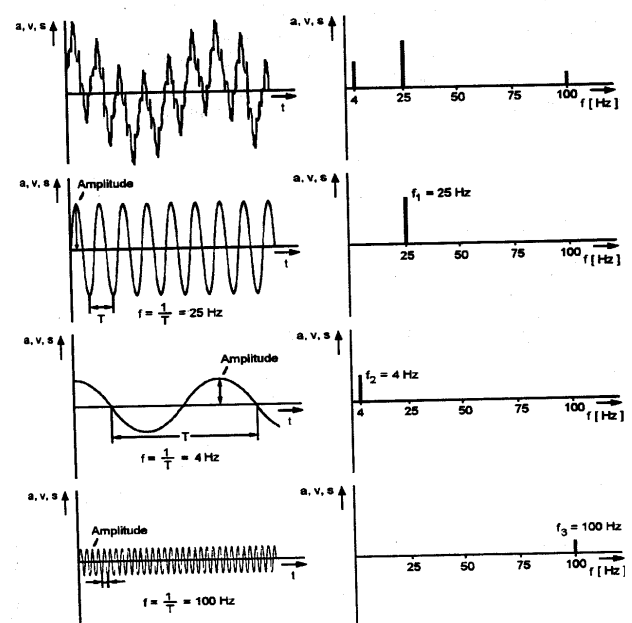
### 1. INTRODUCTION

Machines have their nominal operating mode, and in a design mode that can be with more or less pronounced oscillatory effect both on the machine itself, and on the construction structure and as well on the environment [1]. When designing machines, the measures to prevent vibration impacts on the immediate and further environment, is taken into account. However, there are often disruptions in the operation mode of the machine, which affect its dynamic behavior, manifested with the increase of vibration, noise, increase of the bearings temperature, all of which indicates a disorder in the operation of the machine. Typically, on rotating machines, maintenance procedures prescribed by the manufacturer are known, and can be seen in the replacement of bearings, lubrication of parts that are in direct contact, replacement of the vibration isolation elements in which degenerative processes occurred and other maintenance methods [3]. For cheaper machines, aggregate replacement of the whole assemblies or parts of machines, is most often carried out, while in large and expensive machines and constructions, it is often not possible for financial and logistic reasons, mostly because of the time required for the production of parts, which may take up to several months [2]. The situation is similar with integrated systems that have continuous technology, when without a single segment in a process or machine, production is not possible, and large economic losses are created. One of the most important methods in detecting the cause of faults in machine operation is a vibrodiagnostic analysis.

Vibrodiagnostic methods have been present for several decades and there are diagrams and instructions to compare individual states with known error models that are shown in so-called diagnostic tables [3]. However, these tables are mainly made for conventional rotary machines consisting of an electric motor, a transmission mechanism with couplings and the machine itself. Specific machines and constructions require in addition to the usual vibrodiagnostic methods and special analysis of the cause of the condition disorder. The paper will show some of the examples that deviate from the classic vibrodiagnostic tables and require a different approach.

### 2. VIBRODIAGNOSTIC METHOD FOR FUNCTIONAL MACHINE FAILURE

Vibrodiagnostic tables offered by large manufacturers of diagnostic equipment (such as Bruel & Kjaer, Oneprod, SKF and others) are very effective in detecting functional faults of machines with small and medium-sized rotational movements. Figure 1 shows a conventional rotary machine [3], a fan that functions in air conditioning systems, or in systems with the removal of gases and dust from work spaces as well as with other roles and its oscillatory simple model.



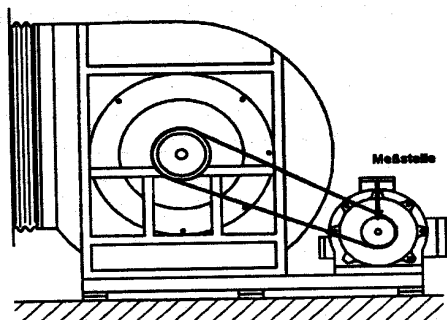


**Fig. 1** The example of the fan in operation and the simplest oscillating model [3]

Figure 1 shows an example of a so-called vibrodiagnostic table for the fan in operation, which FFT analysis indicates possible causes of the problems in the operation of such a system. The task is to carry out vibration measurements on the machine and compare the obtained diagrams with the given tables in order to detect the characteristic frequencies and conclude which is the most likely cause of the increased vibrations, as well as which measure should be applied on the disorder. The intervention measures can be: replacement of bearings, replacement of belts, replacement of pulleys, balancing, adjustment of compatibility and parallelism. As a result of the action of the intervention measure, the improved -regular condition of the dynamic behavior of the machine is obtained.

In this paper, some characteristic examples from industrial practice are given for the easier consideration of the discussed issues.

On the example of one electric motor, shown in figure 2, where the measured FFT spectrum is given to two different characteristic points provided by the literature for such a device (system), and using the methodology of diagnosis diagnostic tables [3], it has been concluded that the measured spectrum coincides with the table values and need the replacement of the bearings. After the indicated intervention, the replacement of the bearings reflected on the measure, the intervention measure gave a positive result.

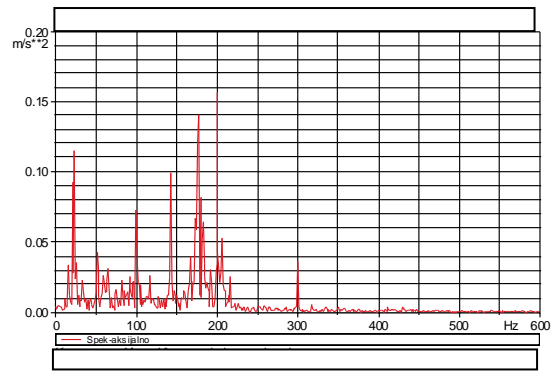
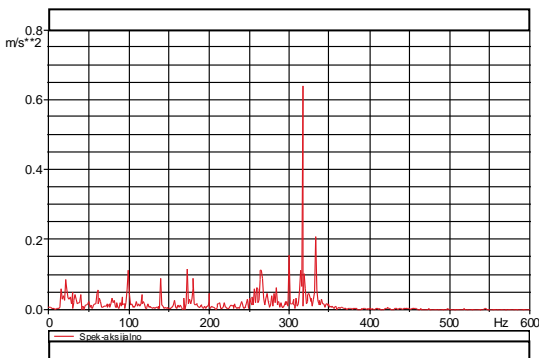


**Fig. 2** Measured FFT spectrum for the vibrations of the electric motor in two control points

The next example is an industrial fan with an increased level of vibration. By analyzing the FFT spectrum and by using the vibrodiagnostic tables and data on the type and characteristics of bearings, a defect of bearings has been identified as a cause of the increased level of vibrations. FFT spectrum for this example is given in the figure 3.

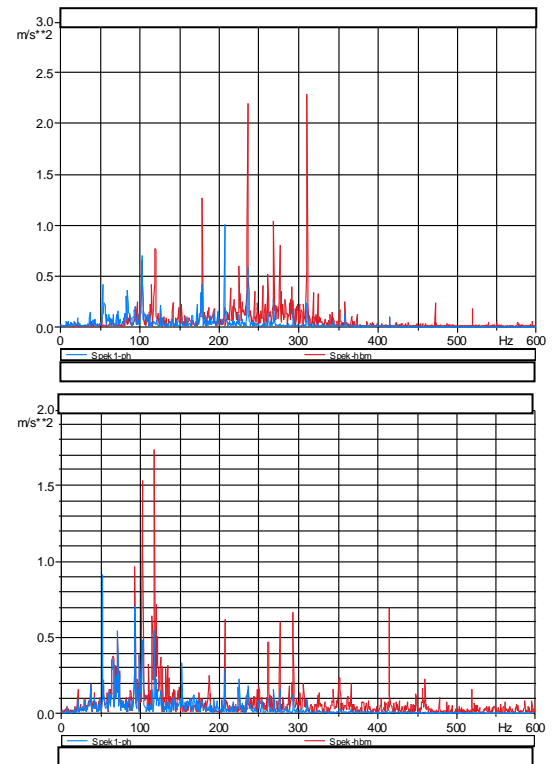


**Fig. 3** FFT spectrum for the example of an industrial fan

FFT analysis before and after an intervention measure was performed, and it is shown on the example of the fan (figure 4). The effects of the interventional measure - balancing the rotary cups of the burner for the fuel oil are shown. The result of this measure is the improved state of the system which is reflected in the reduced vibration level at the same speed.

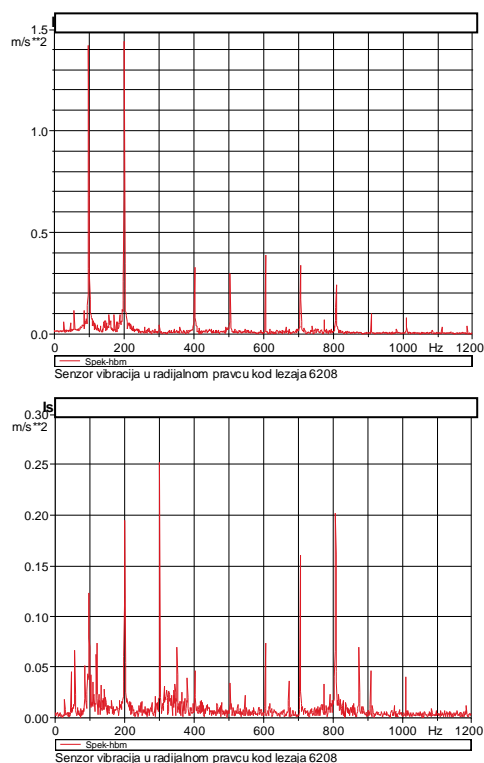


**Fig. 4** An example of a FFT spectrum before and after an intervention measure

In the functional disorders of machine operation, using the appropriate diagnostic tables of the FFT spectrum, we have already discussed, with the adequately completed measurement, allows relatively easily detection of the problems and selection of the adequate corrective measure which is technically most feasible.

### 3. VIBRODYGNOSTIC METHOD FOR COMBINED FUNCTIONAL STRUCTURAL DISORDERS IN MACHINE OPERATION

When disruptions occur in the operation of larger machines, in which, beside the machine, the environment of the machine has a significant influence, most commonly concrete or metal construction, problems are much more complicate, and it can not be reduced to the classic vibrodignostic tables that are applicable to simple systems with a single forced frequency and several oscillating masses and vibration dampers. Such problems in principle are solved multidisciplinary, and it is necessary to look at the dynamic structure of the construction and machine construction. Most often in this case, they are objects of large dimensions, which can not be easily corrected with given measures into the nominal mode of operation. The first step in solving these problems is the vibrodygnostic picture of the machine and the analysis of possible effects where the environment of the machine is taken into account.

This problem has been addressed through several examples from industrial practice. The first is the example of a cement mill. Figure 5 shows the principled scheme of one example for a cement mill, which is considered in this example.

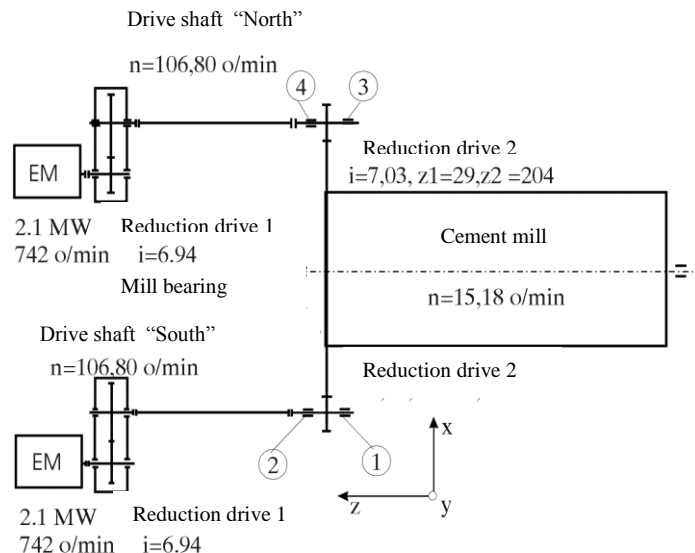


**Fig. 5** Principal scheme of cement mill

The vibrodiagnostic analysis was carried out at the characteristic points, but it was noticed that the problem was manifested in bearings 3 and 4 on the "north" drive shaft because the bearing force was higher than the base, while the problem was less pronounced on the "south" drive shaft where the force operated downwards fundamentals. Figure 6 shows the vibrations in the FFT spectrum, and it was noticed that the vibrations were dominant in the frequencies of  $\approx 52\text{Hz}$ ,  $\approx 105\text{Hz}$ ,  $\approx 150\text{Hz}$  and  $\approx 208\text{Hz}$ .

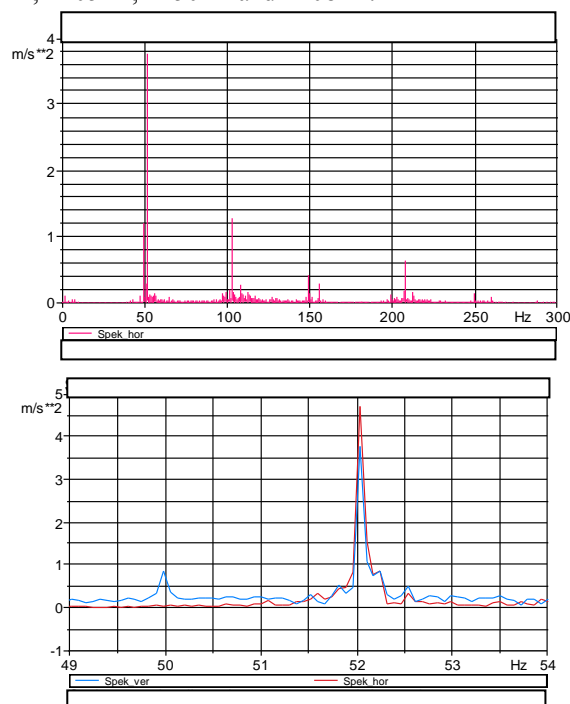


**Fig. 6** FFT spectrum for the vibration level of the cement mill. A detailed analysis taking into account the kinematic scheme shown in Figure 5 and the number of teeth of the mill and drive gear indicated that the problem is caused by the teeth of the larger and smaller gear of the mill when they come in contact. The replacement of the bigger and smaller gear was done, and it lasted a year, and during this time the vibration level on the mill was permanently monitored.

The following example is the Sunds defibrator, which also represents a complex technical dynamic system where vibrodiagnostic tables can only partially indicate the problem. Defibrator is a knife machine that homogenizes the mass of wood parts and necessary ingredients for the production of special wooden boards used in the furniture industry. In the figure 7, the appearance of the machine and simplified scheme are given, while figure 8 shows the FFT spectrum, which is also considered.

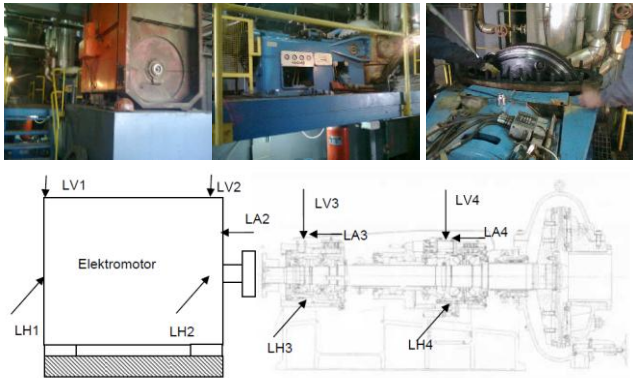


**Fig. 7** Appearance and simplified SUNDs defibrator scheme

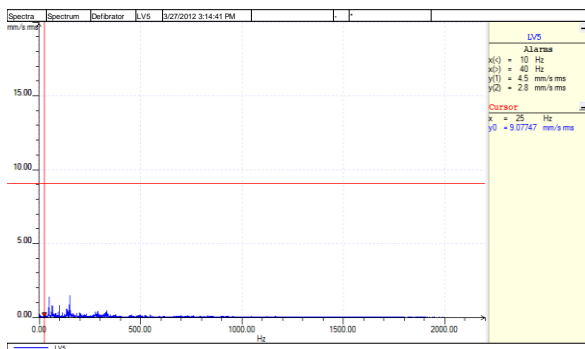


**Fig. 8** FFT spectrum of defibrator SUNDs

Based on the analysis of the FFT spectrum it was noted that the problem is due to the burnt out machine blades and the partial imbalance of the electric motor fan, whose power is 1.6MW at the speed of 1486 rpm, after the change of blades and the balancing of the fan, the problem was solved.

In some cases, it is not enough to perform the machine's vibration diagnostics to solve the problem, but it is necessary to use complex methods in combination with the vibrato-diagnostic.

In the case of a machine placed on an inadequate foundation, it was necessary to decide whether the machine could operate under such conditions. Due to the lack of technical documentation, the method of photogrammetric formation of the CAD model for recording the machine was first used.

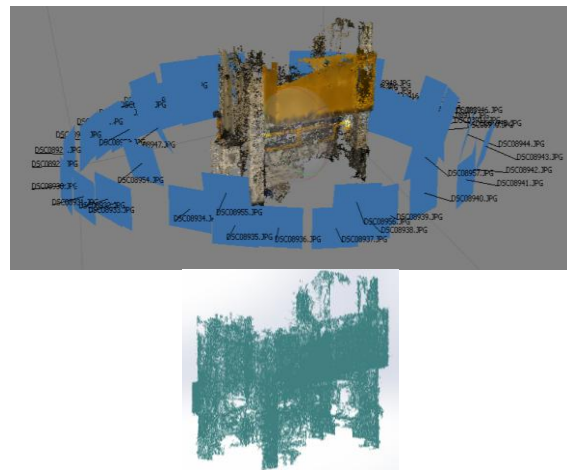


**Fig. 9** Photogrammetric recording of a CAD model for a) recording and b) dot model

By inserting the captured points in the CAD software Solidworks, a simpler but precise model is acquired, and it is shown in figure 10, which can now be used for simulation of the machine's dynamic behavior.

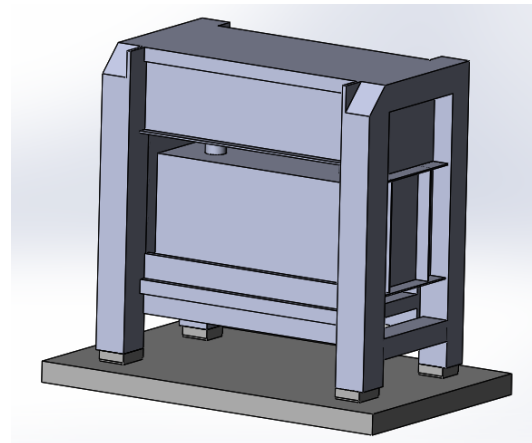


**Fig. 10** The obtained CAD model

The degree of approximation of the obtained model was evaluated based on the data on the weights of the machine parts and data on the total weight of the whole machine, and finally a simplified CAD model in the Solidworks software package was obtained, which was further used for simulation and evaluation of the machine's vibrodynamic behavior.

The simulation was carried out in order to establish the dynamic impact of the work on the floor construction made of concrete MB30 with steel needles ZS/N dimension 0.75x60mm in quantity of 20kg/m<sup>3</sup>.

The results of the dilatation and tension simulation of the concrete plate below the supports and the panel area towards the boundary surfaces showed that the local contact pressure below the supports has an increased value, which is the consequence of the selection of a poor system of vibration isolation, but that there are no increased tensions and dilations on the entire board and boundary surfaces, as shown in figure 11.

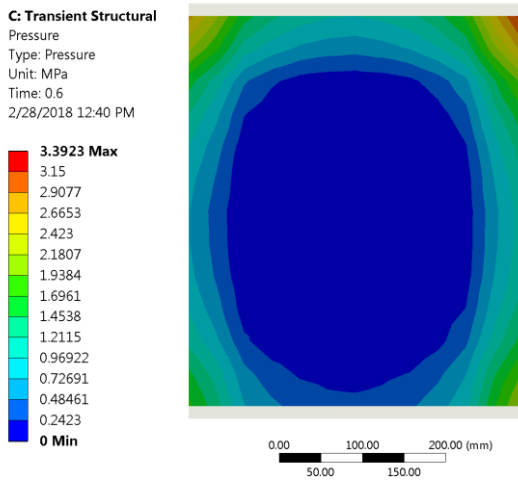
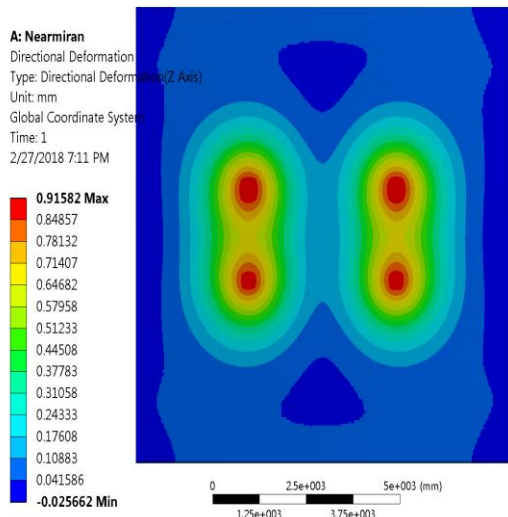


**Fig. 11** Deformation of concrete plate- simulations in the ANSYS software

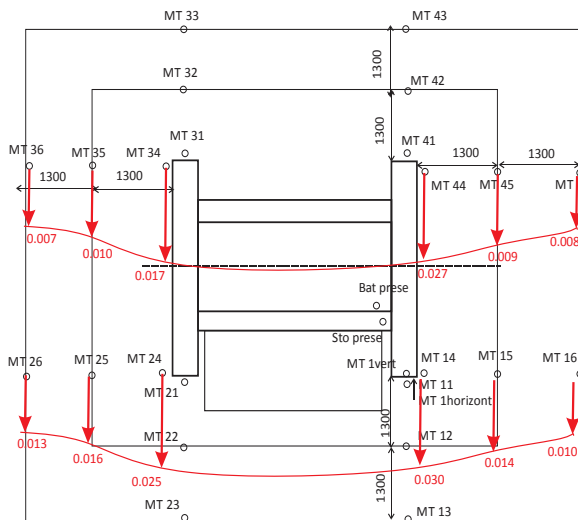


**Fig. 12** Values of the measured acceleration on the concrete plate in the horizontal in relation to the press of the press

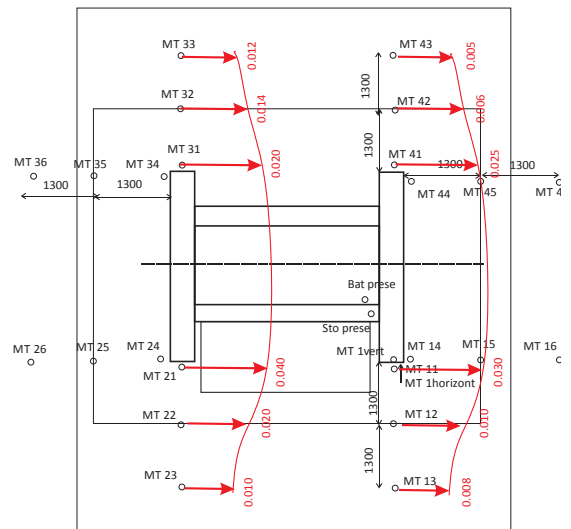


**Fig. 13** Values of the measured acceleration on the concrete slab in the vertical direction in relation to the press of the press

By comparing dynamic behavior obtained by experimentally measuring vibrations with vibrational diagnostic methods with results of dynamic behavior and simulation in the ANSYS software package, a match in the vibration values is seen, which means that the model is verified and based on this it was possible to claim that the machine will be able to work safely under conditions in which it is environmentally free and despite the failure to comply with the conditions set by the machine manufacturer.

#### 4. CONCLUSION

Vibrodyagnostic methods represent the most reliable procedures in troubleshooting of the problems when it comes to machines with rotary masses. The degree of complexity of the method used depends on the type and size of the machine as well as its interaction with the environment. It is very important to observe the transmission of vibrations through the structure of the machine as it determines the influence of certain parts of the machine on its dynamic vibration effect. For simpler machines, it is sufficient to use diagnostic tables offered by manufacturers and by comparing characteristic frequencies to analyze possible causes of the phenomenon and to make corrective measures. The degree of complexity of corrective measures directly affects the cost of troubleshooting, so always use the right measures. In complex vibration systems it is not possible to use only simpler methods, but it is necessary to create simple dynamic models that are checked by simulation in the software for continuum analysis such as ANSYS, as shown in the last example.

#### REFERENCES

- [1] P. Girdhar, C. Scheffer, "Practical Machinery Vibration Analysis and Predictive Maintenance", ISBN 0 7506 6275 1, Elsevier.
- [2] H. Ahmadi, K. Mollazade, "A practical approach to electromotor fault diagnosis of Imam Khomaynei silo by vibration condition monitoring", African Journal of

- Agricultural Research, Vol. 4 (4), pp. 383-388, April 2008.
- [3] ISO 10816-1 - Mechanical vibration -- Evaluation of machine vibration by measurements on non-rotating parts -Part 1: General guidelines.
- [4] ISO 10816-3:2009, „Mechanical vibration -- Evaluation of machine vibration by measurements on non-rotating parts -- Part 3: Industrial machines with nominal power above 15 kW and nominal speeds between 120 r/min and 15 000 r/min when measured in situ”
- [5] K. Bose, “Sliding mode control of induction motor”, in *Proc. IEEE Ind. Appl. Soc. Annu. Meeting*, 1995, pp. 479-486
- [6] EASA Standard AR100-2006., “Recommended practice for the repair electrical apparatus”.
- [7] H. H. Lee, N. Nguyen, J. M.Kwon, “Bearing Fault Diagnosis Using Fuzzy Inference Optimized by Neural Network and Genetic Algorithm”, *Journal of Electrical Engineering & Technology*, Vol. 2, No. 3, pp. 353~357, 2007.
- [8] W. Reimche, U. Südmersen, O. Pietsch, C.Scheer, F. W. Bach, ”Basic of vibration monitoring for fault detection and process control” III, Pan-American Conference on nondestructive testing, Rio de Janeiro, 2003, pp. 1-10.
- [9] M. Samhour, A. Al-Ghandour, S. Alhaj Ali I. Hinti b, W. Massad, “An Intelligent Machine Condition Monitoring System Using Time-Based Analysis: Neuro-Fuzzy Versus Neural Network, *JJMIE*, Volume 3, Number 4, December 2009., pp. 294-305.
- [10] D. Jovanović, N. Živković, M. Raos, Lj. Živković, M. Jovanović, M. Prašćević, “Testing of the level of vibration and parameters of bearings in industrial fan”, *Applied Mechanics and Materials*, Vol. 430, DOI10.4028/www.scientific.net/AMM.430.118, pp 118-122, 2013.
- [11] S. Jovanović, D. Jovanović, 'Dinamičko uravnoteženje kao najvažniji postupak za poboljšanje dinamičkog ponašanja ventilatora", XXII Konferencija Buka i vibracije, Niš, ISBN 978-86-6093-019-6, pp161-164
- [12] D. Jovanovic, M. Jovanovic, M. Raos, N. Živkovic, M. Stankovic, M. Protic, “Vibration analysis of insufficiently repaired well pump - a case study”, *Applied Mechanics and Materials*, Vol. 801 (2015) pp 207-212 doi:10.4028/www.scientific.net/AMM.801.207
- [13] D. Jovanović, M. Jovanović, N. Živković, Lj. Živković, M. Raos, “Belt conveyor drive gearbox problem caused by unpaired gears-a case study”

## EVALUATION OF WBV BY ISO 2631-1 FOR WORKERS OF BROADCASTING AND COMMUNICATIONS COMPANY IN TRANSPORT TO AND FROM MOUNTAIN REPEATER STATION

Jovan Miočinović<sup>1</sup>, Biljana Beljić Durković<sup>2</sup>

<sup>1</sup> TEHPRO d.o.o., Serbia, jovan.miocinovic@tehpro.rs

<sup>2</sup> TEHPRO d.o.o., Serbia, biljana.beljiic@tehpro.rs

**Abstract** - Adding to the expected professional risks arising in their workplaces the workers may be exposed to risks on the way to and from the workplace, by law also considered professional. In this paper is presented the evaluation of WBV for workers of Broadcasting and communications company in transport to and from their workplace in mountain repeater station.

### 1. INTRODUCTION

While people use transportation regularly in their everyday life when going to their work and returning homes, and therefore are exposed to a variety of environmental conditions including whole-body vibration, some are exposed to more extreme conditions. Evaluation of the vibration exposure during transportation in off-road vehicle for the workers of Broadcasting and communications company in transport to and from their workplace in mountain repeater station was made in order to establish probable vibration exposure levels in transport and estimate the possible resulting health risk. Evaluation is made according to ISO 2631-1 [1]. Basic and the additional evaluation method were applied. Measurement results were compared to health guidance caution zones according to ISO 2631-1 and daily exposure action and limit values according to Regulation [2] and Directive 2002/44/EC [3].

### 2. INSTRUMENTATION, SAMPLE AND MEASUREMENT LOCATION AND CONDITIONS

#### 2.1. Instrumentation

For measurements was used SVAN 958 four channels sound (Type 1 IEC 61672-1:2002) and vibration (Type 1 ISO 8041:2005) level meter and analyser with seat accelerometer for whole-body measurements with DYTRAN 3143M1 - IEPE type triaxial accelerometer (Fig. 1).



Fig. 1 SVAN 958 four channels sound and vibration level meter and analyser

#### 2.2. Sample and measurement location and conditions

Measurements were made in vehicle in real conditions, in vehicle model mostly used. All measurements were made in SUV Lada Niva (BA3 2121) (Fig.2). Due to its engine and chassis design, Niva may be defined as one of the first SUV (Sport Utility Vehicle) models, but with the features and possibilities of the real terrain vehicle, made to be functional and durable, and still mostly used in Serbia as company car for bad road conditions and hardly accessible areas.

All measurements were made in the same vehicle.

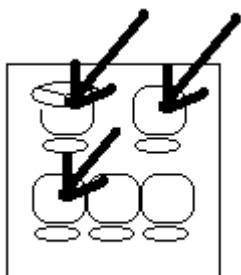


Fig. 2 SUV Lada Niva

Generally there are one-week shifts in repeater station, so workers are exposed to vibration in vehicle twice in week,

when going to and from their work in shift. However, the subcontractors that need to work in repeater station are also exposed when going to and from their work, and that exposition may be more frequent, even twice in a day.

Measurements were taken on the driver's, co-driver's and back left passenger's seat. (Fig.3).



**Fig. 3** Measurement positions in vehicle. Positions are marked with an arrow pointing to the measurement position

**Table 1** Number of measurements per repeater location, driving direction and measurement position

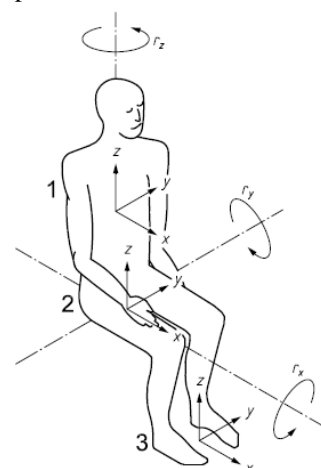
Repeater station location	driving direction (to or from the station)		measurement location (seat)			Number of measurements taken
	to	from	driver's	co-driver's	passenger's	
RS Jastrebac	2	1	1	0	2	3
RS Besna Kobila	1	0	0	0	1	1
RS Kopaonik – Gobelja	1	1	0	1	1	2
RS Ovčar	1	1	0	1	1	2
RS Deli Jovan	1	1	0	0	2	2

Measurements were taken according to ISO 2631-1 in seated position, with a person seated on the seat accelerometer according to a coordinate system in Fig. 4.

Measurements were made in controlled real environment. Measurements were made on the road to and from the repeater station. The road was bumpy macadam road, partly heavily damaged. Mountain roads in rain seasons turn into watercourses and that heavily damages macadam road turning the ride almost into off-road ride. All measurements were taken in September and October 2016 and 2018 in dry conditions.

From possible influences on vibration in vehicle other than road condition one could specify the driver's experience and vehicle speed. The driver's experience may strongly influence the result. Taking that into account the reported measurements were taken with the same driver on all locations. As for the possible correlation with vehicle speed, the present results are inconclusive [4]. However, on the

mountain bumpy roads one can drive only slowly (usually up to 20 km/h) and with utmost care, and that limits the possible variation due to vehicle speed.



**Key**  
 1 seat-back  $r_x$  roll  
 2 seat-surface  $r_y$  pitch  
 3 feet  $r_z$  yaw

**Fig. 4** Basicentric axes of the human body for seated position according to ISO 2631-1

### 3. MEASUREMENT RESULTS

#### 3.1. Weighted r.m.s. accelerations

Measurements were taken in x-, y- and z-axis oriented as in Fig. 4.

The weighted r.m.s. acceleration is determined for each axis (x, y and z) of translational vibration on the surface which supports the person. The assessment of the vibration is made with respect to the highest frequency-weighted acceleration determined in any axis on the seat pan (1), and also the vector sum is used to estimate health risk while the vibration in x, y and z axes is comparable (2), according to [1]:

$$a = \left( \text{Max} \{ k_x^2 a_{w_x}^2, k_y^2 a_{w_y}^2, k_z^2 a_{w_z}^2 \} \right)^{1/2} \quad (1)$$

$$a_v = (k_x^2 a_{w_x}^2 + k_y^2 a_{w_y}^2 + k_z^2 a_{w_z}^2)^{1/2} \quad (2)$$

As the results are presented the average accelerations for each repeater station location. The average value is arithmetic mean value for different measurement locations and driving directions for the same repeater station location.

**Table 2** Measurement results: weighted r.m.s. accelerations for each repeater station location.

Repeater station location	$a_x$ [m/s <sup>2</sup> ]	$a_y$ [m/s <sup>2</sup> ]	$a_z$ [m/s <sup>2</sup> ]	$a$ [m/s <sup>2</sup> ]	$a_v$ [m/s <sup>2</sup> ]
RS Jastrebac	0,396	0,436	0,704	0,704	1,18
RS Besna Kobilja	0,375	0,252	0,506	0,525	0,656
RS Kopaonik – Gobelja	0,479	0,325	0,766	0,766	1,243
RS Ovčar	0,535	0,453	0,635	0,749	1,366
RS Deli Jovan	0,572	0,405	0,730	0,801	1,496

## 4. EVALUATION

### 4.1 Basic evaluation method

As for assessment of whole-body vibration with respect to health, there are several limit values for comparing with daily vibration exposures.

For basic evaluation method in ISO 2631-1 there are health guidance caution zones (Fig. 5), given in Figure B.1 in Annex B of the standard. Zones are defined with equations ([1], eq. (B.1) and (B.2)) :

$$a_{w1} * T_1^{1/2} = a_{w2} * T_2^{1/2} \quad (3)$$

$$a_{w1} * T_1^{1/4} = a_{w2} * T_2^{1/4} \quad (4)$$

where  $a_{w1}$  and  $a_{w2}$  are the weighted r.m.s acceleration values for the first and second exposures and  $T_1$  and  $T_2$  are the corresponding durations. First equation determines zone indicated by dashed lines in figure, and second equation the one indicated by solid lines.

Regulation [2] and Directive 2002/44/EC for basic evaluation method gives daily exposure action value of 0,5 m/s<sup>2</sup> standardised to an eight-hour reference period and daily exposure limit value of 1,15 m/s<sup>2</sup> standardised to an eight-hour reference period, and those values determine zone indicated by red dashed lines in Fig. 5.

When comparing measured values in z direction with zone limits according to B.1, B.2 and Directive (cross section of horizontal red lines and zone borders in the figure) one can see that in average,  $a=0,71$  m/s<sup>2</sup>, health caution zone is achieved when spending 1 hour in transportation, according to eq. B.2. When taking into account vibrations in all directions according to (2) for the average value  $a_v=1,2$  m/s<sup>2</sup>, health caution zone is achieved already in 10 min. As for the maximum acceleration values measured,  $a_v=1,5$  m/s<sup>2</sup>, health caution zone is achieved after 6 minutes spent in the vehicle (first limit of zone B2), spending 35 minutes will bring the passenger in zone B1 and after 55 minutes the exposure exceeds daily exposure action value.

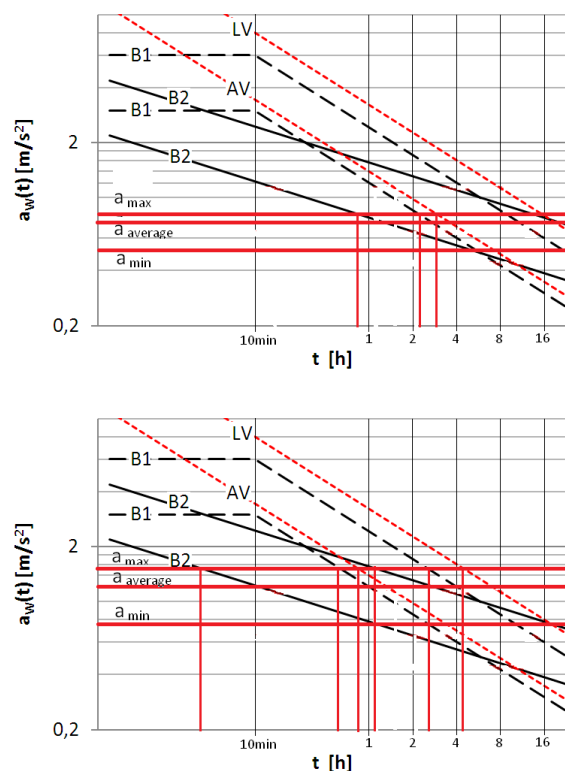


**Fig. 5** Health guidance caution zones. With solid lines is indicated the zone that corresponds the equation B.2 of ISO2631-1, with dashed lines the zone that corresponds the equation B.1. of the same standard and with dotted red lines the zone that is defined with action value and limit value of Directive 2002/44/EC. Horizontal red lines represent the experimental measured weighted r.m.s. acceleration values  $a$  (upper figure) and  $a_v$  (lower figure), maximal, average and minimal. Vertical red lines indicate the time when the corresponding caution zone is reached.

In the table 3 actual daily vibration exposure normalized to a reference period of 8 h,  $A(8)$ , for all the measurements are presented. Here is assumed that the person goes to and from the station in the same day, that is, overestimated for the workers that go for the one week shift and achievable for subcontractors. For the workers that go for the shift the presented values should be divided in half.

**Table 3** Daily vibration exposure normalized to a reference period of 8 h for the actual measurements.

Repeater station location	$a$ [m/s <sup>2</sup> ]	$a_v$ [m/s <sup>2</sup> ]	$A(8)$ [m/s <sup>2</sup> ]	$A_v(8)$ [m/s <sup>2</sup> ]
RS Jastrebac	0,704	1,18	0,302	0,504
RS Besna Kobilja	0,525	0,656	0,198	0,247
RS Kopaonik – Gobelja	0,766	1,24	0,061	0,098
RS Ovčar	0,749	1,37	0,217	0,395
RS Deli Jovan	0,801	1,50	0,329	0,614

We see that limit values are not exceeded. The values that exceed the action values are shaded in gray.

## 4.2 Additional evaluation method

As for the additional evaluation of vibration when the basic evaluation method is not sufficient, the fourth power vibration dose method was used. Additional evaluation method is used in cases where the basic evaluation method may underestimate the effects of vibration (high crest factors, occasional shocks, transient vibration). ISO 2631-1 gives two alternative evaluation methods - the running r.m.s. and the fourth power vibration dose. As a third alternative there is the evaluation method described in ISO 2631-5[4]. The indicators for using the additional method according to ISO 2631-1 are: crest factor greater than 9 and  $VDV/(a_w * T^{1/4})$  greater than 1,75.

Actually all the measurements needed the additional evaluation. The results are presented in table 4.

**Table 4** Additional evaluation method: the fourth power vibration dose.

Repeater station location	Crest factor	$VDV/(a_w * T^{1/4})$	VDV [ $m/s^{1.75}$ ]
RS Jastrebac	12,4	1,37	5,40
RS Besna Kobilja	11,1	2,01	8,43
RS Kopaonik – Gobelja	8,8	2,07	2,77
RS Ovčar	9,0	1,66	8,62
RS Deli Jovan	11,4	1,88	11,33

When comparing measured values with limit values, there are limits defined by B.2 [1] in health guidance caution zones figure (Fig. 6), when taking for estimated vibration dose value,  $eVDV=1,4*a_w*T^{1/4}$ , values  $8,5 m/s^{1.75}$  and  $17 m/s^{1.75}$  for the lower and upper bonds of the zone B.2.

Regulation [2] and Directive 2002/44/EC give for exposure action value vibration dose value of  $9,1 m/s^{1.75}$  and for exposure limit value vibration dose value of  $21 m/s^{1.75}$ .

We see that in two cases the B.2 health caution zone is exceeded (shaded in Table 4) and in one case action value vibration dose value is exceeded (for RS Deli Jovan).

## 5. CONCLUSION

Assuming the average exposure presented in this paper, average value of weighted r.m.s. acceleration,  $0,71 m/s^2$ , first limit of health caution zone (according to eq. B.2 of [1]) is  $9,1 m/s^{1.75}$ . When taking into account vibrations in all directions, for the average value  $a_w=1,2 m/s^2$ , health caution zone is achieved already in 10 min. Driving 55 minutes on the bumpy mountain road would lead to exceeding the daily exposure action value. However, in concrete situations the limit values were not exceeded but the action values were. All the situations considered needed the additional method, and it showed also that limit values were not exceeded but action values were. All this indicates that workers are exposed to a potential health risk.

## REFERENCES

- [1] ISO 2631-1:1997+A1:2010, SRPS ISO 2631-1:2014 Mechanical vibration and shock — Evaluation of human exposure to whole-body vibration — Part 1: General requirements.
- [2] Regulation on preventive measures for health and safety at work regarding vibration exposure. Off. J. RS. 2011, 93, pp. 30-32
- [3] Directive 2002/44/EC of the European Parliament and of the Council of 25 June 2002 on the minimum health and safety requirements regarding the exposure of workers to the risks arising from physical agents (vibration). Off. J. Eur. Commun. 2002, L177, pp. 13-19
- [4] Miočinović, J. “Health risk evaluation of WBV by ISO 2631-1 for passengers in urban public transport road vehicles (buses)”, *24<sup>th</sup> International Conference Noise and Vibration*, Niš, 2014
- [5] ISO 2631-5:2004 Mechanical vibration and shock -- Evaluation of human exposure to whole-body vibration -- Part 5: Method for evaluation of vibration containing multiple shocks



## ANALYTICAL INVESTIGATION TO DUFFING HARMONIC OSCILLATOR

Nicolae Herisanu<sup>1</sup>, Vasile Marinca<sup>1</sup>

<sup>1</sup> University Politehnica Timisoara, Faculty of Mechanical Engineering, nicolae.herisanu@upt.ro

**Abstract** - In this paper, an analytical investigation is proposed for the Duffing harmonic oscillator using a new and reliable method of solution, namely the Optimal Auxiliary Functions Method, which proves to be a powerful tool in analyzing nonlinear problems. An analytical periodic solution and the frequency are obtained using this approach. Very accurate analytical results are obtained after only one iteration, which demonstrates the capabilities of the proposed method to investigate complicated nonlinear problems.

### 1. INTRODUCTION

In the papers [1-6] are presented some conservative nonlinear oscillatory systems which can often be modelled by potentials having a rational form. Such models also lead to differential equations for which the usual expansion in a small parameter perturbation procedure do not apply [2].

Mickens [1,2] applied two non-standard finite difference scheme to numerically integrate the equation of Duffing harmonic oscillator. Tiwari at all [3] presented and approximate frequency-amplitude relation close to the exact one assuming a single term solution and following the Ritz procedure. Also they applied a rational harmonic balance approximation for Duffing harmonic oscillator. Hu and Tang [4] used the first-order harmonic balance via First Fourier coefficient to construct an approximate frequency-amplitude relation. Herisanu and Marinca [6] proposed and optimization procedure, namely the optimal variational iteration method for analytically solving this type of equations. This procedure provides a good approximation for both frequency and periodic solution. Ozis and Yildirim [5] applied the energy balance method obtaining the frequency in the form

$$\omega^2 = 1 - \frac{2}{A^2} \ln \frac{2(1+A^2)}{2+A^2} \quad (1)$$

where A is the initial position of the Duffing harmonic oscillator.

An example of the system which has a rational form is the Duffing harmonic oscillator presented in [2]

$$\frac{d^2y}{dt^2} + \frac{ay^3}{b+cy^2} = 0 \quad (2)$$

where y is the displacement, t is the time, a, b and c are nonnegative parameter.

Defining

$$x = y\sqrt{\frac{b}{a}}, \quad \bar{t} = t\sqrt{\frac{c}{a}} \quad (3)$$

and dropping the bar on t, gives the following non-dimensional equation

$$\ddot{x} + \frac{x^3}{1+x^2} = 0 \quad (4)$$

where dot denotes the derivative with respect to the time t. For small or large x, respectively, the Eq.(4) can be written as

$$\ddot{x} + x^3 \approx 0 \quad \text{for small } x \quad (5)$$

$$\ddot{x} + x \approx 0 \quad \text{for large } x \quad (6)$$

We remark that for small x, the equation of motion (5) is that of a Duffing type nonlinear oscillator, while for large x the equation of motion approximates that of a linear harmonic oscillator. Hence, Eq.(4) is referred to as the Duffing harmonic nature [2]. The restoring force in Eq.(4) is the same for both negative and positive amplitudes.

The initial condition for Eq.(4) are

$$x(0) = A, \quad \dot{x}(0) = 0 \quad (7)$$

### 2. BASICS OF THE OPTIMAL AUXILIARY FUNCTIONS METHOD (OAFM)

In order to emphasize the basics of OAFM, it is useful to consider the nonlinear differential equation under the general form

$$L[u(x)] + g(x) + N[u(x)] = 0 \quad (8)$$

where L is the linear operator, g is a known function depending under the problem under investigation, N is the nonlinear operator, x is the independent variable and u(x) is an unknown function to be determined.

The initial or boundary conditions are given by the operator

$$B\left(u(x), \frac{du(x)}{dx}\right) = 0 \quad (9)$$

In order to find an approximate solution for the considered problem, we assume that this solution can be expressed as

$$\bar{u}(x, C_i) = u_0(x) + u_1(x, C_i), \quad i = 1, 2, \dots, s \quad (10)$$

where the initial approximation  $u_0(x)$  and the first approximation  $u_1(x)$  will be determined as follows.

By substituting Eq.(10) into Eq.(8), it results in

$$L(u_0(x)) + L(u_1(x, C_i)) + g(x) + N[u_0(x) + u_1(x, C_i)] = 0 \quad (11)$$

and the initial approximation  $u_0(x)$  can be obtained from the linear equation

$$\begin{aligned} L[u_0(x)] + g(x) &= 0 \\ B\left(u_0, \frac{du_0}{dx}\right) &= 0 \end{aligned} \quad (12)$$

while the first approximation can be obtained from the equation

$$\begin{aligned} L[u_1(x, C_i)] + N[u_0(x) + u_1(x, C_i)] &= 0 \\ B\left(u_1, \frac{du_1}{dx}\right) &= 0 \end{aligned} \quad (13)$$

The nonlinear term could be expanded as

$$N[u_0(x) + u_1(x, C_i)] = N[u_0(x)] + \sum_{k=1}^{\infty} \frac{u_1^k}{k!} N^{(k)}[u_0(x)] \quad (14)$$

At this point, in order to avoid the difficulties that appear in solving the nonlinear differential equation (13) and to accelerate the convergence of the first approximation  $u_1$  and implicitly of the approximate solution  $\bar{u}(x)$ , instead of the last term arising in Eq.(13), we propose another expression, such that Eq.(13) may be written as

$$\begin{aligned} L[u_1(x, C_i)] + A_1(u_0(x), u_0'(x), C_i)N[u_0(x)] + \\ + A_2(u_0(x), u_0'(x), C_j) &= 0 \\ B\left(u_1(x), \frac{du_1(x)}{dx}\right) &= 0 \end{aligned} \quad (15)$$

where  $A_1$  and  $A_2$  are two arbitrary auxiliary functions depending on the initial approximation  $u_0(x)$  and several unknown convergence-control parameters  $C_i$  and  $C_j$ ,  $i=1,2,\dots,s$ ,  $j=s+1,s+2,\dots,p$ . The auxiliary functions  $A_1$  and  $A_2$  (called as optimal auxiliary functions) are not unique, and are of the same form like  $u_0$ . In some particular cases, if  $N[u_0(x)]=0$ , then  $u_0$  is an exact solution of Eq.(8), but such cases rarely happen to nonlinear problems.

The initially unknown convergence-control parameters  $C_i$  and  $C_j$  may be optimally identified via different approaches, such as the least square method, the Galerkin method, the Ritz method, the collocation method, and so on.

### 3. OAFM FOR DUFFING HARMONIC OSCILLATOR

Using a new independent variable and a new function

$$\tau = \Omega t, \quad x(t) = Au(\tau) \quad (16)$$

the equation (4) can be written in the following form

$$\Omega^2 u'' + A^2 \Omega^2 u^2 u'' + A^2 u^3 = 0 \quad (17)$$

with the corresponding initial conditions

$$u(0) = 1, \quad u'(0) = 0 \quad (18)$$

where prime denotes the derivative with respect to the new variable  $\tau$ .

Applying OAFM [8], [9], [10], the linear and nonlinear operators for Eq.(17) are respectively

$$L[u(\tau)] = \Omega^2 (u'' + u) \quad (19)$$

$$N[u(\tau)] = \Omega^2 (A^2 u^2 u'' - u) + A^2 u^3 \quad (20)$$

The approximate analytical solution is of the form

$$\tilde{u}(\tau) = u_0(\tau) + u_1(\tau) \quad (21)$$

The initial approximation is obtained from the equation

$$L[u_0(\tau)] = 0, \quad u_0(0) = 1, \quad u'(0) = 0 \quad (22)$$

leading to the solution

$$u_0(\tau) = \cos \tau \quad (23)$$

Introducing Eq.(23) into Eq.(20) it follows that

$$N[u_0(\tau)] = \alpha \cos \tau + \beta \cos 3\tau \quad (24)$$

where

$$\alpha = \frac{3}{4} A^2 (1 - \Omega^2) - \Omega^2, \quad \beta = \frac{1}{4} A^2 (1 - \Omega^2) \quad (25)$$

The function "source"  $f_i$  are

$$f_i(\tau) = \cos(2i+1)\tau, \quad i = 1, 2, 3 \quad (26)$$

The auxiliary function  $g$  is

$$g(C_i) = -(C_1 + 2C_2 \cos 2\tau + 2C_3 \cos 4\tau) \quad (27)$$

It follows that the first approximation can be determined from the equation

$$\begin{aligned} L[u_1(\tau, C_i)] = (C_1 + 2C_2 \cos 2\tau + 2C_3 \cos 4\tau)(\alpha \cos \tau + \\ + \beta \cos 3\tau + C_4 \cos 5\tau) \end{aligned} \quad (28)$$

or

$$\begin{aligned} \Omega^2 (u_1'' + u_1) = [\alpha(C_1 + C_2) + \beta(C_2 + C_3) + C_3 C_4] \cos \tau + \\ + (\alpha C_2 + \beta C_1 + C_2 C_4) \cos 3\tau + (\alpha C_3 + \beta C_2 + \\ + C_1 C_4) \cos 5\tau + (\beta C_3 + C_2 C_4) + C_3 C_4 \cos 4\tau \end{aligned} \quad (29)$$

Avoiding the secular term in Eq.(29) we can determine the frequency

$$\Omega^2 = \frac{(3C_1 + 4C_2 + C_3)A^2 + 4C_3 C_4}{A^2(3C_1 + 4C_2 + C_3) + 4C_1 + 4C_2} \quad (30)$$

From Eqs.(29), (23), (15) and (21) we obtain the first-order approximate analytical periodic solution for duffing harmonic oscillator (4)

$$\begin{aligned} x(t) = A \cos \Omega t + \frac{A}{4\Omega^2} \left[ \left( \frac{3A^2}{4} - \frac{3A^2\Omega^2}{4} - \Omega^2 \right) C_2 + \right. \\ \left. + \frac{A^2}{4} (1 - \Omega^2) C_1 + C_2 C_4 \right] (\cos \Omega t - \cos 3\Omega t) + \\ \left. + \frac{A}{24\Omega^2} \left[ \left( \frac{3A^2}{4} - \frac{3A^2}{4} \Omega^2 - 1 \right) C_3 + \right. \right. \\ \left. \left. + \frac{A^2}{4} (1 - \Omega^2) C_2 + C_1 C_4 \right] (\cos \Omega t - \cos 5\Omega t) + \right. \\ \left. + \frac{A}{48\Omega^2} \left[ \frac{A^2}{4} (1 - \Omega^2) C_3 + C_2 C_4 \right] (\cos \Omega t - \cos 7\Omega t) + \right. \\ \left. + \frac{C_3 C_4}{80\Omega^2} (\cos \Omega t - \cos 9\Omega t) \right] \end{aligned} \quad (31)$$

#### 4. NUMERICAL EXAMPLES

The accuracy of our procedure is proved considering two different cases for the initial amplitudes  $A$ :

##### 4.1 Case 1

For the initial amplitude  $A=3$ , the obtained approximate frequency of the system is  $\Omega=0.9231$  and the first-order approximate solution (31) in this case is plotted in fig.1.

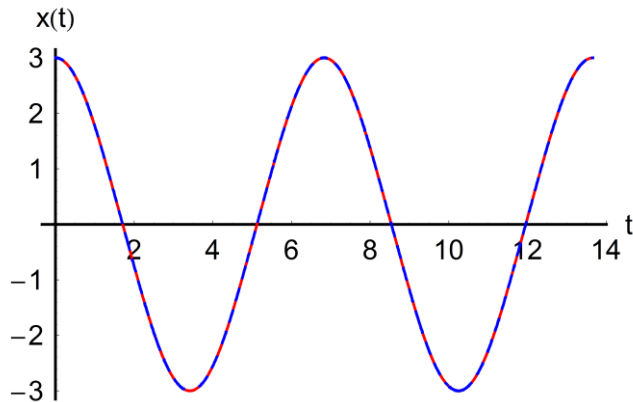


**Fig. 1** The approximate solution in the first case, for the initial amplitude  $A=3$

##### 4.2 Case 2

In the second case, for  $A=5$ , the obtained approximate frequency of the system is  $\Omega=0.9708$  and the first-order approximate solution (31) in this case is plotted in fig.2.

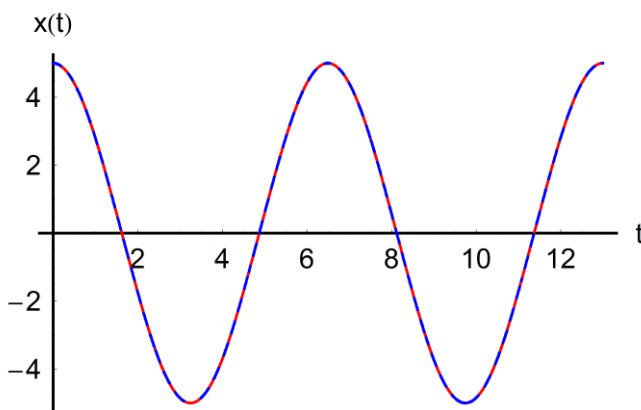


**Fig. 2** The approximate solution in the second case, for the initial amplitude  $A=5$

Fig.1 and 2 show the approximate solutions (31) and the corresponding numerical solutions in two considered cases, for different initial amplitudes of the considered Duffing harmonic oscillator.

#### 5. CONCLUSIONS

In this paper we introduce a new alternative of the OAFM to propose approximate analytical solutions to the Duffing harmonic oscillator equation. Our approach is valid even if the nonlinear equation does not contain small or large parameters. Our construction of the first iteration is different from any other approach especially referring to the auxiliary functions  $g$ , to the functions “source” and the presence of some parameters  $C_1, C_2, C_3$ , and  $C_4$ , which ensure a very rapid convergence of the solutions. We remark that an excellent accuracy of the approximations is obtained after the first iteration. It is worth mentioning that the proposed method is straightforward and can be applied to other nonlinear and strongly nonlinear problems.

#### REFERENCES

- [1] R.E. Mickens, Semi-classical quantization using the method of harmonic balance, *Il Nuova Cimento*, 101 (1989) 359-366
- [2] R.E. Mickens, Mathematical and numerical study of the Duffing-harmonic oscillator, *J. Sound Vibr.* 244 (2001) 563-567
- [3] S.B. Tiwari, S. Nageswara Rao, N.S. Swang, K.S. Sai, H.R. Nataraje, Analytical study on a Duffing-harmonic oscillator, *J. Sound Vibr.* 295 (2005) 1217-1222
- [4] H. Hu, J.H. Tang, Solution of a Duffing-harmonic oscillator by the method of harmonic balance, *J. Sound Vibr.* 294 (2006) 637-639
- [5] T. Ozis, A. Yildirim, Determination of the frequency-amplitude relation for a Duffing-harmonic oscillator by the energy balance method, *Comp. Math. Appl.* 54 (2007) 1184-1187
- [6] N. Herisanu, V. Marinca, A modified variational iteration method for strongly nonlinear problems, *Nonlinear Sci. Lett. A*, 1 (2010) 183-192
- [7] V. Marinca, N. Herisanu, *The optimal homotopy asymptotic method. Engineering applications*. Cham: Springer, 2015
- [8] N. Herisanu, V. Marinca, “Approximate analytical solutions to jerk equations”, *Springer Proc. Math. Stat.*, vol. 182, pp. 169-176, 2016
- [9] B. Marinca, V. Marinca, Approximate analytical solution for thin film flow of a fourth grade fluid down a vertical cylinder, *Proc. Rom. Acad. Ser. A*, vol.19, pp. 69-76, 2018

# KNOW YOUR VIBRATION IMPACT TO REDUCE RISK

Reduce the risk of structural damage, equipment failure and physical harm from excessive vibration with our innovative Vibration Monitoring Terminal.

Vibration Monitoring Terminal Type 3680 enables real-time, continuous, tri-axial measurement for an accurate, uninterrupted record of vibration levels.

## Mining and construction

The simple-to-use device can protect against structural damage from construction and mining operations.

It automatically delivers alerts via email or SMS to avoid breaching set limits; enables remote data transmission to reduce site visits; and provides data to show regulatory compliance and care about neighbour comfort.

## Road and rail traffic

The terminal is also able to assess human response to vibration from road and rail traffic via continuous vibration measurement.

It allows users to efficiently conduct background surveys prior to new construction and routinely assess daily operations. Its data can also be used to evaluate the effectiveness of vibration mitigation techniques.

## Sensitive equipment and artefacts

The unit monitors and sends alerts regarding ambient vibration levels close to sensitive

hospital imaging equipment, semiconductor manufacturing plants, historical buildings and museums.

Its highly sensitive geophone delivers accurate data that helps ensure reliable operation of vibration-sensitive equipment to avoid costly errors, incorrect results and the risk of machine and artefact damage.

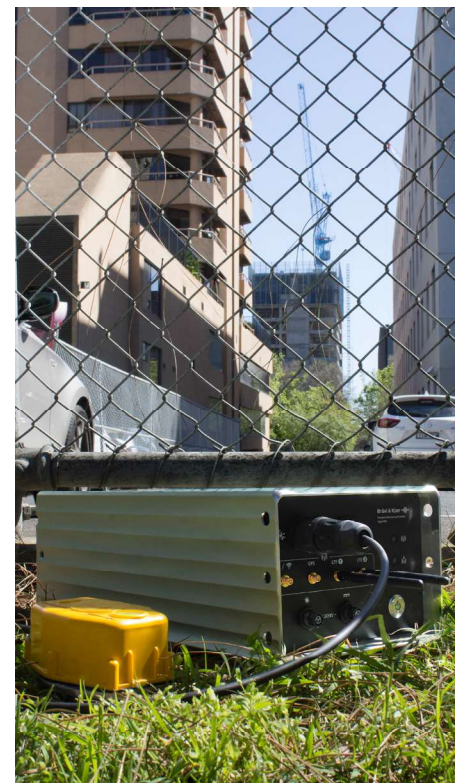
Key features include:

- Real-time data availability, including remote access
- Robust unit with inbuilt communications and system health monitoring
- A complete set of measurement metrics for a wide range of applications
- Alerts based on level and time of day (when used with Sentinel)
- A single geophone capable of measuring to different standards
- Easy installation and high uptime
- Low power consumption and operating costs
- Supported by Brüel & Kjær's service and technical experts

The self-contained unit includes sensor conditioning, processing, storage and communication over Wi-Fi, Bluetooth or digital mobile communications. Its rugged aluminium

enclosure is water and dust proof to an IP67 rating for continuous, long-term use in harsh outdoor environments.

The terminal can be used as a standalone device or with our Sentinel environmental monitoring service for comprehensive, multi-location noise, vibration and dust compliance monitoring.



[www.bksv.com/VMT](http://www.bksv.com/VMT)



## FREE VIBRATIONS OF TAPERED BEAMS

Vasile Marinca<sup>1</sup>, Nicolae Herisanu<sup>2</sup>

<sup>1</sup> Politehnica University of Timisoara, Faculty of Mechanical Engineering, Romania, vasile.marinca@upt.ro

**Abstract** - The aim of this work is to obtain an approximate analytical solution for the fundamental frequency and for the displacement of tapered beams. The Optimal Auxiliary Functions Method (OAFM) is applied to find the solutions of nonlinear governing differential equations. Our results are compared with numerical integration results obtained by using a fourth order Rung-Kutta method.

### 1. INTRODUCTION

Tapered beams can model engineering structures which require a variable stiffness along the length, such as moving arms and turbine blades [1], [2], [3], or can be modelled as a slender, flexible cantilever beam carrying a lumped mass with rotary inertia at an intermediate point along its span hence they exhibit large-amplitude vibrations [4], [5], [6].

Linearization techniques are employed in order to approximate such nonlinear problems. One may question the accuracy of using a linear mode method, which are a frequently used method in the analyses of nonlinear continuous systems to approximate the large amplitude nonlinear behavior [7].

In dimensionless form, the governing differential equation corresponding to fundamental mode of tapered beams is given by

$$\frac{d^2u}{dt^2} + u + a \left[ \frac{d^2u}{dt^2} u^2 + \left( \frac{du}{dt} \right)^2 \right] + bu^3 = 0 \quad (1)$$

where  $a$  and  $b$  are modal constants which result from the discretization procedure [7], describe the large-amplitude free vibration of the considered slender inextensible cantilever beam, which is assumed undergoing planar flexural vibrations. The terms from the brackets in Eq.(1) represent inertia-type cubic nonlinearity arising from the in extensibility assumption. The last term is a static-type cubic nonlinearity associated with the potential energy stored in bending.

For Eq.(1), the initial conditions are

$$u(0) = A, \quad \frac{du}{dt}(0) = 0 \quad (2)$$

Under the transformations

$$\tau = \Omega t, \quad u(\tau) = Ax(\tau) \quad (3)$$

where  $\Omega$  is the natural frequency, Eqs. (1) and (2) can be rewritten in the form

$$\Omega^2 x'' + x + aA^2\Omega^2 x^2 x'' + aA^2\Omega^2 x x'^2 + \lambda A^2 x^3 = 0 \quad (4)$$

$$x(0) = 1, \quad x'(0) = 0 \quad (5)$$

where the prime denotes differentiation with respect to  $\tau$ .

The main objectives of our work are to obtain an analytical solution for the natural frequency  $\Omega$  and corresponding displacement of tapered beams. The OAFM is used to find approximate analytical solutions for the nonlinear governing differential equations (4) and (5). To validate the accuracy and efficiency of our approach, the results are compared with numerical results.

### 2. BASICS OF THE OPTIMAL AUXILIARY FUNCTIONS METHOD

Let us consider the general nonlinear differential equation [5], [8], [9], [10]

$$L[x(\tau)] + N[x(\tau)] = 0, \quad x \in \Omega \quad (6)$$

where  $L$  is a linear operator,  $N$  is a nonlinear operator,  $\tau$  denotes the independent variable,  $\Omega$  is the domain of interest and  $x(\tau)$  is an unknown function. The boundary/initial conditions are

$$B \left( x(\tau), \frac{dx(\tau)}{d\tau} \right) = 0 \quad (7)$$

We suppose that the approximate analytical solution  $\tilde{x}(\tau)$  for Eq.(6) and (7) is

$$\tilde{x}(\tau) = x_0(\tau) + x_1(\tau, C_i), \quad i = 1, 2, \dots, p \quad (8)$$

in which  $x_0(\tau)$  - the initial approximation and  $x_1(\tau, C_i)$  - the first approximation will be determined as follows. Inserting Eq.(8) into Eq.(6) it results in

$$L[x_0(\tau)] + L[x_1(\tau, C_i)] + N[x_0(\tau) + x_1(\tau, C_i)] = 0 \quad (9)$$

The initial approximation  $x_0(\tau)$  is obtained from the linear equation

$$L[x_0(\tau)] = 0 \quad (10)$$

with the corresponding boundary/initial conditions

$$B \left( x_0(\tau), \frac{dx_0(\tau)}{d\tau} \right) = 0 \quad (11)$$

The first approximation  $x_1(\tau)$  is determined from the nonlinear differential equation

$$L[x_1(\tau, C_i)] + N[x_0(\tau) + x_1(\tau, C_i)] = 0 \quad (12)$$

with the boundary/initial conditions

$$B \left( x_1(\tau, C_i), \frac{dx_1(\tau, C_i)}{d\tau} \right) = 0 \quad (13)$$

where  $C_1, C_2, \dots, C_p$  are  $p$  unknown parameters at this moment.

The nonlinear term in Eq.(12) can be expanded in the form

$$N[x_0(\tau) + x_1(\tau, C_i)] = N[x_0(\tau)] + \sum_{k \geq 1} \frac{x_1^k}{k!} N^{(k)}[x_0(\tau)] \quad (14)$$

To avoid the difficulties that can appear in solving the nonlinear differential equation (12) and to accelerate the convergence of the first approximation  $x(\tau, C_i)$ , instead of the last term arising in Eq.(12), we propose another expression, such that Eq.(12) can be rewritten as

$$L[x_1(\tau, C_i)] + \sum_{i=1}^p f_i(\tau) g_i(C_i) = 0, \quad B\left(x_1(\tau), \frac{dx_1(\tau)}{d\tau}\right) = 0 \quad (15)$$

where  $C_i$  are arbitrary unknown parameters,  $f_i$  are auxiliary functions depending on the initial approximation  $x_0(\tau)$ , on the functions which appear into the composition of  $N[x_0(\tau)]$  or are combination of such expressions, and  $g$  are functions which depend on  $C_i$ . In other words,  $x_0(\tau)$  and  $N[x_0(\tau)]$  are "source" for the auxiliary functions  $f_i$ . Auxiliary functions  $f_i$  are not unique and it should be emphasized that we have a great freedom to choose these auxiliary functions. After using the previous considerations, for example if  $x_0(\tau)$  and  $N[x_0(\tau)]$  are polynomial functions, then  $f_i$  are sums of polynomial functions; if  $x_0(\tau)$  and  $N[x_0(\tau)]$  are exponential functions then  $f_i$  are sums of exponential functions; if  $x_0(\tau)$  is trigonometric function and  $N[x_0(\tau)]$  is polynomial function, then  $f_i$  are sums of combinations of trigonometric and polynomial functions, and so on. It is very important to remark that if  $N[x_0(\tau)] = 0$ , then it is clear that  $x_0(\tau)$  is an exact solution of Eqs.(6) and (7).

Now, the unknown parameters  $C_i$  can be optimally identified via rigorous methods such as the least square method, Ritz method, collocation method, Galerkin method, Kantorovich method or by minimizing the square residual error:

$$J(C_1, C_2, \dots, C_p) = \int_{\Omega} R^2(\tau, C_i) d\tau, \quad i = 1, 2, \dots, p \quad (16)$$

where

$$R(\tau, C_i) = L[\tilde{x}(\tau)] + N[\tilde{x}(\tau)] \quad (17)$$

with  $\tilde{x}(\tau)$  given by Eq.(8).

The values of  $C_i$  are obtained by solving the system

$$\frac{\partial J}{\partial C_1} = \frac{\partial J}{\partial C_2} = \dots = \frac{\partial J}{\partial C_i} = 0 \quad (18)$$

By this novel procedure, the approximate analytical solution  $\tilde{x}(\tau)$  is well determined after identification of the optimal values of the initially unknown convergence-control parameters  $C_i$ . It will be proved that our approach is a powerful tool for solving nonlinear problems without small or large parameters into Eqs.(6) and (7).

### 3. OAFM FOR FREE VIBRATION OF TAPERED BEAMS

The Eqs.(4) and (5) can be written in the following form

$$x'' + \frac{x}{\Omega^2} + aA^2(x^2x'' + xx'^2) + \frac{b}{\Omega^2}A^2x^3 = 0 \quad (19)$$

$$x(0) = 1, x'(0) = 0$$

The linear and nonlinear operators are respectively

$$L[x(\tau)] = x'' + x \quad (20)$$

$$N[x(\tau)] = \frac{x}{\Omega^2} - x + aA^2(x^2x'' + xx'^2) + \frac{b}{\Omega^2}A^2x^3 \quad (21)$$

From the equation

$$\begin{aligned} x_0'' + x_0 &= 0, \\ x_0(0) &= 1, x_0'(0) = 0 \end{aligned} \quad (22)$$

it follows that

$$x_0(\tau) = \cos \tau \quad (23)$$

The nonlinear operator for the solution (23) becomes

$$\begin{aligned} N[x_0(\tau)] &= \left( \frac{1}{\Omega^2} - 1 - \frac{1}{2}aA^2 + \frac{3bA^2}{4\Omega^2} \right) \cos \tau + \\ &+ \left( \frac{bA^2}{4\Omega^2} - \frac{aA^2}{2} \right) \cos 3\tau \end{aligned} \quad (24)$$

The functions "source"  $f_i$  are obtained from Eq.(24):

$$f_i(\tau) = \cos(2i+1)\tau, \quad i = 1, 2, 3 \quad (25)$$

and the auxiliary function  $g$  which appear into Eq.(15) is chosen as

$$g(C_i) = -(C_1 + 2C_2 \cos 2\tau + 2C_3 \cos 4\tau) \quad (26)$$

such that Eq.(15) becomes

$$\begin{aligned} x_1'' + x_1 &= (C_1 + 2C_2 \cos 2\tau + 2C_3 \cos 4\tau)(\alpha \cos \tau + \\ &+ \beta \cos 3\tau + C_4 \cos 5\tau) \\ x_1(0) &= x_1'(0) = 0 \end{aligned} \quad (27)$$

where  $\alpha$  and  $\beta$  are obtained from Eq.(24):

$$\alpha = \frac{1}{\Omega^2} - 1 - \frac{1}{2}aA^2 + \frac{3bA^2}{4\Omega^2}; \quad \beta = \frac{bA^2}{4\Omega^2} - \frac{aA^2}{2} \quad (28)$$

and  $C_i, i=1,2,3,4$  are unknown parameters at this moment.

After simple manipulations, Eq.(27) can be rewritten in the form

$$\begin{aligned} x_1'' + x_1 &= [\alpha(C_1 + C_2) + \beta(C_2 + C_3) + C_3C_4] \cos \tau + \\ &+ (\alpha C_2 + \beta C_1 + C_2C_4) \cos 3\tau + (\alpha C_3 + \beta C_2 + \\ &+ C_1C_4) \cos 5\tau + (\beta C_3 + C_2C_4) \cos 7\tau + C_3C_4 \cos 9\tau \\ x_1(0) &= x_1'(0) = 0 \end{aligned} \quad (29)$$

We have the freedom to choose the functions  $g(x)$  in the forms

$$g(C_i) = -(C_1 + 2C_2 \cos 2\tau) \quad (30)$$

or

$$g(C_i) = -(C_1 + 2C_2 \cos 2\tau + 2C_3 \cos 6\tau) \quad (31)$$

or yet

$$\begin{aligned} g(C_i) &= -(2C_1 \cos 2\tau + 2C_2 \cos 4\tau + \\ &+ 2C_3 \cos 6\tau + 2C_4 \cos 8\tau) \end{aligned} \quad (32)$$

and so on.

Avoiding the secular term into Eq.(29), we obtain

$$\alpha(C_1 + C_2) + \beta(C_2 + C_3) + C_3C_4 = 0 \quad (33)$$

From Eqs.(28) and (33) we can determine the frequency

$$\Omega^2 = \frac{(4 + 3bA^2)(C_1 + C_2) + bA^2(C_2 + C_3)}{2aA^2(C_1 + 2C_2 + C_3) + 4C_1 + 4C_2 - 4C_3C_4} \quad (34)$$

Taking into account the solution of Eq.(24), and Eqs.(23), (3) and (8) one can obtain the first-order approximate periodic solution of Eqs.(1) and (2):

$$\begin{aligned} \tilde{u}(t) = & A \cos \Omega t + \frac{A}{8} \left[ \left( \frac{1}{\Omega^2} - 1 - \frac{1}{2} a A^2 + \frac{3bA^2}{4\Omega^2} \right) C_2 + \right. \\ & + \left( \frac{bA^2}{4\Omega^2} - \frac{aA^2}{2} \right) C_1 + C_2 C_4 \left. \right] (\cos \Omega t - \cos 3\Omega t) + \\ & + \frac{A}{24} \left[ \left( \frac{1}{\Omega^2} - 1 - \frac{1}{2} a A^2 + \frac{3bA^2}{4\Omega^2} \right) C_3 + \left( \frac{bA^2}{4\Omega^2} - \frac{aA^2}{2} \right) C_1 + \right. \\ & + C_2 C_4 \left. \right] (\cos \Omega t - \cos 7\Omega t) + \\ & + \frac{C_3 C_4}{80} (\cos \Omega t - \cos 9\Omega t) \end{aligned} \quad (35)$$

#### 4. NUMERICAL EXAMPLES

In what follows we consider two cases in order to prove the accuracy of OAFM.

##### 4.1 Case 1

For  $a=2$ ,  $b=1$ ,  $A=0.5$ , the obtained approximate frequency of the system is  $\Omega=0.7502$  and the first-order approximate solution (35) in this case is plotted in fig.1.

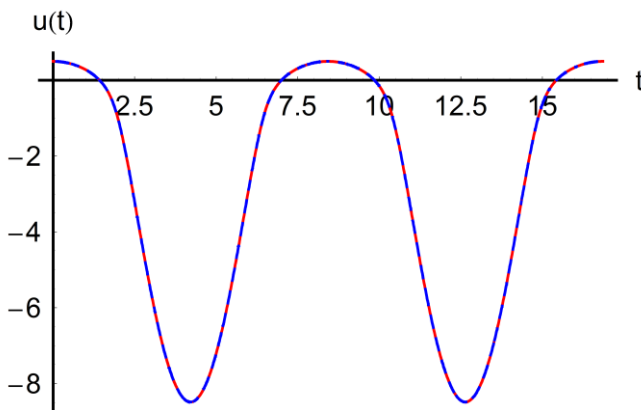


Fig. 1 The approximate solution in the first case, for  $a=2$ ,  $b=1$ ,  $A=0.5$

##### 4.2 Case 2

In the case  $a=1$ ,  $b=3$ ,  $A=0.5$ , the obtained approximate frequency of the system is  $\Omega=1.4591$  and the first-order approximate solution (35) in this case is plotted in fig.2.

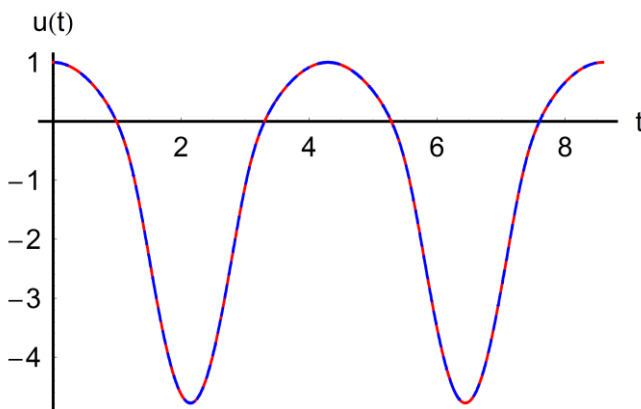


Fig. 2 The approximate solution in the second case, for  $a=1$ ,  $b=3$ ,  $A=1$

Fig.1 and 2 show the approximate solutions (35) and the corresponding numerical solutions in two considered cases, for different physical parameters and initial amplitudes.

#### 5. CONCLUSIONS

In this work, OAFM has been used to obtain approximate analytical solutions for nonlinear oscillations of tapered beams. As shown in this paper, OAFM is a powerful analytical technique providing an effective and convenient mathematical tool for nonlinear differential equations. Our procedure can be easily applied to other strongly nonlinear problems.

#### REFERENCES

- [1] D.J. Goorman, *Free vibrations of beams and shafts*, New York:Wiley, 1975
- [2] S.P. Timoshenko, J.N. Goodier, *Theory of elasticity*, Tokyo :McGraw Hill, 1993
- [3] S.H. Hoseini, T. Pirbodaghi, M.T. Ahmadian, G.H. Farahi, "On large amplitude free vibrations of tapered beams: an analytical approach", *Mechanics Research Communications*, vol. 361, pp. 892-897, 2009
- [4] N. Herisanu, V. Marinca, "Explicit analytical approximations to large-amplitude nonlinear oscillations of a uniform cantilever beam carrying an intermediate lumped mass and rotary inertia", *Meccanica*, vol.45, pp. 847-855, 2010
- [5] V. Marinca, N. Herisanu, *The optimal homotopy asymptotic method. Engineering applications*. Cham: Springer, 2015
- [6] M.N. Hamdan, N.N. Shabaneh, "On the large amplitude free vibration of a restrained uniform beam carrying an intermediate lumped mass", *J. Sound Vibr.*, vol. 199, pp. 711-726, 1997
- [7] M.N. Hamdan, M.A.F. Dado, "Large amplitude free vibration of a uniform cantilever beam carrying an intermediate lumped mass and rotary inertia", *J. Sound Vibr.*, vol. 206, pp. 151-168, 1997
- [8] N. Herisanu, V. Marinca, "Approximate analytical solutions to jerk equations", *Springer Proc. Math. Stat.*, vol. 182, pp. 169-176, 2016
- [9] B. Marinca, V. Marinca, Approximate analytical solution for thin film flow of a fourth grade fluid down a vertical cylinder, *Proc. Rom. Acad. Ser. A*, vol.19, pp. 69-76, 2018
- [10] V. Marinca, N. Herisanu, Vibration of nonlinear nonlocal elastic column with initial imperfection, *Springer Proc. Physics*, vol. 198, pp. 49-56, 2018

**AUSPICE**



**Ministry of Education,  
Science and Technological Development  
Republic Serbia**

**[www.mpn.gov.rs](http://www.mpn.gov.rs)**

**GENERAL SPONSOR**



**Brüel & Kjær**

**[www.bksv.com](http://www.bksv.com)**

